Reversal of immunosenescence by Rab8a empowered dendritic cells

SUDHAKAR SINGH

A thesis submitted for the partial fulfillment of

the degree of Doctor of Philosophy

Department of Biological Sciences

Indian Institute of Science Education and Research Mohali

Sector 81, Knowledge City, SAS Nagar, Manauli PO, Mohali, 140306 Punjab, India.

February 2024

Dedicated to my late grandfather and younger version of myself

Declaration

The work presented in this thesis has been carried out by me under the guidance of **Dr. Sharvan Sehrawat** at the Indian Institute of Science Education and Research Mohali. This work has not been submitted in part or in full for a degree, a diploma, or a fellowship to any other university or institute. Whenever contributions of others are involved, every effort is made to indicate this clearly, with due acknowledgement of collaborative research and discussions. This thesis is a bona fide record of original work done by me and all sources listed within have been detailed in the bibliography

Sudhakar Singh

Place:

Date:

In my capacity as the supervisor of the candidate's thesis work, I certify that the above statements by the candidate are true to the best of my knowledge.

Dr. Sharvan Sehrawat

Associate Professor

Department of Biological Sciences

Indian Institute of Science Education and Research Mohali

Place:

Date:

Acknowledgements

Words in my lexicon fail to express my profound sense of reverence and indebtedness to my mentor **Dr. Sharvan Sehrawat** for his inspiring guidance, outstanding cooperation and constant encouragement during the entire course of study. His constant support, critical appreciation gave a glitter of confidence to my research work during my journey. His intense hard work and countless efforts to provide every possible facility in the lab made this strenuous task achievable. Without his help, it would have been challenging for me to execute all the plans beautifully during the entire study. His motivation, vision and immense knowledge about the field has inspired me throughout these years. I would like to genuinely acknowledge his enlightening guidance and support for being a tremendous mentor to me. I sincerely thank him for his acceptance and patience in planning and executing my research and thesis preparation.

I owe my sincere thanks to the members of my doctoral advisory committee, **Dr. Indranil Banerjee** and **Dr. Kuljeet Sandhu** for their critical evaluation along with prolific ideas and time to time suggestions that helped me in the successful execution of my research work. I am also grateful to all the lab members Dr. Indranil Banerjee for their extensive support in providing me with research facilities of their lab and helping with my experiments.

I am highly thankful to **Indian Council of Medical Research (ICMR) New Delhi** and **IISER Mohali** for providing me financial assistance to perform my research work and all the necessary facilities and research instruments for conducting timely experiments in a conducive research environment. I would also like to extend my thanks and profound gratitude to **Dr. Chander Shekhar** and all the members of animal house facility for their constant and timeless support to

carry out animal experiments. I also thank Prateek Arora for his enduring support and technical help in conducting flow cytometry experiments.

With a debt of gratitude which cannot be adequately expressed in words, I thanks to all my lab members **Surbhi Dahiya, Syed Azeez Tehseen, Sramona Kar, Yuviana J Singh, Mohammad Shaaz, Nimisha, Akshit, Shazia, Gurjinder, Divya, Shreya and Osh** for their scholarly discussion, unconditional support, help during research, company, friendship, encouraging attitude that inspired and helped me to achieve my goal.

I am equally thankful to my ex-lab members and seniors **Dr. Roman Sarkar, Dr. Dhaneshwar Kumar, Dr. Manpreet Kaur, Dr. Jasreen Kaur, Yashu Sharma and Ayush Jain** for their unconditional love and support to complete this strenuous task. My boundless thanks are extended to all of them for the love and concern they showed to me.

As I near the completion of my PhD, wants to extend a special thanks to **Surbhi Dahiya** for her unwavering belief in my abilities, even when I doubted myself, propelled me forward and kept me going during the toughest times of my PhD.

Vocabulary finds no appropriateness to express my heartfelt love and thanks from the very core of my heart to my dearest friends **Nirmal, Adeel, Shraddha, Asis, Archit, Yogesh, Tejal, Kajal Moumita** and **Anshika** for their unconditional love and support.

I am also thankful to my friends and seniors outside the IISER **Dr. Gaurav Chaubey, Dr. Suryakant Verma, Dr. Mamta Pandey, Dr. Ritu Sharma**, **Omprakash**, **Aman K Singh**, **Dr. Vipin Kumar, Dr. Lal Krishan, Dr. Monika**, **Dr. Raghvendra P Singh**, **Manmohan**, **Gaurav and Shalini** for their support throughout my PhD.

Above all, I am indebted to my parents **late Mr. Rajesh Singh**, **Reeta Singh** and **brother, Rajan** for immutable source of inspiration and strength to undertake this PhD degree and successful completion of the same. I am proud to have them to be my parents and there are no words but only feelings to honorably pay my regards to them for their ceaseless perspiration, encouragement, moral support, instilling the research attitude from childhood, unlimited love and affection. Last but not the least, my humble and absolute obeisance to Almighty GOD for his abundant grace, mercy and blessings showered upon me.

Sudhakar Singh

Abstract

Aged population exhibits enhanced susceptibility to viral infection and responds poorly to vaccination. This necessitates devising immune enhancing strategies for this group. Dendritic cells (DCs) because of their unique morphological features and strategic location at tissue sites serve as the sentinels of the immune system and can effectively prime antigen specific cytotoxic T lymphocytes (CTLs), a fraction of which further differentiates into lasting memory. Anamnestic response of memory cells confers to the host a quick protection during a subsequent exposure with homologous infection. Given the critical role of DCs in linking the innate and adaptive immune system, the study was undertaken to gain insights into DCs' biology and their role in immunosenescence. Genome-wide RNAseq analysis of conventional DCs ($CD11b^{+}CD11c^{+}$ cells) isolated from unmanipulated young and aged mice revealed a severely compromised type I interferon signaling in the latter group. Type I IFNs serve as one of the first anti-viral response. Furthermore, DCs of aged animals were severely impaired in antigen presentation and mounted poor response of CTLs *in vitro* and *in vivo*. Genes of PI3K/MtorC1 signaling pathway such as Rab8a, Akt1 and S6K were downregulated in the aging cells. Therefore, the role of Rab8a, a small GTPase downstream to growth factor receptors such as CSF2Ra and IGFR, was evaluated in DCs. Rab8a depleted bone marrow precursors of young animals failed to efficiently differentiate into functionally competent DCs while those from aged animals following reconstitution with Rab8a regained functionality. Accordingly, the Rab8a reconstituted DCs generated a strong anti-viral IFN response when stimulated with two of the viruses viz., IAV and a gamma-herpesvirus (MHV68). Antigen-pulsed DCs enhanced activation of CTLs *in vitro* and mounted a potent primary and memory response of antigen specific CTLs to efficiently control a respiratory infection caused by

Influenza A Virus. Rab8a in conjunction with Rab11 promoted formation of endosomal recycling compartment (ERC) enriched with peptide loaded class I MHC complexes and such complexes were more efficiently displayed on the surface of DCs to engage with antigen specific CTLs. Therefore, the study uncovers a critical role of Rab8a in regulating differentiation and functionality of DCs and that a Rab8a reconstitution of DCs of an aging host could provide a viable approach to achieve immune sufficiency. These observations also have clinical implication in managing viral infections, enhancing vaccine efficacy as well as promoting anti-tumor response in the aging population.

Synopsis

Title of Thesis: Reversal of immunosenescence by Rab8a empowered dendritic cells

Graphical abstract

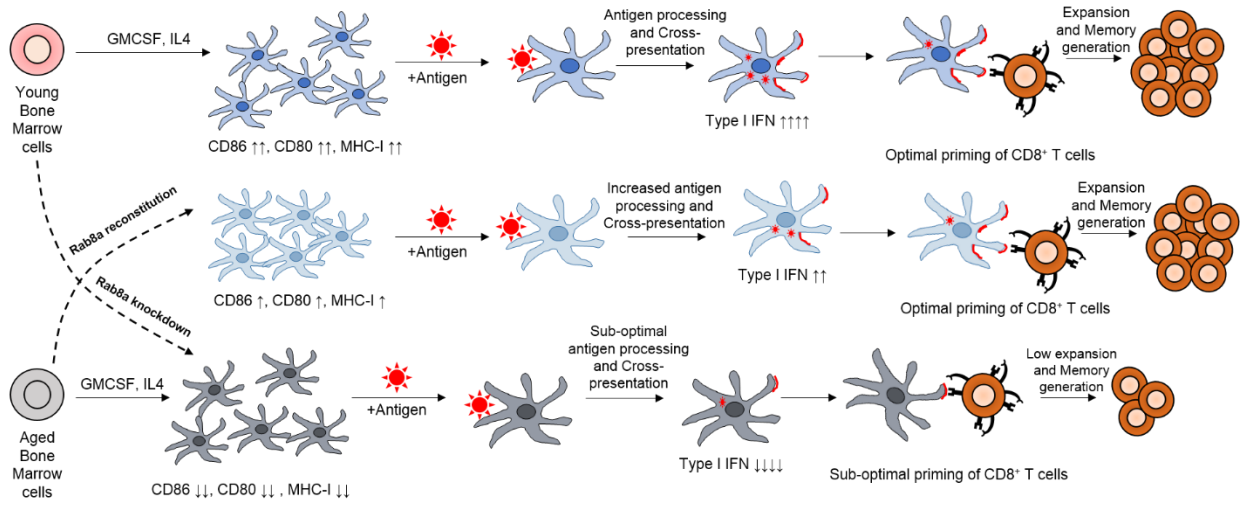

Introduction

Immune induction following infection is a highly regulated process (1). Dendritic cells (DCs) are specialized in sensing the presence of pathogens, internalizing soluble or particulate material, processing and presentation of antigens and eventually priming the T cell responses and thus determining the outcome of an infection (2). Although such homeostatic mechanisms are maintained throughout the lifetime of an individual, aging results in the progressive loss of immune functions, termed as ‘immunosenescence’. Age related alterations in the phenotypic profile and functionality of DCs results in sub optimal T cell priming. Accordingly, an inability to take up,

process and present antigens by DCs result in a diminished response to vaccination in the elderlies. Consequently, aged individuals fail to develop long term immunity in response to immunization and cannot mount proper immune responses against infections, which accounts for high morbidity and mortality (3). Therefore, analyzing the role of DCs in immunosenescence becomes crucial for improving vaccination strategies in the aged population.

Multifactorial etiology of immunosenescence poses a challenge in studying and attempting its reversal. Both cell intrinsic as well as extrinsic factors such as the composition of the microenvironment can result in reduced functionality of immunocytes (4). For example, while a reduction in the absolute counts and clonal diversity of T and B cells contribute to the compromised anti-viral response, the adaptive immune cells in the aging host also exhibit a reduced proliferative potential (5). Innate immune cells also exhibit an age associated diminished cytokine signaling, phagocytic activity and antigen uptake (6). The consequences of immunosenescence have been well-appreciated and investigated but the underlying molecular mechanisms remain to be elucidated. To this end, we performed a genome-wide transcriptomic analysis of DCs isolated from naïve young and aged animals. Genes in multiple pathways responsible for maturation and imparting functionality to DCs were downregulated in the DCs of aged animals when compared with those from their young counterparts. Of note, DCs of aged mice had an impaired type I interferon signaling pathway. We, therefore, decided to characterize the effect that a compromised type I interferon signaling might be having on the differentiation as well as functionality of the DCs in aged individuals. DCs of aged animals exhibited a reduced response of interferons in addition to their compromised ability in antigen presentation and priming $CD8^+$ T cells both *in vitro* and *in vivo*. We also discovered Rab8a (Ras related small GTPase) as a major driver of the immunosenescence in DCs that was significantly downregulated in the aging animals. Its

reconstitution restored differentiation and functionality of DCs generated from aged bone marrow cells. Therefore, reconstitution of Rab8a in the cells of aged individuals could help reverse the effects of immunosenescence.

Objectives

The study was designed with the following objectives.

1. Transcriptomic analysis of DCs of naïve young and aged host

2. Phenotypic and functional analysis of DCs from aged and young host.

3. Investigating the role of Rab8a, a small GTPase in differentiation and function of DCs

    (a) Depletion of Rab8a in DCs of young animals and studying its functional effects

    (b) Reconstitution of Rab8a in DCs of aged animals to restore functionality

Results and discussions in brief

Objective 1. Transcriptomic analysis of DCs of naïve young and aged host.

To unravel the underlying molecular mechanisms responsible for impaired functions of DCs of an aging host, we performed transcriptome analysis of $CD11c^{+}CD11b^{+}$ DCs sorted from the lymphoid tissues of naïve aged (>24 months) and young (2 months) mice. Our analysis revealed an upregulation of 44 genes by DCs of young animals while 123 genes were upregulated in the DCs of aged animals. Of the upregulated genes, a large majority were involved in the regulation of immunological pathways and were predominantly shown to localize to the membrane or nucleus. Genes upregulated in DCs of aged animals included inhibitory molecules such as CD160, and different killer like lectins such as *Klrb1b, Klrb1c, Klrc1* and *Klre1* (7,8). Additionally, a cluster of genes encoding for many GTPase associated nucleotide binding proteins (GIMAPs) and *Arl4d*

were upregulated in DCs of aged animals. These are known modulators of T cell functionality (9, 10). Functional annotation and network analysis of the genes significantly downregulated in DCs of aged animals revealed compromised anti-viral functions that can be attributed to lower expression of multiple Toll-like receptors (TLRs) such as *TLR-9*, *TLR1* and *TLR7* and several anti-viral genes such as *IFITM1, IFI27l2a, IFIT3, IFIT1, OAS1a, OASl2* and *OAS2* in DCs of aged mice suggested their inefficiency in responding to viral infections. Additionally, we observed a downregulation of genes involved in PI3K/MtorC1 signaling axis such as *Rab8a, Akt1* and *S6K*. PI3K/MtorC1 axis is responsible for growth, differentiation and functioning of DCs (24). To validate these observations, we assayed the responsiveness of DCs of aged and young mice to a respiratory virus (Influenza A virus, WSN-SIINFEKL) and a γ-herpesvirus (MHV68-SIINFEKL) by generating BMDCs. *IFNα, IFNβ* and *IFNγ* along with their downstream mediators (STAT1, 2 and IRF9) and interferons stimulated genes (*OAS1A, OAS1G, OAS2, IFIT1, IFITM1* and *ISG15*) levels were reduced in the cells differentiated from precursors of aged as compared to the younger animals (13). Similar observations were made when human PBMCs from healthy young (<25 years) and aged (>65 years) individuals were pulsed with IAV.

Objective 2. Phenotypic and functional analysis of DCs from aged and young host.

Since the type I IFN response was compromised in DCs of aged individuals, we also included young IFN receptor knockout mice (IFNRKO) in the study to explore its role in the differentiation of DCs. Phenotypic profiling of splenic DCs of aged mice revealed a significant higher frequency of splenic DCs (CD11b/CD11c) as compared to young and IFNRKO mice. Even though the expression of class II MHC molecules was comparable in all the groups, the frequencies of class I MHC expressing cells were significantly reduced in the DCs of aged and IFNRKO animals as compared to young mice. DCs from aged mice also showed significantly reduced expression of

CD80 and CD86. These results were indicative of compromised priming potential of DCs from aged as well as young IFNRKO animals. We directly tested this notion by pulsing BMDCs from young, aged and IFNRKO mice with ovalbumin and co-culturing with CFSE labelled antigen-specific OT1 cells ($CD8^+$ T cells bearing TCRs specific for the $Ova_{257-264}$ epitope, SIINFEKL). Upon incubation with Ovalbumin pulsed DCs from aged and IFNRKO mice, OT1 cells proliferated to a lesser extent as compared to those incubated with young DCs. This gave us direct proof of their inefficient T cell priming potential. Subsequently, phenotypic profiling of the *in vitro* generated BMDCs revealed a lower expression of CD80, CD86, MHCI and MHCII on the aged and IFNRKO BMDCs. These results indicated that impaired IFN response in the DCs of aging animals could partly help explain their diminished activity to cross-prime antigens and stimulate $CD8^+$ T cells. Furthermore, to recapitulate these observations *in vivo*, DC immunization experiments were carried out by adoptive transfer of Ova pulsed BMDCs into sex matched congenic young animals, which had previously received OT1 cells. The functionality of the OT1 cells in each recipient group was then measured. A significant increase in the frequencies of OT1 cells in the circulation of young DCs as compared to the aged and IFNRKO DCs recipients was evident. Upon infection with WSN-SIINFEKL, the recipients of the aged and IFNRKO DCs exhibited a sharp decline in body weights as compared to the recipients of DCs from young animals, which could be due to hyper-inflammation in the infected lung tissues and a poor control of the virus by the expanded OT1 cells. Accordingly, the frequencies of OT1 cells expressing CXCR3 (migratory marker) were significantly higher in the recipients of young DCs than those of aged and IFNRKO mice (15). Additionally, the OT1 cells in the recipients of young DCs more abundantly produced IFN-γ, TNF-α or both the cytokines. Consequently, we observed significantly higher titers of IAV in the lungs of the animals receiving DC-therapy from aged and

IFNRKO mice, which was confirmed by hemorrhagic and inflammatory lesions in their lungs. Therefore, we were able to show that DCs of aged animals are compromised in their ability to provide anti-viral protection and a diminished IFN response in the DCs of aged individuals could in part contribute to the observed effects.

Objective 3. Investigating the role of Rab8a, a small GTPase, in differentiation and function of DCs.

(a) Depletion of Rab8a in DCs of young animals and studying its functional effects

Bone marrow cells of aged animals downregulated key genes required for sensing GMCSF such as CSF2Rα along with IGF1R and downstream adaptor molecules Rab8a required for activation of Akt by PI3K (23, 24). Additionally, other genes involved in PI3K-mTOR axis responsible for regulating the growth and differentiation of DCs were reduced in the expression in aged animals (24, 25). Therefore, the analysis suggested diminished proliferative, survival and differentiation potential of bone marrow cells from aged mice. As IGF1R-PI3K pathway critically controls the differentiation program of DCs, we further elucidated its role by shRNA mediated knock down (KD) of Rab8a in the bone marrow cells of young mice. Interestingly, the Rab8a-depleted BM cells when allowed to differentiate, produced significantly less frequency $CD11b^{+}CD11c^{+}$ cells. Moreover, the expression of CD80, CD86, MHCI and MHCII were also lower on Rab8a depleted cells. Therefore, Rab8a deficiency resulted in impaired differentiation as well as maturation of the DCs. We also assayed the functionality of the DCs differentiated from Rab8a depleted bone marrow cells of young animals by pulsing them with and IAV and found that the Rab8a deficient cells produced drastically reduced levels of *IFNα, IFNβ, IFNγ, STAT1* and *STAT2* (4-fold). Therefore, a reduced expression of Rab8a in DCs impedes not only the differentiation program but also attenuates their immunostimulatory potential.

(b) Reconstitution of Rab8a in DCs of aged animals to restore functionality

Since a depletion of Rab8a in the bone marrow of young mice resulted in decreased functionality, we asked whether reconstitution of the same in aged bone marrow (BM) cells could reverse the effects of immunosenescence. To this end, lentivirus mediated overexpression of Rab8a was carried out in bone marrow cells of aged mice. Rab8a reconstituted BM cells of aged animals upregulated the expression of genes involved in nutrient sensing such as *Akt1* and a cell survival factor, *Bcl2*. Rab8a reconstitution also restored the functional differentiation of BMDCs. Accordingly, the production of interferons and their downstream mediators (*IFNα, IFNβ, IFNγ, STAT1* and *STAT2)* upon pulsing with IAV was evident in Rab8a overexpressing (Rab8a-OE) aged BMDCs. Therefore, the DCs of aged animals regained functional competence and mounted elevated response of IFNs following Rab8a reconstitution.

As the cytokine production by the Rab8a reconstituted DCs was enhanced, we assessed whether such cells had improved antigen-presentation potential. Antigen presentation assays by co-culturing CFSE labelled OT1 cells with antigen-pulsed BMDCs generated from Rab8a-OE, bone marrow cells showed a significant increase in the frequencies of dividing OT1 cells as compared to the control BMDCs from aged mice. The restoration of antigen presentation was also seen *in vivo*. Interestingly, the relative abundance of DCs in different lymphoid organs upon adoptive transfer varied amongst the young, aged and Rab8a-OE DC recipients, which could be dictated by the expression of CCR7 and CCR5. Accordingly, these molecules exhibited lower expression on DCs of aged mice than young and Rab8a-OE cells (11). The data, therefore, showed that overexpression of Rab8a in BM cells of aged mice restores their functional differentiation into BMDCs, which exhibited better cross antigen-presentation and migratory potential for efficient sensing of pathogens and priming of antigen specific $CD8^+$ T cells.

To gain mechanistic insights into the molecular events due to the depletion or the overexpression of Rab8a in bone marrow, the transcriptional changes and signaling events following Rab8a knockdown and overexpression were analyzed. Interestingly, the Rab8a depleted bone marrow cells had significantly reduced expression of genes of growth factor receptor-PI3K axis required for cellular growth and survival. The expression of the genes was restored upon Rab8a overexpression in the aged BM cells. Additionally, a baseline expression of Akt1 and phosphorylated Akt1 (pAkt1) was high in the bone marrow cells of young animals as compared to the aged counterparts, which was further increased in differentiated BMDCs. Moreover, following Rab8a depletion, the expression levels of Akt1 as well as pAkt1 reduced while reconstitution of Rab8a led to increased expression of both Akt1 and pAkt1 in steady state and after their differentiation into BMDCs. Therefore, improved growth factor sensing leading to efficient differentiation and enhancement of functionality in DCs following Rab8a reconstitution occurred through PI3K-Akt1 axis activation.

Rab8a reconstituted BMDCs preferentially expanded $CD8^+$ T cells can be attributed to better turnover of peptide loaded class I MHC molecules, which was evident by a significant increase in the surface expression of H-$2K^b$-SIINFEKL in the BMDCs differentiated from young and Rab8a-OE BM cells. Additionally, efficiency of immune synapse formation was improved by DCs of aged animals upon Rab8a reconstitution.

It is well known that Rab8a localizes in different cellular compartments such as plasma membrane (26), macropinosomes (27), recycling endosomes (28) and exocytic vesicles to name a few. It is also essential for the fusion of exocytic vesicles to the plasma membrane (29). Overexpression of Rab8a is also known to promote the formation of cell protrusion and dorsal ruffles (30) and enhances membrane trafficking (27). Therefore, Rab8a could modulate the surface

display of p-MHC class I molecules in the reconstituted DCs and such complexes could better ligate cognate antigen reactive $CD8^+$ T cells. To understand the role of subcellular compartments in facilitating Rab8a-driven cross antigen presentation, we performed confocal analysis of DCs from young and aged animals and Rab8a-OE aged DCs upon antigenic stimulation. A significant increase in the expression of Rab8a along with Rab11 and H-$2K^b$-SIINFEKL was observed in young and Rab8a-OE DCs than those from aged mice following ovalbumin pulse. Rab11 is preferentially localized in recycling endosome, a compartment where class I MHC molecules are abundantly present (18). Colocalization of Rab8a with H-$2K^b$-SIINFEKL and Rab11 was significantly higher in BMDCs generated from young and Rab8a-OE aged cells than the aged BMDCs. Therefore, Rab8a reconstituted DCs of aged animals were enriched with endosomal recycling compartment (ERC) that can then promote efficient trafficking of class I MHC molecules to plasma membrane. Taken together, we conclude that after internalization of Ovalbumin protein, Rab8a modulated the expression of Rab11 and promoted the transport of peptide-MHCI complexes to the ERCs, eventually resulting in efficient antigen display on the surface of the DCs. A significant increase in the frequency of phalloidin^{+ve} cells in BMDCs generated from Rab8a-OE BM cells was indicative of a better cytoskeletal organization within the DCs, which could therefore restore sub-cellular trafficking. Our results also correlated with earlier reports where formation of cell protrusion and dorsal ruffle upon overexpression of Rab8a was observed (20). Therefore, our observation that Rab8a critically controls the functionality and differentiation of DCs and reconstitution of the same in DCs from aged individuals could, therefore, represent a viable option to reconstitute immune function and improve the existing strategies to provide aged individuals with long-term protection against viral infections.

References

1. Janeway Jr, Charles A., et al. "Principles of innate and adaptive immunity." Immunobiology: The Immune System in Health and Disease. 5th edition. Garland Science, 2001.
2. Bousso, P. and Robey, E., 2003. Dynamics of CD8+ T cell priming by dendritic cells in intact lymph nodes. Nature immunology, 4(6), pp.579-585.
3. Nikolich-Žugich, J., 2018. The twilight of immunity: emerging concepts in aging of the immune system. Nature immunology, 19(1), pp.10-19.
4. Ponnappan, S. and Ponnappan, U., 2011. Aging and immune function: molecular mechanisms to interventions.
5. Crooke, S.N., Ovsyannikova, I.G., Poland, G.A. and Kennedy, R.B., 2019. Immunosenescence and human vaccine immune responses. Immunity & ageing, 16, pp.1-16.
6. Pinti, M., Appay, V., Campisi, J., Frasca, D., Fülöp, T., Sauce, D., Larbi, A., Weinberger, B. and Cossarizza, A., 2016. Aging of the immune system: focus on inflammation and vaccination. European journal of immunology, 46(10), pp.2286-2301.
7. Long, E.O., Burshtyn, D.N., Clark, W.P., Peruzzi, M., Rajagopalan, S., Rojo, S., Wagtmann, N. and winter, C.C., 1997. Killer cell inhibitory receptors: diversity, specificity, and function. Immunological reviews, 155(1), pp.135-144.
8. Rodriguez-Barbosa, J.I., Schneider, P., Weigert, A., Lee, K.M., Kim, T.J., Perez-Simon, J.A. and Del Rio, M.L., 2019. HVEM, a co-signaling molecular switch, and its interactions with BTLA, CD160 and LIGHT. Cellular & molecular immunology, 16(7), pp.679-682.

9. Filén, S. and Lahesmaa, R., 2010. GIMAP proteins in T-lymphocytes. Journal of signal transduction, 2010.
10. Tolksdorf, F., Mikulec, J., Geers, B., Endig, J., Sprezyna, P., Heukamp, L.C., Knolle, P.A., Kolanus, W. and Diehl, L., 2018. The PDL1-inducible GTPase Arl4d controls T effector function by limiting IL-2 production. Scientific Reports, 8(1), pp.1-9.
11. Hong, W., Yang, B., He, Q., Wang, J. and Weng, Q., 2022. New insights of CCR7 signaling in dendritic cell migration and inflammatory diseases. Frontiers in Pharmacology, p.523.
12. Nan, Y., Wu, C. and Zhang, Y.J., 2017. Interplay between Janus kinase/signal transducer and activator of transcription signaling activated by type I interferons and viral antagonism. Frontiers in immunology, 8, p.1758.
13. Joffre, O.P., Segura, E., Savina, A. and Amigorena, S., 2012. Cross-presentation by dendritic cells. Nature Reviews Immunology, 12(8), pp.557-569.
14. Sehrawat, S., Koenig, P.A., Kirak, O., Schlieker, C., Fankhauser, M. and Ploegh, H.L., 2013. A catalytically inactive mutant of the deubiquitylase YOD-1 enhances antigen cross-presentation. Blood, The Journal of the American Society of Hematology, 121(7), pp.1145-1156.
15. Hickman, H.D., Reynoso, G.V., Ngudiankama, B.F., Cush, S.S., Gibbs, J., Bennink, J.R. and Yewdell, J.W., 2015. CXCR3 chemokine receptor enables local CD8+ T cell migration for the destruction of virus-infected cells. Immunity, 42(3), pp.524-537.
16. Luo, L., Wall, A.A., Yeo, J.C., Condon, N.D., Norwood, S.J., Schoenwaelder, S., Chen, K.W., Jackson, S., Jenkins, B.J., Hartland, E.L. and Schroder, K., 2014. Rab8a interacts directly with PI3Kγ to modulate TLR4-driven PI3K and mTOR signalling. Nature communications, 5(1), p.4407.

17. Nair-Gupta, P., Baccarini, A., Tung, N., Seyffer, F., Florey, O., Huang, Y., Banerjee, M., Overholtzer, M., Roche, P.A., Tampé, R. and Brown, B.D., 2014. TLR signals induce phagosomal MHC-I delivery from the endosomal recycling compartment to allow cross-presentation. Cell, 158(3), pp.506-521.
18. Pollard, T.D. and Cooper, J.A., 2009. Actin, a central player in cell shape and movement. Science, 326(5957), pp.1208-1212.
19. Peränen, J., Auvinen, P., Virta, H., Wepf, R. and Simons, K., 1996. Rab8 promotes polarized membrane transport through reorganization of actin and microtubules in fibroblasts. The Journal of cell biology, 135(1), pp.153-167.
20. Katze, M.G., He, Y. and Gale, M., 2002. Viruses and interferon: a fight for supremacy. Nature Reviews Immunology, 2(9), pp.675-687.
21. Marckmann, S., Wiesemann, E., Hilse, R., Trebst, C., Stangel, M. and Windhagen, A., 2004. Interferon-β up-regulates the expression of co-stimulatory molecules CD80, CD86 and CD40 on monocytes: significance for treatment of multiple sclerosis. Clinical & Experimental Immunology, 138(3), pp.499-506.
22. Parlato, S., Santini, S.M., Lapenta, C., Di Pucchio, T., Logozzi, M., Spada, M., Giammarioli, A.M., Malorni, W., Fais, S. and Belardelli, F., 2001. Expression of CCR-7, MIP-3β, and Th-1 chemokines in type I IFN-induced monocyte-derived dendritic cells: importance for the rapid acquisition of potent migratory and functional activities. Blood, The Journal of the American Society of Hematology, 98(10), pp.3022-3029.
23. Van de Laar, L., Coffer, P.J. and Woltman, A.M., 2012. Regulation of dendritic cell development by GM-CSF: molecular control and implications for immune homeostasis

and therapy. Blood, The Journal of the American Society of Hematology, 119(15), pp.3383-3393.

24. Sukhbaatar, N., Hengstschläger, M. and Weichhart, T., 2016. mTOR-mediated regulation of dendritic cell differentiation and function. Trends in immunology, 37(11), pp.778-789.
25. Linke, M., Fritsch, S.D., Sukhbaatar, N., Hengstschläger, M. and Weichhart, T., 2017. mTORC 1 and mTORC 2 as regulators of cell metabolism in immunity. FEBS letters, 591(19), pp.3089-3103.
26. Armstrong, J., Thompson, N., Squire, J.H., Smith, J., Hayes, B. and Solari, R., 1996. Identification of a novel member of the Rab8 family from the rat basophilic leukaemia cell line, RBL. 2H3. Journal of cell science, 109(6), pp.1265-1274.
27. Hattula, K., Furuhjelm, J., Tikkanen, J., Tanhuanpää, K., Laakkonen, P. and Peränen, J., 2006. Characterization of the Rab8-specific membrane traffic route linked to protrusion formation. Journal of cell science, 119(23), pp.4866-4877.
28. Rowe, R.K., Suszko, J.W. and Pekosz, A., 2008. Roles for the recycling endosome, Rab8, and Rab11 in hantavirus release from epithelial cells. Virology, 382(2), pp.239-249.
29. Grigoriev, I., Yu, K.L., Martinez-Sanchez, E., Serra-Marques, A., Smal, I., Meijering, E., Demmers, J., Peränen, J., Pasterkamp, R.J., van der Sluijs, P. and Hoogenraad, C.C., 2011. Rab6, Rab8, and MICAL3 cooperate in controlling docking and fusion of exocytotic carriers. Current Biology, 21(11), pp.967-974.
30. Peränen, J., 2011. Rab8 GTPase as a regulator of cell shape. Cytoskeleton, 68(10), pp.527-539.

31. Cebrian, I., Croce, C., Guerrero, N.A., Blanchard, N. and Mayorga, L.S., 2016. Rab22a controls MHC-I intracellular trafficking and antigen cross-presentation by dendritic cells. EMBO reports, 17(12), pp.1753-1765.

Table of Contents

Contents **Page No.**

Declaration……i

Acknowledgement…….……....iii

Abstract…….....vi

Synopsis…….....viii

List of figures…….xxvii

List of tables……xxix

Abbreviations……...xxx

Part I…….1

Background and overview……...1

Immunosenescence……..…….2

Microenvironment in the aging host……..4

Aging and primary lymphoid organs…….…….……....5

Homeostasis of HSCs in bone marrow of aging host …….....6

Aging and stromal compartment of bone marrow……...7

Aging and thymus…….....8

Aging and secondary lymphoid organs…….10

Age related defects in the immune cells ……11

Effects of aging on the cells of innate immune system……...11

Homeostasis of granulocytes in an aging host……...……12

Monocytes and macrophages in aging host……..……..13

Natural killer cell response pattern in aging host ……..……14

Aging and natural killer T (NKT) cells……..…15

Aging and dendritic cells……..……...16

Aging and adaptive immune system…….……...17

Aging and B lymphocytes……...…….17

T lymphocytes homeostasis with …….……18

Molecular understanding of cellular senescence……..…….20

Differentiation of BMDCs from precursor cells……...…….23

JAK/STAT mediated DCs differentiation…….……24

PI3K/PKB and DCs differentiation ……..……...25

MAPK pathway in DCs differentiation…….……...26

NF-κβ in the differentiation of DCs……...……...27

Age related impairment in the differentiation of BMDCs ……27

Conclusion…….....……..28

References ……..……...31

Part II……....67

Rab8a restores function in dendritic cells of an aging host……..67

Abstract……...69

Introduction……70

Materials and methods……73

Mice viruses and cells ……...73

Ethics statement for human study……...73

Antibody and other reagents……...73

Next generation sequencing and differential gene expression……74

Functional annotation and network analysis of differentially expressed genes in DCs of aged mice……...75

In-vitro BMDCs generation……..……75

Cloning of Rab8a-shRNA into pLKO.1GFP for knockdown and Rab8a into pLenti-GFP for overexpression and generation of lentiviruses and transduction of bone marrow cells……76

Staining of samples and flow cytometric analysis……77

qRT-PCR for measuring the mRNA level of different genes ……79

Antigen presentation assay……81

DCs immunization assay……82

Rab8a reconstitution in BM cells of aged mice and functional characterization of Rab8a-OE BMDCs…….…….82

Measuring the surface expression of H-2k^{b} bound to SIINFEKL on antigen pulsed BMDCS ……...……..84

In vitro immune synapse formation assay by flow cytometry……...84

Confocal microscopy…….85

Fluorescence microscopy……...86

Cell lysate preparation and western blotting …….....86

Plaque assay to measure the viral titer ……..**.....**87

Statistical analysis……...87

Results……....88

Transcriptome analysis of DCs reveals compromised function in aging host ……..88

DCs of an aging host are phenotypically and functionally impaired ……101

DCs immunization impaired cross-presentation by DCs of aged mice…….110

Rab8a dependent deficit in differentiation program and type I IFN response in DCs of an aging host ……..112

Restoring functional competence in aging DCs by Rab8a reconstitution ……123

Reconstitution of Rab8a in aging DCs enhances antigen cross-presentation and facilitates their homing to secondary lymphoid organs (SLO)……125

Rab8a reconstituted DCs generate effective antigen-specific memory $CD8^+$ T cell response……...141

Rab8a reconstitution in bone marrow cells promoted signalling via mTOR pathway for enhancing survival …….151

Rab8a controls the turnover of class I MHC molecules to enhance antigen presentation ……155

Discussion…… 165

References…….169

Appendix……176

List of Figures

Figures **Pages No.**

Part II

FIGURE 2.1. DCs of aging host mount an inhibited type I IFN response……91

FIGURE 2.2. Transcriptome profiling of dendritic cells of young and aged mice reveals the downregulation of antiviral genes ……..…….93

Figure 2.3 Reconstitution of Rab8a in bone marrow cells of aged animals restored the TLR related function…….96

FIGURE 2.4. Functional annotation and network analysis of SDE genes expressed in dendritic cells of aged animals reveals down regulation of antiviral pathways ……..99

FIGURE 2.5. DCs of an aging host exhibits phenotypic and functional impairment. ……..103

FIGURE 2.6. Phenotypic profiling of splenic DCs and BMDCs reveals downregulation of key molecules required for CD8+ T cells priming ……106

FIGURE 2.7. Sorting strategy for BMDCs and OT1 transfer status for in-vivo DCs immunization experiments ……..108

FIGURE 2.8. Rab8a critically influences the differentiation and functionality of DCs ……..114

FIGURE 2.9. Knocking down of Rab8a in bone marrow cells of young mice compromised the differentiation and functionality of BMDCs ……..117

FIGURE 2.10. BMDCs of aged mice reconstituted of Rab8a regain functionality……..120

FIGURE 2.11. Restoration of Rab8a in bone marrow cells of aged mice enhances the antigen presentation ability of aged BMDCs ……129

Figure 2.12. Reconstitution of Rab8a in aged BMDCs promotes antigen cross presentation…...131

FIGURE 2.13. Phenotypic profiling of splenic DCs and BMDCs generated using GMCSF/IL4…….133

FIGURE 2.14. Gating strategy and depletion of key molecules (Ly6G/Ly6C/F4/80/NK1.1) expressing cDC2s in order to reveals its role in antigen presentation ……....135

FIGURE 2.15. A comparative analysis of GM-CSF/IL-4 and Flt-3l induced BMDCs reconstituted of Rab8a in enhancing in-vitro antigen presentation.…… ……...137

FIGURE 2.16. Reconstitution of Rab8a in bone marrow cells of aged animals restored the functionality of Flt3l derived cDC2s *in-vivo.* ……..143

FIGURE 2.17. Reconstitution of Rab8a in the bone marrow of aged animals led to the restoration of the priming and presentation abilities to T cells in the BMDCs recipient animals……....144

FIGURE 2.18. OT1 transfer status for in-vivo DCs immunization experiment and in-vitro antigen presentation ability of DCs generated from Rab8a overexpressing BM cells of aged mice 146

FIGURE 2.19. Rab8a overexpressing DCs of aged animals expand antigen-specific $CD8^+$ T cells in vivo.....148

FIGURE 2.19. Rab8a is critically required for functional differentiation of BMDCs ……152

FIGURE 2.20. Rab8a is critical for the formation of immunological synapse using DCs and $CD8^+$ T cells…..……158

FIGURE 2.21. Reconstitution of Rab8a in BM cells of aged mice restore the antigen display on BMDCs.…….....161

FIGURE 2.23. Overexpression of Rab8a in BM cells of aged mice modulates the expression of Rab11 and H-2Kb-SIINFEKL upon pulsing with ovalbumin. ……...163

List of Tables

TABLE 2.1. List of qpcr primers (5'-3') used for measuring the expression of respective genes in mouse cDNA……177

TABLE 2.2. List of qPCR primers (5'-3') used for assessing the expression of respective genes in human PBMCs…….178

TABLE 2.2. List of qPCR primers (5'-3') used for measuring the expression of genes of mTOR pathway ……..…….179

TABLE 2.4. List of PCR primers (5'-3') used for the cloning of Rab8a shRNA into pLKO.1-GFP and cDNA sequences into pLenti-GFP vector. ……....180

Abbreviations

APCs	Antigen presenting cells
DCs	Dendritic cells
SPDCs	Splenic dendritic cells
BMDCs	Bone marrow derived dendritic cells
FPKM	Fragments per kilobase per million mapped fragments
SDE	Significantly differentially expressed gene
Klr	Killer cell lectin like receptor
GIMAP	GTPase of immunity associated protein
Arl4d	ADP-ribosylation factor 4d
Hic1	Hypermethylated in cancer 1
TLR	Toll like receptor
OAS	2’-5’-oligoadenylate synthetase 1
IFITM1	Interferon induced transmembrane protein 1
IFIT1	Interferon induced protein with tetratricopeptide repeat1
PLSCR1	Phospholipid scramblase 1
Rab8a	Ras related protein Rab8a
Akt	Akt serine/threonine kinase1 (Protein kinase B)

S6K	Ribosomal protein S6 kinase
Nr1h3	Nuclear receptor subfamily 1 group H member 3
CCR5	Chemokine (C-C motif) receptor 5
CCR7	Chemokine (C-C motif) receptor 5
CXCR3	Chemokine (C-X-C motif) receptor 3
CD	Cluster of differentiation
CMP	Common myeloid progenitor
CLP	Common lymphoid progenitor
CTL	Cytotoxic T lymphocyte
GM-CSF	Granulocyte-macrophage colony stimulating factor
GTP	Guanosine triphosphate
HSC	Hematopoietic stem cell
HIV	Human immunodeficiency virus
IAV	Influenza A virus
γ-MHV-68	γ-murine herpes virus
IFNRKO	Interferon receptor knockout
IFN-α	Interferon α
IFN-β	Interferon β

IFN-γ	Interferon γ
IL	Interleukin
MHC	Major histocompatibility complex
ERC	Endosomal recycling complex
MLN	Mediastinal lymph node
NF-kB	Nuclear factor kappa B
NK cell	Natural killer cell
PBMCs	Peripheral blood mononuclear cells
PFU	Plaque forming unit
CSF2Rα	Colony stimulating factor 2 receptor α
IGF1R	Insulin like growth factor 1 receptor
mTOR	Mammalian target of rapamycin
TSC	Tuberous sclerosis
PRAS40	Proline-rich AKT substrate, 40kDa
mTORC1	Mammalian target of rapamycin complex 1
PI3K	Phosphoinositide 3-kinase
Bcl2	B-cell lymphoma 2
ROS	Reactive oxygen species

JAK	Janus kinase
STAT	Signal transducer and activator of transcription factor
IRF9	Interferon regulatory factor 9
TCR	T cell receptor
TLR	Toll-like receptor
TNF-α	Tumor necrosis factor α
Rab8a-OE	Rab8a overexpressing
Rab8aKD	Rab8a knockdown
BM	Bone marrow
CFSE	Carboxyfluorescein succinimidyl ester
PI	Propidium Iodide
Dpt	Day post transfer
MDCK	Madin-Darby Canine Kidney Epithelial Cells
HEK293T	Human embryonic kidney cells

PART I

Background and overview

Immunosenescence

The complex structure of multicellular organisms originates from the cellular organization into tissues, organs, and organ systems. Cells are held together by various types of junctions, such as tight junctions, adherens junctions, and gap junctions. Cell to cell communication leads to the activation of various signaling pathways. The associated function and architecture of tissues and organs can decline with age, and this can lead to reduced response to various stimuli. Various factors can contribute to such effects which include changes in the gene expression, DNA damage, changes in cellular metabolism and altered composition of extracellular matrix. Age-related alterations can adversely affect all tissues and organ systems leading to deterioration of health, increased risk of acquiring infection, inefficient resolution of diseases and enhanced susceptibility to developing chronic diseases such as cancer and vasculopathies. Deteriorating functionality of immune system in the aging population is also known as immunosenescence (1).

Age associated attrition of immune functions can lead to an increased susceptibility to various infections, decreased efficacy of vaccines, and a higher risk of developing certain diseases (2, 3,4). Several changes occur in the immune system during immunosenescence which include diminished function of immune cells, such as T cells (5, 6) and B cells (7, 8) Thymus, a primary lymphoid organ, which is responsible for the maturation of T cells, also shrinks and becomes less efficient in cellular output as the host ages (9). The ability of the host to mount a robust and coordinated immune response becomes impaired, making it more challenging to effectively control infections. The production of antibodies by B cells is inhibited and with this the control of microbes in extracellular spaces or at the portal of entry is rendered inefficient. Immunosenescence can also lead to chronic low-grade inflammation, known as inflammaging. This persistent inflammation can lead to age-related diseases such as cardiovascular diseases, cancers, and neurodegenerative

disorders (10). These changes in the immune system are influenced not only by a variety of physiological and environmental factors as well as the genetics of host (11).

The adaptive immune system consists of a diverse repertoire of T and B cells, which differentiate into effectors and memory cells following a well-orchestrated transcriptionally controlled program triggered following antigen-stimulation. While naïve lymphocytes provide the host the ability to mount specific immune response to antigens during initial encounter, memory lymphocytes can rapidly respond to the previously encountered antigens. The number of naïve lymphocytes gradually declines with aging but the abundance of memory lymphocytes with known as well as unknown antigen specificities (virtual memory) expands. Such a response pattern could compromise the efficacy of immune reactions against newly acquired infections. Furthermore, because of the intrinsically impaired functionality of the existing immune memory, such cells may not provide efficient protection during reinfection with certain agents. Lymphopoiesis is reduced post puberty and a further expansion of repertoire becomes limited. While the specificities of adaptive immune cells remain largely unchanged but the accumulating cues in lymphoid organs tend to readjust and fine tune the response pattern of existing cells to confer to the host some level of protection against the encountered pathogen. This is established for the responsiveness of helper T cells but not well understood for CTLs. Plasticity of Th cells could contribute to such effects. However, in the later phase of aging, a progressive decline in immune function and enhanced susceptibility to infection induces high morbidity and mortality of the infected aged individuals. Such largely irreversible alterations in the aging host also impair vaccine induced protection and fail to adequately control carcinogenesis. One of the most prominent features of immunosenescence is the reduction in the output of naïve T lymphocytes due to thymic atrophy (12). The repertoire of B cells generated in bone marrow is also reduced (12, 13). The analysis of

TCR Vβ chain usage in human peripheral T cells showed a reduction in the diversity of T cell clones. Goronzy and Weyand, 2005 have demonstrated a significant decrease in the repertoire of T cells from 10^8 in younger to 10^6 in the elderly (14). Both intrinsic and extrinsic factors could contribute to the age-related decline in the generation of naïve immune cells. Genetic alterations in the immune cells or cellular damage constitute some of the cell-intrinsic factors while the altered composition of growth factors or hormones including the microenvironment, anatomical disruption in the lymphoid and non-lymphoid organs serve as extrinsic factors. These factors could also control the homeostatic turnover of naïve lymphocytes (15).

Microenvironment in the aging host

Microenvironment prevailing in both lymphoid and non-lymphoid organs constitutes one of the critical factors in immune cell homeostasis. Primary lymphoid organs, such as the bone marrow and thymus, play a crucial role in the production and maturation of immune cells. The bone marrow is the site of hematopoiesis after birth in most vertebrates where the immune cells of different types and lineages are generated. B cells, one of the critical arms of adaptive immune system, develop and mature in bone marrow before populating secondary lymphoid organs. Thymus, located in the thoracic cavity, is primarily responsible for the maturation and development of T cells and these cells are key players in cell-mediated immunity. Secondary lymphoid organs, such as the spleen and lymph nodes present throughout the body constitute drainage system for the extracellular spaces. Secondary lymphoid organs provide necessary microenvironment for facilitating cellular interaction and activating immune cells. Lymph nodes are small, bean-shaped structures that filter and trap antigens (foreign substances) present in the extracellular spaces in addition to housing immune cells that traverse through circulatory system. Spleen, located in the upper left abdomen, filters blood, and helps remove old or damaged red blood cells and participates in immune

responses. Structural integrity of both primary and secondary lymphoid organs is crucial for a healthy host as well as for the induction of an effective immune response. Disrupted architecture of these organs can have a significant impact on the quality and magnitudes of immune responses leading to inefficient control of infections and increased susceptibility of the host to other immune disorders.

Aging and primary lymphoid organs

Bone marrow and thymus are the sites for maturation of B and T cells, respectively. Aging reduces the number and functionality of hematopoietic stem cells (HSCs), resulting in the decreased production of common lymphoid progenitors (CLPs) and B as well as T cells. Furthermore, the microenvironment within bone marrow of an aging host becomes less supportive of B cell development, resulting in the compromised antibody response to infections. Similarly, thymic atrophy reduces the output of T cells, and consequently the composition of T cell subpopulations is also changed. This leads to the impaired immune surveillance and enhances susceptibility of the host to develop severe reactions following infection (11). The bone marrow microenvironment, or hematopoietic niche, plays a crucial role in supporting the development and maintenance of HSCs and the generation of various immune cells. Aging can significantly affect the architecture and function of the hematopoietic niche and in so doing impacts immune cell differentiation. The stromal compartment within the bone marrow microenvironment consists of different types of cells, including mesenchymal stem cells (MSCs), osteoblasts, adipocytes, and endothelial cells. These stromal cells provide physical and regulatory support to the HSCs. With aging, there is a decline in the number and function of HSCs, which are responsible for generating different cell types, including immune cells. The composition and functionality of the stromal compartment within the hematopoietic niche is altered with aging. For example, the altered composition of

MSCs, adipocytes, and osteoblasts can affect the regulatory signals and adversely affect the differentiation of HSCs. Additionally, the regenerative capacity of the niche is reduced. This results in compromised humoral and cell mediated immunity.

Homeostasis of HSCs in bone marrow of aging host

The aging host exhibits dysregulated hematopoiesis but underlying mechanisms are not well understood. Strain and species of animals used in different studies might introduce variations in the composition of HSCs. Therefore analyzing different strains during the aging process might present discordant results (19, 20). For example, aged DBA/2 strain of mouse possess a higher frequency of HSCs in the bone marrow as compared to CBA/J, BALB/c, or C57BL/6 mice (16). Differential representation of HSCs is also evident in the aged mouse and paradoxically some strains of mice show more pronounced HSCs response as compared to their younger counterparts (16-18). Frequencies of HSCs in bone marrow of aged humans could decrease (21), increase (22), or remain unchanged (23) depending on the genetic variations or the underlying conditions. It is known that DBA/2 genotype of mouse have competitive advantage over C57BL/6 strain of mouse in terms of higher rates of cellular division which could be due to intrinsic differences in the proliferation of stem cells (24, 25). However, this advantage wanes as the C57BL/6 animals age and eventually this strain shows elevated frequencies of HSCs due to their increased proliferation rates. It was shown that approximately 12.5% of HSCs were in S/G2/M phases of their cell cycle in 23-month-old mice, while such cells were 2.6 – 3.9% in younger mice (26). HSCs were more frequent in the aged mice but when adoptively transferred in the irradiated recipients such cells were compromised in self-renewal and lymphopoiesis (18, 26, and 27). The reasons for such a discrepancy are not clear but could relate to the differences in niche in the two conditions. Additionally increased frequency of HSCs could skew the generation of myeloid cells as compared

to the lymphoid cells as was evident by transcriptional profiling of such cells from different age groups. More of the myeloid lineage genes were found upregulated than those involved in the differentiation of lymphoid cells which could suggest for specific reduction in the cells of lymphoid cells in the aged mice (17). The skewing of HSCs differentiating towards myeloid lineage in the aged mice was accompanied by decreased production of CLPs, pre-pro-B cells, pro-B cells, pre-B cells, and total B cells (17, 28, and 29). The reduction in the proliferation of CLPs and inefficient expression of recombination activating gene 2 (RAG2) as well as V(D)J recombinase activity could account for decreased output of pro-B cells and pre-B cells in bone marrow, respectively (30, 31).

Elevated oxidative stress induced higher production of reactive oxygen species (ROS) by bone marrow HSCs in the aging host diminishes their function. ROS mediated DNA damage in HSCs and their reduced expression levels of genes required for repairing DNA damage in the aged individuals could results in dysfunctional HSCs (27, 32, and 33). Accordingly, age related alterations could reduce the frequency of HSCs by ~25% and the persisting cells show lower threshold of ROS mediated impaired functions (32). Partial restoration of HSCs functions by treatment with antioxidants such as N-acetyl-cysteine or catalase was also reported (34, 35). That stromal cells in the bone marrow of aged host are limited in the production of antioxidants such as glutathione (36) and peroxiredoxin-2 (36, 37) was also reported. Therefore, the generated ROS are majorly responsible for the reduced homeostasis of HSCs in the aging host.

Aging and stromal compartment of bone marrow

Not only the progenitor cells but also the niche contributing cells crucially control hematopoiesis in the aging host. Accumulation of senescent stromal cells including mesenchymal stem cells (MSCs), that give rise to osteoblasts and adipocytes, could affect hematopoiesis and lymphopoiesis

(39). A conditional depletion of osteoblasts in mouse resulted in increased myelopoiesis and decreased lymphopoiesis leading to ~30% reduction in the numbers of B cells and HSCs in bone marrow (40). Adipocytes antagonize HSCs response and within adipocyte rich region of bone marrow there is upto a 3-fold reduction in the population of HSCs (41). Senescent cells exhibit a state of irreversible cell cycle arrest and are compromised in the secretion of pro-inflammatory cytokines, chemokines, and growth factors, collectively known as the senescence-associated secretory phenotype (SASP). The SASP can disrupt the microenvironment and impair the function of HSCs, leading to the decreased production of immune cells (38). Age related changes in the stromal compartment impair the function of HSCs and promote stromal growth (42). Furthermore, aging can also alter the differentiation pattern of MSCs, leading to a skewed adipogenic cell differentiation while reducing their osteogenic differentiation (43, 21). Not only the frequencies but also the number as well as functionality of osteoblasts is increased in the aging population (44, 45). This eventually leads to removal of HSCs from osteoblastic niches which could be facilitated by the loss of adhesion to stroma (46). Skewing of MSCs towards adipogenic response in aged individuals is regulated by peroxisome proliferator-activated receptor gamma 2 (PPARγ2) which is master regulator of osteoblast/adipocyte balance (47). Upto a 10-fold increase in the expression of *PPARγ2* mRNA was shown in the bone marrow stroma of elderly as compared to the young animals (48).

Aging and thymus

Thymus is one of the primary lymphoid organs where T cells develop. It undergoes age-related changes by a process known as thymic involution. Thymus is at its maximum size and remains most active during childhood and adolescence, and thereafter it gradually decreases in size and exhibits impaired functionality as the host ages. By middle age, the thymus is only a fraction of its

original size, and the output of naive T cells is greatly reduced. The thymic stroma, consisting mainly of thymic epithelial cells (TECs), plays a crucial role in the maturation and selection of T cells. TECs not only provide crucial signals to the developing T cells to guide them through various differentiation and selection processes but also help create the unique microenvironment in the thymus, which is essential for developing the functional T cell repertoire (11). During thymic involution, the number and function of TECs decline, which can contribute to the reduced output of naïve T cells and a decline in immune function. As a result, the host becomes more susceptible to contract infections, develop cancer and other age-related diseases.

TECs originate from the endodermal cells during mid-gestation period (49). Post-natal thymus serves as the site for the development and education of T cells. Non-lymphoid tissue aggregates composed of stromal cells as well as TECs, the surrounding mesenchyme along with the complex set of cellular interactions with the immigrating lymphoid and endothelial progenitors constitute the complex cellular environment within thymus (50). The compartmentalization of thymus continues after birth where hematopoietic progenitors of T cells are periodically seeded by bone marrow leading to its increased size (51). The increased thymic size is also accompanied by more of fully mature T cells of appropriate specificity making it to periphery (52, 53). The compartmentalized postnatal thymus is divided into different compartments; the outer cortex, inner medulla and cortico-medullary junction (CMJ). These different thymic compartments serve distinct functions during the maturation and selection of T cells. Cortical TECs (cTECs) play a crucial role in positive selection, maintaining T cell lineage commitment, and supporting early thymocyte proliferation and differentiation. Medullary TECs (mTECs) are specialized in inducing central tolerance and facilitating the maturation of thymocytes prior to their exit from the thymus.

As the thymus undergoes age-related changes, compartmentalization can become disorganized, and the ratios of the subsets of TEC can shift, leading to a reduction in the output of naïve T cells.

Aging and secondary lymphoid organs

Age-related changes in the architecture of secondary lymphoid organs, such as lymph nodes and spleen, can alter the microenvironment required for immune cell interactions and the generation of adaptive immune responses to infections as well as vaccines. Consequently, aging population exhibits an increased susceptibility to infections and tumors (54). Lymph nodes (LNs) are critical for the activation and proliferation of antigen-specific T and B cells. LNs serve as the drainage sites for lymph transported via lymphatics from various tissues and therefore any antigenic organic material contained can traverse through these organs. Antigen carrying antigen presenting cells (APCs) traverse through LNs interact with the T cells of appropriate specificity at specialized sites to activate the latter. Once expanded the effector T or B cells via direct activity or through their products help neutralize the infectious agent (55). Passage of blood into LNs is governed by arterioles of hilum. Inside the LNs, blood enters the parenchyma through post-capillary venules (PCVs), also known as high endothelial venules (HEVs) which are lined by tall, cuboidal endothelial cells, and it exits via venules of the hilum (55). Migration of antigen experienced immune cells to the LNs is also governed by the expression of surface adhesion molecules and their interacting molecules expressed by the endothelial venules. Migration of immune cells also helps in wound healing, angiogenesis, and inflammation as well as tumor control (56). It has been shown that the total numbers of LNs in the human body which ranges from 300 to 500, and their total weight (~100 grams) decreases with age. Age associated deterioration in the LNs involves fibrosis, vitrification, reduction in the number of PCVs, and changes in the morphology and function of the specialized endothelial cells also known as venous capillaries (57). Aging related

impairment also includes reduction in the amount of cortical and medullary zones of lymphoid tissues and reduction in the number and size of germinal centers in lymphoid follicles leading to compromised immunological response against infections. Furthermore, aging related impairment of LNs not only reduces the number of follicular dendritic cells (FDCs) but also their antigen uptake ability which adversely affects humoral immunity in the older individuals (58). Enhanced susceptibility of aged population to infections is evident in people over 65 years of age (59-62). Spleen, a reservoir of immune cells serves as a primary site for the initiation of adaptive immune responses against blood-borne pathogens. Age-related changes in the splenic architecture can lead to reduced number and function of immune cells. Overall, the age-related changes in the architecture of secondary lymphoid organs can have a significant impact on immune function and increased risk of acquiring infections and developing other age-related diseases.

Age related defects in the immune cells

Both innate and adaptive arms of the immune system are compromised in aged individuals and consequently, the frequency and severity of infection, immune surveillance against developing malignancies, and response against vaccinations are compromised in older individuals (63-65). The ability of T cells to discriminate self from non-self-antigens can also be impaired, leading to an increased risk of developing autoimmune diseases.

Effects of aging on the cells of innate immune system

Age-related defects in the innate immune system includes decreased production of cytokines and chemokines. This can result in a diminished recruitment of immune cells to sites of infection. A decline in the production of antimicrobial peptides is also evident in aged individuals. This can lead to an increased susceptibility to bacterial infections (68). Epithelial barriers of different organs

such as skin, lung, and gastrointestinal tract also increase as we age (69-71). How aging impacts the functioning of innate immune cells is debatable with some reporting no change, and others showing a significant decline in functionality in aged individuals (72-75). Some of the proinflammatory cytokines such as interleukin IL-6, IL-1β, tumor necrosis factor (TNFα), and TGFβ which mediate chronic inflammation are preferentially induced in aging individuals causing a process commonly known as inflammaging (76-79). Age associated discrepancy in the innate immune system has also been studied in murine models which show a slower recovery, prolonged morbidity, and persisted viremia following influenza A virus (IAV) infection in aged C57BL/6 mice and these results were attributed to the delayed recruitment of granulocytes and DCs as well as the prolonged persistence of macrophages in the infected lungs (67). It was also noted that aging also results in diminished protective pro-inflammatory response (IL-12 and MCP1) and a delayed peak of IL-6 in the lungs tissues of aged mice but the levels of TNF-α and IL-1α were significantly increased (66).

Homeostasis of granulocytes in an aging host

Age associated impairment in the functionality of granulocytes can lead to a delayed response against different microbial infections. This impairment can manifest in several ways including a reduced production of reactive oxygen and nitrogen species (ROS and RNS) which help in direct killing of invading microbes. Granulocytes also produce a wide range of degradative enzymes and antimicrobial peptides (AMPs) that can help clear infections and such products may be less efficiently produced in older individuals. Neutrophils or polymorphonuclear cells (PMNs) being the most abundant and short-lived leukocytes with an average span of ~8-12 hours in the blood. Neutrophils are the first immune cells which migrate at the sites of infection and try to clear the pathogen by ingesting them through phagocytosis or by releasing microbicidal granules. After

phagocytosis, neutrophils produce a wide range of toxic products such as nitric oxide, super oxide, oxy halides, and hydrogen peroxide to cytolyze the ingested microbes. Rather than to their reduced frequencies, the compromised functionality of PMNs in the aging host is largely attributed to diminished chemotaxis and phagocytosis as well as reduced production of superoxide in response to the ligation of innate immune receptors such as toll like receptors (TLRs) or formyl peptide receptor 1 (FMLP) or by the opsonized microbial products in aged individuals (80-83). Even though most of the studies suggest a compromised production of ROS by PMNs in aging host but their spontaneity in production was increased (84). A delayed and overall reduction in the production of ROS was observed by some investigators (85). It is also noticed that neutrophils of elderly are less responsive to GM-CSF and can more frequently undergo apoptosis at the infected tissues leading to an inefficient control of infection and a persisting inflammation (86, 87, and 83). Studies involving murine models have shown that there is a sharp decrease in the number of neutrophils recruited to site of infection which can be attributed to their altered genesis in bone marrow (86, 71). Other types of granulocytes such as eosinophils, basophils and mast cells which provide defense against parasites and airway inflammation can be adversely affected by aging. Aging associated decline in the functionality of eosinophils is largely attributed to their enhanced degranulation in the aged asthmatic people (89).

Monocytes and macrophages in aging host

Monocytes which transform into macrophages with specialized functions are abundantly present in connective tissue, sub-mucosal layer of the gastro-intestinal tract, lung, liver, spleen, bone, brain, and skin. Submucosal tissues entrapped macrophages tend to preferentially lose functionality in aging host. It is also reported that the surface expression of class II MHC molecules on macrophages is reduced with aging both in mice and humans (90, 91). Another study

corroborated such observations by showing that macrophages from aged mice showed 50% lesser upregulation of class II MHC molecule as compared to those from younger animals following stimulation with IFNγ and this led to compromised antigen presentation (90). A decline in the phagocytic activity of macrophages from the aged host was also reported and this likely caused reduced production of super-oxide anions (94). Super oxides are involved in the respiratory burst of macrophages and are critically involved for bactericidal effects (92, 93). Such macrophages also produced lower levels of chemokines, such as macrophage inflammatory protein (MIP)-1β, MIP-1α, Eotaxin, and MIP-2 (95). Monocytes collected from the peripheral blood of aged humans showed a decline in the surface expression of pattern recognition receptors (PRR) such as TLR1, 2, and 4 to varying levels (96). Consequently, such cells produced lower levels of TNFα, and IL-6 post TLR1/2 ligation but their production of pro-inflammatory cytokines at basal levels was elevated (97). Factors such as the microenvironment, shortening of telomeres and presence of higher levels of pro-inflammatory cytokine especially IL-6 in the circulation of aged individuals could explain the skewed differentiation of macrophages into M1 than M2 types (73). Aging related impairment has also been shown in LPS activated splenic macrophages by microarray-based analysis (98). Cells from aged mice were reduced in the expression of genes involved in TLR-signaling and NF-κβ pathway but that of a negative regulator, IL-1 receptor-associated kinase-3 (IRAK3), was exclusively upregulated in those from young mice. This effect could be attributed to the high levels of intracellular ROS in the cells of aged mice.

Natural killer cell response pattern in aging host

NK cells provide anti-viral and anti-tumor defense in addition to performing immune surveillance. NK cells are heterogeneous population of lymphoid origin and differ in their proliferative potential which correlates with their surface expression of CD56. $CD56^{high}$ cells are less abundant (10%) as

compared to the $CD56^{low}$ cells (90%) in the peripheral blood of humans (74). $CD56^{low}$ NK cells are highly cytotoxic, less proliferative and produce fewer cytokines but $CD56^{high}$ NK cells are highly proliferative and produce a wide range of cytokines such as IFNγ, TNF-β and IL-10, and chemokines, such as RANTES and MIP-1α, but their cytotoxicity is limited. With aging there is a preferential accumulation of $CD56^{low}$ NK cells in the humans (97). It has also been shown by various studies involving humans that the circulating NK cells were increased with age but their net influence on cytolytic activity against tumorigenesis is not appreciably enhanced (100, 101). Therefore, relative abundance of $CD56^{low}$ NK cells is considered as a compensatory mechanism to account for the reduced activity and proportion of different subsets (102). It is also noticed that NK cells in the aging host were defective in cytotoxicity and lymphokine-activated killer (LAK) cell activity. These defects are due to their compromised inositol phosphate metabolism, a signaling pathway involved in cellular functions. The impairment in inositol phosphate metabolism may affect the signaling pathways and intracellular processes necessary for efficient cytotoxicity and LAK cell activity of NK cells. Inositol phosphates are important second messengers involved in cell signaling, and disruptions in their metabolism can have downstream effects on various cellular functions (103). The spontaneous cytotoxic activity of NK cells which occurs independently of antibody response is specifically reduced with aging. Therefore, immune surveillance by KN cells is compromised and the aged population also tends to develop cancers.

Aging and natural killer T (NKT) cells

Age-associated changes in the immune system also involve alterations in the population of natural killer T (NKT) cells. NKT cells are a unique subset of T cells that express an invariant T cell receptor (TCR) and are restricted by the CD1d molecule. They can respond rapidly to certain antigens, such as α-Galactosyl Ceramide (106). NKT cells are reduced in numbers in aged mice as

well as humans. While the mechanisms underlying such a reduction are not fully understood, factors such as thymic involution, altered T cell development and changes in the microenvironment could contribute. Accumulation of memory-like NKT cells at the expense of naïve NKT cells is also evident. Aging can also impact the functionality of NKT cells by compromising the NKT cell activation and impaired cytokine production in response to antigenic stimulation. Moreover, there is a shift in the cytokine production pattern of NKT cells from a type I to type II response and the latter is primarily involved in antibody production and eliciting allergic responses. This skewing of the cytokine profile may have implications for elevated immune-regulatory response in older individuals (107). NKT cells play important roles in bridging innate and adaptive immunity, regulating inflammation, and maintaining immune balance. Therefore, age-related alterations in NKT cells may contribute to immune dysregulation, increased susceptibility to infections, and impaired immune surveillance against cancers.

Aging and dendritic cells

Dendritic cells (DCs) serve as the sentinel cells because of their unique anatomical localization, morphology, and ability to traverse to secondary lymphoid organs. These cells phagocytose antigen, process them and eventually present antigenic peptides to T cells. Immature DCs home to tissues, take up antigens by phagocytosis or macropinocytosis and subsequently get activated to home to the draining LNs. Number and functionality of various subsets of DCs such as myeloid DC (mDC) and plasmacytoid DC (pDC), and their relative abundance at different sites could vary as the host ages. However, the tissue specific DCs such as Langerhans cells present in the skin, are consistently reduced in aged population (108). Aging also impacts the cytokine production, some cytokines such as IFNα and IL-12 are produced less abundantly while others such as IL-6 and TNFα are produced more abundantly following stimulation with various infections, agonists such

as LPS and ssRNA (109, 110). Age associated defects also include the impaired macropinocytosis, phagocytosis, migration of DCs and reduced signaling events such as decreased phosphorylation due to deficiency of PI3K as the latter is required for phosphorylation of serine/threonine-protein-kinase/PKB (AKT) in DCs (111).

Aging and adaptive immune system

Defects arising in the cells of adaptive immune system have been more commonly studied as compared to those in the other arm of immunity in the aging population. These could originate from the reduced repertoire of antigen-specific cells, impaired activation of antigen-specific T cells because of the mis-directed interaction between DCs and T cells which impacts production of cytokines and other signaling molecules. These changes can affect the ability of the immune system to clear infections. The altered cytokine production can also affect the balance between Th1 and Th2 responses and inadequate control of microbial infections (112).

Aging and B lymphocytes

A diminished response of B lymphocytes is observed in aged individuals which can be attributed to reduced production of B lymphocytes from bone marrow. Precursor of B lymphocytes are pro-B cells which differentiate into pre-B cells which after immunoglobulin gene rearrangement are converted to become B cells and after passing through a selection process migrate to periphery. A decline in the B lymphocytes results in compromised antibody response as is observed in aging population of both humans and mice (113- 116). These defects are largely governed by intrinsic defects of B cells as serum immunoglobulin levels remain unchanged in both aged mice and humans. However, the affinities of antibodies are often lower (117). The diminished antibody affinity response can occur due to reduced somatic hyper-mutation because of the inefficiency of

germinal center reaction (GCR) and isotype switching (118). A transcription factor E47 which is responsible for class switching in B cells is reduced in the expression in aging individuals (119). As alluded to earlier, the decline in the frequency of precursors B cells results in limited naïve B cells output. This can eventually lead to the preferential accumulation of antigen-experienced memory B cells and blunt overall repertoire (120). Antigen experienced B cells with limited specificities are maintained by homeostatic proliferation mechanisms. The memory B cells are less prone to undergo apoptosis and persist in the system for long-term survival at the expense of naïve cells (121, 122). Studies involving murine models have shown a reduction in the expression of genes responsible for the lineage commitment and differentiation of B (123, 124). Additionally, significant alterations in the downstream signaling events following antigen recognition by B cells are more commonly evident in aged people (125, 126).

T lymphocytes homeostasis with aging

T cells are a critical component of the adaptive immune system and act as center regulator of defense against various pathogens by producing effectors molecules that endow them with the ability to kill infected cells. Altered composition of T cell pool and their compromised functionality are common features of immunosenescence. It is shown that aging induced effects on thymic activity and the output of naïve T cells could be partially reversed by systemic administration of cytokines and hormones or by bone marrow transplantation (127, 128). A study showed that thymic ablation resulted in premature aging of naïve T cells. Aging associated changes also include the attrition of TCR diversity and consequently oligoclonal expansion of T cells is evident (129, 130). It was also observed that aging skews TCR repertoire and KIR (Killer inhibitory receptor) are more frequently expressed by T cells (131, 132). KIRs are usually expressed by NK cells but the consequences of their expression by T cells are not known.

Additionally, it is also known that the thymic involution leads to reduced frequencies of naïve T cells in the periphery which is compensated by increased number of effector and memory T cells (133). Antigen independent proliferation of T cells is also observed in aged individuals which could help explain their comparable numbers in the aged and young individuals (134). Age associated downregulation of surface CD28 by $CD8^+$ T cells was observed in the older people which could suggest for their functional incompetence (134). Naïve $CD4^+$ T cells of aged mice showed a relative increase in the lifespan but such cells were functionally deficient (135). The accumulated memory $CD8^+$ T cell population ($CD8^+CD28^-$) had shortened telomeres and a major fraction was reactive to cytomegalovirus. Microarray analysis of T cells obtained from young and aged donors, showed a differential transcriptome in $CD8^+CD28^-$ T cells and $CD8^+CD28^+$ T cells. A hierarchical clustering of T cells subsets could be derived from their expression profile. On one extreme of the spectrum were the antigen unexperienced $CD8^+$ T cells from young individuals with a phenotype of $CD8^+CD28^+$ while the antigen-experienced $CD8^+CD28^-$ T cells from young and the older people constituted the other end of spectrum. $CD8^+CD28^+$ T cells obtained from the elderly representing an intermediate population (136). A significant increase in the number of effectors and memory T cells in the aged individuals is accompanied with a concomitant decline in the response against new antigens and consequently poor response to vaccination is noticed (137-139). The milieu conducive for the differentiation of Th2 over Th1 cells exists in aged host (104, 105, 140-142). Comparative analysis of the response of regulatory T cells in aged and young host has provided inconsistent results (143, 144). Numbers of $CD4^+CD25^+$ or $CD4^+Foxp3^+$ were comparable in young and aged individuals but such cells from the aged individuals efficiently inhibited the production of IL-10 in when added to the co-culture of effector $CD4^+$ T cells. Th17 responses were more abundant in the aged individuals, and this could be attributed to increased

IL-6 levels (145). The downstream signaling via TCR was hampered in the T cells of aged host which could be due to reduced IL-2 production as well as impaired recruitment of molecules at the immune synapse. These observations were made for the cells of murine as well as humans (146-153). Enhanced levels oxidative stress in the T cells from aged host could also partially account for such results (150-153).

Molecular understanding of cellular senescence

HSCs are reduced by 2-10-fold in aged humans as well as mice and such cells are additionally compromised in their proliferation and differentiation (154-158). Both cell-intrinsic factors such as DNA damage, production of ROS, changes in polarity and cell extrinsic factors such as hematopoietic niche or the microenvironment could cause such effects (154, 159). Dysfunctional HSCs lead to declining immunity and precipitate various diseases such as myeloid and lymphoid leukemia, autoimmunities and enhanced susceptibility of the host to acquire infections and controlling it poorly (160, 156 and 167). Senescence of BM cells is also driven by the reduced response of cells to nutrient sensing via mTOR axis. GM-CSF promotes the growth and survival of precursor BM cells by engaging PI3K-mTOR pathways and subsequently such cells differentiate into BMDCs by engaging STAT5. Development, maturation and functionality of aging cells is compromised (161). A limitation of growth factors leads to the inhibition of MAPK/mTOR pathway and consequently cell cycle is arrested. Such cells show impaired metabolism, protein synthesis and cellular functions (161). Cell cycle arrest in the aging cells could also be caused by dysregulated autophagy, mitochondrial oxidative phosphorylation, or systemic inflammation. An active mTOR signal in the absence of growth factors leads to direct or indirect inhibition of cyclin-dependent kinase (CDK) such as p21 and p16 that causes arrest of cells in G1 phase, while the cells remain metabolically active via mTOR pathway (161, 162). The mTOR

activation in the cells arrested in G1 phase promotes cellular senescence and such cells show hypertrophic changes with flattened morphology in addition to producing pro-inflammatory molecules. The irreversible cell cycle arrest in the G1 phase promotes cell injury, decreasing physiological cell capacities, leading to an unnatural aging process. A hyper activation of mTOR also promotes neoplastic cell transformation so inhibiting mTOR might prevent age associated neoplastic disease *(163).* Therefore, a regulated expression of mTOR is necessary for the growth and development of cells.

It is known that mTOR exists as multiprotein complex (mTORC1 and mTORC2) and constitutes a central integrator of cell metabolism and promotes lineage commitment in T cells (164). mTORC1 promotes the transcription of genes involved in cellular metabolism and affects glycolysis, pentose phosphate pathway (PPP) and de novo lipogenesis as it was evident in both Tsc1/Tsc2 depleted or rapamycin treated cells (165). mTORC1 signaling increases flux through oxidative PPP to generate NADPH, which provides the reducing environment for many biosynthetic processes. The production of ribose sugar required for synthesis of nucleotides is also enhanced which promotes anabolic cell growth and proliferation (165). A dramatic up-regulation of glucose consumption through PPP was observed which further increased myc- and mTORC1-dependent activation of T cells. The deletion of myc impeded glutamine oxidation which is essential for the growth of T cells through the mTOR pathway (166).

Inhibition of mTOR induces T-cell anergy even in the presence of an adequate co-stimulation which can be attributed to down-regulation of the metabolic machinery (168, 169) and such cells are preferentially retained in lymphoid tissues (170, 171). That the signaling via mTOR affects differentiation of $CD4^+$ helper T cells was shown. While an inhibition of mTORC1 impairs the differentiation of Th1 and Th17 cells without affecting Th2 response, a deficiency of mTORC2

in T cells impairs the differentiation of Th2 cells with no effect of the differentiation of Th1 and Th17 cells (172). An inhibition of mTOR also influences the differentiation of T regulatory cells (Tregs) (173, 174) by promoting the expansion of naturally occurring Tregs ($CD4^+CD25^+FoxP3^+$) as well as by generating inducible Tregs from conventional $CD4^+$ T cells (173-176). While the mTOR inhibition suppresses the proliferation of activated $CD4^+$ T cells in addition to enhancing their susceptibility to apoptosis, the response of memory $CD8^+$ T cells is promoted (177, 179). Studies involving murine model of acute LCMV infection revealed significant enhancement in the frequencies of CD127 (IL-7Rα), CD62L (lymph node homing marker) and the anti-apoptotic molecule, B-cell lymphoma 2 (Bcl2), expressing cells following mTOR targeting by pharmacological antagonism with rapamycin and or its genetic ablation (178). The mTOR depleted cells showed reduced expression of T-bet, a master regulator of Th1 and $CD8^+$ T cells activity and such cells preferentially generated memory T cells (179, 180).

Inhibition of mTOR by using rapamycin has significant effects on DCs biology. The mTOR inhibited cells were compromised in phenotypic and functional maturation of DCs following addition of IL-4, LPS or CD40 ligation (181-183) as well as upon their fms-like tyrosine 3 kinase ligand (Flt3L) induced differentiation (184, 185). Additionally, mTOR-inhibition also promoted apoptosis of human monocyte and $CD34^+$ derived DCs, without affecting other immune cells such as macrophages or myeloid cells (186). However, mTOR inhibition enhanced CCR7 expression on DCs which is required for migration of DCs to the secondary lymphoid organs (187). Furthermore, mTOR inhibition also regulated the plasmacytoid DCs (pDC) which are responsible for the anti-viral immune response and produce enormous amounts of type I IFN during viral infection and activate NK cells (188). mTOR inhibitors can also regulates the functional fate of

antigen presenting cells by upregulating ILT3 and ILT4 and downregulating CD40. This results in the increase in the frequency of circulating $CD8^{+}CD28^{-}$T cells as well as Tregs (189).

Differentiation of BMDCs from precursor cells

Generation of dendritic cells (DCs) from bone marrow is required for the maintenance of DCs pool in the host throughout the life-time of an individual (191). Since DCs are relatively short-lived cells, a continuous replenishment from bone marrow, blood or tissue-derived precursors is required (192). Hematopoietic stem cells (HSCs) generate the precursor cells such as CMP (common myeloid progenitor) and MDP (macrophage and DC progenitors) whose proliferation, survival and functional differentiation are required for efficient generation of DCs (190). It has been shown that the GM-CSF is required for *in vitro* induction and efficient development of DCs in both humans and mice (193, 194). A significant increase in the number of DCs in spleen and thymus of mice was observed following supplementation of GM-CSF suggesting its critical role *in vivo* for the expansion of DCs (195, 196). A substantial decrease in the number of migratory DCs in skin and gut of mice lacking GM-CSF or the GM-CSF receptor (CSFR), supports the hypothesis that this subset requires GM-CSF under steady-state conditions (197-199). Additionally, GM-CSF is known to inhibit the differentiation of BM precursors to plasmacytoid DCs but supports the survival and terminal differentiation of circulating interferon (IFN)-producing cells, also known as precursors of pDCs (200, 201). DCs expand following infection or an inflammatory response which can be attributed to the increased GM-CSF secretion (202). Additionally, GM-CSF is also known to induce the development of immunogenic DCs which produce NOS and TNF-α (203, 205). Bone marrow differentiation to BMDCs is initiated following sensing of GM-CSF by the GM-CSF receptor (GM-CSFR) which comprises of 2 distinct subunits, GM-CSFRα or CD116 and a shared β-receptor (βc; CD131). While CD116 is unique to GM-CSF receptor, CD131 is shared

between GM-CSFR, IL-3R and IL-5R receptor (205, 207). Downstream signaling cascades starts with the ligation of GM-CSF and interaction of different effector proteins with the common βc subunit. Initiation of signaling starts with the activation of a cytoplasmic tyrosine kinase janus kinase 2 (JAK2), which leads to the activation of different downstream proteins such as STAT5 (JAK/STAT) pathway, MAPK pathway, PI3K pathway and canonical NF-κβ pathway (205-208). It was also observed that a direct activation of canonical NF-κβ pathway in which βc-bound TRAF6 mediates the translocation of NF-κβ by degrading Iκβα. This step also promotes a direct interaction between Iκβ kinase (IKK) and GM-CSFRα unit which demonstrates that this signaling is triggered as a direct consequence of GM-CSFR engagement (209, 210).

JAK/STAT mediated DCs differentiation

JAK/STAT pathway is required for proper differentiation of DCs. Accordingly, it was shown that a conditional ablation of JAK2 in adult mice significantly impaired the number of splenic DCs. Similarly, the GM-CSF supplemented cultures of bone marrow cells of JAK2 deficient mice generated reduced number of conventional DCs (cDCs) (211). GM-CSF induced the activation of STAT3 and 5. STAT3 response was found to be critically involved in differentiation of DCs with Flt3L but was not necessary for DCs generated by GM-CSF (212, 213). However, STAT5 has been studied to support GM-CSF mediated differentiation of human migratory and murine bone marrow derived conventional DCs. (214-218). The STAT5 promotes differentiation of interstitial DCs (iDCs) from human $CD34^+$ hematopoietic progenitor cells (HPCs) with GM-CSF but its inhibition facilitates the development of $CD34^-$ HPCs to become Langerhans cells which suggests a subset-specific regulation of migratory DCs (216). Additionally ectopic expression of STAT5 leads to the reduced production of cDCs *in vitro* in addition to negatively impacting the differentiation of human $CD34^+$ HPCs to become iDCs and Langerhans cells. Elevated STAT5

activity also promotes the terminal differentiation of human $CD34^-$derived pre-iDCs ($CD14^+CD1a^-$) and pre-Langerhans cells ($CD14^-CD1a^+$) (216, 219). Studies in murine models have also shown the GM-CSF induced activation of STAT5 which eventually promoted the development of migratory and cDCs but inhibits the generation of pDCs (200, 214 and 215). It was also observed that treatment of IFN-producing pDCs with GM-CSF helped promote their terminal differentiation which attested to the critical role of context and temporally regulated processes in generation of different subsets of DCs.

PI3K/PKB and DCs differentiation

Sensing of extracellular GM-CSF produced during an inflammatory response or that supplemented to the culture media induced activation of phosphatidylinositol 3-kinase class I- serine/threonine protein kinase B (PI3K-PKB) or (PI3K-Akt) pathways. Activation of PI3K-PKB cascade is dependent upon the downstream molecules such as phosphatidylinositol-3,4,5-triphosphate ($PtdIns(3,4,5)P_3$), a secondary messenger whose response is inhibited by phosphatases, PTEN and SHIP. A reduction in the number of splenic DCs was recorded in the mice lacking p85α subunit of class IA PI3K (220). The phenotype could be copied with the specific deletion of PTEN in the bone marrow precursors as well as their reconstitution in the irradiated mice (220, 221). Such mice showed high frequencies of DCs. Similarly, $SHIP^{-/-}$ mice showed increased population of splenic $CD11C^+$ DCs indicating the role of PI3K activity in the development of DCs (222). Protein kinase B (PKB/c-AKT), is the major target of PI3K which gets activated upon phosphorylation by phosphoinositide-dependent kinase-1 (PDK1). Increased number of human BDCA-1^+ DCs in β2-microglobulin$^{-/-}$NOD/SCID mice transplanted with human $CD34^+$ HPCs expressing constitutively active mutant of PKB than the control HPCs indicating the supportive role of PKB in DCs' development (223). Inhibition of mTOR using rapamycin resulted in reduced numbers of DCs

which suggested the role of downstream effectors of PI3K/PKB axis in activating of mTOR complex 1 (mTORC1) (224). Furthermore, a pharmacological inhibition of PI3K or mTOR inhibited GM-CSF induced DC differentiation *in-vitro* from monocytes as well as hematopoietic precursors (223-226). An enhanced activity of PI3K promotes the survival of DCs and their precursors in addition to inhibiting the apoptosis because of GM-CSF deprivation (223, 227 and 228). Even though it is known that the survival of most DC lineages is supported by PI3K-dependent signaling, its effect varies between distinct subsets and the phase of differentiation. The survival of human derivatives of $CD34^-$ iDCs and pre-Langerhans was dependent on activity of PI3K but the survival of terminally differentiated DCs did not show PI3K or mTOR dependency (223, 225). Similarly, the survival of monocyte derived DCs was dependent on the PI3K signaling but that of monocytes was independent on either PI3K or mTOR in humans (225, 226). A reduced number of DCs with normal phenotype but impaired functionality was observed in GM-CSF added cultures of PI3K or mTOR inhibited cells which attested to the role of PI3K-PKB axis in promoting the survival and proliferation (224, 225, 229 and 230).

MAPK pathway in DCs differentiation

GM-CSF mediated activation of MAPK pathway in the development of DCs involve signaling events, regulated by MEK/ERK pathway. Accordingly, the generated DCs from bone marrow of $ERK^{-/-}$ mice showed increased expression of surface molecules such as MHC-II and CD86 suggested that ERK negatively regulated the functional differentiation of DCs (231). Pharmacological inhibition of MEK or ERK impaired the survival and differentiation of human monocyte-derived DC (226, 232). It was also observed that the activation of p38 of MAPK59 by factors secreted in tumor microenvironment induced DCs differentiation while the effect was reversed upon pharmacological inhibition p38 MAPK (232-234). Above results suggest that the

GM-CSF induces the activation of MEK/ERK signaling cascade and promotes the development of DCs by regulating the survival, proliferation, and differentiation.

NF-κβ in the differentiation of DCs

Addition of GM-CSF in the culture to generate differentiation of BMDCs triggers signaling via NF-kβ pathway. Studies involving individual knockout of canonical NF-κβ proteins such as RelA, c-Rel, or p50 did not affect the frequency of splenic DCs in mice but a combined deficiency of RelA and p50 led to the reduced population of $CD11c^{+}$DCs. An impaired differentiation of DCs was also observed from $RelA^{-/-}p50^{-/-}$ hematopoietic progenitors subjected to GM-CSF induced cultures (235). It was also shown that the addition of GM-CSF induced activation of canonical NF-κβ pathway and its critical involvement in generating migratory DCs either from monocytes or from $CD34^{+}$ hematopoietic progenitors in humans (223, 236 and 237). Pharmacological or shRNA mediated inhibition of NF-κβ reduces the yields of BMDCs in GM-CSF added culture of hematopoietic progenitors of mice or human (235, 190). The role of canonical NF-κβ signaling in the survival of both precursors as well as the differentiated DCs was also shown (236, 237) (190, 238). Further the role NF-κβ in the impacting the functionality of cDCs has also been shown and BMDCs from $p50^{-/-}$c-$Rel^{-/-}$ mice showed a reduced ability to produce IL-12 (235). Whereas a continued NF-κβ inhibition in BMDCs leads to an impaired functionality of DC and such cells induce compromised activation of T cells through different signals induced by pathogens and inflammatory cytokines. (239).

Age related impairment in the differentiation of BMDCs

Immunosenescence can lead to a decreased expression of key molecules that are essential for the growth, survival, and development of bone marrow-derived dendritic cells (BMDCs) (240, 241).

Sensing of GM-CSF through growth factor receptors follows activation of downstream molecules, Rab8a, an adaptor molecules that helps recruit PI3K to the receptor complex. Such signaling events lead to the activation and phosphorylation of Akt proteins which causes the suppression of TSC1 and TSC2 proteins to activate mToRC1 complex. Active mTORC1 eventually leads to the phosphorylation of S6 kinase (S6K) which is the positive regulator of cellular survival and maintaining homeostasis (242). Impaired differentiation of DCs from aging precursors upon GM-CSF addition has been observed (243). Some studies have reported reduced capacity for the differentiation of DCs from progenitors or the monocytes of aged individuals as compared to the younger individuals in GM-CSF supplemented cultures (244, 245). Aging can result in dysregulated expression of signaling molecules and transcription factors critical for inducing an optimal response following GM-CSF ligation. Furthermore, altered microenvironment and cellular interactions within the bone marrow or peripheral tissues can contribute to the impaired differentiation and functionality of DCs in older population (246-250). DCs are crucial for initiating and modulating immune responses, and their impaired differentiation can reduce antigen presentation, altered immune cell activation, and compromised immune surveillance (251, 252). Understanding the mechanisms underlying dysfunctionality in DCs is important for improving their differentiation and functionality in older individuals. Approaches such as targeting specific signaling pathways or modifying the microenvironment could enhance generation and activation of DCs in aging individuals. The study described in this thesis involve restoration in the functionality and differentiation of aged BMDCs upon reconstitution of a small GTPase Rab8a. It is also shown earlier that overexpression of Ras kinase promotes the expression of anti-apoptotic molecules Bcl2 and promotes the survival of the cells. Depletion of PI3K which is an upstream mediator of Rab8a leads to reduced production of IFNβ from bone marrow derived macrophages

(241). Depletion of Rab8a also inhibits the cilliogenesis and fusion of exocytic vesicles to the plasma membrane (253, 255). These observations indicated a crucial role of Rab8a in biology of DCs.

Conclusion

The immune response against invading pathogens in healthy individuals involves the coordinated action of both innate and adaptive immune systems. The innate immune system provides immediate, non-specific defense while the adaptive immune system mounts a more targeted response and generates immunological memory. DCs capture antigens and process them into small peptide fragments, which are then presented on their cell surface in context with major histocompatibility complex (MHC) molecules. During the interaction of DCs and T cells, three signals are required for T cell activation and differentiation. Signal 1 involves the interaction between the T cell receptor (TCR) on the surface of T cells and the peptide-MHC complex presented by the APC. Signal 2 and signal 3 involve co-stimulation and cytokines, respectively. Naïve T cells following sensing the three signals expand and differentiate into effector T cells, which have specialized functions such as killing infected cells or secreting cytokines to control infection. After the infection is resolved, most effector T cells are removed by apoptosis leaving behind a pool as memory T cells which exhibit longevity and provide the basis for immunological memory. In subsequent encounters with the same pathogen, memory T cells are rapidly reactivated, leading to a faster and more robust immune response, thereby conferring a quick protection against reinfection. Long-term protection against viral infections relies on the ability of DCs to effectively prime antigen specific T cells to generate lasting memory. However, age-related perturbation in antigen processing and presentation can result in attenuation of antigen-specific T cell responses leading to a weaker immune response against the invading pathogens or

vaccination in elderlies. Therefore, for improving immunity in the elderlies it becomes imperative to understand the molecular mechanisms underlying age-related immune impairment of DCs. This could provide critical insights in devising strategies to restore immune functions. Following objectives were defined for the investigations.

1. Transcriptomic analysis of DCs of naïve young and aged host.

2. Phenotypic and functional analysis of DCs from aged and young host.

3. Investigating the role of Rab8a, a small GTPase in differentiation and function of DCs

    (a) Depletion of Rab8a in DCs of young animals and studying its functional effects

    (b) Reconstitution of Rab8a in DCs of aged animals to restore functionality

References

1. Aw, D., Silva, A.B. and Palmer, D.B., 2007. Immunosenescence: emerging challenges for an ageing population. *Immunology*, 120(4), pp.435-446.
2. Chinn, I.K., Blackburn, C.C., Manley, N.R. and Sempowski, G.D., 2012, October. Changes in primary lymphoid organs with aging. *In Seminars in immunology* (Vol. 24, No. 5, pp. 309-320).
3. Simpson, R.J., 2011. Aging, persistent viral infections, and immunosenescence: can exercise" make space"? Exercise and sport sciences reviews, 39(1), pp.23-33.
4. Santoro, A., Bientinesi, E. and Monti, D., 2021. Immunosenescence and inflammaging in the aging process: age-related diseases or longevity. Ageing Research Reviews, 71, p.101422.
5. Mancuso, S., Carlisi, M., Santoro, M., Napolitano, M., Raso, S. and Siragusa, S., 2018. Immunosenescence and lymphomagenesis. Immunity & Ageing, 15, pp.1-7.
6. Tu, W. and Rao, S., 2016. Mechanisms underlying T cell immunosenescence: aging and cytomegalovirus infection. Frontiers in microbiology, 7, p.2111.
7. Rodriguez, I.J., Lalinde Ruiz, N., Llano León, M., Martínez Enríquez, L., Montilla Velásquez, M.D.P., Ortiz Aguirre, J.P., Rodríguez Bohórquez, O.M., Velandia Vargas, E.A., Hernández, E.D. and Parra López, C.A., 2021. Immunosenescence study of T cells: a systematic review. Frontiers in immunology, 11, p.604591.
8. Frasca, D., Diaz, A., Romero, M., Garcia, D. and Blomberg, B.B., 2020. B cell immunosenescence. Annual review of cell and developmental biology, 36, pp.551-574.

9. Buffa, S., Bulati, M., Pellicano, M., Dunn-Walters, D.K., Wu, Y.C., Candore, G., Vitello, S., Caruso, C. and Colonna-Romano, G., 2011. B cell immunosenescence: different features of naive and memory B cells in elderly. Biogerontology, 12, pp.473-483.
10. Rezzani, R., Nardo, L., Favero, G., Peroni, M. and Rodella, L.F., 2014. Thymus and aging: morphological, radiological, and functional overview. Age, 36, pp.313-351.
11. Ferrucci, L. and Fabbri, E., 2018. Inflammageing: chronic inflammation in ageing, cardiovascular disease, and frailty. Nature Reviews Cardiology, 15(9), pp.505-522.
12. Linton, P.J. and Dorshkind, K., 2004. Age-related changes in lymphocyte development and function. *Nature immunology* 5(2), pp.133-139.
13. Allman, D. and Miller, J.P., 2005. B cell development and receptor diversity during aging. *Current opinion in immunology* 17(5), pp.463-467.
14. Goronzy, J.J. and Weyand, C.M., 2005. T cell development and receptor diversity during aging. Current opinion in immunology, 17(5), pp.468-475.
15. Weng, N.P., 2006. Aging of the immune system: how much can the adaptive immune system adapt?. *Immunity* 24(5), pp.495-499.
16. de Haan, G., Nijhof, W. and Van Zant, G., 1997. Mouse strain-dependent changes in frequency and proliferation of hematopoietic stem cells during aging: correlation between lifespan and cycling activity. *Blood, The Journal of the American Society of Hematology* 89(5), pp.1543-1550.
17. Rossi, D.J., Bryder, D., Zahn, J.M., Ahlenius, H., Sonu, R., Wagers, A.J. and Weissman, I.L., 2005. Cell intrinsic alterations underlie hematopoietic stem cell aging. *Proceedings of the National Academy of Sciences* 102(26), pp.9194-9199.

18. Hotta, T., Hirabayashi, N., Utsumi, M., Murate, T. and Yamada, H., 1980. Age-related changes in the function of hemopoietic stroma in mice. *Experimental hematology* 8(7), pp.933-936.
19. Müller-Sieburg, C.E. and Riblet, R., 1996. Genetic control of the frequency of hematopoietic stem cells in mice: mapping of a candidate locus to chromosome 1. *The Journal of experimental medicine* 183(3), pp.1141-1150.
20. Phillips, R.L., Reinhart, A.J. and Van Zant, G., 1992. Genetic control of murine hematopoietic stem cell pool sizes and cycling kinetics. *Proceedings of the National Academy of Sciences* 89(23), pp.11607-11611.
21. Tuljapurkar, S.R., McGuire, T.R., Brusnahan, S.K., Jackson, J.D., Garvin, K.L., Kessinger, M.A., Lane, J.T., O'Kane, B.J. and Sharp, J.G., 2011. Changes in human bone marrow fat content associated with changes in hematopoietic stem cell numbers and cytokine levels with aging. *Journal of anatomy* 219(5), pp.574-581.
22. Kuranda, K., Vargaftig, J., de la Rochere, P., Dosquet, C., Charron, D., Bardin, F., Tonnelle, C., Bonnet, D. and Goodhardt, M., 2011. Age-related changes in human hematopoietic stem/progenitor cells. *Aging cell* 10(3), pp.542-546.
23. Povsic, T.J., Zhou, J., Adams, S.D., Bolognesi, M.P., Attarian, D.E. and Peterson, E.D., 2010. Aging is not associated with bone marrow–resident progenitor cell depletion. *Journals of Gerontology Series A: Biomedical Sciences and Medical Sciences* 65(10), pp.1042-1050.
24. Chen, J., Astle, C.M. and Harrison, D.E., 2000. Genetic regulation of primitive hematopoietic stem cell senescence. Experimental Hematology, 28(4), pp.442-450.

25. Van Zant, G., Holland, B.P., Eldridge, P.W. and Chen, J.J., 1990. Genotype-restricted growth and aging patterns in hematopoietic stem cell populations of allophenic mice. The Journal of experimental medicine, 171(5), pp.1547-1565.
26. Morrison, S.J., Wandycz, A.M., Akashi, K., Globerson, A. and Weissman, I.L., 1996. The aging of hematopoietic stem cells. *Nature medicine* 2(9), pp.1011-1016.
27. Chambers, S.M., Shaw, C.A., Gatza, C., Fisk, C.J., Donehower, L.A. and Goodell, M.A., 2007. Aging hematopoietic stem cells decline in function and exhibit epigenetic dysregulation. *PLoS biology* 5(8), p.e201.
28. Johnson, K.M., Owen, K. and Witte, P.L., 2002. Aging and developmental transitions in the B cell lineage. *International immunology* 14(11), pp.1313-1323.
29. Miller, J.P. and Allman, D., 2003. The decline in B lymphopoiesis in aged mice reflects loss of very early B-lineage precursors. *The Journal of Immunology* 171(5), pp.2326-2330.
30. Labrie III, J.E., Sah, A.P., Allman, D.M., Cancro, M.P. and Gerstein, R.M., 2004. Bone marrow microenvironmental changes underlie reduced RAG-mediated recombination and B cell generation in aged mice. *The Journal of experimental medicine* 200(4), pp.411-423.
31. Min, H., Montecino-Rodriguez, E. and Dorshkind, K., 2006. Effects of aging on the common lymphoid progenitor to pro-B cell transition. *The Journal of Immunology* 176(2), pp.1007-1012.
32. Jang, Y.Y. and Sharkis, S.J., 2007. A low level of reactive oxygen species selects for primitive hematopoietic stem cells that may reside in the low-oxygenic niche. *Blood, The Journal of the American Society of Hematology* 110(8), pp.3056-3063.
33. Ito, K., Hirao, A., Arai, F., Matsuoka, S., Takubo, K., Hamaguchi, I., Nomiyama, K., Hosokawa, K., Sakurada, K., Nakagata, N. and Ikeda, Y., 2004. Regulation of oxidative

stress by ATM is required for self-renewal of haematopoietic stem cells. *Nature* 431(7011), pp.997-1002.

34. Tothova, Z., Kollipara, R., Huntly, B.J., Lee, B.H., Castrillon, D.H., Cullen, D.E., McDowell, E.P., Lazo-Kallanian, S., Williams, I.R., Sears, C. and Armstrong, S.A., 2007. FoxOs are critical mediators of hematopoietic stem cell resistance to physiologic oxidative stress. *Cell* 128(2), pp.325-339.
35. Shipounova, I.N., Svinareva, D.A., Petrova, T.V., Lyamzaev, K.G., Chernyak, B.V., Drize, N.I. and Skulachev, V.P., 2010. Reactive oxygen species produced in mitochondria are involved in age-dependent changes of hematopoietic and mesenchymal progenitor cells in mice. A study with the novel mitochondria-targeted antioxidant SkQ1. *Mechanisms of ageing and development* 131(6), pp.415-421.
36. Wilson, A., Shehadeh, L.A., Yu, H. and Webster, K.A., 2010. Age-related molecular genetic changes of murine bone marrow mesenchymal stem cells. *BMC genomics* 11(1), pp.1-14.
37. Wang, W., Gou, L., Xie, G., Tong, A., He, F., Lu, Z., Yao, Y., Liu, K., Li, J., Tang, M. and Chen, L., 2010. Proteomic analysis of interstitial fluid in bone marrow identified that peroxiredoxin 2 regulates H2O2 level of bone marrow during aging. *Journal of proteome research* 9(8), pp.3812-3819.
38. Beresford, J.N., Bennett, J.H., Devlin, C., Leboy, P.S. and Owen, M.E., 1992. Evidence for an inverse relationship between the differentiation of adipocytic and osteogenic cells in rat marrow stromal cell cultures. *Journal of cell science* 102(2), pp.341-351.

39. Zhang, J., Niu, C., Ye, L., Huang, H., He, X., Tong, W.G., Ross, J., Haug, J., Johnson, T., Feng, J.Q. and Harris, S., 2003. Identification of the haematopoietic stem cell niche and control of the niche size. *Nature* 425(6960), pp.836-841.

40. Visnjic, D., Kalajzic, Z., Rowe, D.W., Katavic, V., Lorenzo, J. and Aguila, H.L., 2004. Hematopoiesis is severely altered in mice with an induced osteoblast deficiency. *Blood* 103(9), pp.3258-3264.

41. Naveiras, O., Nardi, V., Wenzel, P.L., Hauschka, P.V., Fahey, F. and Daley, G.Q., 2009. Bone-marrow adipocytes as negative regulators of the haematopoietic microenvironment. *Nature* 460(7252), pp.259-263.

42. Chertkov, J.L. and Gurevitch, O.A., 1981. Age-related changes in hemopoietic microenvironment. Enhanced growth of hemopoietic stroma and weakened genetic resistance to hemopoietic cells in old mice. *Experimental Gerontology* 16(2), pp.195-198.

43. Muguruma, Y., Yahata, T., Miyatake, H., Sato, T., Uno, T., Itoh, J., Kato, S., Ito, M., Hotta, T. and Ando, K., 2006. Reconstitution of the functional human hematopoietic microenvironment derived from human mesenchymal stem cells in the murine bone marrow compartment. *Blood* 107(5), pp.1878-1887.

44. Kassem, M. and Marie, P.J., 2011. Senescence-associated intrinsic mechanisms of osteoblast dysfunctions. *Aging cell* 10(2), pp.191-197.

45. Jiang, S.Y., Shu, R., Xie, Y.F. and Zhang, S.Y., 2010. Age-related changes in biological characteristics of human alveolar osteoblasts. *Cell proliferation* 43(5), pp.464-470.

46. Köhler, A., Schmithorst, V., Filippi, M.D., Ryan, M.A., Daria, D., Gunzer, M. and Geiger, H., 2009. Altered cellular dynamics and endosteal location of aged early hematopoietic

progenitor cells revealed by time-lapse intravital imaging in long bones. *Blood, The Journal of the American Society of Hematology* 114(2), pp.290-298.

47. Shockley, K.R., Lazarenko, O.P., Czernik, P.J., Rosen, C.J., Churchill, G.A. and Lecka-Czernik, B., 2009. PPARγ2 nuclear receptor controls multiple regulatory pathways of osteoblast differentiation from marrow mesenchymal stem cells. *Journal of cellular biochemistry* 106(2), pp.232-246.
48. Moerman, E.J., Teng, K., Lipschitz, D.A. and Lecka-Czernik, B., 2004. Aging activates adipogenic and suppresses osteogenic programs in mesenchymal marrow stroma/stem cells: the role of PPAR-γ2 transcription factor and TGF-β/BMP signaling pathways. *Aging cell* 3(6), pp.379-389.
49. Gordon, J., Wilson, V.A., Blair, N.F., Sheridan, J., Farley, A., Wilson, L., Manley, N.R. and Blackburn, C.C., 2004. Functional evidence for a single endodermal origin for the thymic epithelium. *Nature immunology* 5(5), pp.546-553.
50. Gordon, J. and Manley, N.R., 2011. Mechanisms of thymus organogenesis and morphogenesis. *Development* 138(18), pp.3865-3878.
51. Goldschneider, I., 2006. Cyclical mobilization and gated importation of thymocyte progenitors in the adult mouse: evidence for a thymus-bone marrow feedback loop. *Immunological reviews* 209(1), pp.58-75.
52. Adkins, B., 2003. Peripheral $CD4^+$ lymphocytes derived from fetal versus adult thymic precursors differ phenotypically and functionally. *The Journal of Immunology* 171(10), pp.5157-5164.
53. Min, B., McHugh, R., Sempowski, G.D., Mackall, C., Foucras, G. and Paul, W.E., 2003. Neonates support lymphopenia-induced proliferation. *Immunity* 18(1), pp.131-140.

54. Bueno, V. (2022). Age-Related Changes in Primary and Secondary Lymphoid Organs. In: Bueno, V., Pawelec, G. (eds) Healthy Longevity and Immune System. Healthy Ageing and Longevity, vol 16. *Springer, Cham*. https://doi.org/10.1007/978-3-030-87532-9_2.

55. Miranda, R.N., Khoury, J.D. and Medeiros, L.J., 2013. Normal lymph node architecture and function. *In Atlas of Lymph Node Pathology* (pp. 3-7). Springer, New York, NY.

56. Ruddle, N.H., 2016. High endothelial venules and lymphatic vessels in tertiary lymphoid organs: characteristics, functions, and regulation. *Frontiers in immunology* 7, p.491.

57. Murakami, G. and Taniguchi, I., 2004. Histologic heterogeneity and intranodal shunt flow in lymph nodes from elderly subjects: a cadaveric study. *Annals of Surgical Oncology* 11(3), pp.279S-284S.

58. Turner, V.M. and Mabbott, N.A., 2017. Structural and functional changes to lymph nodes in ageing mice. *Immunology* 151(2), pp.239-247.

59. Briceño, O., Lissina, A., Wanke, K., Afonso, G., Von Braun, A., Ragon, K., Miquel, T., Gostick, E., Papagno, L., Stiasny, K. and Price, D.A., 2016. Reduced naïve CD 8^+ T-cell priming efficacy in elderly adults. *Aging cell* 15(1), pp.14-21.

60. Govaert, T.M., Thijs, C.T.M.C.N., Masurel, N., Sprenger, M.J.W., Dinant, G.J. and Knottnerus, J.A., 1994. The efficacy of influenza vaccination in elderly individuals: a randomized double-blind placebo-controlled trial. *Jama* 272(21), pp.1661-1665.

61. Weinberger, B. and Grubeck-Loebenstein, B., 2012. Vaccines for the elderly. *Clinical Microbiology and Infection* 18, pp.100-108.

62. Ciabattini, A., Nardini, C., Santoro, F., Garagnani, P., Franceschi, C. and Medaglini, D., 2018, December. Vaccination in the elderly: the challenge of immune changes with aging. *In Seminars in immunology* (Vol. 40, pp. 83-94). Academic Press.

63. Larbi, A., Franceschi, C., Mazzatti, D., Solana, R., Wikby, A. and Pawelec, G., 2008. Aging of the immune system as a prognostic factor for human longevity. *Physiology* 23(2), pp.64-74.

64. McElhaney, J.E. and Effros, R.B., 2009. Immunosenescence: what does it mean to health outcomes in older adults?. *Current opinion in immunology* 21(4), pp.418-424.

65. Weinberger B. Herndler-Brandstetter D. Schwanninger A. Weiskopf D. Grubeck-Loebenstein B. Biology of immune responses to vaccines in elderly persons. *Clin Infect Dis*. 2008; 46:1078–1084.

66. Toapanta, F.R. and Ross, T.M., 2009. Impaired immune responses in the lungs of aged mice following influenza infection. *Respiratory research* 10(1), pp.1-19.

67. Shaw, A.C., Joshi, S., Greenwood, H., Panda, A. and Lord, J.M., 2010. Aging of the innate immune system. *Current opinion in immunology* 22(4), pp.507-513.

68. Ponnappan, S. and Ponnappan, U., 2011. Aging and immune function: *molecular mechanisms to interventions*.

69. Enck, P., Zimmermann, K., Rusch, K., Schwiertz, A., Klosterhalfen, S. and Frick, J.S., 2009. The effects of ageing on the colonic bacterial microflora in adults. *Zeitschrift für Gastroenterologie* 47(07), pp.653-658.

70. Gomez, C.R., Boehmer, E.D. and Kovacs, E.J., 2005. The aging innate immune system. *Current opinion in immunology* 17(5), pp.457-462.

71. Nomellini, V., Gomez, C.R. and Kovacs, E.J., 2008. Aging and impairment of innate immunity. *Trends in Innate Immunity* 15, pp.188-205.

72. Fulop, T., Larbi, A., Douziech, N., Fortin, C., Guérard, K.P., Lesur, O., Khalil, A. and Dupuis, G., 2004. Signal transduction and functional changes in neutrophils with aging. *Aging cell* 3(4), pp.217-226.

73. Kovacs, E.J., Palmer, J.L., Fortin, C.F., Fülöp Jr, T., Goldstein, D.R. and Linton, P.J., 2009. Aging and innate immunity in the mouse: impact of intrinsic and extrinsic factors. *Trends in immunology* 30(7), pp.319-324.

74. Shodell, M. and Siegal, F.P., 2002. Circulating, interferon-producing plasmacytoid dendritic cells decline during human ageing. *Scandinavian journal of immunology* 56(5), pp.518-521.

75. Van Duin, D., Mohanty, S., Thomas, V., Ginter, S., Montgomery, R.R., Fikrig, E., Allore, H.G., Medzhitov, R. and Shaw, A.C., 2007. Age-associated defect in human TLR-1/2 function. *The Journal of Immunology* 178(2), pp.970-975.

76. Caligiuri, M.A., 2008. Human natural killer cells. Blood, *The Journal of the American Society of Hematology* 112(3), pp.461-469.

77. Ershler, W.B. and Keller, E.T., 2000. Age-associated increased interleukin-6 gene expression, late-life diseases, and frailty. *Annual review of medicine* 51, p.245.

78. Franceschi, C., Bonafè, M., Valensin, S., Olivieri, F., De Luca, M., Ottaviani, E. and De Benedictis, G., 2000. Inflamm-aging: an evolutionary perspective on immunosenescence. *Annals of the new York Academy of Sciences* 908(1), pp.244-254.

79. O'mahony, L., Holland, J., Jackson, J., Feighery, C., Hennessy, T.P.J. and Mealy, K., 1998. Quantitative intracellular cytokine measurement: age-related changes in proinflammatory cytokine production. *Clinical & Experimental Immunology* 113(2), pp.213-219.

80. Chatta, G.S., Andrews, R.G., Rodger, E., Schrag, M., Hammond, W.P. and Dale, D.C., 1993. Hematopoietic progenitors and aging: alterations in granulocytic precursors and responsiveness to recombinant human G-CSF, GM-CSF, and IL-3. *Journal of gerontology* 48(5), pp.M207-M212.
81. Fortin, C.F., McDonald, P.P., Lesur, O. and Fülöp Jr, T., 2008. Aging and neutrophils: there is still much to do. *Rejuvenation research* 11(5), pp.873-882.
82. Lord, J.M., Butcher, S., Killampali, V., Lascelles, D. and Salmon, M., 2001. Neutrophil ageing and immunesenescence. *Mechanisms of ageing and development* 122(14), pp.1521-1535.
83. Wessels, I., Jansen, J., Rink, L. and Uciechowski, P., 2010. Immunosenescence of polymorphonuclear neutrophils. *The Scientific World Journal* 10, pp.145-160.
84. Ogawa, K., Suzuki, K., Okutsu, M., Yamazaki, K. and Shinkai, S., 2008. The association of elevated reactive oxygen species levels from neutrophils with low-grade inflammation in the elderly. *Immunity & Ageing* 5(1), pp.1-8.
85. Fulop, T., Larbi, A., Douziech, N., Fortin, C., Guérard, K.P., Lesur, O., Khalil, A. and Dupuis, G., 2004. Signal transduction and functional changes in neutrophils with aging. *Aging cell* 3(4), pp.217-226.
86. Fortin, C.F., Larbi, A., Dupuis, G., Lesur, O. and Fülöp, T., 2007. GM-CSF activates the Jak/STAT pathway to rescue polymorphonuclear neutrophils from spontaneous apoptosis in young but not elderly individuals. *Biogerontology* 8(2), pp.173-187.
87. Lord, J.M., Phillips, A.C. and Arlt, W., 2009. Synergistic effects of ageing and stress on neutrophil function. *In Handbook on Immunosenescence* (pp. 475-495). Springer, Dordrecht.

88. Biasi, D., Bambara, L.M., Carletto, A., Caramaschi, P., Andrioli, G., Urbani, G. and Bellavite, P., 1999. Neutrophil migration, oxidative metabolism and adhesion in early onset periodontitis. *Journal of clinical periodontology* 26(9), pp.563-568.

89. Mathur, S.K., Schwantes, E.A., Jarjour, N.N. and Busse, W.W., 2008. Age-related changes in eosinophil function in human subjects. *Chest* 133(2), pp.412-419.

90. Herrero Mateu, C., Marqués Soler, L., Lloberas Cavero, J. and Celada Cotarelo, A., 2001. IFN-gamma-dependent transcription of MHC class II IA is impaired in macrophages from aged mice. *Journal of Clinical Investigation* 2001, vol. 107, núm. 4, p. 485-493.

91. Solana, R., Pawelec, G. and Tarazona, R., 2006. Aging and innate immunity. *Immunity* 24(5), pp.491-494.

92. Sindrilaru, A. and Scharffetter-Kochanek, K., 2013. Disclosure of the culprits: macrophages—versatile regulators of wound healing. *Advances in wound care* 2(7), pp.357-368.

93. Piazzolla, G., Tortorella, C., Serrone, M., Jirillo, E. and Antonaci, S., 1998. Modulation of cytoskeleton assembly capacity and oxidative response in aged neutrophils. *Immunopharmacology and immunotoxicology* 20(2), pp.251-266.

94. Rabatić, S., Sabioncello, A., Dekaris, D. and Kardum, I., 1988. Age-related changes in functions of peripheral blood phagocytes. *Mechanisms of ageing and development* 45(3), pp.223-229.

95. Swift, M.E., Burns, A.L., Gray, K.L. and DiPietro, L.A., 2001. Age-related alterations in the inflammatory response to dermal injury. *Journal of Investigative Dermatology* 117(5), pp.1027-1035.

96. Panda, A., Arjona, A., Sapey, E., Bai, F., Fikrig, E., Montgomery, R.R., Lord, J.M. and Shaw, A.C., 2009. Human innate immunosenescence: causes and consequences for immunity in old age. *Trends in immunology* 30(7), pp.325-333.

97. Van Duin, D. and Shaw, A.C., 2007. Toll-like receptors in older adults. *Journal of the American Geriatrics Society* 55(9), pp.1438-1444.

98. RL, C., Liu Y. Popa D. Getchell ML. Getchell TV. Stromberg AJ. Bondada S. 2006. Molecular basis of age-associated cytokine dysregulation in LPS-stimulated macrophages. *J Leukoc Biol* 79(6), pp.1314-1327.

99. Krishnaraj, R., 1992. Immunosenescence of human NK cells: effects on tumor target recognition, lethal hit and interferon sensitivity. *Immunology letters* 34(1), pp.79-84.

100. Franceschi, C., Monti, D., Barbier, D., Salvioli, S., Grassilli, E., Capri, M., Troiano, L., Guido, M., Bonafe, M., Tropea, F. and Salomon, P., 1996. Successful immunosenescence and the remodelling of immune responses with ageing. *Nephrology Dialysis Transplantation* 11(supp9), pp.18-25.

101. Franceschi, C., Monti, D., Sansoni, P. and Cossarizza, A., 1995. The immunology of exceptional individuals: the lesson of centenarians. *Immunology today* 16(1), pp.12-16.

102. Miyaji, C., Watanabe, H., Toma, H., Akisaka, M., Tomiyama, K., Sato, Y. and Abo, T., 2000. Functional alteration of granulocytes, NK cells, and natural killer T cells in centenarians. *Human immunology* 61(9), pp.908-916.

103. Mariani, E., Mariani, A.R., Meneghetti, A., Tarozzi, A., Cocco, L. and Facchini, A., 1998. Age-dependent decreases of NK cell phosphoinositide turnover during spontaneous but not Fc-mediated cytolytic activity. *International immunology* 10(7), pp.981-989.

104. Lee, H.K. and Marzella, L., 1994. Regulation of intracellular protein degradation with special reference to lysosomes: role in cell physiology and pathology. *International Review of Experimental Pathology* 35, pp.39-147.

105. Gayoso, I., Sanchez-Correa, B., Campos, C., Alonso, C., Pera, A., Casado, J.G., Morgado, S., Tarazona, R. and Solana, R., 2011. Immunosenescence of human natural killer cells. *Journal of innate immunity* 3(4), pp.337-343.

106. DelaRosa, O., Tarazona, R., Casado, J.G., Alonso, C., Ostos, B., Peña, J. and Solana, R., 2002. Vα24+ NKT cells are decreased in elderly humans. *Experimental gerontology* 37(2-3), pp.213-217.

107. Jing, Y., Gravenstein, S., Chaganty, N.R., Chen, N., Lyerly, K.H., Joyce, S. and Deng, Y., 2007. Aging is associated with a rapid decline in frequency, alterations in subset composition, and enhanced Th2 response in CD1d-restricted NKT cells from human peripheral blood. *Experimental gerontology* 42(8), pp.719-732.

108. Bhushan, M., Cumberbatch, M., Dearman, R.J., Andrew, S.M., Kimber, I. and Griffiths, C.E.M., 2002. Tumour necrosis factor-α-induced migration of human Langerhans cells: the influence of ageing. *British Journal of Dermatology* 146(1), pp.32-40.

109. Della Bella, S., Bierti, L., Presicce, P., Arienti, R., Valenti, M., Saresella, M., Vergani, C. and Villa, M.L., 2007. Peripheral blood dendritic cells and monocytes are differently regulated in the elderly. *Clinical immunology* 122(2), pp.220-228.

110. Shodell, M. and Siegal, F.P., 2002. Circulating, interferon-producing plasmacytoid dendritic cells decline during human ageing. *Scandinavian journal of immunology* 56(5), pp.518-521.

111. Agrawal, A., Agrawal, S., Cao, J.N., Su, H., Osann, K. and Gupta, S., 2007. Altered innate immune functioning of dendritic cells in elderly humans: a role of phosphoinositide 3-kinase-signaling pathway. *The Journal of Immunology*, 178(11), pp.6912-6922.

112. Alberti, S., Cevenini, E., Ostan, R., Capri, M., Salvioli, S., Bucci, L., Ginaldi, L., De Martinis, M., Franceschi, C. and Monti, D., 2006. Age-dependent modifications of Type 1 and Type 2 cytokines within virgin and memory CD4+ T cells in humans. *Mechanisms of ageing and development* 127(6), pp.560-566.

113. Aw, D., Silva, A.B. and Palmer, D.B., 2007. Immunosenescence: emerging challenges for an ageing population. *Immunology* 120(4), pp.435-446.

114. Cancro, M.P., Hao, Y., Scholz, J.L., Riley, R.L., Frasca, D., Dunn-Walters, D.K. and Blomberg, B.B., 2009. B cells and aging: molecules and mechanisms. *Trends in immunology* 30(7), pp.313-318.

115. Frasca, D. and Blomberg, B.B., 2009. Effects of aging on B cell function. *Current opinion in immunology* 21(4), pp.425-430.

116. Harrison, D.E., Strong, R., Sharp, Z.D., Nelson, J.F., Astle, C.M., Flurkey, K., Nadon, N.L., Wilkinson, J.E., Frenkel, K., Carter, C.S. and Pahor, M., 2009. Rapamycin fed late in life extends lifespan in genetically heterogeneous mice. *Nature* 460(7253), pp.392-395.

117. Gibson, K.L., Wu, Y.C., Barnett, Y., Duggan, O., Vaughan, R., Kondeatis, E., Nilsson, B.O., Wikby, A., Kipling, D. and Dunn-Walters, D.K., 2009. B-cell diversity decreases in old age and is correlated with poor health status. *Aging cell* 8(1), pp.18-25.

118. Rogerson, B.J., Harris, D.P., Swain, S.L. and Burgess, D.O., 2003. Germinal center B cells in Peyer's patches of aged mice exhibit a normal activation phenotype and highly mutated IgM genes. *Mechanisms of ageing and development* 124(2), pp.155-165.

119. Frasca, D., Landin, A.M., Lechner, S.C., Ryan, J.G., Schwartz, R., Riley, R.L. and Blomberg, B.B., 2008. Aging down-regulates the transcription factor E2A, activation-induced cytidine deaminase, and Ig class switch in human B cells. *The Journal of Immunology* 180(8), pp.5283-5290.

120. Stephan, R.P., Sanders, V.M. and Witte, P.L., 1996. Stage-specific alterations in murine B lymphopoiesis with age. *International immunology* 8(4), pp.509-518.

121. Huppert, F., Solomou, W., O'Connor, S., Morgan, K., Sussams, P. and Brayne, C., 1998. Aging and lymphocyte subpopulations: whole-blood analysis of immune markers in a large population sample of healthy elderly individuals. *Experimental gerontology* 33(6), pp.593-600.

122. Kline, G.H., Hayden, T.A. and Klinman, N.R., 1999. B cell maintenance in aged mice reflects both increased B cell longevity and decreased B cell generation. *The Journal of Immunology* 162(6), pp.3342-3349.

123. Corcoran, L.M., 2005. Transcriptional control of B cell activation. *Molecular Analysis of B Lymphocyte Development and Activation* pp.105-146.

124. Labrie III, J.E., Sah, A.P., Allman, D.M., Cancro, M.P. and Gerstein, R.M., 2004. Bone marrow microenvironmental changes underlie reduced RAG-mediated recombination and B cell generation in aged mice. *The Journal of experimental medicine* 200(4), pp.411-423.

125. Souvannavong, V., Lemaire, C., Andréau, K., Brown, S. and Adam, A., 1998. Age-associated modulation of apoptosis and activation in murine B lymphocytes. *Mechanisms of ageing and development* 103(3), pp.285-299.

126. Whisler, R.L. and Grants, I.S., 1993. Age-related alterations in the activation and expression of phosphotyrosine kinases and protein kinase C (PKC) among human B cells. *Mechanisms of ageing and development* 71(1-2), pp.31-46.

127. Aspinall, R., Pitts, D., Lapenna, A. and Mitchell, W., 2010. Immunity in the elderly: the role of the thymus. *Journal of comparative pathology* 142, pp.S111-S115.

128. Goldberg GL. Chidgey A. Van den Brink MRM. Boyd R. Sempowski GD 2009. Thymic involution and immune reconstitution. *Trends Immunol* 30:366–373.

129. Naylor, K., Li, G., Vallejo, A.N., Lee, W.W., Koetz, K., Bryl, E., Witkowski, J., Fulbright, J., Weyand, C.M. and Goronzy, J.J., 2005. The influence of age on T cell generation and TCR diversity. *The Journal of Immunology* 174(11), pp.7446-7452.

130. Vallejo, A.N., 2007. Immune remodeling: lessons from repertoire alterations during chronological aging and in immune-mediated disease. *Trends in molecular medicine* 13(3), pp.94-102.

131. Otsuji, M., Kimura, Y., Aoe, T., Okamoto, Y. and Saito, T., 1996. Oxidative stress by tumor-derived macrophages suppresses the expression of CD3 ζ chain of T-cell receptor complex and antigen-specific T-cell responses. *Proceedings of the National Academy of Sciences* 93(23), pp.13119-13124.

132. Ouyang, Q., Wagner, W.M., Voehringer, D., Wikby, A., Klatt, T., Walter, S., Müller, C.A., Pircher, H. and Pawelec, G., 2003. Age-associated accumulation of CMV-specific CD8+ T cells expressing the inhibitory killer cell lectin-like receptor G1 (KLRG1). *Experimental gerontology* 38(8), pp.911-920.

133. Stulnig, T., Maczek, C., Böck, G., Majdic, O. and Wick, G., 1995. Reference intervals for human peripheral blood lymphocyte subpopulations from 'healthy'young and aged subjects. *International archives of allergy and immunology* 108(3), pp.205-210.

134. Sansoni, P., Vescovini, R., Fagnoni, F., Biasini, C., Zanni, F., Zanlari, L., Telera, A., Lucchini, G., Passeri, G., Monti, D. and Franceschi, C., 2008. The immune system in extreme longevity. *Experimental gerontology* 43(2), pp.61-65.

135. Tsukamoto, H., Clise-Dwyer, K., Huston, G.E., Duso, D.K., Buck, A.L., Johnson, L.L., Haynes, L. and Swain, S.L., 2009. Age-associated increase in lifespan of naive $CD4^+$ T cells contributes to T-cell homeostasis but facilitates development of functional defects. *Proceedings of the National Academy of Sciences* 106(43), pp.18333-18338.

136. Lazuardi, L., Herndler-Brandstetter, D., Brunner, S., Laschober, G.T., Lepperdinger, G. and Grubeck-Loebenstein, B., 2009. Microarray analysis reveals similarity between $CD8^+$ $CD28^-$ T cells from young and elderly persons, but not of $CD8^+$ $CD28^+$ T cells. *Biogerontology* 10(2), pp.191-202.

137. Hodes, R.J., 1997. Aging and the immune system. *Immunological reviews* 160(1), pp.5-8.

138. Saurwein-Teissl, M., Lung, T.L., Marx, F., Gschösser, C., Asch, E., Blasko, I., Parson, W., Böck, G., Schönitzer, D., Trannoy, E. and Grubeck-Loebenstein, B., 2002. Lack of antibody production following immunization in old age: association with $CD8^+$ $CD28^-$ T cell clonal expansions and an imbalance in the production of Th1 and Th2 cytokines. *The Journal of Immunology* 168(11), pp.5893-5899.

139. Weinberger, B., Herndler-Brandstetter, D., Schwanninger, A., Weiskopf, D. and Grubeck-Loebenstein, B., 2008. Biology of immune responses to vaccines in elderly persons. *Clinical Infectious Diseases* 46(7), pp.1078-1084.

140. Carlin, L.M., Yanagi, K., Verhoef, A., Hoen, E.N.N.T., Yates, J., Gardner, L., Lamb, J., Lombardi, G., Dallman, M.J. and Davis, D.M., 2005. Secretion of IFN-γ and not IL-2 by anergic human T cells correlates with assembly of an immature immune synapse. *Blood* 106(12), pp.3874-3879.

141. Rink, L., Cakman, I. and Kirchner, H., 1998. Altered cytokine production in the elderly. *Mechanisms of ageing and development* 102(2-3), pp.199-209.

142. Weyand, C.M., Brandes, J.C., Schmidt, D., Fulbright, J.W. and Goronzy, J.J., 1998. Functional properties of $CD4^+$ $CD28^-$ T cells in the aging immune system. *Mechanisms of ageing and development* 102(2-3), pp.131-147.

143. Hwang, K.A., Kim, H.R. and Kang, I., 2009. Aging and human $CD4^+$ regulatory T cells. *Mechanisms of ageing and development* 130(8), pp.509-517.

144. Nishioka, T., Shimizu, J., Iida, R., Yamazaki, S. and Sakaguchi, S., 2006. CD4+ $CD25^+$ $Foxp3^+$ T cells and $CD4^+$ $CD25^-$ $Foxp3^+$ T cells in aged mice. *The Journal of Immunology* 176(11), pp.6586-6593.

145. Huang, M.C., Liao, J.J., Bonasera, S., Longo, D.L. and Goetzl, E.J., 2008. Nuclear factor-κβ-dependent reversal of aging-induced alterations in T cell cytokines. *The FASEB Journal* 22(7), pp.2142-2150.

146. Adolfsson, O., Huber, B.T. and Meydani, S.N., 2001. Vitamin E-enhanced IL-2 production in old mice: naive but not memory T cells show increased cell division cycling and IL-2-producing capacity. *The Journal of Immunology* 167(7), pp.3809-3817.

147. Linton, P.J., Haynes, L., Tsui, L., Zhang, X. and Swain, S., 1997. From naive to effector-alterations with aging. *Immunological reviews* 160(1), pp.9-18.

148. Nagel, J.E., Chopra, R.K., Chrest, F.J., McCoy, M.T., Schneider, E.L., Holbrook, N.J. and Adler, W.H., 1988. Decreased proliferation, interleukin 2 synthesis, and interleukin 2 receptor expression are accompanied by decreased mRNA expression in phytohemagglutinin-stimulated cells from elderly donors. *The Journal of clinical investigation* 81(4), pp.1096-1102.

149. Eisenbraun, M.D., Tamir, A. and Miller, R.A., 2000. Altered composition of the immunological synapse in an anergic, age-dependent memory T cell subset. *The Journal of Immunology* 164(12), pp.6105-6112.

150. Das, R., Ponnappan, S. and Ponnappan, U., 2007. Redox regulation of the proteasome in T lymphocytes during aging. *Free Radical Biology and Medicine* 42(4), pp.541-551.

151. Flescher, E., Ledbetter, J.A., Schieven, G.L., Vela-Roch, N., Fossum, D., Dang, H., Ogawa, N. and Talal, N., 1994. Longitudinal exposure of human T lymphocytes to weak oxidative stress suppresses transmembrane and nuclear signal transduction. *The Journal of Immunology* 153(11), pp.4880-4889.

152. Haynes, L., Linton, P.J., Eaton, S.M., Tonkonogy, S.L. and Swain, S.L., 1999. Interleukin 2, but not other common γ chain–binding cytokines, can reverse the defect in generation of CD4 effector T cells from naive T cells of aged mice. *The Journal of experimental medicine* 190(7), pp.1013-1024.

153. Thoman ML. Weigle WO., 1981. Lymphokines and aging: interleukin-2 production and activity in aged animals. *The Journal of Immunology* 127:2102–2106.

154. Bhat, M., Robichaud, N., Hulea, L., Sonenberg, N., Pelletier, J. and Topisirovic, I., 2015. Targeting the translation machinery in cancer. *Nature reviews Drug discovery* 14(4), pp.261-278.

155. Iglesias-Bartolome, R., Patel, V., Cotrim, A., Leelahavanichkul, K., Molinolo, A.A., Mitchell, J.B. and Gutkind, J.S., 2012. mTOR inhibition prevents epithelial stem cell senescence and protects from radiation-induced mucositis. *Cell stem cell* 11(3), pp.401-414.

156. Hara, K., Maruki, Y., Long, X., Yoshino, K.I., Oshiro, N., Hidayat, S., Tokunaga, C., Avruch, J. and Yonezawa, K., 2002. Raptor, a binding partner of target of rapamycin (TOR), mediates TOR action. *Cell* 110(2), pp.177-189.

157. Kim DH, Sarbassov DD, Ali SM., 2002. mTOR Interacts with Raptor to Form a Nutrient-Sensitive Complex that Signals to the Cell Growth Machinery. *Cell* 110(2):163–75. 10.1016/S0092-8674(02)00808-5

158. Sarbassov, D.D., Ali, S.M., Kim, D.H., Guertin, D.A. and Latek, R.R., H. 41 Erdjument-Bromage, P. Tempst, and DM Sabatini. 2004. Rictor, a novel 42 binding partner of mTOR, defines a rapamycin-insensitive and raptor-43 independent pathway that regulates the cytoskeleton. *Current Biology* 14, pp.1296-302.

159. Uchenunu, O., Pollak, M., Topisirovic, I. and Hulea, L., 2019. Oncogenic kinases and perturbations in protein synthesis machinery and energetics in neoplasia. *Journal of Molecular Endocrinology* 62(2), pp.R83-R103.

160. Takahara, T. and Maeda, T., 2013. Evolutionarily conserved regulation of TOR signalling. *The journal of biochemistry* 154(1), pp.1-10.

161. Blagosklonny, M.V., 2014. Geroconversion: irreversible step to cellular senescence. *Cell cycle* 13(23), pp.3628-3635.

162. Campisi, J. and d'Adda di Fagagna, F., 2007. Cellular senescence: when bad things happen to good cells. *Nature reviews Molecular cell biology* 8(9), pp.729-740.

163. Althubiti, M., Lezina, L., Carrera, S., Jukes-Jones, R., Giblett, S.M., Antonov, A., Barlev, N., Saldanha, G.S., Pritchard, C.A., Cain, K. and Macip, S., 2014. Characterization of novel markers of senescence and their prognostic potential in cancer. *Cell death & disease* 5(11), pp.e1528-e1528.

164. Delgoffe, G.M., Pollizzi, K.N., Waickman, A.T., Heikamp, E., Meyers, D.J., Horton, M.R., Xiao, B., Worley, P.F. and Powell, J.D., 2011. The kinase mTOR regulates the differentiation of helper T cells through the selective activation of signaling by mTORC1 and mTORC2. *Nature immunology* 12(4), pp.295-303.

165. Düvel, K., Yecies, J.L., Menon, S., Raman, P., Lipovsky, A.I., Souza, A.L., Triantafellow, E., Ma, Q., Gorski, R., Cleaver, S. and Vander Heiden, M.G., 2010. Activation of a metabolic gene regulatory network downstream of mTOR complex 1. *Molecular cell* 39(2), pp.171-183.

166. Wang, R., Dillon, C.P., Shi, L.Z., Milasta, S., Carter, R., Finkelstein, D., McCormick, L.L., Fitzgerald, P., Chi, H., Munger, J. and Green, D.R., 2011. The transcription factor Myc controls metabolic reprogramming upon T lymphocyte activation. *Immunity* 35(6), pp.871-882.

167. Stallone, G., Infante, B., Prisciandaro, C. and Grandaliano, G., 2019. mTOR and aging: an old fashioned dress. *International journal of molecular sciences* 20(11), p.2774.

168. Powell, J.D., Lerner, C.G. and Schwartz, R.H., 1999. Inhibition of cell cycle progression by rapamycin induces T cell clonal anergy even in the presence of costimulation. *The Journal of Immunology* 162(5), pp.2775-2784.

169. Zheng, Y., Delgoffe, G.M., Meyer, C.F., Chan, W. and Powell, J.D., 2009. Anergic T cells are metabolically anergic. *The Journal of Immunology* 183(10), pp.6095-6101.

170. Sinclair, L.V., Finlay, D., Feijoo, C., Cornish, G.H., Gray, A., Ager, A., Okkenhaug, K., Hagenbeek, T.J., Spits, H. and Cantrell, D.A., 2008. Phosphatidylinositol-3-OH kinase and nutrient-sensing mTOR pathways control T lymphocyte trafficking. *Nature immunology* 9(5), pp.513-521.

171. Thomson, A.W., Turnquist, H.R. and Raimondi, G., 2009. Immunoregulatory functions of mTOR inhibition. *Nature Reviews Immunology* 9(5), pp.324-337.

172. Lee, K., Gudapati, P., Dragovic, S., Spencer, C., Joyce, S., Killeen, N., Magnuson, M.A. and Boothby, M., 2010. Mammalian target of rapamycin protein complex 2 regulates differentiation of Th1 and Th2 cell subsets via distinct signaling pathways. *Immunity* /32(6), pp.743-753.

173. Wing, K. and Sakaguchi, S., 2010. Regulatory T cells exert checks and balances on self-tolerance and autoimmunity. *Nature immunology* 11(1), pp.7-13.

174. Guillonneau, C., Picarda, E. and Anegon, I., 2010. CD8+ regulatory T cells in solid organ transplantation. Current opinion in organ transplantation, 15(6), pp.751-756.

175. Dai, Z., Zhang, S., Xie, Q., Wu, S., Su, J., Li, S., Xu, Y. and Li, X.C., 2014. Natural CD8+ CD122+ T cells are more potent in suppression of allograft rejection than CD4+ CD25+ regulatory T cells. *American Journal of Transplantation* 14(1), pp.39-48.

176. Battaglia, M., Stabilini, A. and Roncarolo, M.G., 2005. Rapamycin selectively expands CD4+ CD25+ FoxP3+ regulatory T cells. *Blood* 105(12), pp.4743-4748.

177. Strauss, L., Whiteside, T.L., Knights, A., Bergmann, C., Knuth, A. and Zippelius, A., 2007. Selective survival of naturally occurring human $CD4^+$ $CD25^+$ $Foxp3^+$ regulatory T cells cultured with rapamycin. *The Journal of Immunology* 178(1), pp.320-329.

178. Kopf, H., Gonzalo, M., Howard, O.Z. and Chen, X., 2007. Rapamycin inhibits differentiation of Th17 cells and promotes generation of FoxP3^{+} T regulatory cells. *International immunopharmacology* 7(13), pp.1819-1824.

179. Araki, K., Turner, A.P., Shaffer, V.O., Gangappa, S., Keller, S.A., Bachmann, M.F., Larsen, C.P. and Ahmed, R., 2009. mTOR regulates memory CD8 T-cell differentiation. *Nature* 460(7251), pp.108-112.

180. Rao, R.R., Li, Q., Odunsi, K. and Shrikant, P.A., 2010. The mTOR kinase determines effector versus memory CD8^{+} T cell fate by regulating the expression of transcription factors T-bet and Eomesodermin. *Immunity* 32(1), pp.67-78.

181. Kapsenberg, M.L., 2003. Dendritic-cell control of pathogen-driven T-cell polarization. *Nature Reviews Immunology* 3(12), pp.984-993.

182. Taner, T., Hackstein, H., Wang, Z., Morelli, A.E. and Thomson, A.W., 2005. Rapamycin-treated, alloantigen-pulsed host dendritic cells induce ag-specific T cell regulation and prolong graft survival. *American Journal of Transplantation* 5(2), pp.228-236.

183. Turnquist, H.R., Raimondi, G., Zahorchak, A.F., Fischer, R.T., Wang, Z. and Thomson, A.W., 2007. Rapamycin-conditioned dendritic cells are poor stimulators of allogeneic CD4^{+} T cells, but enrich for antigen-specific Foxp3+ T regulatory cells and promote organ transplant tolerance. *The Journal of Immunology* 178(11), pp.7018-7031.

184. Hackstein, H., Taner, T., Zahorchak, A.F., Morelli, A.E., Logar, A.J., Gessner, A. and Thomson, A.W., 2003. Rapamycin inhibits IL-4 induced dendritic cell maturation in vitro and dendritic cell mobilization and function in vivo. *Blood* 101(11), pp.4457-4463.

185. Waskow, C., Liu, K., Darrasse-Jèze, G., Guermonprez, P., Ginhoux, F., Merad, M., Shengelia, T., Yao, K. and Nussenzweig, M., 2008. The receptor tyrosine kinase Flt3 is

required for dendritic cell development in peripheral lymphoid tissues. *Nature immunology* 9(6), pp.676-683.

186. Woltman, A.M., de Fijter, J.W., Kamerling, S.W., van der Kooij, S.W., Paul, L.C., Daha, M.R. and van Kooten, C., 2001. Rapamycin induces apoptosis in monocyte-and CD34-derived dendritic cells but not in monocytes and macrophages. *Blood, The Journal of the American Society of Hematology* 98(1), pp.174-180.
187. Sordi, V., Bianchi, G., Buracchi, C., Mercalli, A., Marchesi, F., D'Amico, G., Yang, C.H., Luini, W., Vecchi, A., Mantovani, A. and Allavena, P., 2006. Differential effects of immunosuppressive drugs on chemokine receptor CCR7 in human monocyte-derived dendritic cells: selective upregulation by rapamycin. *Transplantation* 82(6), pp.826-834.
188. Swiecki, M. and Colonna, M., 2015. The multifaceted biology of plasmacytoid dendritic cells. *Nature Reviews Immunology* 15(8), pp.471-485.
189. Stallone, G., Pontrelli, P., Infante, B., Gigante, M., Netti, G.S., Ranieri, E., Grandaliano, G. and Gesualdo, L., 2014. Rapamycin induces ILT3^{high}ILT4^{high} dendritic cells promoting a new immunoregulatory pathway. *Kidney International* 85(4), pp.888-897.
190. Van de Laar, L., Coffer, P.J. and Woltman, A.M., 2012. Regulation of dendritic cell development by GM-CSF: molecular control and implications for immune homeostasis and therapy. *Blood, The Journal of the American Society of Hematology* 119(15), pp.3383-3393.
191. Banchereau, J. and Steinman, R.M., 1998. Dendritic cells and the control of immunity. *Nature* 392(6673), pp.245-252.
192. Merad, M. and Manz, M.G., 2009. Dendritic cell homeostasis. *Blood, The Journal of the American Society of Hematology* 113(15), pp.3418-3427.

193. Inaba, K., Steinman, R.M., Pack, M.W., Aya, H., Inaba, M., Sudo, T., Wolpe, S. and Schuler, G., 1992. Identification of proliferating dendritic cell precursors in mouse blood. *The Journal of experimental medicine* 175(5), pp.1157-1167.

194. Sallusto, F. and Lanzavecchia, A., 1994. Efficient presentation of soluble antigen by cultured human dendritic cells is maintained by granulocyte/macrophage colony-stimulating factor plus interleukin 4 and downregulated by tumor necrosis factor alpha. *The Journal of experimental medicine* 179(4), pp.1109-1118.

195. Daro, E., Pulendran, B., Brasel, K., Teepe, M., Pettit, D., Lynch, D.H., Vremec, D., Robb, L., Shortman, K., McKenna, H.J. and Maliszewski, C.R., 2000. Polyethylene glycol-modified GM-CSF expands $CD11b^{high}CD11c^{high}$ but not $CD11bl^{ow}CD11c^{high}$ murine dendritic cells in vivo: a comparative analysis with Flt3 ligand. *The Journal of Immunology* 165(1), pp.49-58.

196. Vremec, D., Lieschke, G.J., Dunn, A.R., Robb, L., Metcalf, D. and Shortman, K., 1997. The influence of granulocyte/macrophage colony-stimulating factor on dendritic cell levels in mouse lymphoid organs. *European journal of immunology* 27(1), pp.40-44.

197. Kingston, D., Schmid, M.A., Onai, N., Obata-Onai, A., Baumjohann, D. and Manz, M.G., 2009. The concerted action of GM-CSF and Flt3-ligand on in vivo dendritic cell homeostasis. *Blood, The Journal of the American Society of Hematology* 114(4), pp.835-843.

198. Bogunovic, M., Ginhoux, F., Helft, J., Shang, L., Hashimoto, D., Greter, M., Liu, K., Jakubzick, C., Ingersoll, M.A., Leboeuf, M. and Stanley, E.R., 2009. Origin of the lamina propria dendritic cell network. *Immunity* 31(3), pp.513-525.

199. Varol, C., Vallon-Eberhard, A., Elinav, E., Aychek, T., Shapira, Y., Luche, H., Fehling, H.J., Hardt, W.D., Shakhar, G. and Jung, S., 2009. Intestinal lamina propria dendritic cell subsets have different origin and functions. *Immunity* 31(3), pp.502-512.

200. Gilliet, M., Boonstra, A., Paturel, C., Antonenko, S., Xu, X.L., Trinchieri, G., O'Garra, A. and Liu, Y.J., 2002. The development of murine plasmacytoid dendritic cell precursors is differentially regulated by FLT3-ligand and granulocyte/macrophage colony-stimulating factor. *The Journal of experimental medicine* 195(7), pp.953-958.

201. Ghirelli, C., Zollinger, R. and Soumelis, V., 2010. Systematic cytokine receptor profiling reveals GM-CSF as a novel TLR-independent activator of human plasmacytoid predendritic cells. *Blood, The Journal of the American Society of Hematology* 115(24), pp.5037-5040.

202. Hamilton, J.A., 2008. Colony-stimulating factors in inflammation and autoimmunity. *Nature Reviews Immunology* 8(7), pp.533-544.

203. Xu, Y., Zhan, Y., Lew, A.M., Naik, S.H. and Kershaw, M.H., 2007. Differential development of murine dendritic cells by GM-CSF versus Flt3 ligand has implications for inflammation and trafficking. *The Journal of Immunology* 179(11), pp.7577-7584.

204. Shortman, K. and Naik, S.H., 2007. Steady-state and inflammatory dendritic-cell development. *Nature Reviews Immunology* 7(1), pp.19-30.

205. Barreda, D.R., Hanington, P.C. and Belosevic, M., 2004. Regulation of myeloid development and function by colony stimulating factors. *Developmental & Comparative Immunology* 28(5), pp.509-554.

206. Shearer, W.T., Rosenwasser, L.J., Bochner, B.S., Martinez-Moczygemba, M. and Huston, D.P., 2003. Biology of common β receptor–signaling cytokines: IL-3, IL-5, and GM-CSF. *Journal of Allergy and Clinical Immunology* 112(4), pp.653-665.

207. Geijsen, N., Koenderman, L. and Coffer, P.J., 2001. Specificity in cytokine signal transduction: lessons learned from the IL-3/IL-5/GM-CSF receptor family. *Cytokine & growth factor reviews*, 12(1), pp.19-25.

208. Hercus, T.R., Thomas, D., Guthridge, M.A., Ekert, P.G., King-Scott, J., Parker, M.W. and Lopez, A.F., 2009. The granulocyte-macrophage colony-stimulating factor receptor: linking its structure to cell signaling and its role in disease. *Blood, The Journal of the American Society of Hematology* 114(7), pp.1289-1298.

209. Meads, M.B., Li, Z.W. and Dalton, W.S., 2010. A novel TNF receptor-associated factor 6 binding domain mediates NF-κB signaling by the common cytokine receptor β subunit. *The Journal of Immunology* 185(3), pp.1606-1615.

210. Ebner, K., Bandion, A., Binder, B.R., de Martin, R. and Schmid, J.A., 2003. GMCSF activates NF-κB via direct interaction of the GMCSF receptor with IκB kinase β. *Blood* 102(1), pp.192-199.

211. Zhong, J., Yang, P., Muta, K., Dong, R., Marrero, M., Gong, F. and Wang, C.Y., 2010. Loss of Jak2 selectively suppresses DC-mediated innate immune response and protects mice from lethal dose of LPS-induced septic shock. *PLoS One* 5(3), p.e9593.

212. Laouar, Y., Welte, T., Fu, X.Y. and Flavell, R.A., 2003. STAT3 is required for Flt3L-dependent dendritic cell differentiation. *Immunity* 19(6), pp.903-912.

213. Onai, N., Obata-Onai, A., Tussiwand, R., Lanzavecchia, A. and Manz, M.G., 2006. Activation of the Flt3 signal transduction cascade rescues and enhances type I interferon–

producing and dendritic cell development. *The Journal of experimental medicine* 203(1), pp.227-238.

214. Cohen, P.A., Koski, G.K., Czerniecki, B.J., Bunting, K.D., Fu, X.Y., Wang, Z., Zhang, W.J., Carter, C.S., Awad, M., Distel, C.A. and Nagem, H., 2008. STAT3-and STAT5-dependent pathways competitively regulate the pan-differentiation of CD34pos cells into tumor-competent dendritic cells. *Blood, The Journal of the American Society of Hematology* 112(5), pp.1832-1843.

215. Esashi, E., Wang, Y.H., Perng, O., Qin, X.F., Liu, Y.J. and Watowich, S.S., 2008. The signal transducer STAT5 inhibits plasmacytoid dendritic cell development by suppressing transcription factor IRF8. *Immunity* 28(4), pp.509-520.

216. Van de Laar, L., van den Bosch, A., Wierenga, A.T., Janssen, H.L., Coffer, P.J. and Woltman, A.M., 2011. Tight control of STAT5 activity determines human CD34$^-$derived interstitial dendritic cell and langerhans cell development. *The Journal of Immunology* 186(12), pp.7016-7024.

217. Choi, Y.E., Yu, H.N., Yoon, C.H. and Bae, Y.S., 2009. Tumor-mediated down-regulation of MHC class II in DC development is attributable to the epigenetic control of the CIITA type I promoter. *European journal of immunology* 39(3), pp.858-868.

218. Sebastián, C., Serra, M., Yeramian, A., Serrat, N., Lloberas, J. and Celada, A., 2008. Deacetylase activity is required for STAT5-dependent GM-CSF functional activity in macrophages and differentiation to dendritic cells. *The Journal of Immunology* 180(9), pp.5898-5906.

219. Fujita, J., Mizuki, M., Otsuka, M., Ezoe, S., Tanaka, H., Satoh, Y., Fukushima, K., Tokunaga, M., Matsumura, I. and Kanakura, Y., 2011. Myeloid neoplasm-related gene

abnormalities differentially affect dendritic cell differentiation from murine hematopoietic stem/progenitor cells. *Immunology Letters* 136(1), pp.61-73.

220. Fukao, T., Tanabe, M., Terauchi, Y., Ota, T., Matsuda, S., Asano, T., Kadowaki, T., Takeuchi, T. and Koyasu, S., 2002. PI3K-mediated negative feedback regulation of IL-12 production in DCs. *Nature immunology* 3(9), pp.875-881.
221. Sathaliyawala, T., O'Gorman, W.E., Greter, M., Bogunovic, M., Konjufca, V., Hou, Z.E., Nolan, G.P., Miller, M.J., Merad, M. and Reizis, B., 2010. Mammalian target of rapamycin controls dendritic cell development downstream of Flt3 ligand signaling. *Immunity* 33(4), pp.597-606.
222. Antignano, F., Ibaraki, M., Kim, C., Ruschmann, J., Zhang, A., Helgason, C.D. and Krystal, G., 2010. SHIP is required for dendritic cell maturation. *The Journal of Immunology* 184(6), pp.2805-2813.
223. Van de Laar, L., Buitenhuis, M., Wensveen, F.M., Janssen, H.L., Coffer, P.J. and Woltman, A.M., 2010. Human CD34$^-$derived myeloid dendritic cell development requires intact phosphatidylinositol 3-kinase–protein kinase B–mammalian target of rapamycin signaling. *The Journal of Immunology* 184(12), pp.6600-6611.
224. Haidinger, M., Poglitsch, M., Geyeregger, R., Kasturi, S., Zeyda, M., Zlabinger, G.J., Pulendran, B., Hörl, W.H., Säemann, M.D. and Weichhart, T., 2010. A versatile role of mammalian target of rapamycin in human dendritic cell function and differentiation. *The Journal of Immunology* 185(7), pp.3919-3931.
225. Woltman, A.M., de Fijter, J.W., Kamerling, S.W., van der Kooij, S.W., Paul, L.C., Daha, M.R. and van Kooten, C., 2001. Rapamycin induces apoptosis in monocyte-and CD34$^-$

derived dendritic cells but not in monocytes and macrophages. *Blood, The Journal of the American Society of Hematology* 98(1), pp.174-180.

226. Woltman, A.M., van der Kooij, S.W., Coffer, P.J., Offringa, R., Daha, M.R. and van Kooten, C., 2003. Rapamycin specifically interferes with GM-CSF signaling in human dendritic cells, leading to apoptosis via increased p27KIP1 expression. *Blood, The Journal of the American Society of Hematology* 101(4), pp.1439-1445.
227. Kim, J.H., Kang, T.H., Noh, K.H., Kim, S.H., Lee, Y.H., Kim, K.W., Bae, H.C., Ahn, Y.H., Choi, E.Y., Kim, J.S. and Lee, K.M., 2010. Enhancement of DC vaccine potency by activating the PI3K/AKT pathway with a small interfering RNA targeting PTEN. *Immunology letters* 134(1), pp.47-54.
228. Park, D., Lapteva, N., Seethammagari, M., Slawin, K.M. and Spencer, D.M., 2006. An essential role for Akt1 in dendritic cell function and tumor immunotherapy. *Nature biotechnology* 24(12), pp.1581-1590.
229. Hackstein, H., Taner, T., Logar, A.J. and Thomson, A.W., 2002. Rapamycin inhibits macropinocytosis and mannose receptor–mediated endocytosis by bone marrow–derived dendritic cells. *Blood, The Journal of the American Society of Hematology* 100(3), pp.1084-1087.
230. Turnquist, H.R., Raimondi, G., Zahorchak, A.F., Fischer, R.T., Wang, Z. and Thomson, A.W., 2007. Rapamycin-conditioned dendritic cells are poor stimulators of allogeneic $CD4^+$ T cells, but enrich for antigen-specific $Foxp3^+$ T regulatory cells and promote organ transplant tolerance. *The Journal of Immunology* 178(11), pp.7018-7031.
231. Bendix, I., Pfueller, C.F., Leuenberger, T., Glezeva, N., Siffrin, V., Müller, Y., Prozorovski, T., Hansen, W., Topphoff, U.S., Loddenkemper, C. and Zipp, F., 2010.

MAPK3 deficiency drives autoimmunity via DC arming. *European journal of immunology* 40(5), pp.1486-1495.

232. Xie, J., Qian, J., Yang, J., Wang, S., Freeman III, M.E. and Yi, Q., 2005. Critical roles of Raf/MEK/ERK and PI3K/AKT signaling and inactivation of p38 MAP kinase in the differentiation and survival of monocyte-derived immature dendritic cells. Experimental hematology, 33(5), pp.564-572.

233. Wang, S., Yang, J., Qian, J., Wezeman, M., Kwak, L.W. and Yi, Q., 2006. Tumor evasion of the immune system: inhibiting p38 MAPK signaling restores the function of dendritic cells in multiple myeloma. *Blood* 107(6), pp.2432-2439.

234. Xie, J., Qian, J., Wang, S., Freeman, M.E., Epstein, J. and Yi, Q., 2003. Novel and detrimental effects of lipopolysaccharide on in vitro generation of immature dendritic cells: involvement of mitogen-activated protein kinase p38. *The Journal of Immunology* 171(9), pp.4792-4800.

235. Ouaaz, F., Arron, J., Zheng, Y., Choi, Y. and Beg, A.A., 2002. Dendritic cell development and survival require distinct NF-κB subunits. *Immunity* 16(2), pp.257-270.

236. Gu, X.Y., Zhou, L.F., Zhang, M.S., Dai, W.J., Chen, S.Y., He, S.H., Ji, X.H. and Yin, K.S., 2009. Targeted NF-κB inhibition of asthmatic serum-mediated human monocyte-derived dendritic cell differentiation in a transendothelial trafficking model. *Cellular immunology* 260(1), pp.14-20.

237. Zhou, L.F., Zhang, M.S., Yin, K.S., Ji, Y., Xie, W.P., Cui, X.F. and JI, X.H., 2006. Effects of adenoviral gene transfer of mutated IκBα, a novel inhibitor of NF-κB, on human monocyte-derived dendritic cells 1. *Acta Pharmacologica Sinica* 27(5), pp.609-616.

238. Platzer, B., Jörgl, A., Taschner, S., Höcher, B. and Strobl, H., 2004. RelB regulates human dendritic cell subset development by promoting monocyte intermediates. *Blood* 104(12), pp.3655-3663.

239. Hayden, M.S., West, A.P. and Ghosh, S., 2006. NF-κB and the immune response. *Oncogene* 25(51), pp.6758-6780.

240. Sukhbaatar, N., Hengstschläger, M. and Weichhart, T., 2016. mTOR-mediated regulation of dendritic cell differentiation and function. *Trends in immunology* 37(11), pp.778-789.

241. Clements, S.J., Maijo, M., Ivory, K., Nicoletti, C. and Carding, S.R., 2017. Age-associated decline in dendritic cell function and the impact of Mediterranean diet intervention in elderly subjects. Frontiers in Nutrition, 4, p.65.

242. Zacca, E.R., Crespo, M.I., Acland, R.P., Roselli, E., Núñez, N.G., Maccioni, M., Maletto, B.A., Pistoresi-Palencia, M.C. and Morón, G., 2015. Aging impairs the ability of conventional dendritic cells to cross-prime CD8+ T cells upon stimulation with a TLR7 ligand. PloS one, 10(10), p.e0140672.

243. Luo, L., Wall, A.A., Yeo, J.C., Condon, N.D., Norwood, S.J., Schoenwaelder, S., Chen, K.W., Jackson, S., Jenkins, B.J., Hartland, E.L. and Schroder, K., 2014. Rab8a interacts directly with PI3Kγ to modulate TLR4-driven PI3K and mTOR signalling. *Nature communications* 5(1), p.4407.

244. Chatta, G.S., Andrews, R.G., Rodger, E., Schrag, M., Hammond, W.P. and Dale, D.C., 1993. Hematopoietic progenitors and aging: alterations in granulocytic precursors and responsiveness to recombinant human G-CSF, GM-CSF, and IL-3. Journal of gerontology, 48(5), pp.M207-M212.

245. Grolleau-Julius, A., Garg, M.R., Mo, R., Stoolman, L.L. and Yung, R.L., 2006. Effect of aging on bone marrow-derived murine $CD11c^{+}$ $CD4^{-}$ $CD8\alpha^{-}$ dendritic cell function. The Journals of Gerontology Series A: Biological Sciences and Medical Sciences, 61(10), pp.1039-1047.

246. Shurin, M.R., Shurin, G.V. and Chatta, G.S., 2007. Aging and the dendritic cell system: implications for cancer. Critical reviews in oncology/hematology, 64(2), pp.90-105.

247. Ho, Y.H. and Méndez-Ferrer, S., 2020. Microenvironmental contributions to hematopoietic stem cell aging. Haematologica, 105(1), p.38.

248. Lefebvre, J.S., Maue, A.C., Eaton, S.M., Lanthier, P.A., Tighe, M. and Haynes, L., 2012. The aged microenvironment contributes to the age-related functional defects of CD4 T cells in mice. Aging cell, 11(5), pp.732-740.

249. Zhang, L., Mack, R., Breslin, P. and Zhang, J., 2020. Molecular and cellular mechanisms of aging in hematopoietic stem cells and their niches. Journal of Hematology & Oncology, 13, pp.1-22.

250. Leimkühler, N.B. and Schneider, R.K., 2019. Inflammatory bone marrow microenvironment. Hematology 2014, the American Society of Hematology Education Program Book, 2019(1), pp.294-302.

251. Kennedy, D.E. and Knight, K.L., 2017. Inflammatory changes in bone marrow microenvironment associated with declining B lymphopoiesis. The Journal of Immunology, 198(9), pp.3471-3479.

252. Del Prete, A., Salvi, V., Soriani, A., Laffranchi, M., Sozio, F., Bosisio, D. and Sozzani, S., 2023. Dendritic cell subsets in cancer immunity and tumor antigen sensing. Cellular & Molecular Immunology, 20(5), pp.432-447.

253. Veglia, F. and Gabrilovich, D.I., 2017. Dendritic cells in cancer: the role revisited. Current opinion in immunology, 45, pp.43-51.

254. Grigoriev, I., Yu, K.L., Martinez-Sanchez, E., Serra-Marques, A., Smal, I., Meijering, E., Demmers, J., Peränen, J., Pasterkamp, R.J., van der Sluijs, P. and Hoogenraad, C.C., 2011. Rab6, Rab8, and MICAL3 cooperate in controlling docking and fusion of exocytotic carriers. *Current Biology* 21(11), pp.967-974.

255. Nachury, M.V., Loktev, A.V., Zhang, Q., Westlake, C.J., Peränen, J., Merdes, A., Slusarski, D.C., Scheller, R.H., Bazan, J.F., Sheffield, V.C. and Jackson, P.K., 2007. A core complex of BBS proteins cooperates with the GTPase Rab8 to promote ciliary membrane biogenesis. *Cell* 129(6), pp.1201-1213.

PART II

Rab8a restores function in dendritic cells of an aging host

The research work described in the thesis is a slight modification of the manuscript entitled, "Rab8a restores function in dendritic cells of an aging host" submitted for publication.

The terms "our" and "we" refers to me and the co-authors. My contribution includes

(1) Selection of the topic

(2) Compiling and interpretation of the literature

(3) Designing experiments

(4) Understanding the literature and interpretation of the results

(5) Providing comprehensible structure to the paper

(6) Preparation of graphs and figures

(7) Writing and editing of the manuscript.

Abstract

Dendritic cells (DCs) of un-manipulated aged (>20 months) and young (2 months) mice when subjected to genome wide RNAseq analysis revealed a compromised IFN response. Influenza A virus (IAV) or a γ-herpesvirus (MHV68) stimulated DCs from aged humans and mice mounted inhibited type I IFN response. Furthermore, DCs of aged animals were found deficient in processing and presentation of exogenous antigens that led to poor expansion of ovalbumin specific TCR transgenic $CD8^+$ T cells (OT1 cells) *in vitro* as well as *in vivo* in DC-immunization protocols. Reconstituting DCs with Rab8a, a small GTPase, acting downstream to growth factor receptor and known to enhance membrane trafficking restored impaired differentiation and maturation of DCs from aging host. Such DCs induced potent anti-viral IFNs response and more vigorously activated specific $CD8^+$ T cells to efficiently control IAV infection. Rab8a colocalized with Rab11 marked endosomal recycling compartment (ERC) that preferentially stored the generated peptide-MHC I complexes for their efficient surface display to engage with specific $CD8^+$ T cells. We therefore demonstrated Rab8a as a critical regulator of DCs in aging host controlling their differentiation and functionality and its immune potentiating effects following reconstitution.

Introduction

Dendritic cells (DCs) serve as the sentinel cells of the immune system because of their strategic location at tissue sites. Following recognition of invading pathogens, these cells produce effector molecules such as type I IFNs that have direct anti-viral functions. A compromised type I IFN response due to genetic deficiencies in the innate immune receptors or their downstream adaptor molecules results in poor viral control and sets the stage for a protracted immunopathological reaction. DCs are also crucial for an efficient activation of T cells, a subset of which exhibits cytolytic activity against the infected targets (1). A progressive loss of immune functions is also evident in the aging population and consequently this group shows enhanced mortality following viral infection (2). Therefore, the molecular analysis of DCs in contributing to the process of immunosenescence could help understand better the age related aberrations leading to immune impairment, and it can further help devise strategies not only to improve the outcome of infection but also in enhancing the efficacy of vaccines in the aging population.

Several factors such as the altered architecture of lymphoid organs, dysregulated migratory patterns of immune cells, inefficient production of soluble and cellular mediators, altered composition of milieu in secondary lymphoid tissues leading to an impaired T cell priming could all contribute to compromised immune functions in the aging host (3). Absolute numbers as well as the clonal diversity of adaptive immune cells are reduced in an aging host (4). Furthermore, the turnover rates and functionality of the residual cells of adaptive immune system are also diminished (5). The age-related impairment also occurs in innate immune cells and such cells exhibit impaired cytokine signalling, phagocytosis as well as antigen-uptake (6). Immunosenence, therefore, is a complex process and its reversal is challenging. While the consequences of immunosenescence have been studied, molecular mechanisms underlying such processes remain

largely unexplored that we aimed at investigating in this study. Given the critical roles of DCs in linking innate and adaptive immune defenses, we performed a genome-wide transcriptomic analysis of $CD11b^{+}CD11c^{+}$ DCs isolated from lymphoid organs of unmanipulated young and aged mice.

Genes encoding the products of multiple pathways known to drive the differentiation, maturation and functionality of DCs were downregulated in the aged animals. Majority of genes in type I IFN signalling pathway showed significantly reduced expression in DCs of aged animals as well as humans as compared to their younger counterparts. Since IFN response critically controls the maturation of DCs, we analyzed the effects that a lack of IFN signalling might have in their differentiation and functionality in aged mice. Bone marrow derived DCs (BMDCs) as well as splenic DCs (spDCs) of animals depleted of IFN signalling (IFNRKO) expressed lower level of costimulatory as well as class I and II MHC molecules and antigen pulsed DCs form IFNRKO failed to efficiently prime specific $CD8^{+}$ T cells *in vitro* as well as *in vivo*. Further analysis revealed that both spDCs and BMDCs of aged mice had reduced expression of *Rab8a*, a Ras-related small GTPase, which acts downstream to the growth factor receptor signalling. That the expression of Rab8a controlled the differentiation and functionality of DCs was shown by gene knockdown as well as reconstitution experiments. Accordingly, Rab8a depleted bone marrow precursors of young animals were not only compromised in ability to differentiate into mature DCs but also in their associated functions such as the production of cytokines, expression of costimulatory and homing molecules as well as antigen-presentation to stimulate antigen-specific $CD8^{+}$ T cells. DCs from aging animals reconstituted of Rab8a largely regained all the associated functions and conferred to the host an enhanced protection during respiratory virus infection with IAV. Rab8a reconstitution of DCs of aged animals showed enhanced levels of peptide-MHC I

complexes carrying Rab8a marked ERCs for an efficient surface display of antigenic peptides to induce $CD8^+$ T cell response. Our data, therefore, underpin a critical role of Rab8a in the response pattern of DCs in the aging host and showed that a reversal of immune functions could be achieved by reconstituting this molecule to improve outcome of viral infection.

Material and Methods

Mice, viruses and cells

The animal experiments were performed strictly in accordance with the protocols (IISERM/SAFE/PRT/2022/015, IISERM/SAFE/PRT/2022/028, IISERM/SAFE/PRT/2022/016 and IISERM/SAFE/PRT/2022/016) approved by the Institute Animal Ethics Committee (IAEC). The IAEC was constituted under the aegis of the Committee for the Purpose of Control and Supervision of Experiments on Animals (CPCSEA). Wild type C57BL/6 (Stock No. 000664), IFNR-KO (B6.Cg-Ifngr1tm1Agt Ifnar1tm1.2Ees/J; Stock no- 029098) and OT1 (C57BL/6-Tg (TcraTcrb)1100Mjb/J; Stock No. 003831) mice were obtained from Jackson laboratory, USA and bred at the Small Animal Facility for Experimentation (SAFE), IISER Mohali. Aged mice used for the experiments were between 18-24 months old. For adoptive transfer experiments, sex-matched CD45.1+ (B6.SJL-Ptprca Pepcb/BoyJ; Stock No. 002014) congenic mice were used. MHV68-SIINFEKL and IAV-WSN-SIINFEKL were grown and titrated using Vero and MDCK cells, respectively as described earlier (45, 46).

Ethics statement for human study

All the work with humans was approved by the institute ethics committee (IEC/2022/05) of the Indian Institute of Science Education and Research.

Antibody and other reagents

Antibodies used for measuring the expression of different molecules were obtained from BD biosciences, eBiosciences, Tonbo biosciences and BioLegend. The antibodies were against CD11c-PE-Cy7/PE (N418) (Dendritic cells marker), CD11b-FITC (M1/70), CCR5-(HM-CCR5),

CCR7-(4B12) CD80-PE (16-10A1), CD86-APC (GL-1), CD8-PerCP-Cy5.5 (530-6.7), CD44-APC (IM7), CD45.2-FITC, CD45.2-PE (104), CXCR3-FITC (173), TNFα-APC (TN3-19.12), IFNγ-PE (XMG1.2), MHCI-APC (28-8-6) and MHCII-APC (M5/114.15.2). CFSE (Carboxyfluorescein succinimidyl ester) and Cell-Trace^{TM} Far Red to label the live CD8^{+} T cells and BMDCs respectively were obtained from Invitrogen. PI staining was also done for assessing apoptotic cell frequency. Alexa Fluor^{TM} 488 Phalloidin (A12379) used for actin staining was obtained from Invitrogen. Anti-mouse-GAPDH (GA1R), anti-Akt pan (40D4), anti-Pakt1 (D25E6), anti-Rab11 (5589S), anti-mouse-Rab8a (261CT1.3.1) along with anti-mouse Alexa-Flour568 (A11004) were used in western blotting. GM-CSF (315-03) and IL-4 (214-14) cytokine obtained from peprotech were used in differentiation of BMDCs. The BMDCs were generated in 10% RPMI (10% FBS, and 10% Pen-strep). The HEK293T, VeroE6 and MDCK cells were maintained in 10% DMEM. Lentiviruses for knockdown (Rab8a-shRNA) and overexpression (Rab8a-OE) of Rab8a were generated using HEK293T cells and concentrated using PEG-NaCl (20% PEG-8000 and 1.2M NaCl).

Next-Generation Sequencing and differential gene expression

Total RNA samples from CD11b^{+}CD11c^{+} splenic dendritic cells of young and aged mice were sequenced using next generation sequencing. cDNA library preparation from the RNA samples was done using Illumina® TruSeq® Sample Preparation protocol. The generated cDNA libraries were sequenced using Illumina Hi-Seq-2000 platform. The data generated was analyzed by Tuxedo protocol where raw reads which were in of FAST-Q format were aligned to the reference genome of *Mus musculus* (mm9) using Tophat. Only high-quality reads with QC score of more than 20 were used for alignment. The obtained BAM (Binary version of SAM file) and SAM (Sequence alignment mapping) files, which were processed for abundance estimation by

cufflinks. For generating the list of differentially expressed genes the files were processed using Cuffdiff.

Functional annotation and network analysis of differentially expressed genes in DCs of aged mice

RNA-seq data was generated as described earlier (45). A threshold of 5 RPKM in either condition was set to narrow down the differentially expressed genes. To obtain a list of significantly differentially expressed (SDE) genes between the groups, another cut off of 1.5-fold change in young vs aged condition was applied. The functional annotation and gene ontology was performed using WEB-based Gene SeT AnaLysis Toolkit (Webgestalt, (http://webgestalt.org/option.php by considering *Mus musculus* genome as a reference genome. All the SDE genes were used as input for network analysis using STRING database (Search Tool for the Retrieval of Interacting Genes, https://string-db.org/). All the networks were generated using STRING default parameters (45).

***In vitro* BMDC generation**

Young (4–6-week-old), aged (>18 months old) Wild Type and IFNR-KO mice were sacrificed and bone marrow cells were isolated by flushing the femur and tibia with 10% RPMI. This was followed by RBC lysis using 1x RBC lysis buffer (155mM NH_4Cl, 12mM $NaHCO_3$, 0.1mM EDTA, pH 7.3). $15x10^6$ of the bone marrow cells were then re-suspended in 15 mL of 10% RPMI supplemented with 5ng/mL of GM-CSF and IL-4 and seeded in 100 mm petri dish for 6 days in a humidified CO_2 incubator. On alternate days after seeding, half of the culture medium was replaced with complete RPMI supplemented with 5ng/ml of IL-4 and GM-CSF. 5 days after culture the cells were harvested using a cell scrapper and washed twice with 10% RPMI at 4°C for 5 minutes at 200xg. Viability of the *in-vitro* generated BMDCs was assessed using trypan

blue staining. These cells were used for further characterisation as described below. Additionally 15 million bone marrow cells from young, aged and Rab8a-OE conditions were re-suspended in 15 mL of 10% RPMI supplemented with 20ng/mL of Flt3l and seeded in 100 mm petri dish for 6 days in a humidified CO2 incubator. On alternate day's medium change with 10%RPMI and 20ng/mL FLT3l was similar as expalained above.

Cloning of Rab8a-shRNA into pLKO.1GFP for knockdown and Rab8a into pLenti-GFP for overexpression and generation of lentiviruses and transduction of bone marrow cells

For the knockdown of Rab8a in bone marrow of young WT (C57BL/6) mice, shRNA sequences for Rab8a and scramble control were designed using default settings on www-data@wi.mit.edu site and cloned into a modified pLKO.1-GFP RNAi cloning vector (Figure 2.9.H). For generating lentiviruses 100-mm petri-dish seeded with HEK293T cells at 80% confluency were co-transfected with 5 plasmids, *viz.* 10µg Rab8a shRNA/scrambled construct, 9.8µg pCMVR8.74 (packaging vector), 6µg pMD2.G (envelope vector), 6µg Tat and 6µg Rev plasmids. The transfection mixture was prepared by mixing the plasmids in 1 mL of serum free DMEM containing PEI in a 1:3 ratio (DNA: PEI). The mixture was immediately vortexed for 20 seconds and then incubated at room temperature for 15 minutes. Post of incubation, the transfection mixture was overlaid carefully onto the HEK293T cells and plates were kept in humidified CO_2 incubator for 6 hours, following which the media was replaced with 10% DMEM and plates were left in the CO_2 incubator for 72 hours. Transfection of HEK293T cells were checked by visualization of GFP (Figure 2.9.H and 2.10.A). 72 hours post transfection, the supernatant was collected and centrifuged at 200g to remove cell debris. The generated lentiviruses were then concentrated using PEG-NaCl. The concentrated lentiviruses were used for the knockdown of Rab8a using spin transduction and GFP

positive cells used for measuring the for the further analysis (Figure 2.9.K) .Knockdown was confirmed by Western Blotting and qRT-PCR (47).

Rab8a gene was cloned between *XbaI* and *BamHI* sites in pLenti-GFP vector for overexpression in bone marrow cells of aged mice (Figure 2.10.A). Lentivirus generation and concentration was performed as described earlier (47). Expression of Rab8a in lentiviral soup was measured by PCR (Figure 2.10.B). Overexpression was confirmed by qPCR and western blot.

Staining of samples and flow cytometric analysis

Peripheral blood samples were collected in 1.5mL of micro-centrifuge tubes containing in 10µL 500mM EDTA. 35µL of the blood samples were taken and incubated with 7µL of antibody mix for 30 minutes on ice. The Red blood cells were then lysed by adding 400µL of RBC lysis buffer (155mM NH_4Cl, 12mM $NaHCO_3$, 0.1mM EDTA, pH 7.3). The cells were analysed flow cytometrically using BD C6 Flow cytometer.

For surface staining of the cells from different organs of were harvested in 10% RPMI, and single cell suspensions were made by placing the organs in a 70µm strainer and gently crushing them using a 2mL syringe plunger. In case of spleen RBC lysis was also performed. The cells were stained using the indicated antibodies on ice for 30 minutes. The cells were then washed by centrifugation at 200g for 5 minutes in 1x PBS at 4ºC and acquired using BD C6 flow cytometer. For surface staining of immune cells from lungs, the tissue was first digested with collagenase (0.5mg/mL) for 1hr at 37°C. The single cell suspensions were then made as described. The cells were then stained using the indicated fluorescent antibodies at 4ºC for 30 minutes.

For phenotyping of the *in-vitro* generated BMDCs, cells were gently removed from the culture plate using a cell scrapper and washed twice using complete RPMI by centrifugation at 200g for 5 minutes at 4°C. The staining was performed as described. Similarly, splenic DCs were phenotypically characterized. Single-cell suspensions for splenic DC characterisation were prepared as described (48).

For the intracellular cytokine staining (ICCS) assays, equal number ($5x10^5$) of cells from different organs were pulsed with 10µg/mL of $Ova_{257-264}$ (SIINFEKL) for 4 hours at 37ºC for 4hrs. This was followed by incubation with 1x Brefeldin A for 4 hours at 37ºC. The cells were then surface stained and treated with IC fixation buffer for 30 minutes on ice. This was followed by permeabilization using IC permeabilization buffer for 15 minutes. The intracellular cytokines were stained by incubating the surface-stained cells with the antibody cocktail prepared in permeabilization buffer for 45 minutes on ice. The cells were the washed twice with 1X-PBS and acquired using BD C6 flow cytometer.

For sorting of BMDCs, *in-vitro* generated BMDCs were harvested and washed twice in 10%RPMI. The cells were then incubated with the antibody cocktail for 30 minutes on ice. The cells were then washed and sorted based on CD11b and CD11c staining using BD FACSAria Fusion III. Additionally for some experiments in-vitro generated BMDCs were first stained with CD11b/CD11c for double positive dendritic cells then double positive cells were stained with F4/80 and GR1 (Ly6G and Ly6C) and in other case double positive cells were stained NK1.1 and GR1 (Ly6G and Ly6C). Followed by the double negative cells NKD ($NK1.1^-/GR1^-$) or MKD ($F4/80^-/GR1^-$) $CD11b^+/CD11c^+$ cells were sorted.

For measuring the expression of Rab8a along with Akt1 and Pakt1 in bone marrow and BMDCs, the cells were first surface stained with CD11b. This was followed by Fc blocking. The cells were then fixed and permeabilized using IC fixation and permeabilization buffer. The primary antibodies against Akt1 and p-Akt1 were then added for 30 minutes at room temperature. The cells were then washed, and the bound primary antibodies were then probed with secondary antibodies tagged with Alexa-Fluor 568. Similar analysis was performed on Rab8a-KD BM/BMDCs cells along with their scrambled control. A similar approach was employed to detect the expression of Rab8a and Rab11 upon antigenic stimulation (Ova pulsed) in BMDCs generated from young, aged and Rab8a overexpressing aged BM cells.

qRT-PCR for measuring the mRNA levels of different genes

In vitro generated BMDCs (from young or aged mice) or PBMCs (from young or aged humans) were stimulated with UV inactivated Influenza-A Virus (IAV-WSN-SIINFEKL) and γ-herpesvirus (MHV-68-SIINFEKL) for 3 different time points (30minutes, 3hrs and 6hrs). Unstimulated cells from each group were taken as a control for normalization of the expression data. At the indicated time points, RNA was isolated using Trizol. The concentration and quality of the RNA preparation was assessed using OD_{280} and $OD_{260/280}$ measurements, respectively. Equal concentration of RNA was then used for cDNA preparation using verso cDNA kit (Thermo Fisher Scientific). qPCR was then performed using 2X-DyNamo ColorFlash SYBR Green qPCR kit (ThermoFisher). The relative expression of HPRT or 18s rRNA were taken as the endogenous control for estimating the transcript abundance using 2^{-ddCT} method (49).

To measure type I IFN response, *in-vitro* generated BMDCs from young and aged mice were sorted as double positive cells using CD11b and CD11c staining. Equal number of the sorted DCs were

then pulsed *in vitro* with 0.5 multiplicity of infection (MOI) of IAV (WSN-SIINFEKL) or MHV68-SIINFEKL for different time intervals (30 minutes, 3hrs and 6hrs). RNA was then isolated at the indicated time points and cDNA was prepared. Expression of genes involved in type I IFN pathway was measured by qRT-PCR as described in the previous sections. Human blood samples were collected from from young (~25 years) and aged (>65 years) healthy donors in EDTA tubes followed by isolating PBMCs using histopaque. Equal numbers of the isolated PBMCs were pulsed with 0.5 MOI of IAV for 30 minutes, 3hrs and 6hrs. The cells were then harvested for RNA isolation and analysed for measuring the expression of different genes involved in type I IFN pathway by qRT-PCR.

Bone marrow cells of young mice were subjected to shRNA mediated knockdown of Rab8a by spin transduction of lentiviruses containing the Rab8a shRNA constructs. The cells were then used for generation of BMDCs by culturing them in media supplemented with 5ng/mL GM-CSF and IL-4. Five days later, the cells were harvested and equal number of the cells were pulsed with 0.5MOI of IAV for 6hrs. The cells were processed for RNA isolation to measure the expression of different genes by qRT-PCR. BMDCs generated from scrambled control transduced BM cells served as control for normalization.

In separate experiments, Rab8a expression was reconstituted in aged BM cells by transduction with viruses containing the Rab8a overexpression construct. The transduced cells were then used for BMDC generation by culturing them in media supplemented with GM-CSF and IL-4 for 5 days. Equal number of the sorted BMDCs were then pulsed with 0.5MOI of either live or UV-inactivated IAV for 6hrs. The cells were then used for RNA isolation followed by cDNA preparation. qRT-PCR was then performed to measure the expression of various genes. BMDCs from aged and young animals were also generated for comparison. For assessing the

kinetics of expression of genes encoding for IGF1R and Rab8a, BM cells from young and aged mice were cultured in the presence of 5ng/mL of IL-4 and GM-CSF for 12, 24 and 48 hrs. At the indicated time points, the cells were isolated to prepare RNA samples. qRT-PCR was performed onto the converted cDNA to measure the transcript abundance. Additionally in separate experiments in-vitro generated $CD11b^{+}/CD11c^{+}$ BMDCs were sorted which were double negative for NK1.1 and GR1 (Ly6G and Ly6C) NKD ($NK1.1^{-}/GR1^{-}$) or MKD ($F4/80^{-}/GR1^{-}$). Followed by these NKD or MKD cells were pulsed with 0.5MOI of IAV and the expression of Rab8a along with IFNα, IFNβ and IFNγ were measured. Separately in order to show the expression of Rab8a along with the interferons such as IFNα, IFNβ and IFNγ from bonafide cDC2s ($CD11b^{+}/CD11c^{+}$) Flt3l was used to generate DCs and were also pulsed in similar fashion.

Antigen presentation assay

In-vitro generated BMDCs from young and aged animals were sorted as double positive cells using anti-CD11b and anti-CD11c antibodies. The sorted BMDCs were then pulsed with 25μg/mL of $Ova_{257-264}$ (SIINFEKL) for 45 minutes or 200μg/mL of chicken ovalbumin protein for 2hrs. The cells were then washed twice using complete RPMI. These cells were used for co-culture with CFSE labelled OT-I cells to assess antigen presentation. 72hrs after co-culture, the cells were washed twice with 1xPBS and stained with anti-CD8 antibody. The stained samples were acquired using BD Accuri C6 flow cytometer and the data was analysed using flowJo (BD Biosciences) software. Additionally $CD11b^{+}/CD11c^{+}$ dendritic cells were also stained with F4/80 and GR1 (Ly6G and Ly6C) in one case and in other double positive cells were stained NK1.1 and GR1 (Ly6G and Ly6C) and then the double negative cells, NKD ($NK1.1^{-}/GR1^{-}$) or MKD ($F4/80^{-}/GR1^{-}$) $CD11b^{+}/CD11c^{+}$ cells were sorted. Above NKD/MKD depleted cells were also pulsed with ovalbumin and were co-cultured with CellTrace Far RedTM labelled OT1 cells.

DC immunization assay

In-vitro generated BMDCs from young, aged and IFNR-KO mice were sorted based upon CD11b and CD11c staining. The sorted BMDCS were washed once with complete RPMI and equal numbers of cells from each group were pulsed with OVA protein (200µg/ml) for 2 hrs. The cells were then washed thrice with 1xPBS and adoptively transferred into sex matched CD45.1^{+} mice previously infused with OT1 cells. The frequency of OT-I cells were checked in circulation of the recipients at 7- and 14-days post transfer. The recipients were then infected intranasally with WSN-SIINFEKL to recall persisting OT-1 cells generated following DC immunization. The kinetics of the expansion of OT-I cells was measured at different days post infection (dpi). The animals were sacrificed at 8 dpi for cellular analysis. ICCS assays were performed to assess the functionality of the recruited OT-I cells. The abundance of replicating virus particles in the lungs was gauged by performing viral titration on MDCK cells and qRT-PCR to measure abundance of viral nucleoprotein (NP) and RNA dependent RNA polymerase (RdRP).

Rab8a reconstitution in BM cells of aged mice and functional characterization of Rab8a-OE BMDCs

BM cells of aged mice were transduced with lentiviruses harbouring the Rab8a overexpression construct by spin transduction (48). The cells were then cultured in media supplemented with 5ng/mL of GM-CSF and IL4 for 5 days for differentiation of BMDCs. 5 days post onset of culture, the BMDCs were harvested by gently scraping and DCs were sorted based upon CD11c staining. The cells were then pulsed with 200µg/mL of OVA for 2 hours and washed twice with 1xPBS. The pulsed cells were then co-cultured with CFSE labelled OT1 cells for 72 hours to assess antigen presentation as a function of OT-I cell proliferation.

In another set of experiments, equal number of BMDCs from young, aged and Rab8a-Overexpressing conditions were pulsed with Ovalbumin (200μg/mL) for 2 hours, washed twice and transferred into gender matched CD45.1 mice which were previously infused with CFSE labelled OT1 cells. 72 hours post BMDCs transfer, peripheral blood was collected to check the expansion of the CFSE labelled OT1 cells. The animals were left for one month for generation of memory. The efficiency of priming was then assessed by recalling the memory OT-I cells by infecting the recipients intranasally (i.n) with 200 pfu of WSN-SIINFEKL. The animals were then sacrificed and subjected to cellular analysis. Viral load assessment was performed by plaque assays and qRT-PCR for measuring the transcript abundance viral NP and RdRP. Additionally similar experimental setup was used for Flt3l based DCs and virus specific expanded donor cells was measured in IAV infected different DCs recepients upon recall of infection.

In an additional experiment, $3x10^4$ of BMDCs differentiated from aged and young animals as well as those from aged mice but overexpressing Rab8a (Rab8a-OE) were pulsed with different concentrations of either ovalbumin or $Ova_{257-264}$ (SIINFEKL) peptide. The cells were then washed twice and co-cultured with $1.5x10^4$ CFSE labelled OT1 cells for assessment of proliferation of OT1 cells using flow cytometry.

In a separate experiment, BMDCs generated from different conditions were pulsed with ovalbumin (200μg/mL) for 2 hours, washed twice with 1xPBS and transferred into sex matched congenic ($CD45.1^+$) mice which were previously infused with CFSE labelled OT1 cells. 72 hours post BMDC transfer, different lymphoid organs were collected to check the expansion of CFSE labelled OT1 cells. In the same experiment, the distribution of the BMDCs within the organs was also assessed using CD45.2 and CD11c staining. The expression of chemokine receptors such as CCR5 and CCR7 was also measured on IAV pulsed BMDCs from each group. Additionally Flt3l based

DCs were also generated from young, aged and Rab8a-OE bone marrow cells. Later on the OVA pulsed BMDCs were from above conditions were infused into gender matched CD45.1^{+} congenic mice which were already transferred with CFSE labelled OT1 cells. After 72hrs of post DCs transfer these animals were sacrificed and different lymphoid and non-lymphoid organs along with peripheral blood was collected in order to measure *in vivo* antigen presentation.

Measuring surface expression of H-2k^{b} bound to SIINFEKL on antigen pulsed BMDCs

BMDCs were generated as described above from young, aged and Rab8aOE conditions and pulsed with different concentrations of either complete ovalbumin or Ova$_{257-274}$ (SIINFEKL) peptide for 6- and 24-hrs. The pulsed cells were then stained with antibodies against CD11c, class I MHC and H2K^{b}-SIINFEKL for 30 minutes on room temperature for detection of H-2K^{b}-SIINFEKL positive DCs out of class I MHC positive cells. The stained cells were washed twice with 1xPBS and then acquired using BD Acuri C6 flow cytometer.

***In-vitro* immune synapse formation assay by flow cytometry**

BMDCs were generated from young, aged and Rab8a reconstituted aged BM cells by culturing them in media supplemented with 5ng/mL of GM-CSF and IL-4 for 5 days for generation of BMDCs. The BMDCs were sorted and labelled with cell-Trace^{TM} Far Red and pulsed with either complete ovalbumin or Ova$_{257-274}$ (SIINFEKL) peptide. The cells were then washed twice with 1xPBS and co-cultured with CFSE labelled OT1 cells for two different time points (6hrs and 16hrs). The cells were then washed and acquired using BD Accuri C6 flow cytometer.

Confocal microscopy

BM cells from young and aged animals were isolated and those from aged mice were then either transduced with lentiviruses packaged with Rab8a overexpressing constructs or vector controls. Following transduction, the young and aged cells were used to generate BMDCs by culturing them in the presence of GM-CSF and IL-4 as mentioned earlier. The frequency of $CD11c^{+}$ cells were assessed using flow cytometry and the cells were then seeded onto gelatin coated coverslips overnight. The cells were then pulsed with 200μg/mL concentration of ovalbumin for different time intervals (0hrs, 2hrs, 6hrs, 12hrs and 24hrs). The cells were then washed twice with 1x PBS followed by fixation with 4% PFA for 20 minutes at room temperature. This was followed by blocking with 1% BSA in 1x PBS for 45 minutes. The cells were then washed and the Fc receptors were blocked using Fc block reagent for 1 hour at room temperature. Fc blocking was followed by incubation with primary antibodies against Rab8a (mouse IgG) and Rab11 (rabbit IgG) for 2 hours. The primary antibody cocktail was prepared in IC permeabilization solution procured from Invitrogen. The coverslips were then washed thrice with 1xPBS. This was followed by incubation with a cocktail of Hoechst, fluorescent tagged secondary antibodies (anti-mouse IgG-Alex Fluor 488 and anti-Rabbit IgG-Alexa Fluor 647) and anti-H-$2k^{b}$-SIINFEKL-PE prepared in IC permeabilization buffer for 2 hours. Following the incubation, the cells were washed thrice with 1xPBS and mounted on slides for image acquisition. The images were acquired using Nikon A1 confocal microscope at 60x magnification. All the captured images were analysed by using ImageJ software. In the same experiment in order to visualize the total actin content inside the cells CD11c positive cells generated from different conditions were fixed, permeabilized and stained with Alexa Fluor™ 488 Phalloidin and acquired using BD Accuri C6 flow cytometer.

Fluorescence microscopy

Successful transfection of HEK293T cells for generation of Rab8a-shRNA and Rab8a-OE lentiviruses was confirmed using fluorescence microscopy after 72hrs of transfection. All the images were captured using Leica microscope and analyzed using ImageJ software.

Cell lysate preparation and western blotting

Cell lysates were prepared from the indicated cells by using a hypotonic lysis buffer (20mM HEPES, 0.2mM EDTA, 1.5mM $MgCl_2$, 100mM KCl, 20 % (V/V) glycerol, 0.02% (V/V) NP-40, pH 7.5). The lysates were normalized using OD_{280} and resolved through SDS-PAGE (15% resolving, 4% stacking). The gels were transferred onto a PVDF membrane and blocked overnight at 4ºC using 5% skim milk in 0.05% PBST solution under slow rotation. On next day, the membranes were washed thrice for 5 minutes each using 0.05% PBST solution and the blot was incubated with primary antibodies against Rab8a, Akt1, and pAkt1 (1:2000 dilution) for 1 hr at room temperature. GAPDH was used as an endogenous loading control. Following primary antibody incubation, the blot was washed 5 times with 0.05% PBST and the blot was incubated with alkaline phosphatase conjugated secondary antibodies for 45 minutes at room temperature. Following secondary antibody incubation, the blots were washed 5 times using 0.05% PBST and probed using femtolucent AP substrate solution. Additionally, cell lysate from ova pulsed BMDCs from young, aged and Rab8a-OE were probed using primary anti-Rab8a and anti-Rab11 antibodies.

Plaque assay to measure the viral titer

For measuring the viral load in the lungs of infected mice, lungs were homogenized in serum free DMEM using a tissue homogenizer. The homogenized samples were spun at 13,000rpm for 10 minutes at 4ºC and the supernatants were collected for viral titration on MDCK cells. After 5 days of infection, the plaques were developed by staining with crystal violet.

Statistical analysis

GraphPad Prism 9 was used for statistical analysis. The data was analyzed either by one way ANOVA or by two way ANOVA (in case of multiple variables) and for some data type non-parametric t test was also done as indicated in the figure legends. All the data represents mean ± SEM and the level of statistical significance was determined as; $****p < 0.0001$, $***p < 0.001$, $*p < 0.01$ and $*p < 0.05$.

Results

Transcriptome analysis of DCs reveals compromised function in aging host

To gain insights into the molecular mechanisms responsible for impaired functions of DCs of an aging host, we performed transcriptional analysis of $CD11c^{+}CD11b^{+}$ cells sorted from the lymphoid tissues of unmanipulated aged (>24 months) and young (2 months) mice (Fig 2.1.A). Out of 21519 genes, those showing an FPKM value of >5 in either of the samples were analyzed for differential expression (Fig 2.1.A and 2.2.A). A cutoff value of 1.5-fold change was set to classify significantly differentially expressed (SDE) gene as the samples were obtained from unmanipulated young and aged animals (Fig 2.2.A). We identified 44 genes upregulated by DCs of young animals while 123 genes were upregulated in the DCs of aged animals (Figure 2.1.A and 2.2.A). Of the upregulated genes, a large majority were involved in regulation of signal transduction, regulation of biological processes and cell to cell communication, protein-protein or protein-nucleic acid interaction and hence were predominantly shown to localise in membrane or nucleus (Fig 2.2.B-G). Genes upregulated in DCs of aged animals included inhibitory molecules such as CD160 (5-fold), *Klrb1b* (3-fold), *Klrb1c* (4.5-fold), *Klrc1* (3.8 fold) and *Klre1*(3.2-fold) (Figure 2.1.B) (7,8). Genes encoding for GTPase associated nucleotide binding proteins were upregulated in DCs of aged animals. These included *GIMAP3* (4.15-fold), *GIMAP4* (3.7-fold), *GIMAP7* (3.6-fold), *GIMAP5* (3.3-fold), *GIMAP8* (3.2-fold), *GIMAP6* (2.9-fold), *GIMAP9* (2.3-fold), *GIMAP1* (2.19-fold) (Fig 2.1.C). GIMAPs were shown to be critical for T cells survival but their influence in DCs physiology is not established (9). *Arl4d*, a GTPase shown to negatively regulate the function in $CD8^{+}$ T cells, was increased in the expression by ~3.6-fold in the DCs of aged mice (10). *Hic1*, a gene that directly suppresses class II trans-activator (CIITA) to modulate the expression of class II MHC molecule was increased in expression by ~3.5-fold in the DCs of

aged mice (Fig 2.1.B) (11). The functional annotation, network and pathway analysis of the genes significantly downregulated in DCs of aged animals revealed compromised anti-viral functions, tissue remodeling as well as those involved in fine-tuning immune responses such as Th1, Th2 and Th17 cell differentiation, functioning of NK cells, cytokine receptor as well as TCR signaling, migration of leukocytes from lymphoid organs to tissue sites (Figure 2.3.A-D). A lower expression of multiple surface and endosomal Toll-like receptors (TLRs) such as TLR1, TLR2 and TLR4 along with TLR-7, TLR8 and TLR9 were significantly downregulated in cDC2s of aged animals upon IAV stimulation. The downstream adaptor molecules such as MyD88 and other downstream mediator such TRAF6 and IRF7 which eventually leads to the production of pro-inflammatory (IL6 and IL1β) and anti-inflammatory (IL4 and IL10) molecules were also compromised in IAV pulsed DCs from aged individuals (Figure 2.4). Expression of several anti-viral genes such as *IFITM1* (~2.4 fold), *IFI27l2a* (2 fold), *IFIT3* (1.74 fold), *IFIT1* (1.7 fold), *OAS1a* (2.5 fold), *OASl2* (2.27 fold) and *OAS2* (1.9-fold), was observed in DCs of aged mice which indicated their inefficiency in responding to viral infections (Fig 2.1.D, 2.3.I). *PLSCR1* encodes a product that control HCMV infection via IFN, was reduced in expression by ~1.73-fold. Genes of PI3K/MtorC1 signaling axis such as *Rab8a, Akt1* and *S6K* responsible for growth, differentiation and functioning of DCs were downregulated in the aging animals (Fig 2.1.E). Following an initial interaction with the invading pathogen at infection sites DCs migrate to secondary lymphoid organs to activate T cells. Molecules involved in modulating the migratory properties of DCs such as *CD103* (1.5-fold), *CCR7, Nr1h3* (1.5-fold) showed reduced expression in DCs of aged mice (Fig 2.1.A and D) (12,13).

Since the IFN pathway was severely compromised in DCs of aged animals as compared to their counterparts from younger animals, we analyzed its impact in their differentiation and

responsiveness to viral recognition. We first compared the IFN response in BMDCs generated *in-vitro* from young (~6-8 weeks old) and aged (>18 months old) mice. Sorted double positive ($CD11b^+CD11c^+$) DCs (purity ~95%) were pulsed with two different viruses viz., Influenza A virus (WSN-SIINFEKL) and a γ-herpesvirus (MHV68-SIINFEKL) and the mRNA expression of genes involved in type I IFN pathway was measured (Fig 2.1.F-J and 2.3.E-H). We observed significantly reduced expression levels of several IFN genes and the effectors of IFN signaling in IAV pulsed BMDCs (Fig 2.1.G-J). *IFNα, IFNβ* and *IFNγ* levels were reduced by more than 15, 12 and 2-fold at all the time points in the cells differentiated from precursors of aged as compared to the younger animals (Fig 2.1.F). Similar results were obtained for the MHV68-stimulated BMDCs (Fig 2.3.E-H). Following IFNR ligation, signal is transduced via JAK/STAT pathway (14). The expression levels of transcription factors STAT1, 2 and IRF9 were significantly lower in BMDCs of aged as compared to their younger counterparts following a pulse with either IAV or MHV68 (Fig 2.1.H and 2.3.F). The expression profile of downstream effectors induced following signaling via IFNR was measured in IAV as well as MHV68 pulsed BMDCs differentiated from precursor cells of aged and young animals. BMDCs of aged animals pulsed with either IAV or MHV68 showed reduced expression of *OAS1A* (80 and 140-fold), *OAS1G* (8 and 4-fold), *OAS2* (5 and 4-fold), *OAS3* (9 and 4-fold), respectively (Fig 2.1.I and 2.3.H). Similarly, *IFIT1* (3 and 3-fold), *IFITM1* (6 and 2-fold) and *ISG15 (6.4 and 4-fold)* were also significantly downregulated in the IAV or MHV68-pulsed cells of aged mice, respectively (Fig 2.1.J, Fig 2.3.G). To assess whether such a downregulation was specific to murine cells or occurred in a generic manner, we performed a similar analysis on human PBMCs isolated from healthy young (<25 years) and aged (>65 years) individuals following pulsing with IAV (Figure 2.1.K-N). PBMCs of aged individuals showed reduction in the expression levels of most of the genes of IFN pathways albeit at varying levels

following IAV pulsing. Therefore, DCs of aged mice as well as humans exhibited compromised IFN signaling following recognition of two distinct viral agents which could account for the enhanced susceptibility of an aging host to viral infections.

Figure2.1

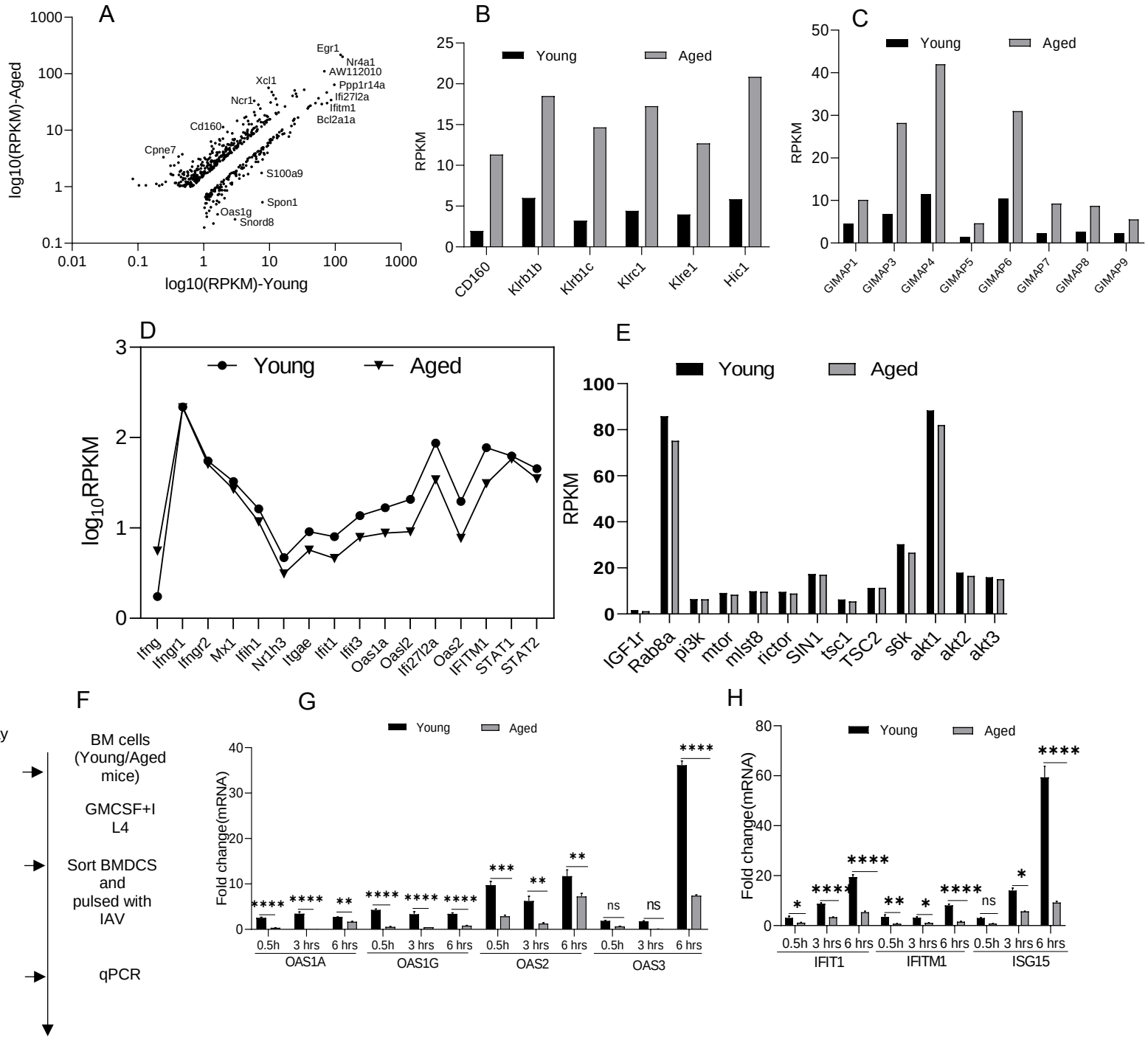

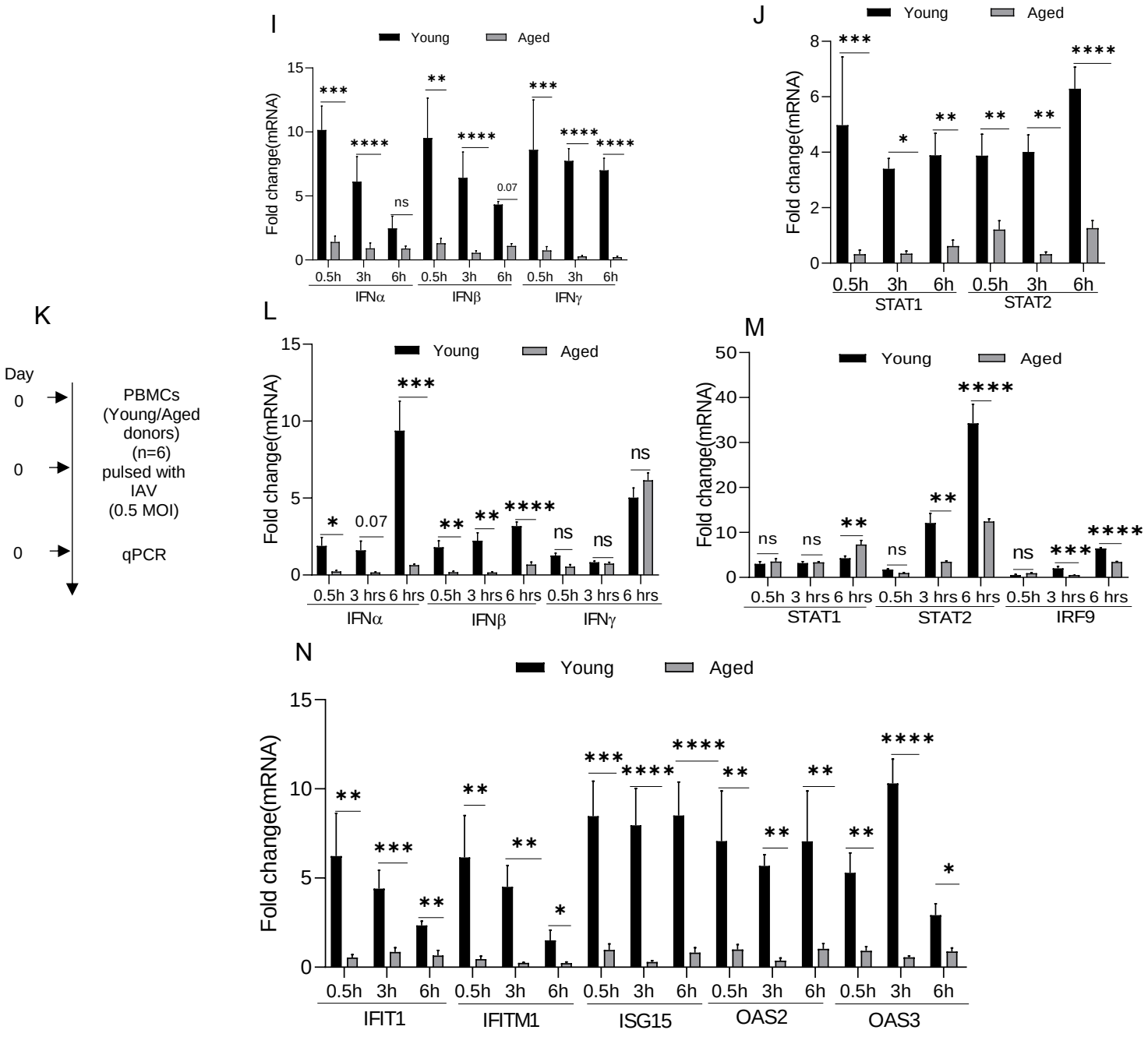

Figure 2.1 DCs of aging host mount an inhibited type I IFN response.

A. Dot plot shows the expression of genes in DCs of aged and young animals. B. Bar graph for show the expression of key inhibitory genes in aged and young DCs. C. Bar-graph show the expression of a cluster of GIMAP genes. D. Line graph showing the log10 RPKM value for genes involved in type I IFN pathway of DCs of young and aged animals. E. Bar graph shows the RPKM

of different genes in DCs of aged and young animals. F-J. Assessing the expression of IFNs and ISGs in virus stimulated BMDCs of young and aged mice. F. A schematic of the experiments is shown. The generated BMDCs from young and aged mice were pulsed with IAV for different time points. The cells were then processed for RNA isolation and cDNA preparation. The relative abundance of different genes of type I IFN pathways was then measured by qRT-PCR. G-J. Bar graph show the relative expression of different genes of type I IFN pathway is shown. K-N. Assessing the expression of IFNs and ISGs in virus stimulated PBMCs of young and aged humans. K. Schematic for the experiment is shown. PBMCs isolated from aged and young individuals were pulsed with IAV for the indicated time points and were then analysed for the expression of different genes. L-N. Bar graphs show the expression data of different genes of type I IFN pathways in IAV pulsed human PBMCs is shown. The experiments were repeated at least three times and representative data from one of the experiment is shown (n=3 for animal experiments and for human PBMCs analysis n=6 donor were considered). Mean ± SEM values are shown and the levels of statistical significance was analysed by two way ANOVA. ****p<0.0001; ***p<0.001;**p<0.01;*p<0.05, ns p>0.05.

Figure2.2

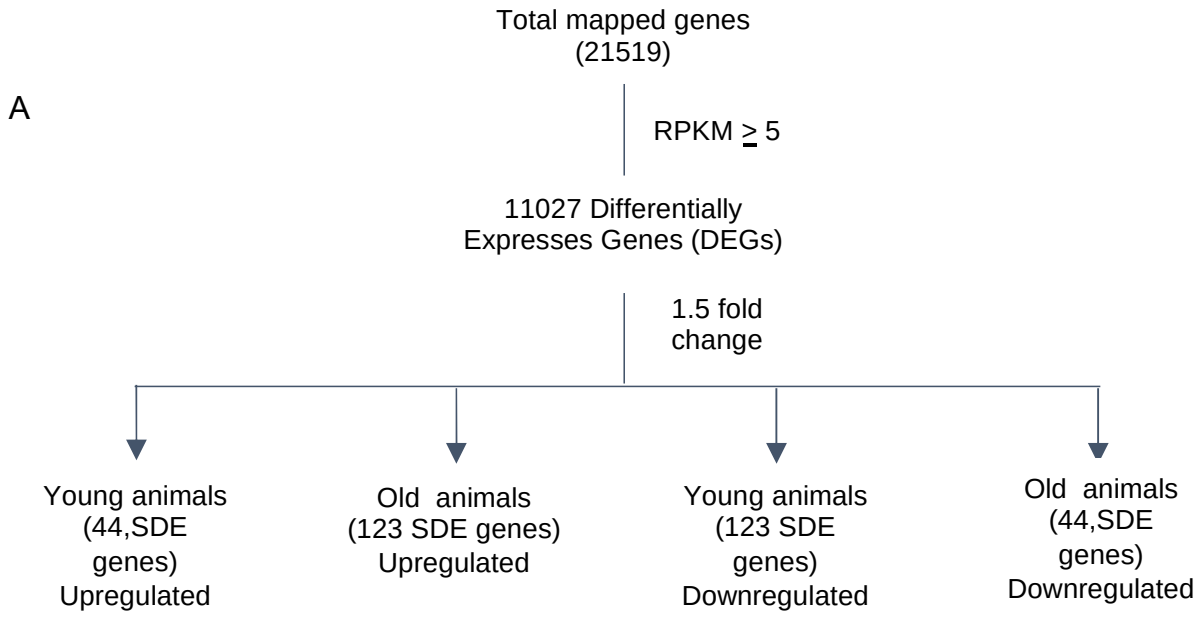

B

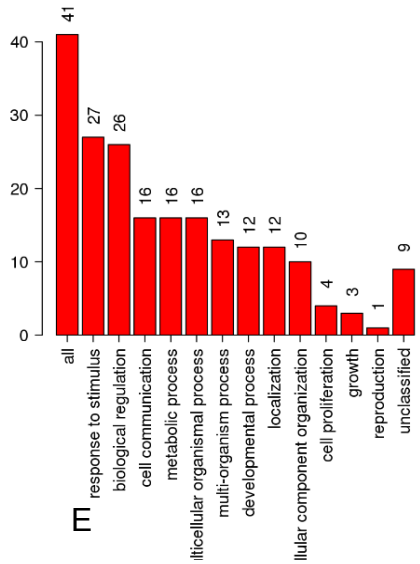
Bar chart of Biological Process categories
all
response to stimulus
biological regulation
cell communication
metabolic process
lticellular organismal process
multi-organism process
developmental process
localization
llular component organization
cell proliferation
growth
reproduction
unclassified

C

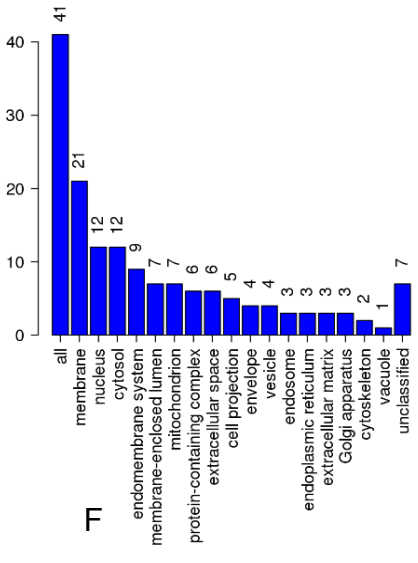
Bar chart of Cellular Component categories
all
membrane
nucleus
cytosol
endomembrane system
membrane-enclosed lumen
mitochondrion
protein-containing complex
extracellular space
cell projection
envelope
vesicle
endosome
endoplasmic reticulum
extracellular matrix
Golgi apparatus
cytoskeleton
vacuole
unclassified

D

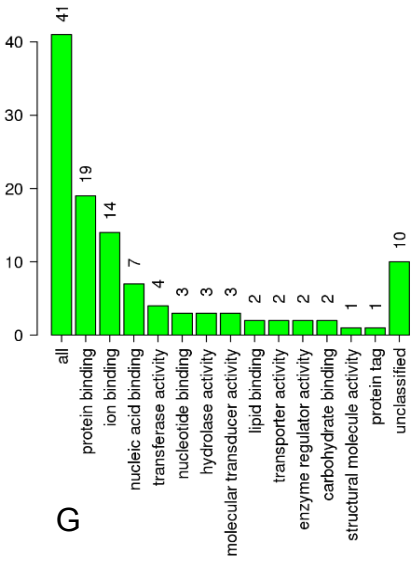
Bar chart of Molecular Function categories
all
protein binding
ion binding
nucleic acid binding
transferase activity
nucleotide binding
hydrolase activity
molecular transducer activity
lipid binding
transporter activity
enzyme regulator activity
carbohydrate binding
structural molecule activity
protein tag
unclassified

E

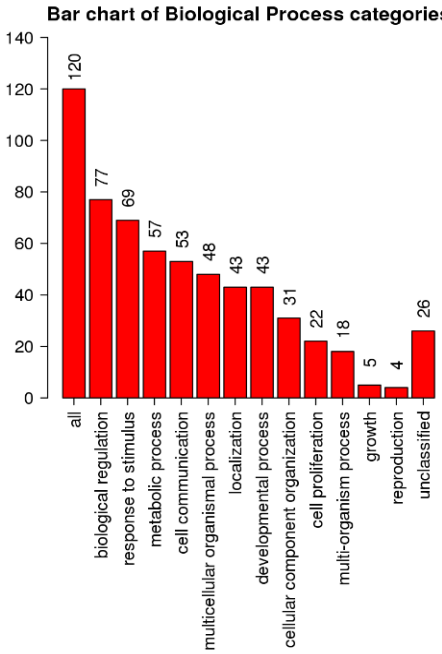
Bar chart of Biological Process categories
all
biological regulation
response to stimulus
metabolic process
cell communication
multicellular organismal process
localization
developmental process
cellular component organization
cell proliferation
multi-organism process
growth
reproduction
unclassified

F

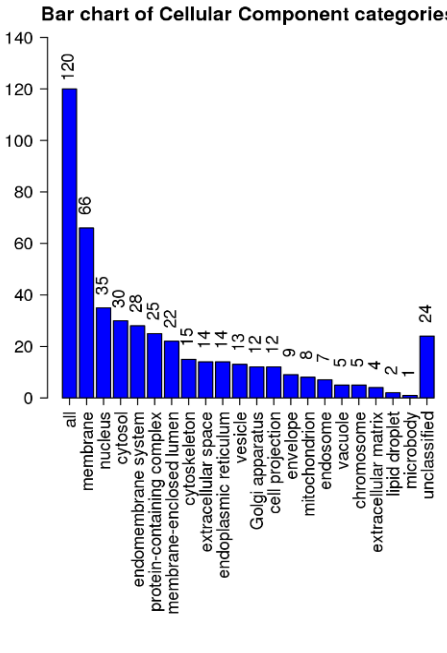
Bar chart of Cellular Component categories
all
membrane
nucleus
cytosol
endomembrane system
protein-containing complex
membrane-enclosed lumen
cytoskeleton
extracellular space
endoplasmic reticulum
vesicle
Golgi apparatus
cell projection
envelope
mitochondrion
endosome
vacuole
chromosome
extracellular matrix
lipid droplet
microbody
unclassified

G

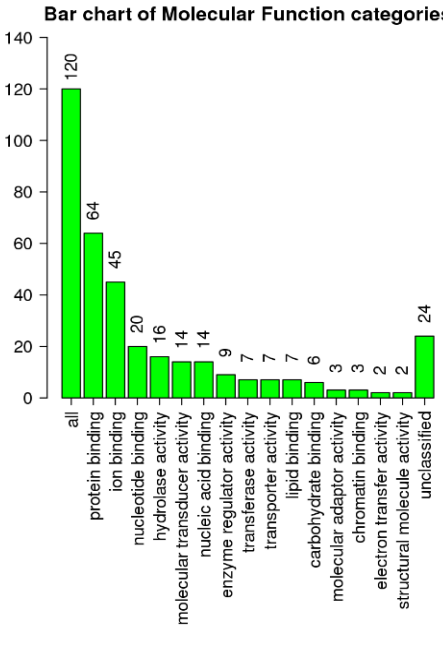
Bar chart of Molecular Function categories
all
protein binding
ion binding
nucleotide binding
hydrolase activity
molecular transducer activity
nucleic acid binding
enzyme regulator activity
transferase activity
transporter activity
lipid binding
carbohydrate binding
molecular adaptor activity
chromatin binding
electron transfer activity
structural molecule activity
unclassified

H

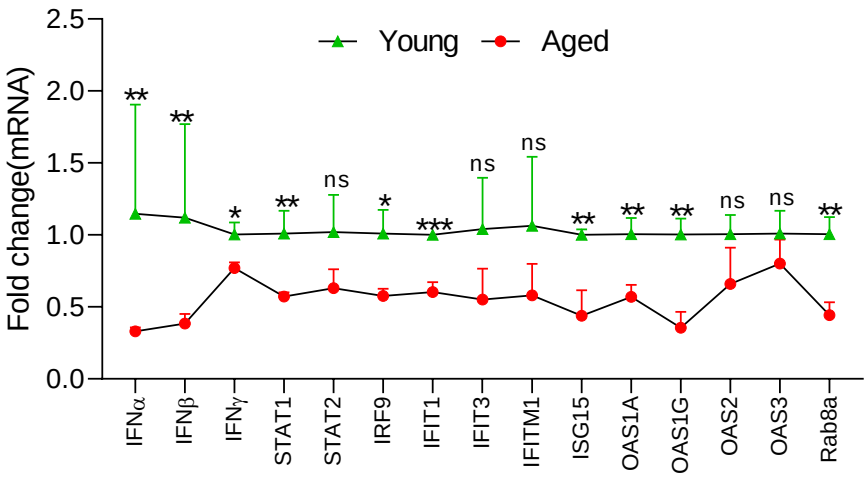
Young
Aged
Fold change(mRNA)
IFNα
IFNβ
IFNγ
STAT1
STAT2
IRF9
IFIT1
IFIT3
IFITM1
ISG15
OAS1A
OAS1G
OAS2
OAS3
Rab8a

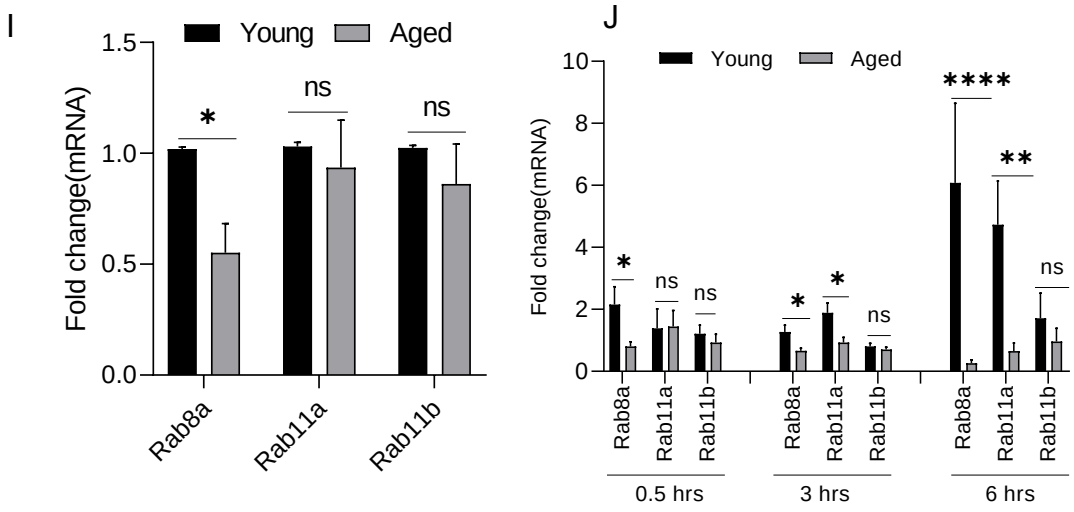

Figure2.2: Transcriptome profiling of dendritic cells of young and aged mice reveals the downregulation of antiviral genes.

A. Schematic for RNA-seq data analysis to obtain significantly differently expressed (SDE) genes in DCs of aged and young mice. B-G. Bar-graph represents the functional annotations using go-slim analysis of 44 SDE genes upregulated in young or downregulated in aged animals (B-D) or 123 SDE genes upregulated in aged or downregulated in young animals (E-G) using Webgestalt. H. Bar graph show the expression profile of different genes of interferon pathways at basal level in BMDCs generated from young and aged animals. I-J. Bar graphs show the gene expression profile of Rab8a along with Rab11a and Rab11b in human PBMCs both at basal level (I) and upon stimulation with 0.5 MOI IAV. Cumulative data is summarized by bar diagram (n=3). Mean ± SEM values are shown and non-parametric t test was used to assess statistical differences. ****$p<0.0001$; ***$p<0.001$;**$p<0.01$;*$p<0.05$, ns $p>0.05$.

Figure2.3

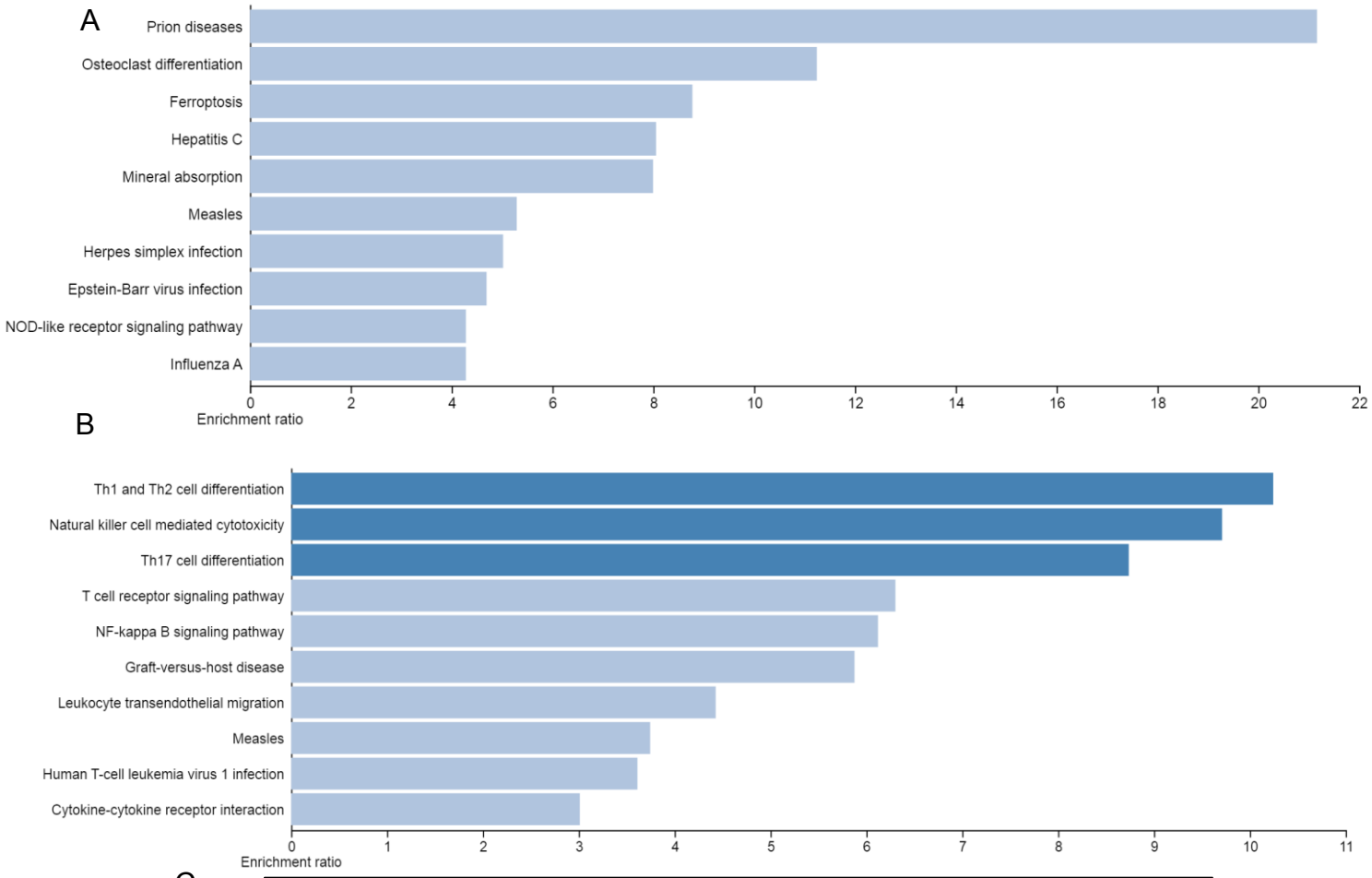
A
Prion diseases
Osteoclast differentiation
Ferroptosis
Hepatitis C
Mineral absorption
Measles
Herpes simplex infection
Epstein-Barr virus infection
NOD-like receptor signaling pathway
Influenza A
0 2 4 6 8 10 12 14 16 18 20 22
Enrichment ratio
B
Th1 and Th2 cell differentiation
Natural killer cell mediated cytotoxicity
Th17 cell differentiation
T cell receptor signaling pathway
NF-kappa B signaling pathway
Graft-versus-host disease
Leukocyte transendothelial migration
Measles
Human T-cell leukemia virus 1 infection
Cytokine-cytokine receptor interaction
0 1 2 3 4 5 6 7 8 9 10 11
Enrichment ratio
C
Mmp14
Prnp
Cd300ld
Fam43a
Clec4a1
Cdk5rap1
Fabp5
Ifitm1
Pla2g7
Ceacam16
Oas1a
Plscr1
Clec4a3
C1qb
Ocstamp
Gm14446
Ifit1
Oas2
Ifit3
Cabp4
Gm14548
Cd300e
Timm10
Isg15
Oasl2
Agrn
Rtp4
Cd5
Ly6a
Itgae
Ifi27l2a
Flot1
Ryden
Ppp1r14a
Mt1
Sirpb1c
Gpr82
Htr7
Gm5150
Bcl2a1a

D

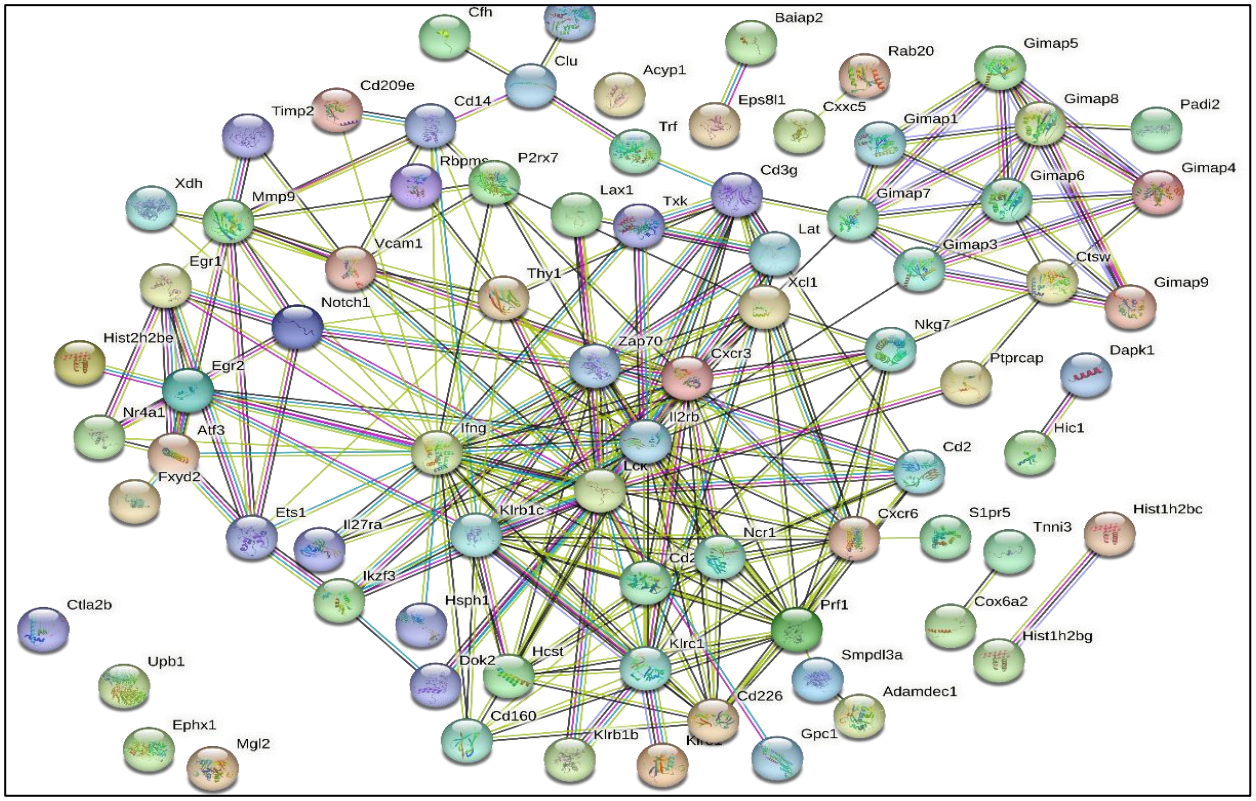
Cfh
Clu
Baiap2
Rab20
Gimap5
Acyp1
Cd209e
Timp2
Cd14
Eps8l1
Cxxc5
Gimap8
Padi2
Trf
Gimap1
Rbpms
P2rx7
Cd3g
Gimap6
Gimap4
Xdh
Mmp9
Lax1
Txk
Gimap7
Lat
Vcam1
Gimap3
Ctsw
Egr1
Thy1
Xcl1
Gimap9
Notch1
Nkg7
Hist2h2be
Zap70
Cxcr3
Ptprcap
Dapk1
Egr2
Nr4a1
Atf3
Ifng
Il2rb
Hic1
Cd2
Fxyd2
Klrb1c
Cxcr6
S1pr5
Hist1h2bc
Ets1
Il27ra
Ncr1
Tnni3
Ikzf3
Ctla2b
Hsph1
Prf1
Cox6a2
Klrc1
Hist1h2bg
Upb1
Dok2
Hcst
Smpdl3a
Cd226
Adamdec1
Ephx1
Cd160
Klrb1b
Gpc1
Mgl2

E

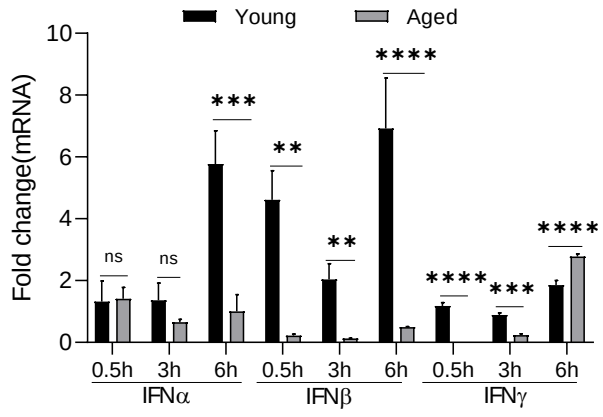
Young
Aged
Fold change(mRNA)
0.5h
3h
6h
IFNα
IFNβ
IFNγ

F

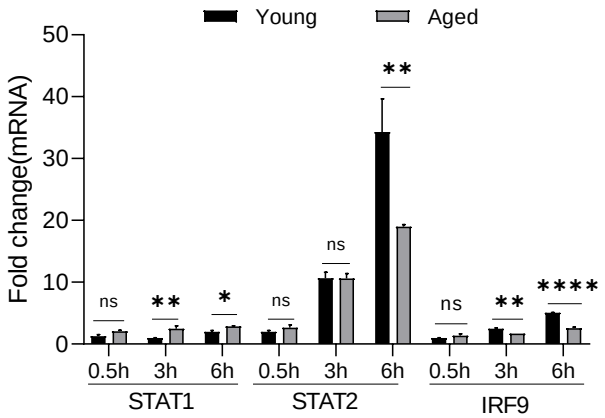
Young
Aged
Fold change(mRNA)
0.5h
3h
6h
STAT1
STAT2
IRF9

G

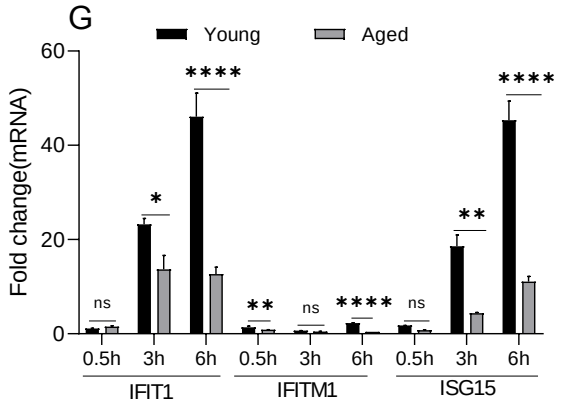
Young
Aged
Fold change(mRNA)
0.5h
3h
6h
IFIT1
IFITM1
ISG15

H

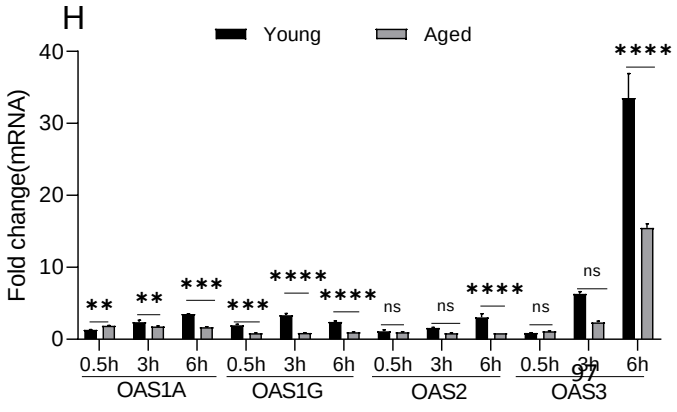
Young
Aged
Fold change(mRNA)
0.5h
3h
6h
OAS1A
OAS1G
OAS2
OAS3

I

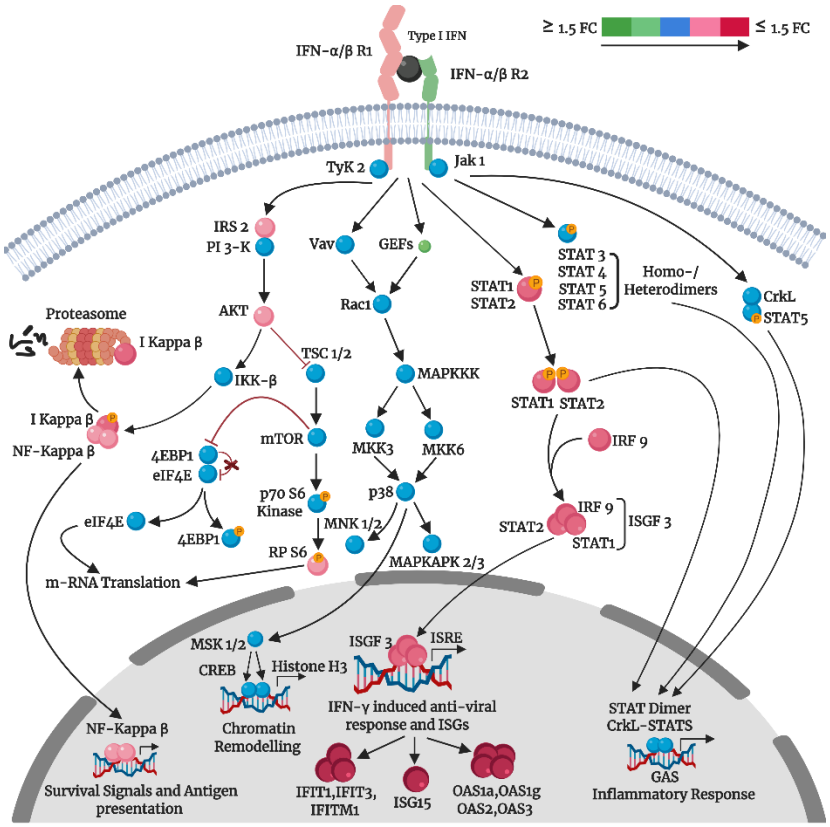

Figure2.3: Functional annotation and network analysis of SDE genes expressed in dendritic cells of aged animals reveals down regulation of antiviral pathways.

A-B. Represents the pathway analysis of 44 SDE genes upregulated in young or downregulated in aged animals (A) or 123 SDE genes upregulated in aged or downregulated in young animals (B). C-D. STRING based network analysis of total SDE genes upregulated in young or downregulated in aged animals. E-H. Bar graph show the expression data in terms of fold change of different genes of type I IFN pathways in each group. The experiments were repeated at least three times and representative data from one of the experiment is shown. Data represents Means ± SEM. ****p<0.0001; ***p<0.001;**p<0.01;*p<0.05, ns p>0.05 (two way ANOVA). I. Expression data of genes of type I IFN pathways are shown in a pathway where genes labelled with red dots represents downregulation of SDE in aged animals, green shows the upregulation whereas blue dot shows no significance.

Figure2.4

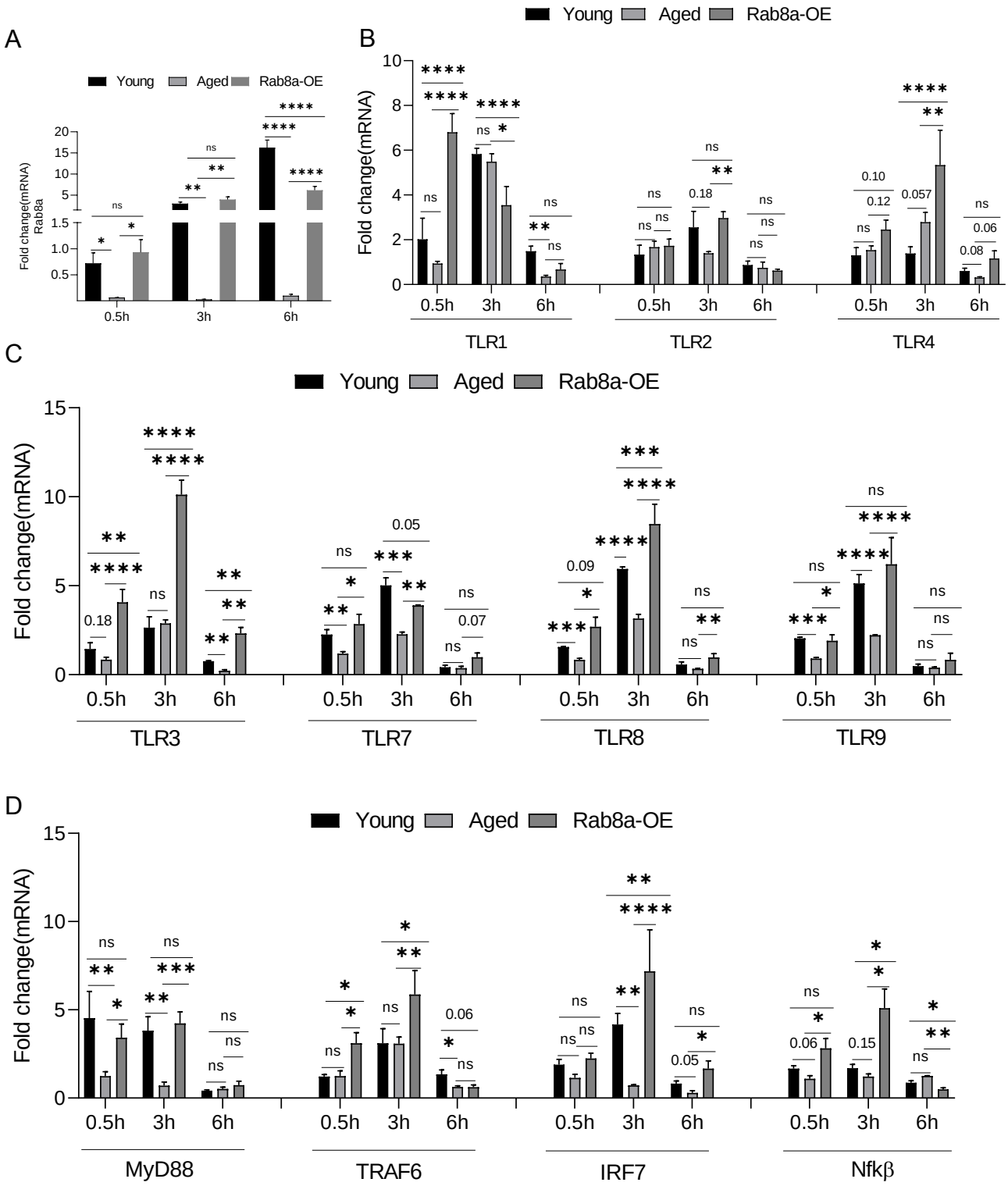
A
Young
Aged
Rab8a-OE
Fold change(mRNA) Rab8a
0.5h
3h
6h
B
Young
Aged
Rab8a-OE
Fold change(mRNA)
TLR1
TLR2
TLR4
C
Young
Aged
Rab8a-OE
Fold change(mRNA)
TLR3
TLR7
TLR8
TLR9
D
Young
Aged
Rab8a-OE
Fold change(mRNA)
MyD88
TRAF6
IRF7
Nfkβ

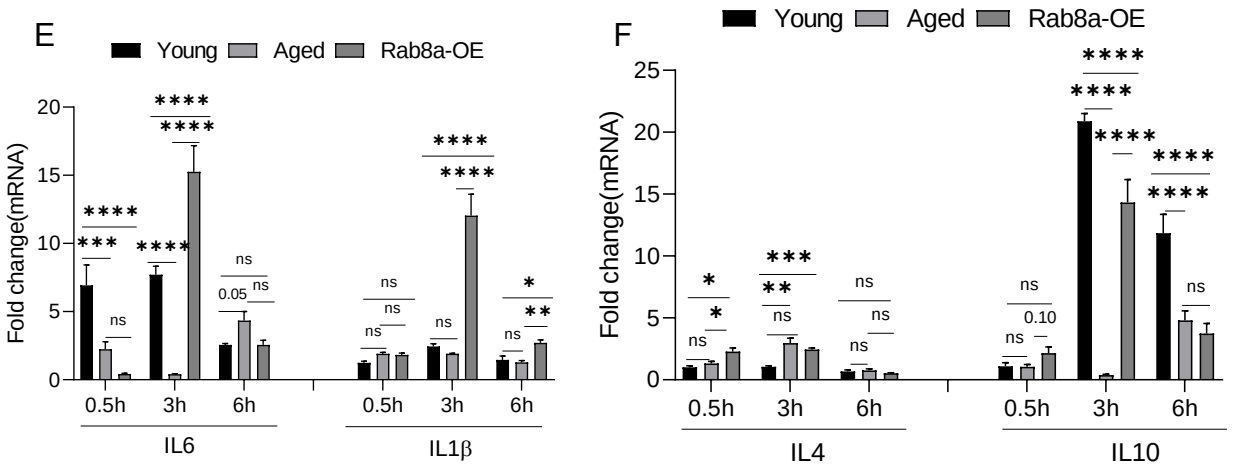

Figure 2.4: Reconstitution of Rab8a in bone marrow cells of aged animals restored the TLR related function.

A. Bar graphs shows the expression of surface TLRs such as TLR1, TLR2 and TLR4 from IAV stimulated DCs at different time points in indicated groups. B. Bar graphs shows the expression of endosomal TLRs such as TLR3, TLR7, TLR8 and TLR9 from IAV stimulated DCs at different time points. C. Bar graphs revealing the expression pattern of Rab8a in young, aged, and Rab8a-OE DCs upon pulsing them with IAV. D. Bar Graphs shows the transcript abundance of different adaptor and downstream mediator of TLRs such as MYD88, TRAF6, IRF7 and NFKβ in different indicated groups. E. Bar graphs shows the expression profile of pro-inflammatory cytokines such as IL6 and IL1β. F. Bar graphs shows the expression profile of anti-inflammatory cytokines such as IL4 and IL10. Cumulative data is summarized by bar diagram (n=3). Mean ± SEM values are shown and two way ANOVA was used to assess statistical differences. ****p<0.0001; ***p<0.001;**p<0.01;*p<0.05, ns p>0.05.

DCs of an aging host are phenotypically and functionally impaired

We compared the phenotype of splenic DCs of aged, young and IFNRKO mice. As DCs of aged animals were compromised in their response via IFN signaling, we also evaluated its role in the DC maturation by including young IFNRKO animals in the analysis. The frequencies of splenic DCs ($CD11b^+CD11c^+$ cells) in aged (~6.62% ± 0.2) as compared to young (~1.14% ± 0.2) and IFNR-KO mice (~1.91% ± 0.47) had significantly higher frequencies (Figure 2.6.A and B). While the expression levels of class II MHC molecules were comparable in all the groups, those of class I MHC were significantly reduced in the DCs of aged (~ 69.16 % ± 1.2) and IFNRKO animals (~59.9% ± 1.4) as compared to those from the young (~79.9% ± 2.17) mice (Figure 2.6.C and D). DCs from aged mice showed significantly reduced expression levels of co-stimulatory molecules and the $CD80^+CD86^+$ cells among $CD11b^+CD11c^+$ were ~49.03% ± 7.3 in young and 35.43% ± 1.5 in aged animals (Fig 2.6.E and F). These results were indicative of compromised activity of DCs from aged as well as young IFNRKO animals in activating antigen specific T cells despite their elevated frequencies.

Does IFN signaling in DCs impact their ability to prime $CD8^+$ T cells? BMDCs were differentiated from young, aged and IFNRKO mice. Thereafter, the ovalbumin pulsed BMDCs (purity ~95%) were co-cultured with OT1 cells to analyze their responsiveness. The frequency of $CD11b^+CD11c^+$ DCs from young (~39.67% ± 3.51), aged (~44.5% ± 0.55), and IFNRKO (~45.1% ± 0.26) were comparable, but those expressing CD80 and CD86 were significantly decreased in aged (~17.3% ± 0.36) and IFNRKO (~27.2% ± 0.15) in comparison to young (~35.0% ± 1.2) mice (Figure 2.5.A and 2.6.G, H and J). Per cell basis expression as measured by MFI values showed a similar trend (Figure 2.6.J). Significant differences in the expression of CD80 and CD86 by BMDCs of the age matched WT and IFNRKO mice attested to the role of IFN signaling in their

maturation. We also measured the frequencies of $CD11b^{+}CD11c^{+}$ DCs expressing class I and II MHC molecules and observed significant reduction in the frequencies of cells expressing both the molecules in IFNRKO (class I MHC^{+ve} cells ~42.0% ± 1.04, class II MHC^{+ve} cells ~56.07% ± 0.15) as compared to those in the WT young (class I MHC^{+ve} cells ~84.60% ± 0.17, class II MHC^{+ve} cells ~82.7% ± 0.37) mice. The cells from WT aged mice preferentially showed reduction in levels of class I MHC (~70.60% ± 1.68 vs 84.60% ± 0.17) than those of class II MHC (~77.3% ± 0.89 vs 82.7% ± 0.37) molecules in both percent positivity and MFI values in a head-to-head comparison with their younger counterparts (Figure 2.5.A and 2.6.I and J). DCs are particularly efficient in uptake and cross-presentation of exogenous antigens to activate specific $CD8^{+}$ T cells, a process more relevant during vaccination and resolution of infection with some viruses (15,16). Frequencies of proliferating OT1 cells co-cultured with the Ova-pulsed BMDCs from young vs aged and IFNRKO vs young mice, respectively, were five-fold (7.48% ± 0.51 versus ~36.3% ± 3.2) and two-fold (21.7% ± 1.90 versus 36.3% ± 3.2) lower when compared with those from young animals (Figure 2.5.B and C). Additionally we also compared the antigen presentation ability of OVA pulsed cDC2s for two different time points viz 2hr and 24hrs which were generated from young, aged and IFNRKO animals. The CFSE dilution was plotted for individual peaks from different conditions and found a significant decrease in the CFSE diluting cells in the last peak where cDC2s were generated from aged and IFNRKO animals than young animals (Figure 2.5D, E and 2.7A-B). These results indicated that impaired IFN response in the DCs of aging animals could partly help explain the diminished activity of DCs to cross-present antigens in stimulating $CD8^{+}$ T cells.

Figure2.5

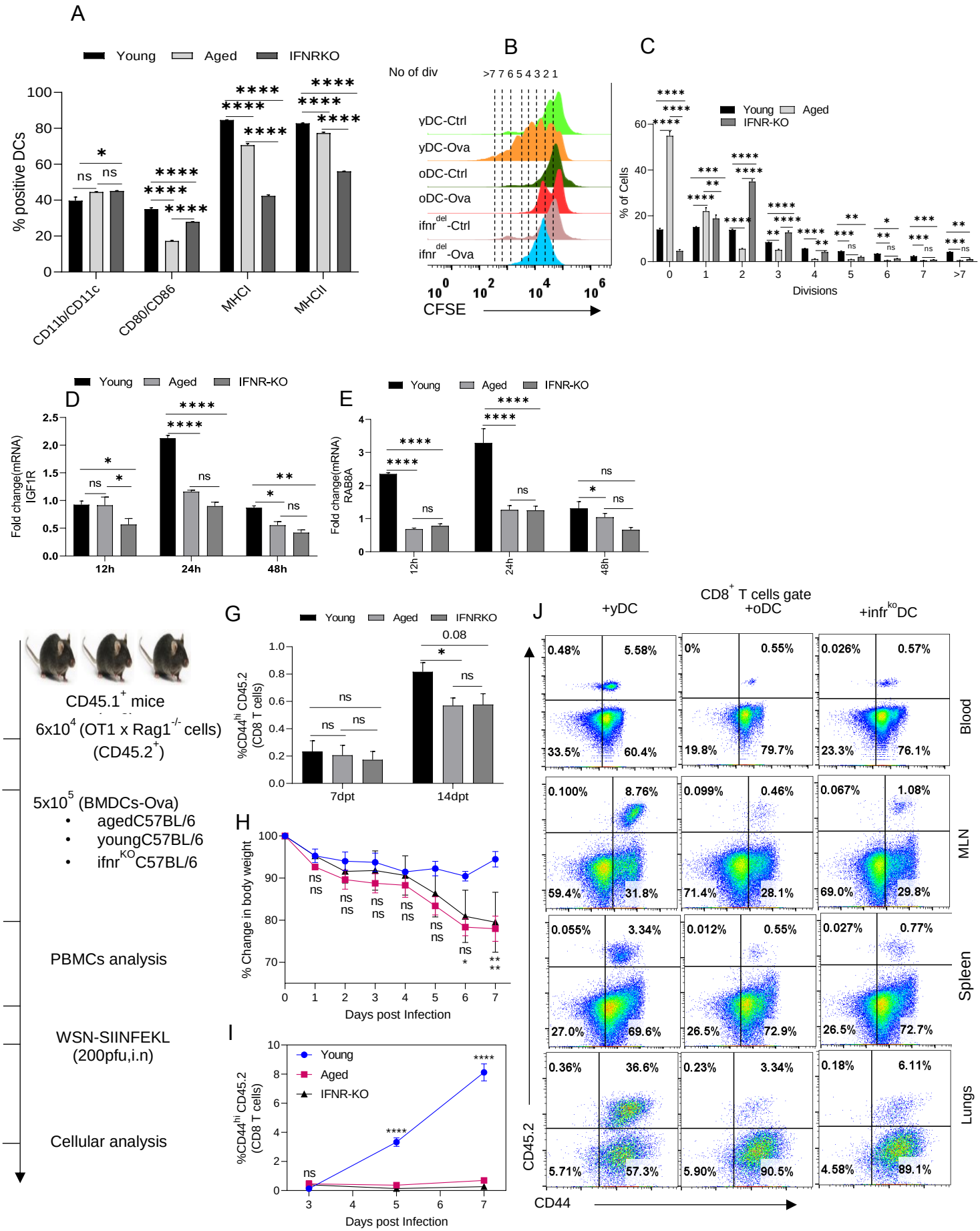
A
Young
Aged
IFNRKO
% positive DCs
CD11b/CD11c
CD80/CD86
MHCI
MHCII
B
No of div
>7 7 6 5 4 3 2 1
yDC-Ctrl
yDC-Ova
oDC-Ctrl
oDC-Ova
ifnr del -Ctrl
ifnr del -Ova
CFSE
C
Young
Aged
IFNR-KO
% of Cells
Divisions
D
Young
Aged
IFNR-KO
Fold change(mRNA) IGF1R
12h
24h
48h
E
Young
Aged
IFNR-KO
Fold change(mRNA) RAB8A
12h
24h
48h
F
Days
CD45.1+ mice
6x10^4 (OT1 x Rag1-/- cells) (CD45.2+)
5x10^5 (BMDCs-Ova)
agedC57BL/6
youngC57BL/6
ifnrKOC57BL/6
PBMCs analysis
WSN-SIINFEKL (200pfu,i.n)
Cellular analysis
1
2
9
16
17
25
G
Young
Aged
IFNRKO
%CD44hi CD45.2 (CD8 T cells)
7dpt
14dpt
H
% Change in body weight
Days post Infection
I
Young
Aged
IFNR-KO
%CD44hi CD45.2 (CD8 T cells)
Days post Infection
J
CD8+ T cells gate
+yDC
+oDC
+infrkoDC
Blood
MLN
Spleen
Lungs
CD45.2
CD44

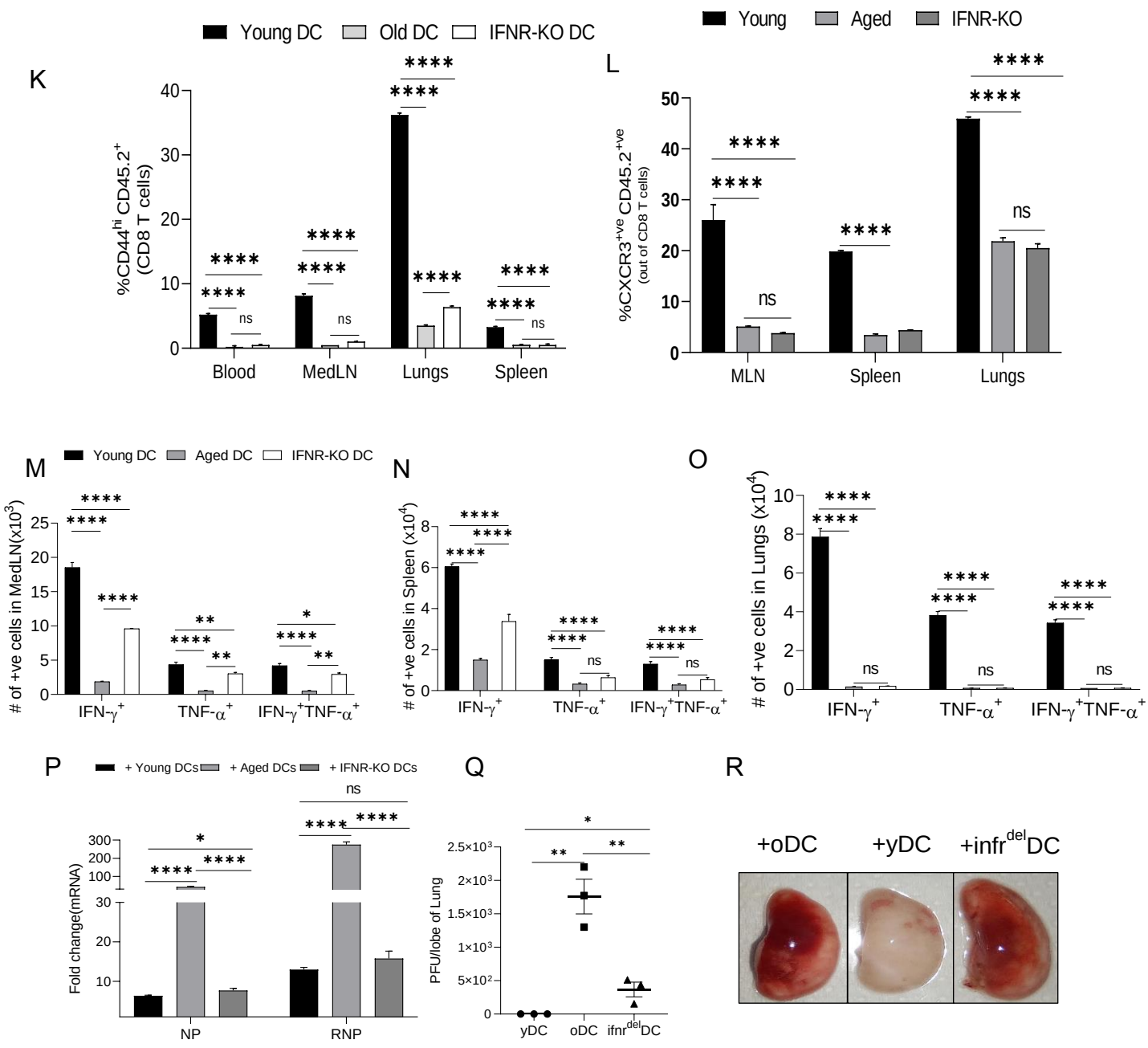
K
Young DC
Old DC
IFNR-KO DC
%CD44hi CD45.2+ (CD8 T cells)
Blood
MedLN
Lungs
Spleen
L
Young
Aged
IFNR-KO
%CXCR3+ve CD45.2+ve (out of CD8 T cells)
MLN
Spleen
Lungs
M
Young DC
Aged DC
IFNR-KO DC
of +ve cells in MedLN(x10^3)
IFN-γ+
TNF-α+
IFN-γ+TNF-α+
N
of +ve cells in Spleen (x10^4)
O
of +ve cells in Lungs (x10^4)
P
+ Young DCs
+ Aged DCs
+ IFNR-KO DCs
Fold change(mRNA)
NP
RNP
Q
PFU/lobe of Lung
yDC
oDC
ifnrdelDC
R
+oDC
+yDC
+infrdelDC

Figure 2.5 DCs of an aging host exhibits phenotypic and functional impairment

Bone marrow from young, aged and IFNR-KO mice were cultured in the presence of GM-CSF and IL-4 for 6 days to differentiate into DCs. The cells were then phenotypically characterized. A. Representative bar graphs summarize the frequency of cells stained for the indicated markers. B-C. *In-vitro* generated BMDCs were harvested and sorted as double positive cells by staining with anti-CD11b and CD11c antibodies. The sorted cells were pulsed with ovalbumin for 2 hours and were co-cultured with CFSE labelled OT1 cells for 72 hours. The extent of proliferating cells was measured by CFSE dilution. B. Representative offset histograms show the frequency of proliferating $CD8^+$ T cells in the indicated conditions. C. Cumulative data is summarised by bar diagram (n=3). Mean ± SEM values are shown and one way ANOVA was used to assess statistical differences. ****p<0.0001; ***p<0.001;**p<0.01;*p<0.05, ns p>0.05.(One way ANOVA). D. Representative overlaid histogram show the frequency of CFSE diluting OT1 cells D-E. Bar graph showing the fold change expression of IGF1R (D) and Rab8a (E) in the cytokine mediated differentiation of BMDCs at indicated time post culture using qRT-PCR (n=3). Means ± SEM values are shown and the data are analysed by two way ANOVA. ****p<0.0001; ***p<0.001;**p<0.01;*p<0.05, ns p>0.05. G. In-vitro generated BMDCs were sorted and equal number of BMDCs were pulsed with ovalbumin for 2 hours. The cells were then washed and 5x105 cells were transferred into $CD45.1^+$ animals which were previously infused with OT1 cells. The mice were infected intranasally with an IAV (WSN-SIINFEKL) two weeks later to assess cellular and viral parameters. H. Bar diagram summarize the frequency of expanded donor cells at 7 and 14 days post DC transfer. I. Line graph shows the change in body weights of different groups of animals at different dpi. J. Line graph show the kinetics of virus specific donor CD8+ T cell expansion in the blood of BMDCs recipients (n=3). Data are shown as Mean ± SEM values and analysed by one way ANOVA. ****p<0.0001; ***p<0.001;**p<0.01;*p<0.05, ns p>0.05. K. Representative FACS plot from different lymphoid and non-lymphoid organs are shown for assessing specific donor cells. L. Bar graph summarizes the cumulative data for the frequencies of donor cells in different organs. M. Bar graph represents the frequency of $CXCR3^+CD45.2^+$ cells out of total $CD8^+$ T cells in different organs of BMDCs recipients. N-P. Bar graphs summarize the data from ICCS assays to assess the functionality of expanded donor cells in draining MLN (N), spleen (O) and lungs (P) are shown. Q. Bar graph shows the viral load in the lungs of infected

animals using influenza NP and RdRP specific primers. R. Dot plots show the viral titres in the lungs as measured by plaque forming assays. S. Representative gross images of lungs of each recipients are shown (n=3). Data are shown as Mean ± SEM and analysed by two way ANOVA. ****p<0.0001; ***p<0.001;**p<0.01;*p<0.05, ns p>0.05.. The experiments were repeated at least twice and representative data from one of the experiment is shown.

Figure2.6

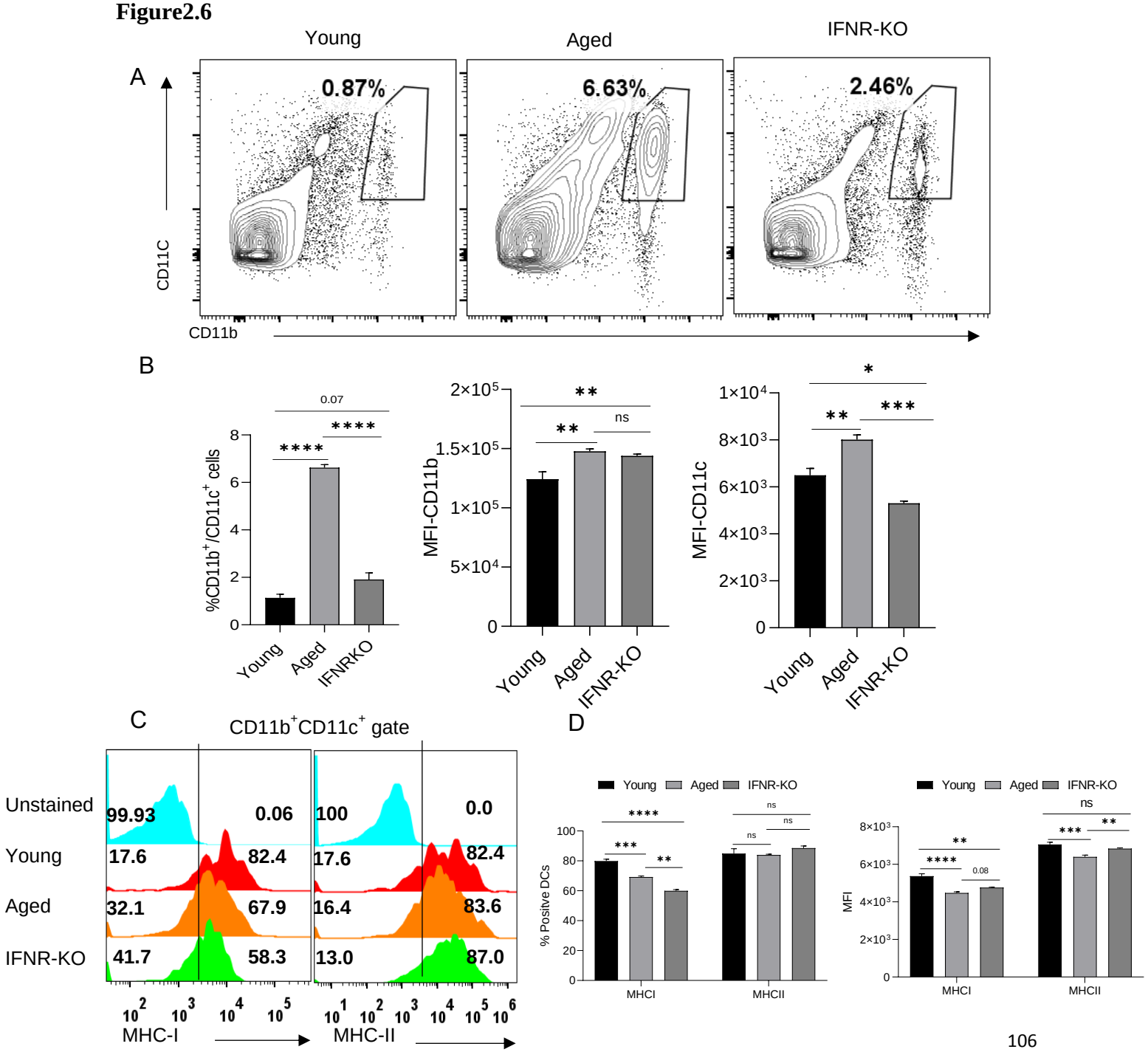

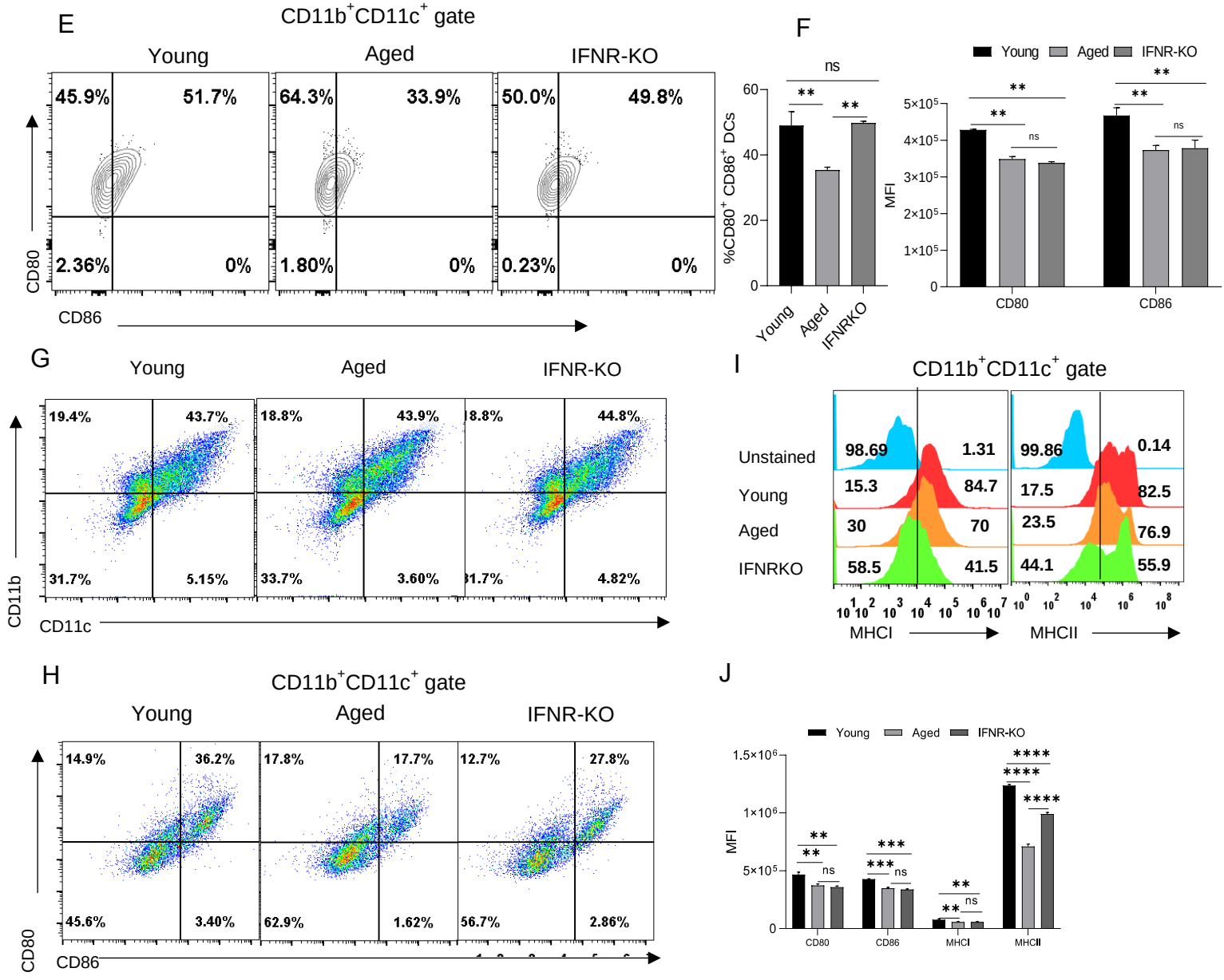
E
CD11b+CD11c+ gate
Young
Aged
IFNR-KO
45.9%
51.7%
2.36%
0%
64.3%
33.9%
1.80%
0%
50.0%
49.8%
0.23%
0%
CD80
CD86
F
Young
Aged
IFNR-KO
ns
%CD80+ CD86+ DCs
MFI
CD80
CD86
G
Young
Aged
IFNR-KO
19.4%
43.7%
31.7%
5.15%
18.8%
43.9%
33.7%
3.60%
8.8%
44.8%
1.7%
4.82%
CD11b
CD11c
I
CD11b+CD11c+ gate
Unstained
Young
Aged
IFNRKO
98.69
1.31
15.3
84.7
30
70
58.5
41.5
99.86
0.14
17.5
82.5
23.5
76.9
44.1
55.9
MHCI
MHCII
H
CD11b+CD11c+ gate
Young
Aged
IFNR-KO
14.9%
36.2%
45.6%
3.40%
17.8%
17.7%
62.9%
1.62%
12.7%
27.8%
56.7%
2.86%
CD80
CD86
J
Young
Aged
IFNR-KO
MFI
CD80
CD86
MHCI
MHCII

Figure2.6: Phenotypic profiling of splenic DCs and BMDCs reveals downregulation of key molecules required for CD8$^+$ T cells priming.

A. Representative FACS plot show the frequency of DCs in the spleens of young, aged and IFNRKO mice. B. Bar graph show the cumulative data of frequency and MFI of (A). C. Overlaid histogram show the frequency of MHCI and MHCII expression on DCs from young, aged and IFNRKO mice. D. Bar graphs show the cumulative data of frequency and MFI of indicted molecules of (C). E. Representative FACS plots show the frequency and MFI of DCs staining for costimulatory molecules CD80 and CD86. F. Bar graphs show the cumulative data of (E). Data represents Means ± SEM. ****p<0.0001; ***p<0.001;**p<0.01;*p<0.05, ns p>0.05 (one way ANOVA). G. Representative FACS plot show the frequency of BMDCs generated from aged, young and IFNRKO bone marrow. H. Representative FACS plot show the frequency of BMDCs staining for the costimulatory receptors CD80 and CD86. I. Overlaid histogram show the frequency of MHCI and MHCII positive BMDCs from each group is shown. J. Bar diagrams summarize the expression of the indicated molecule on a per cell basis in each group are shown. Data represents Means ± SEM. ****p<0.0001; ***p<0.001;**p<0.01;*p<0.05, ns p>0.05 (one way ANOVA). The experiments were repeated at least three times and representative data from one of the experiment is shown.

Figure 2.7

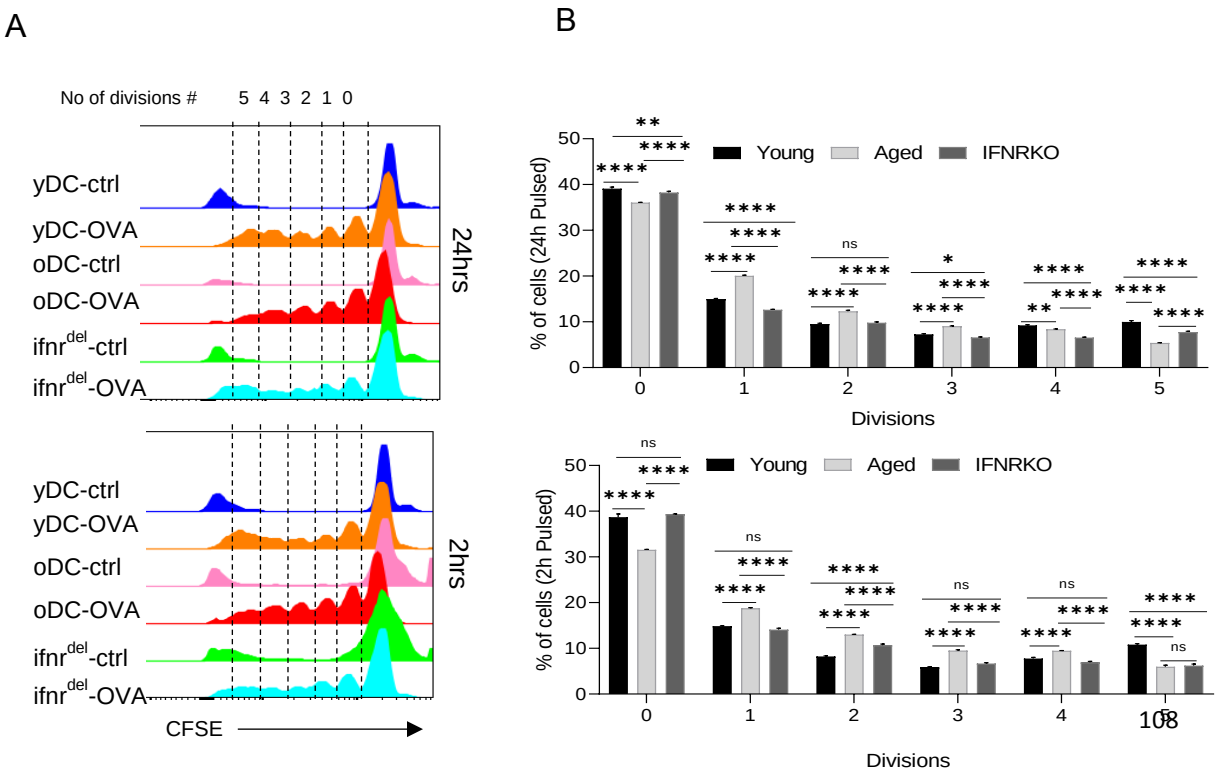

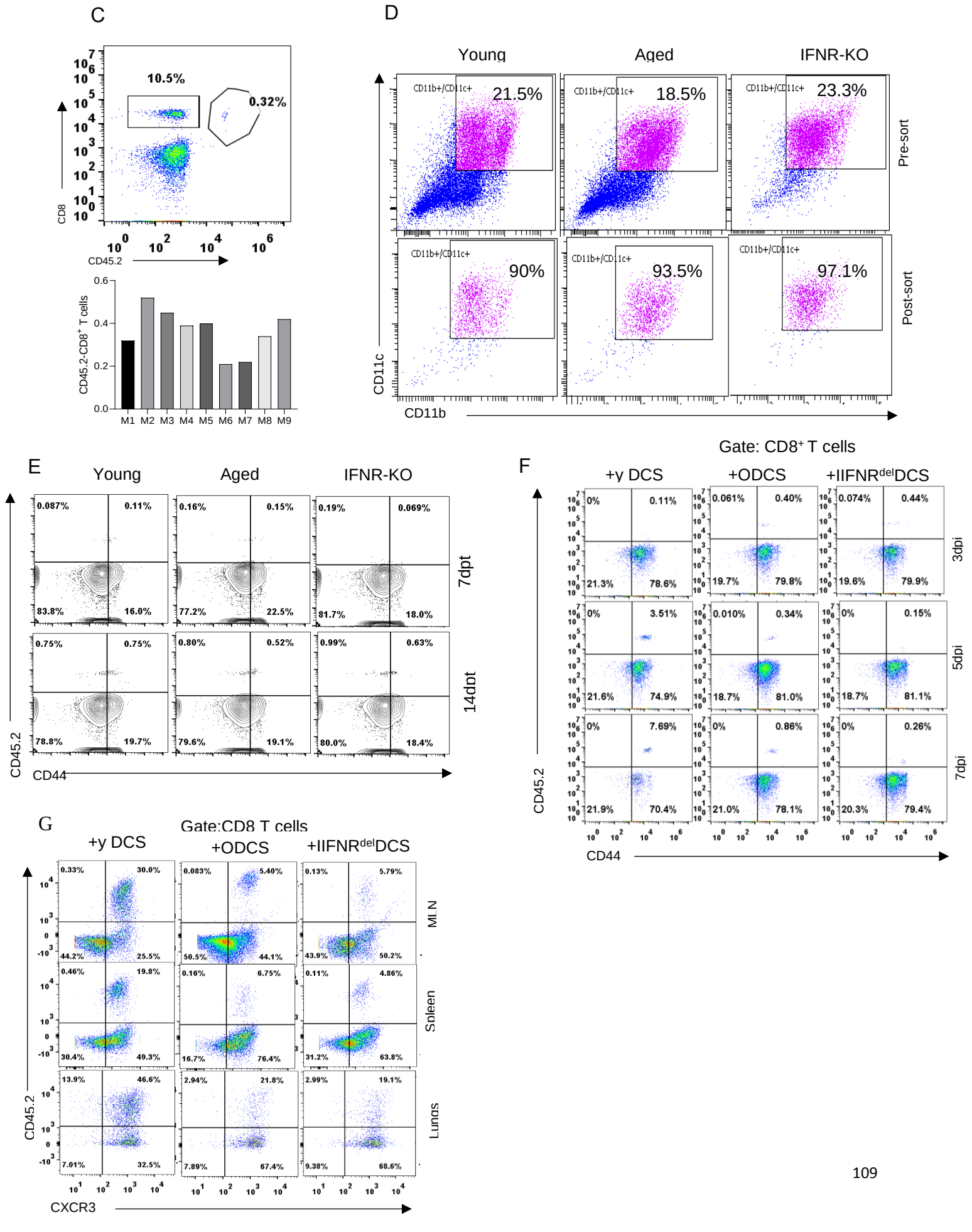
C
10.5%
0.32%
CD8
CD45.2
CD45.2-CD8+ T cells
M1 M2 M3 M4 M5 M6 M7 M8 M9
D
Young
Aged
IFNR-KO
CD11b+/CD11c+
21.5%
18.5%
23.3%
90%
93.5%
97.1%
Pre-sort
Post-sort
CD11c
CD11b
E
Young
Aged
IFNR-KO
0.087%
0.11%
83.8%
16.0%
0.16%
0.15%
77.2%
22.5%
0.19%
0.069%
81.7%
18.0%
7dpt
0.75%
0.75%
78.8%
19.7%
0.80%
0.52%
79.6%
19.1%
0.99%
0.63%
80.0%
18.4%
14dpt
CD45.2
CD44
F
Gate: CD8+ T cells
+y DCS
+ODCS
+IIFNRdelDCS
0%
0.11%
21.3%
78.6%
0.061%
0.40%
19.7%
79.8%
0.074%
0.44%
19.6%
79.9%
3dpi
0%
3.51%
21.6%
74.9%
0.010%
0.34%
18.7%
81.0%
0%
0.15%
18.7%
81.1%
5dpi
0%
7.69%
21.9%
70.4%
0%
0.86%
21.0%
78.1%
0%
0.26%
20.3%
79.4%
7dpi
CD45.2
CD44
G
Gate:CD8 T cells
+y DCS
+ODCS
+IIFNRdelDCS
0.33%
30.0%
44.2%
25.5%
0.083%
5.40%
50.5%
44.1%
0.13%
5.79%
43.9%
50.2%
MLN
0.46%
19.8%
30.4%
49.3%
0.16%
6.75%
16.7%
76.4%
0.11%
4.86%
31.2%
63.8%
Spleen
13.9%
46.6%
7.01%
32.5%
2.94%
21.8%
7.89%
67.4%
2.99%
19.1%
9.38%
68.6%
Lungs
CD45.2
CXCR3

Figure2.7: Sorting strategy for BMDCs and OT1 transfer status for in-vivo DCs immunization experiments.

A. Representative overlaid histogram show the frequency of CFSE diluted cells at the level of different peaks in indicated conditions. B. Bar graph show the MFI of CFSE diluting cells in indicated conditions. C. FACS plot show the frequency of $CD45.2^{+}CD8^{+}$ T (OT1) transferred cells in individual biological replicates before the transfer of ovalbumin pulsed BMDCs. D. FACS plot showing the pre-sort (Top panel) and post sort purity of sorted BMDCs. E. FACS plot show the frequency of donor OT-I cells at 7 and 14 days post BMDC immunisation. F. Representative FACS plot show the frequency of expanded donor cells in the blood at different days of post infection in each group of animals is shown. G. Representative FACS plot show the frequency of $CXCR3^{+}CD45.2^{+}CD8^{+}$ T cells in different cellular compartments of different BMDCs recipient animals.

DCs immunization impaired cross-presentation by DCs of aged mice

Having assessed the phenotypic differences and reduced *ex vivo* cross-priming potential of DCs from aged mice, we evaluated *in vivo* activity in a normalized environment. Antigen-pulsed DCs ($5x10^5$ of the sorted $CD11b^{+}CD11c^{+}$ BMDCs) (purity ~95%) from young, aged and IFNRKO young mice were injected in congenic $CD45.1^{+}$ young animals that were adoptively transferred with $6x10^4$ of $CD45.2^{+}$ OT1 cells one day earlier (Figure 2.7.C and 2.7.D). The recipients showed equal distribution of OT1 cells the following day (Figure 2.7.D). We observed upto a two-fold increase in the frequencies of OT1 cells in the peripheral blood of animals receiving DC-therapy of young animals' origin as compared to those injected with DC of aged animals 15 days later (Figure 2.5.H and 2.6.E). The animals were then infected with IAV (WSN-SIINFEKL) intranasally to recall OT1 cells. The recipients of the aged and IFNRKO DCs showed a sharp decline in body weights in the acute phase of infection, while those receiving DC-therapy of young animals' origin showed only a slight and transient reduction in body weights (Figure 2.5.I). A rapid recovery in

body weights of animals in the latter group of animals could be due to an efficient viral control by the activity of the expanded OT1 cells. Frequencies of OT1 cells in the peripheral blood were 5.20% ± 0.34, 0.21% ± 0.29 and 0.52% ± 0.10 in the group that received ovalbumin pulsed DCs of young, aged and IFNRKO mice, respectively (Figure 2.5.J-K and 2.7.E). We then analysed the distribution of $CD8^+$ T cells in different lymphoid and non-lymphoid organs the next day (Figure 2.5.K and L). Such cells were >10, 5 and 7-fold more abundant in medLN, spleen and lungs of animals receiving DCs from young as compared to those infused with DCs from aged and IFNRKO animals, respectively (Figure 2.5.K and L). Recalled OT1 cells expressing CXCR3 were significantly reduced in the recipients of DC-therapy from aged and IFNRKO in comparison to those from younger mice (Figure 2.5.M and 2.7.F). CXCR3 is expressed on inflammatory tissue homing $CD8^+$ T cells (17). Cognate peptide stimulated OT1 cells that produced IFN-γ, TNF-α or both the cytokines were 20-times more abundant in the medLN of animals receiving DC-therapy of young as compared to that from aged animals (Figure 2.5.N, O and P). We then assessed the anti-viral effects of differentially expanded $CD8^+$ T cells and observed significantly reduced titres of IAV as well as the expression of viral genes in the lungs of the animals receiving DC-therapy from aged and IFNRKO mice as compared to the animals receiving DC-therapy from young animals (Figure 2.5.Q and R). Furthermore, haemorrhagic, and inflammatory lesions were more pronounced in the animals receiving DC-therapy from aged and IFNRKO mice as compared to the recipients of young animals' origin (Figure 2.5.S). Therefore, we show that DCs of aged animals are compromised in their ability to provide anti-viral protection and a diminished IFN response in the DCs of aged individuals could in part contribute to the observed effects. However, factors other than the compromised IFN response, which is more likely to occur in the aging innate immune

cells such DCs, could also contribute to poor priming of antigen specific $CD8^+$ T cells leading to an inefficient protection to the aging host against viral infections.

Rab8a dependent deficit in differentiation program and type I IFN response in DCs of an aging host

Next, we focused our analysis on the differentiation of DCs from precursor cells in the aged and young animals as the maturation status directly impacts their function. Bone marrow cells from aged and young animals cultured in the presence of GM-CSF and IL-4 were processed for RNA isolation to analyze the expression profile of genes downstream to the growth factor receptor such as CSF2Ra and IGFR. Bone marrow cells of young as compared to the aged animals expressed significantly higher levels of *CSF2Ra, IGF1R* and *Rab8a* (Figure 2.5.E and 2.9.A-E). During the differentiation of BMDCs the expression of *IGF1R* and *Rab8a* was increased by upto 3-fold in younger animals but remain unchanged in those of aged and IFNRKO mice (Figure 2.5. E). Several other genes involved in mTOR signaling *viz. PI3K, mTOR, SIN1, Akt1, 2* and *3, S6K* and *PRAS40* were significantly downregulated whereas the inhibitors of mTORC1 signaling, *Tsc1* and *Tsc2* were found significantly upregulated in bone marrow cells of aged animals (Figure 2.9.F-G). This was indicative of diminished proliferative, survival and differentiation potential of aged bone marrow cells. As IGF1R-PI3K pathway critically controls the differentiation program of DCs, we further elucidated its role by shRNA mediated knock down (KD) of *Rab8a*, an adaptor molecule downstream to IGF1R in the bone marrow cells (Figure 2.9.H-J). Following disruption of Rab8a function in DCs of young mice, the expression of gene encoding for the receptor *IGF1R* (~30-fold) and a downstream kinase, *Akt1* (~17-fold) were significantly reduced (Figure 2.9.J). That a knockdown of Rab8a also downregulates expression of IGF1R was shown previously (18). The

data suggest that the cytokine mediated impaired differentiation of precursor cells into DCs is critically dependent on Rab8a.

Does the deficiency of Rab8a in DCs affect their function? We firstly characterised the Rab8a-depleted BMDCs and the control counterparts phenotypically. The frequencies of $CD11b^{+}CD11c^{+}$ cells were significantly reduced following Rab8a deficiency in the cells during their differentiation (Rab8a-KD ~33.17% ± 0.37, Control >39.97 % ± 0.72) (Figure 2.8.A-C). Among $CD11b^{+}CD11c^{+}$ cells, those expressing costimulatory molecules (CD80 and CD86) were also significantly reduced in the Rab8a-KD cells (~24.17% ± 0.86) as compared to the scrambled controls (~49.3% ± 0.75) (Figure 2.8.C and 2.9.L and M). Not only the percent positive but also the MFI values for CD86 were significantly lower in the shRNA treated group (Figure 2.9.N). Furthermore, the frequency of class I and II MHC expressing DCs were significantly reduced in the Rab8a-KD cells (Figure 2.8.C, and 2.9.N-O). Frequencies of live cells were comparable within control and the Rab8a-KD cells negating the toxic effects of the shRNA mediated KD of Rab8a (Figure 2.9.P-R). Therefore, Rab8a deficiency resulted in impaired differentiation as well as maturation of DCs. Given an essential role of DCs in mounting the first anti-viral response following an infection, we compared the expression levels of genes of type I IFN pathway in control and Rab8a deficient cells following stimulation with IAV (Figure 2.8.D and E). Rab8a deficient cells were drastically reduced in the expression of *IFNα* (70-fold), *IFNβ* (50-fold), *IFNγ* 46-fold), *STAT1* (80-fold) and *STAT2* (4-fold) (Figure 2.8.D-E). Therefore, a reduced expression of Rab8a in DCs impedes not only the differentiation program but also their virus sensing and the production anti-viral IFNs.

Figure 2.8

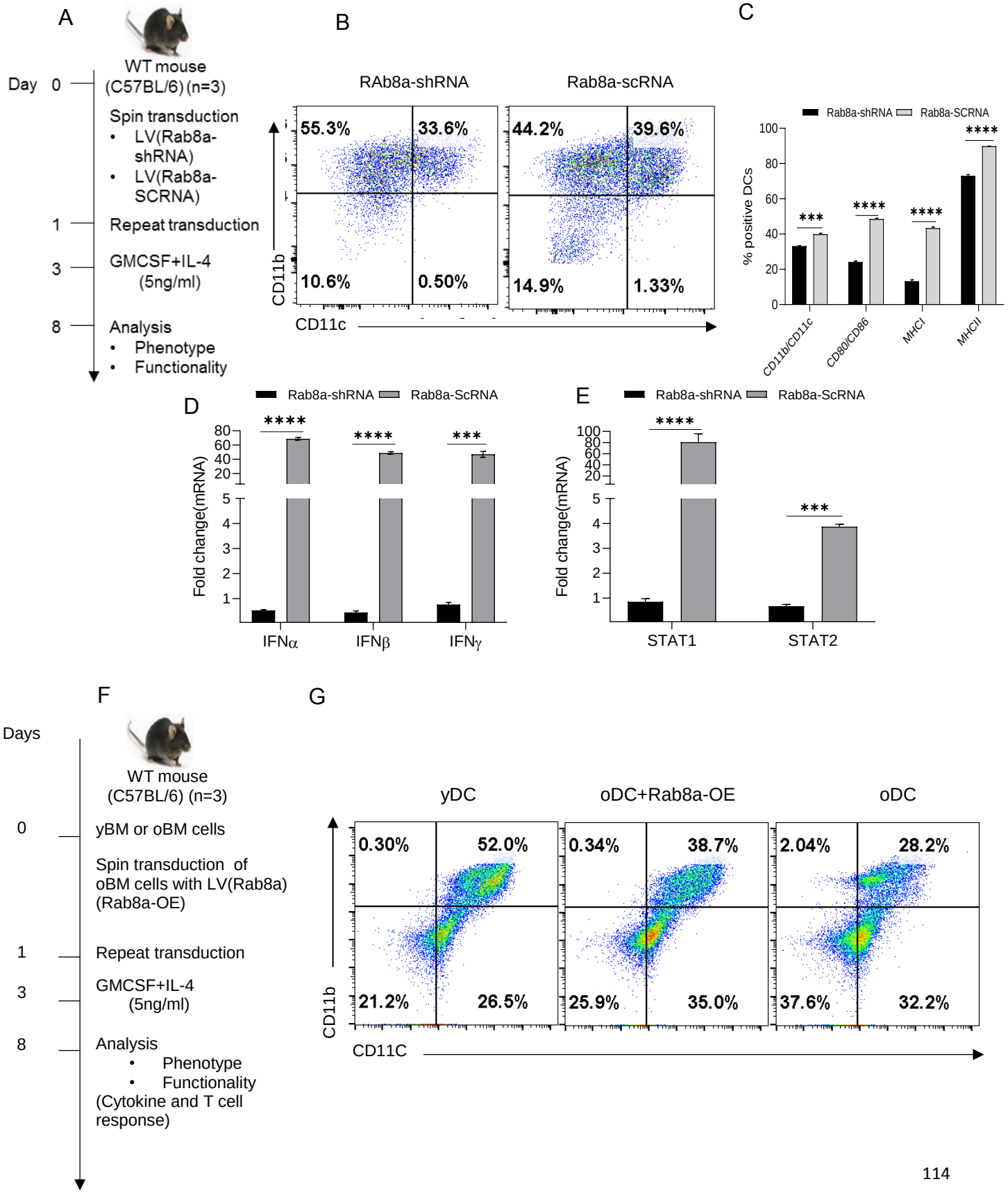
A
WT mouse
(C57BL/6) (n=3)
Day 0
Spin transduction
• LV(Rab8a-shRNA)
• LV(Rab8a-SCRNA)
1
Repeat transduction
3
GMCSF+IL-4
(5ng/ml)
8
Analysis
• Phenotype
• Functionality
B
RAb8a-shRNA
Rab8a-scRNA
55.3%
33.6%
10.6%
0.50%
44.2%
39.6%
14.9%
1.33%
CD11b
CD11c
C
Rab8a-shRNA
Rab8a-SCRNA
% positive DCs
CD11b/CD11c
CD80/CD86
MHCI
MHCII
D
Rab8a-shRNA
Rab8a-ScRNA
Fold change(mRNA)
IFNα
IFNβ
IFNγ
E
Rab8a-shRNA
Rab8a-ScRNA
Fold change(mRNA)
STAT1
STAT2
F
Days
WT mouse
(C57BL/6) (n=3)
0
yBM or oBM cells
Spin transduction of oBM cells with LV(Rab8a) (Rab8a-OE)
1
Repeat transduction
3
GMCSF+IL-4
(5ng/ml)
8
Analysis
• Phenotype
• Functionality
(Cytokine and T cell response)
G
yDC
oDC+Rab8a-OE
oDC
0.30%
52.0%
21.2%
26.5%
0.34%
38.7%
25.9%
35.0%
2.04%
28.2%
37.6%
32.2%
CD11b
CD11C

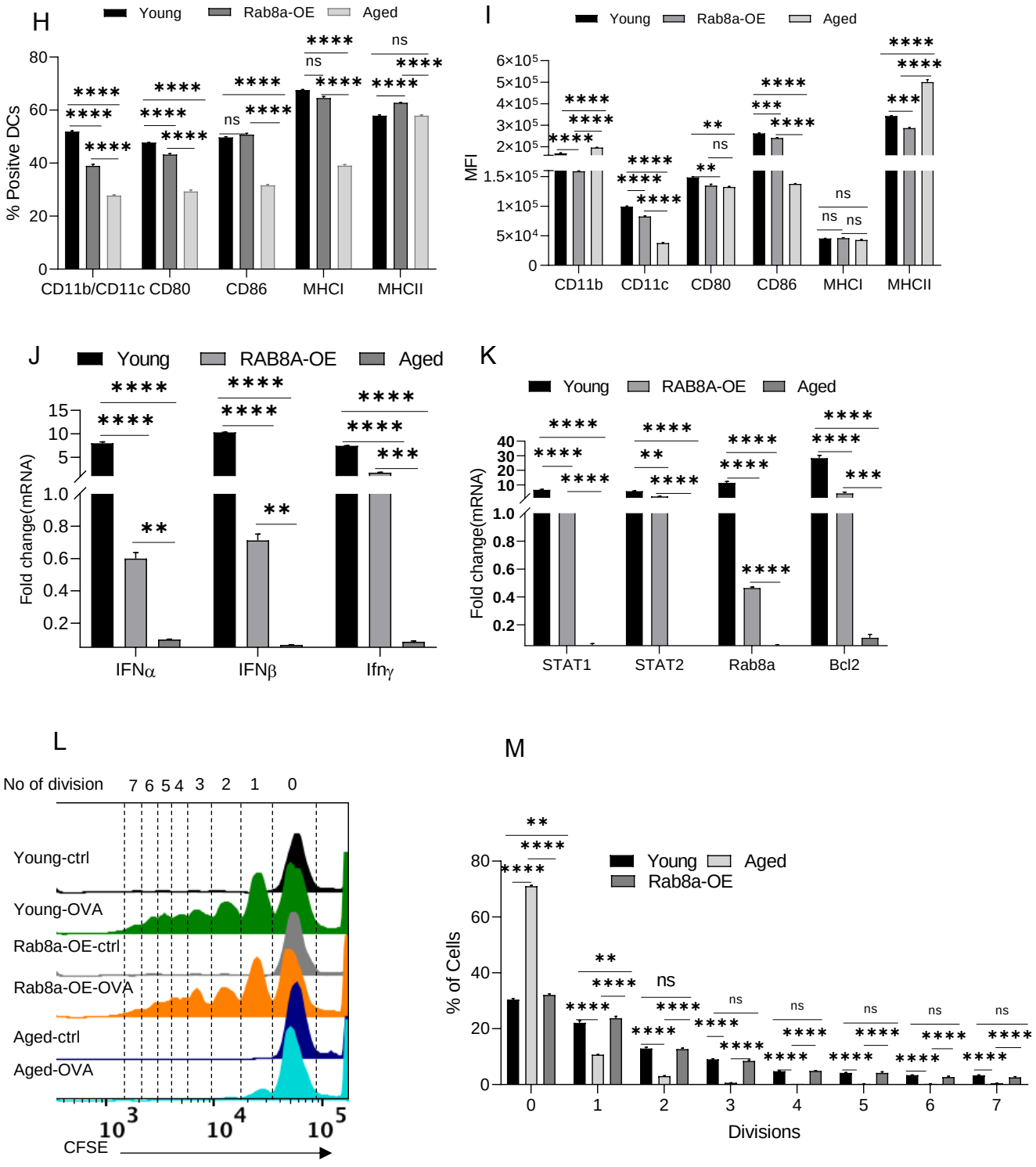
H
Young
Rab8a-OE
Aged
% Positive DCs
CD11b/CD11c
CD80
CD86
MHCI
MHCII
I
MFI
CD11b
CD11c
CD80
CD86
MHCI
MHCII
J
RAB8A-OE
Fold change(mRNA)
IFNα
IFNβ
Ifnγ
K
STAT1
STAT2
Rab8a
Bcl2
L
No of division
7 6 5 4 3 2 1 0
Young-ctrl
Young-OVA
Rab8a-OE-ctrl
Rab8a-OE-OVA
Aged-ctrl
Aged-OVA
CFSE
M
% of Cells
Divisions

Figure 2.8: Rab8a critically influences the differentiation and functionality of DCs.

A. Schematic of experiments is shown. Bone marrow cells from young animals were spin transduced to knockdown the expression of Rab8a. The cells lacking Rab8a were then cultured in media supplemented with GM-CSF and IL-4 for 6 days and were then assessed for phenotypic profiling and functionality. B. Representative FACS plots show the frequency of DCs ($CD11b^+/CD11c^+$) in shRNA and scrambled-construct transduced cells. C. Bar-graph show the frequency of different molecules on the surface of dendritic cells. D-E. Bar-graph show the expression of different key genes involved in type I IFN response upon pulsing with influenza A virus (n=3). Data represents Means ± SEM. ****p<0.0001; ***p<0.001;**p<0.01;*p<0.05, ns p>0.05. (one way ANOVA). F. Schematic of experiments where bone marrow cells from aged mice were transduced for Rab8a overexpression and then allowed to differentiate into DCs in presence of GMCSF and IL4 for 6 days. The cells were harvested and phenotypic profiling along with their functionality assays were performed. G. Representative FACS plot showing the frequency of dendritic cells ($CD11b^+/CD11c^+$) in the indicated groups are shown. H. Bar-graph show the frequency of DCs staining for different markers are shown. I. Bar-graph show the MFI of data represented in (H). J-K. Bar-graph show the expression of different key genes involved in Type I IFN response upon pulsing with influenza-A virus. L. Representative histogram show the proliferation of OTI cells co-incubated with ovalbumin stimulated BMDCs generated from young, aged and Rab8a-OE is shown. M. Bar-graph summarizing the frequency of proliferating $CD8^+$ T cells in the indicated conditions is shown (n=3). Data represents Means ± SEM. ****p<0.0001; ***p<0.001;**p<0.01;*p<0.05, ns p>0.05. (one way ANOVA). The experiments were repeated at least three times and representative data from one of each experiment is shown.

Figure 2.9

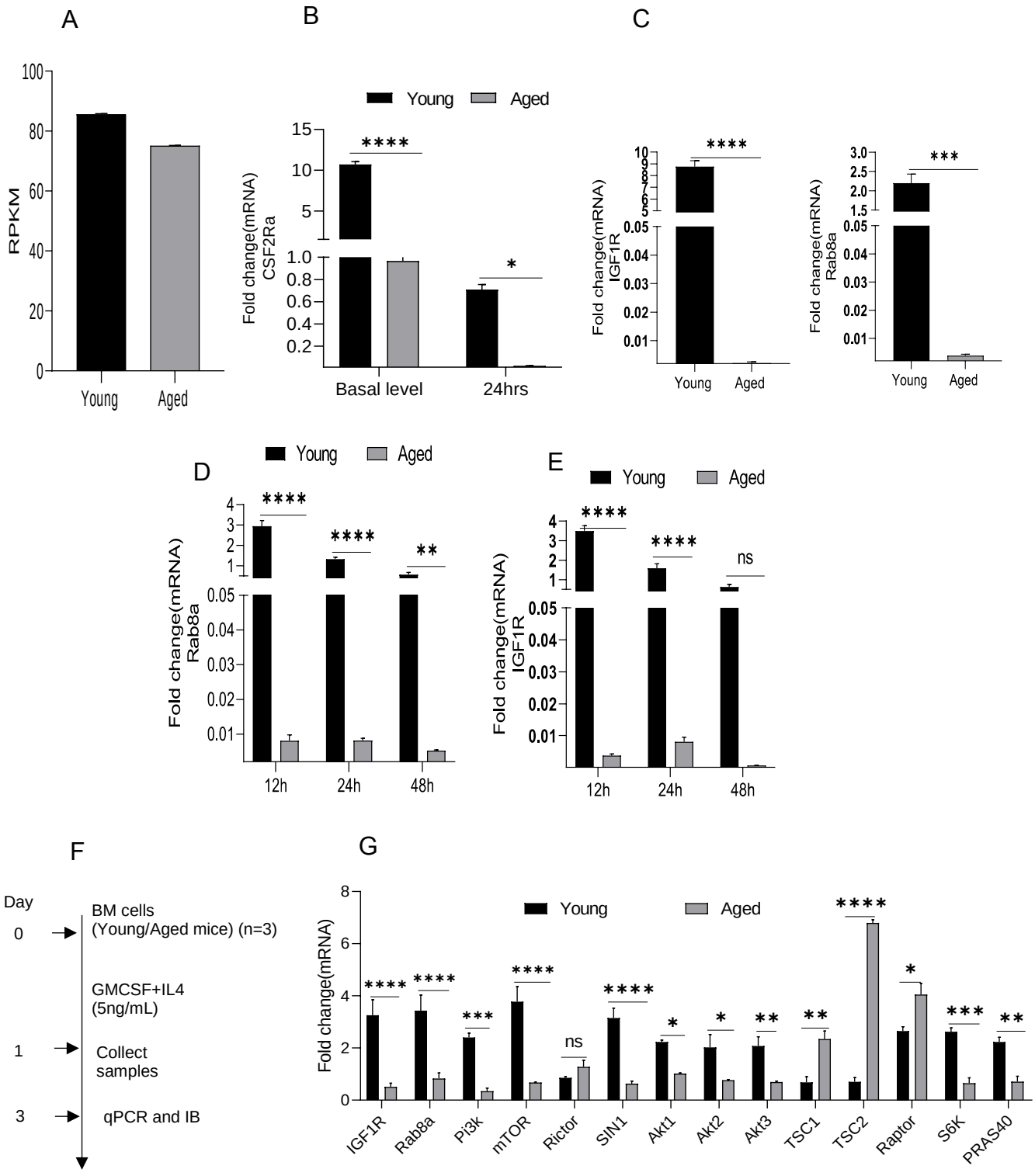
A
B
C
RPKM
Young
Aged
Fold change(mRNA) CSF2Ra
Basal level
24hrs
Fold change(mRNA) IGF1R
Fold change(mRNA) Rab8a
D
E
12h
24h
48h
ns
F
Day
0
BM cells
(Young/Aged mice) (n=3)
GMCSF+IL4
(5ng/mL)
1
Collect
samples
3
qPCR and IB
G
IGF1R
Rab8a
Pi3k
mTOR
Rictor
SIN1
Akt1
Akt2
Akt3
TSC1
TSC2
Raptor
S6K
PRAS40

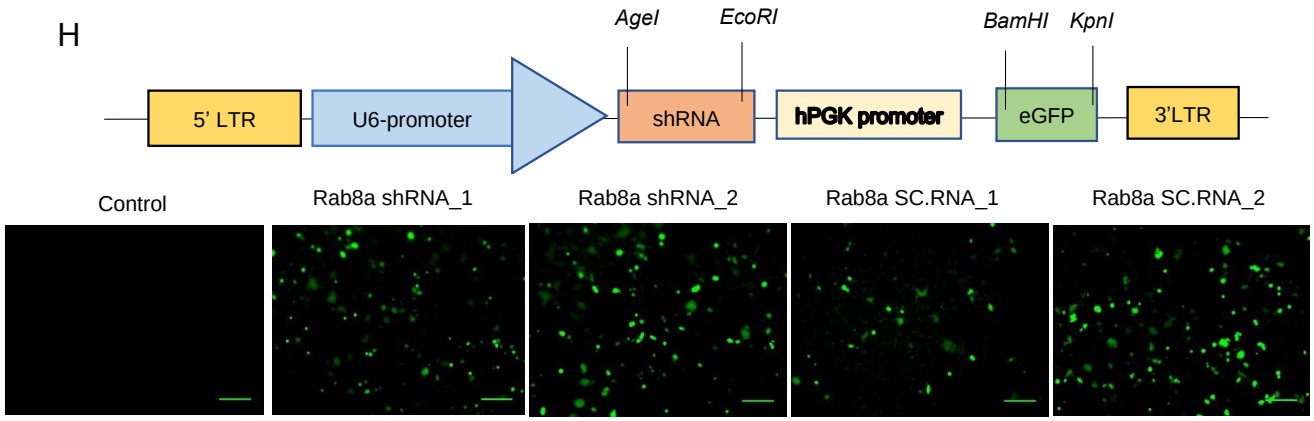
H
AgeI
EcoRI
BamHI
KpnI
5' LTR
U6-promoter
shRNA
hPGK promoter
eGFP
3'LTR
Control
Rab8a shRNA_1
Rab8a shRNA_2
Rab8a SC.RNA_1
Rab8a SC.RNA_2

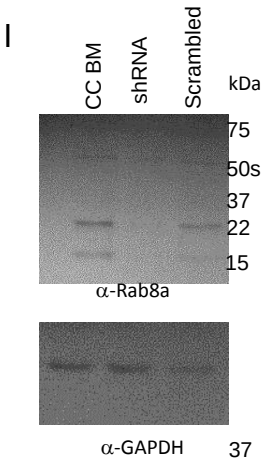
I
CC BM
shRNA
Scrambled
kDa
75
50s
37
22
15
α-Rab8a
α-GAPDH
37

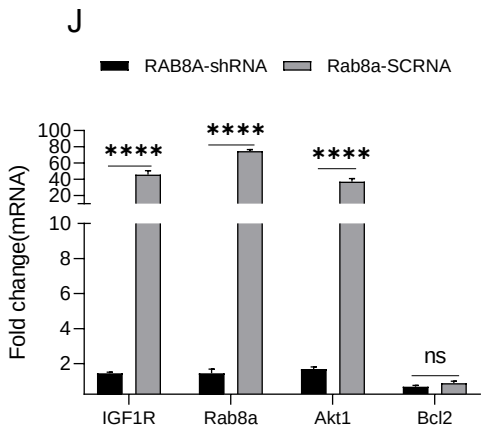
J
RAB8A-shRNA
Rab8a-SCRNA
Fold change(mRNA)
****
****
****
ns
IGF1R
Rab8a
Akt1
Bcl2

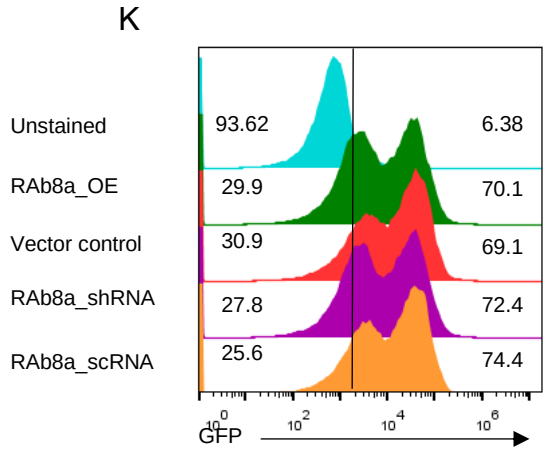
K
Unstained
RAb8a_OE
Vector control
RAb8a_shRNA
RAb8a_scRNA
93.62
6.38
29.9
70.1
30.9
69.1
27.8
72.4
25.6
74.4
GFP

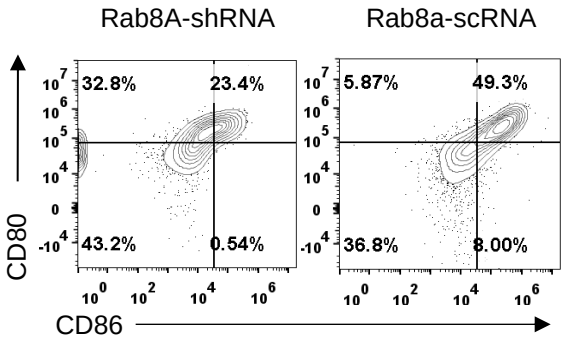
L
Rab8A-shRNA
Rab8a-scRNA
CD80
CD86
32.8%
23.4%
43.2%
0.54%
5.87%
49.3%
36.8%
8.00%

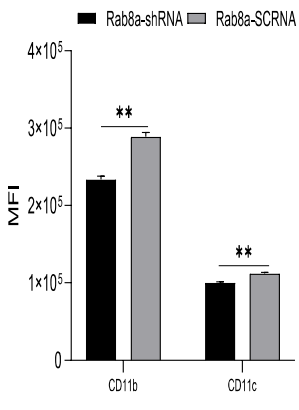
M
Rab8a-shRNA
Rab8a-SCRNA
MFI
**
**
CD11b
CD11c

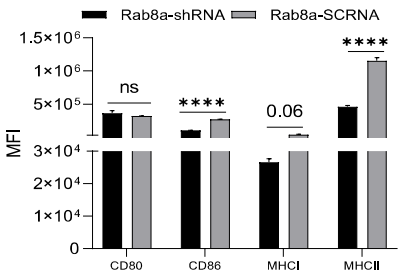
N
Rab8a-shRNA
Rab8a-SCRNA
MFI
ns
****
0.06
****
CD80
CD86
MHCI
MHCII

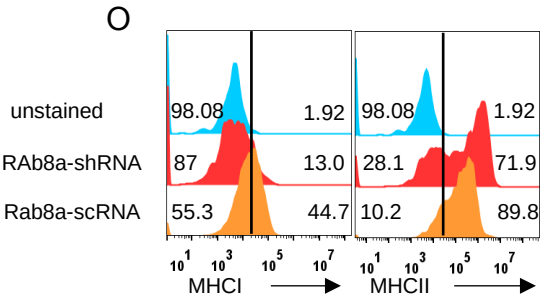
O
unstained
RAb8a-shRNA
Rab8a-scRNA
98.08
1.92
87
13.0
55.3
44.7
98.08
1.92
28.1
71.9
10.2
89.8
MHCI
MHCII

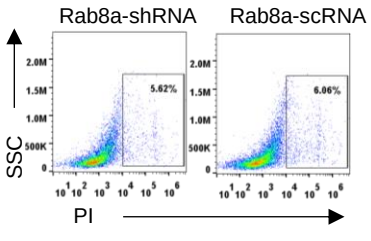
P
Rab8a-shRNA
Rab8a-scRNA
SSC
PI
5.62%
6.06%

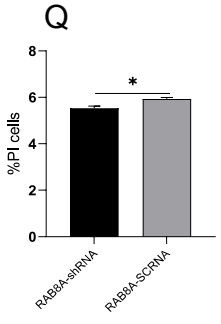
Q
%PI cells
*
RAB8A-shRNA
RAB8A-SCRNA

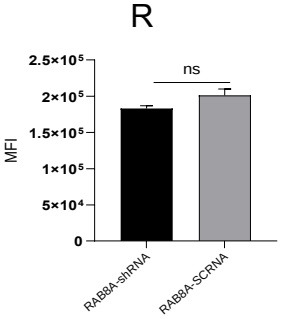
R
MFI
ns
RAB8A-shRNA
RAB8A-SCRNA

Figure 2.9: Knocking down of Rab8a in bone marrow cells of young mice compromised the differentiation and functionality of BMDCs.

A. Bar graph show the RPKM of Rab8a in DCs of aged and young mice. B. Bar graph shows the expression of CSF2Ra in absence and presence of GMCSF and IL4. C. Bar graph show the expression of IGF1R and Rab8a using qPCR in young and aged mice. D-E. Bar graph showing the expression of IGF1R (D) and Rab8a (E) in terms of fold change after pulsing with GMCSF and IL4 in young and aged mice at different time intervals. F. Schematic of experiments wherein BM from young and aged animals were culture in media supplemented with GMCSF and IL4 for 24hrs along with control cells (cultured in normal media) were collected, and transcript abundance of different key genes required for the growth and functional differentiation of DCs were measured. G. Bar graph showing the expression data in terms of fold change in each group. Data represents Means ± SEM. ****p<0.0001; ***p<0.001;**p<0.01;*p<0.05, ns p>0.05 (one way ANOVA). H. Schematic of cloning strategy for cloning of Rab8a in pLKO.1-GFP vector where shRNA and scrambled sequences for Rab8a were cloned downstream of the U6 promoter, between AgeI and EcoRI sites and fluorescence microscopy images showing GFP signal in HEK293T transfected for shRNA/Scrambled construct harbouring lentiviruses. Scale bar: 160μm. I. Western blot showing the knockdown efficiency at protein level using anti-Rab8a antibody. GAPDH served as an endogenous loading control J. Bar graph show the expression data to show the knockdown of Rab8a at mRNA level and other key genes using qPCR in the indicated groups. Data represents Means ± SEM. ****p<0.0001; ***p<0.001;**p<0.01;*p<0.05, ns p>0.05 (two way ANOVA). K. Overlaid histograms showing the transduction efficiency of BM cells in each group. L. FACS plot show the frequency of BMDCs staining for CD80 and CD86 generated from Rab8a-shRNA/SC-RNA BM cells. M-N Bar graph show the MFI of different molecules in the indicated groups. O. Overlaid histograms show the frequency of BMDCs expressing MHCI and MHCII molecules in the indicated groups. P. Representative FACS plot show the frequency of PI positive cells in each group. Q-R. Bar graphs show the frequency (Q) and MFI (R) of PI positive cells. The experiments were repeated at least three times and representative data from one of the experiment is shown.

Figure 2.10

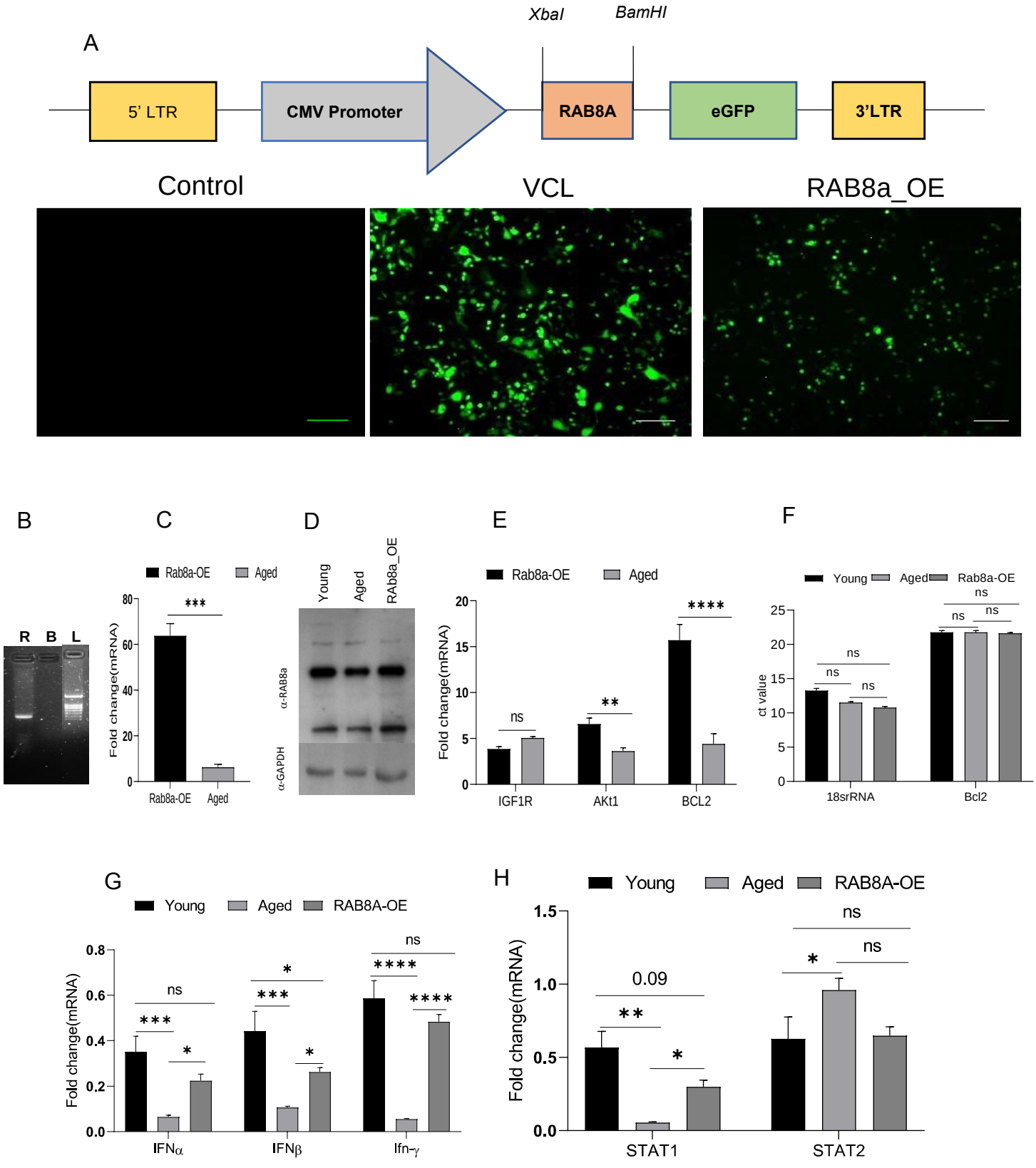
A
XbaI
BamHI
5' LTR
CMV Promoter
RAB8A
eGFP
3'LTR
Control
VCL
RAB8a_OE
B
R B L
C
Rab8a-OE
Aged
Fold change(mRNA)
***
Rab8a-OE
Aged
D
Young
Aged
RAb8a_OE
α-RAB8a
α-GAPDH
E
Rab8a-OE
Aged
Fold change(mRNA)
ns
**
****
IGF1R
AKt1
BCL2
F
Young
Aged
Rab8a-OE
ct value
ns
18srRNA
Bcl2
G
Young
Aged
RAB8A-OE
Fold change(mRNA)
IFNα
IFNβ
Ifn-γ
H
Young
Aged
RAB8A-OE
Fold change(mRNA)
0.09
STAT1
STAT2

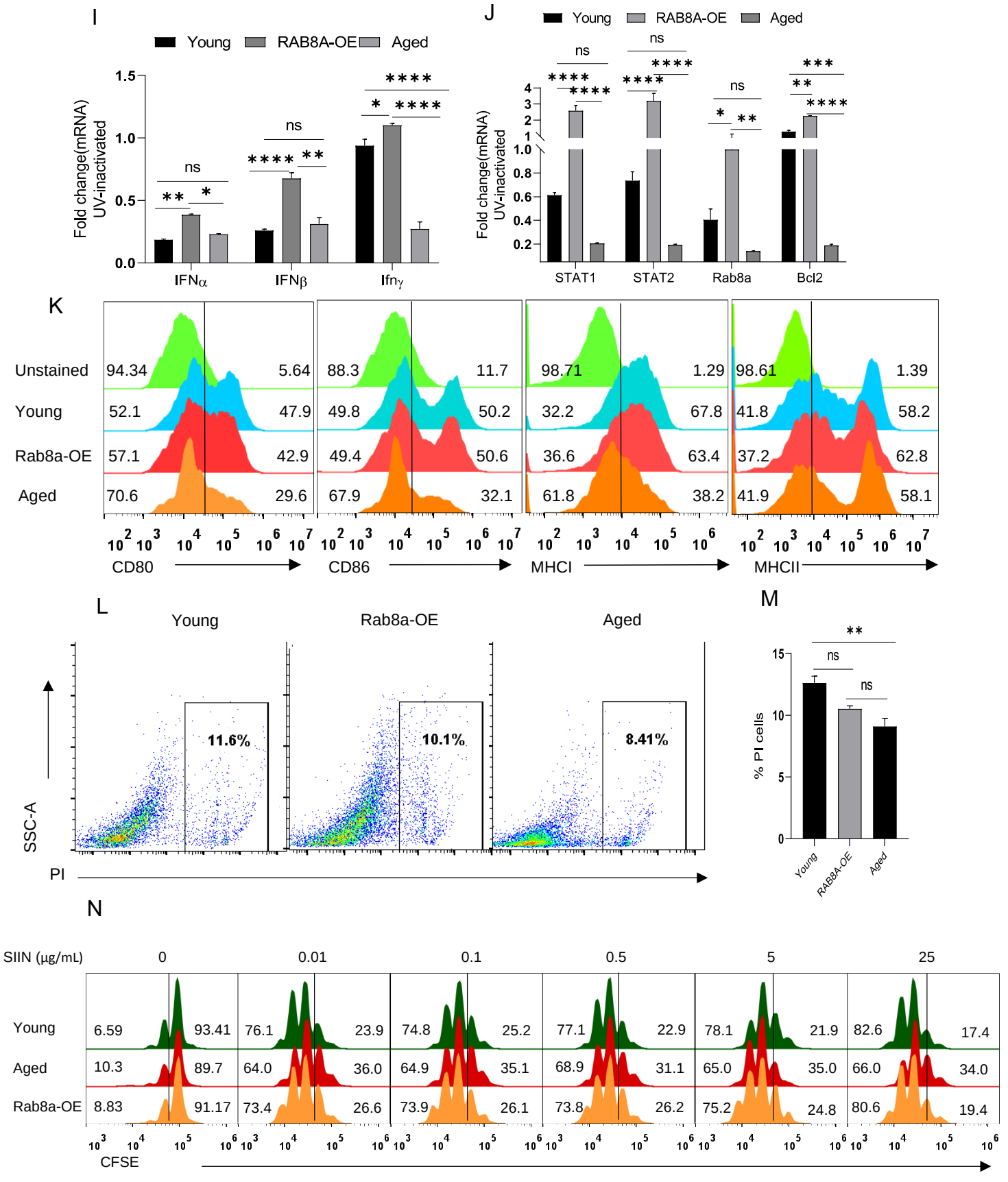
I
Young
RAB8A-OE
Aged
Fold change(mRNA) UV-inactivated
IFNα
IFNβ
Ifnγ
J
STAT1
STAT2
Rab8a
Bcl2
K
Unstained
Young
Rab8a-OE
Aged
CD80
CD86
MHCI
MHCII
L
SSC-A
PI
11.6%
10.1%
8.41%
M
% PI cells
N
SIIN (μg/mL)
0
0.01
0.1
0.5
5
25
CFSE

O

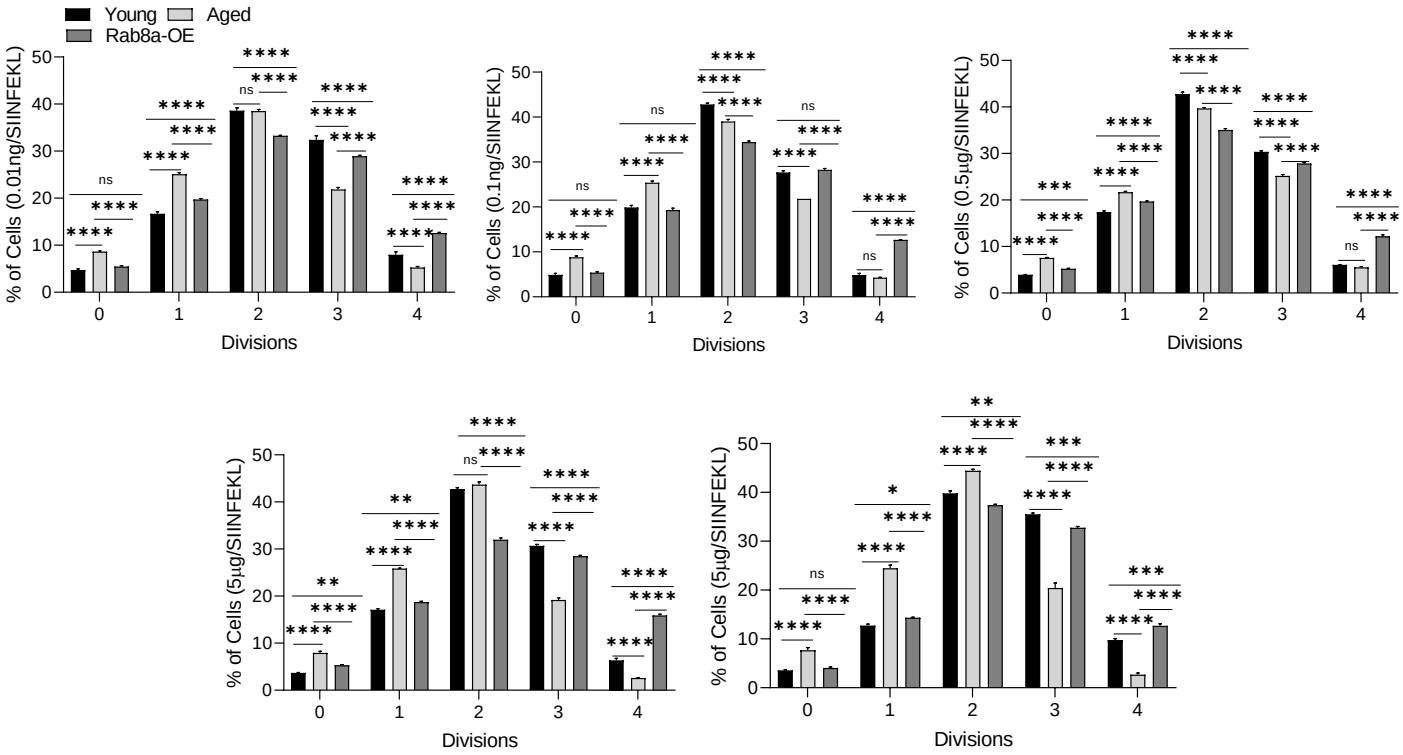

Figure 2.10: BMDCs of aged mice reconstituted of Rab8a regain functionality.

A. Schematic of strategy for cloning Rab8a in pLenti-GFP vector for the overexpression of Rab8a is shown (upper panel) and fluorescence microscopic images of transfected HEK293T cells to produce lentiviruses expressing Rab8a. Scale bar: 160µm. B. Agarose gel electrophoresis gel image shows Rab8a specific amplification in Rab8a (R) transduced cells and blank (B). C. Bar graph show the overexpression of Rab8a in lentivirus transduced bone marrow cells of aged mice and their control counterparts as assessed by qPCR. Mean ± SEM values are shown and the statistical analysis was performed by non-parametric t test. ****p<0.0001; ***p<0.001;**p<0.01;*p<0.05, ns p>0.05. D. Western blot shows the polypeptide bands of Rab8a ~22kDa in the indicated conditions. GAPDH was used as an endogenous loading control. E. Bar graph shows the abundance of transcripts for IGF1R, Akt1 and Bcl2 in Rab8a overexpressing aged bone marrow cells in comparison to aged bone marrow cells. Mean ± SEM values are shown and statistical analysis was done non-parametric t test. ****p<0.0001; ***p<0.001;**p<0.01;*p<0.05, ns p>0.05. F. Bar graph showing the ct value of Bcl2 and 18s rRNA in indicated groups. G. Offset histograms show the expression of indicated markers in BMDCs derived from different conditions. H and I. BMDCs generated from young, aged and aged

cells reconstituted of Rab8a were pulsed with IAV for 6 hours. Thereafter, the cells were processed for RNA isolation. The expression profile of genes involved in the type I IFN pathways was measured by qRT-PCR. Bar graphs show the expression of IFNα, IFNβ and IFN-γ (H), and STAT1 and STAT2 (I). J-K. Bar-graphs show the transcript abundance of different genes of type I IFN pathways from aged and Rab8a-OE BMDCs which were pulsed with UV inactivated IAV for 6hrs. L. Representative FACS plots show the frequency of PI positive cells in each group. M. Bar graphs show the frequency of PI positive cells in BMDCs generated from each group. N-O Representaive histogram and Bar graphs shows the frequency of CFSE dilution in respective case. Mean ± SEM values are shown and one way ANOVA was applied for calculating the level of statistical significance. ****$p<0.0001$; ***$p<0.001$; **$p<0.01$; *$p<0.05$, ns $p>0.05$.

Restoring functional competence in aging DCs by Rab8a reconstitution

We next investigated whether a reconstitution of Rab8a in bone marrow cells of aged individuals could help restore function. Bone marrow cells of aged animals were transduced with non-replicating lentivirus (LV) encoding Rab8a and the overexpression was established by qRT-PCR and western blotting (Figure 2.10.C and D). Rab8a reconstituted bone marrow cells of aged animals upregulated the expression of genes involved in nutrient sensing such as *Akt1* (upto 2-fold) and a cell survival factor, *Bcl2* (>3-fold) (Figure 2.10.E and F). The frequency of $CD11b^+CD11c^+$ cells increased among the differentiated bone marrow cells of aged animals that over expressed Rab8a (Rab8a-OE) (~38.93% ± 01.0) as compared to the control aged cells (~27.7% ± 0.51) while such cells were 51.87% ± 0.51 in young animals (Figure 2.8.G, H and I). $CD11b^+CD11c^+$ cells expressing co-stimulatory molecules were also increased significantly following Rab8a overexpression with the frequencies of $CD80^+$ cells increasing from 29.7% ± 1.13 to 43.20% ± 0.60 and those of $CD86^+$ cells from 31.67% ± 0.56 to 50.7% ± 0.86) (Figure 2.8.H, I and 2.10.K). Surprisingly, the increased frequencies of $CD80^+$ and $CD86^+$ cells following Rab8a overexpression in bone marrow precursors of aged animals were comparable to those in the

differentiated DCs from young animals in which such cells were ~47.7% ± 0.15 and 49.70% ± 0.5, respectively (Figure 2.8.H, I and 2.10.K). Rab8a overexpression also increased the frequencies of class I MHC expressing cells from 39% ± 0.75 to 64.53% ± 1.02 in the BMDCs of aged animals (Fig 2.8.H, I and 2.10.K). That the overexpression of Rab8a did not cause toxicity of cells was shown by PI staining (Figure 2.10.L and M). Rab8a reconstituted BMDCs from aged animals mounted significantly improved IFN response when stimulated with either UV-inactivated or the replicating IAV (Fig 2.8.J-K and 2.10.G-J). Following Rab8a reconstitution of bone marrow cells of aged animals, *IFNα* (6.6-fold), *IFNβ* (11.6-fold), *IFNγ* (16.6-fold), *STAT1* (24.4-fold), *STAT2* (41.6-fold) and an anti-apoptotic molecule, *Bcl2* (35.7-fold) were increased in the expression in comparison to the control cells from aged animals (Figure 2.8.J-K). As compared to the Rab8a-OE cells from aged animals, the cells from younger animals expressed upto a 10-fold higher level of these molecules suggesting for a partial regain of their direct anti-viral functions following reconstitution of Rab8a (Figure 2.8.J-K). Similar trends were also observed for the expression of genes involved in the type I IFN pathway such as *IFNα, IFNβ, IFNγ*, *STAT1* and *STAT2* in the BMDCs pulsed with replication incompetent or heat inactivated viruses (Figure 2.10.G-J). The above obtained results were also confirmed on bonafide cDC2s ($CD11b^+/CD11c^+$) which were generated using Flt3l and pulsed with IAV for 3hrs, a similar trend were observed for the expression of Rab8a along with IFN genes (IFNα, IFNβ, and IFNγ) as it was observed for IAV pulsed GMCSF derived cDC2s (Figure 2.15.E and J). Addionally while profiling the splenic cDC2s we observed a significant expression of F4/80, NK1.1 and GR1 (Ly6G/Ly6C) onto the cDC2s (Figure 2.13.A) later on the cDC2s differentiated from bone marrow precursor of young, aged and RAb8a-OE conditions using GMCSF+IL4 (Figure 2.13.B-E) were also checked for the expression above mentioned molecules. In order to observe the influence of these molecules on *in*

vitro generated cDC2s, the above $CD11b^{+}/CD11c^{+}$ cDC2s were depleted for the NK cells, monocytes and Neutrophils (NKD: $NK1.1^{-}/GR1^{-}$) markers in one case and in other case monocytes, neutrophils and macrophages (MKD: $F4/80^{-}/GR1^{-}$) (Figure 2.14.A-B). Followed by these NKD and MKD cDC2s were pulsed with IAV and the expression of interferons was measured and a similar trend was observed for these depleted as was observed un-depleted cells, however the intensity was lower which suggested that indeed the expression of above molecules influenced the expression of genes upon viral pulsing (Figure 2.14.C). Our data suggested that the DCs of aged animals regained functional competence and mounted elevated IFN response following Rab8a reconstitution. Additionally we also observed an enhanced expression of TLR related genes and their downstream mediator which could dictates the gain in the functionality of aged DCs upon overexpression of Rab8a (Figure 2.4). While we did not establish a direct role of Rab8a in a compromised IFN response leading to reduced functions of DCs of aging host, such events might be connected given its defined role in facilitating cellular secretions. Our data suggest that the DCs of aged animals regained functional competence and mounted elevated response of IFNs following Rab8a reconstitution.

Reconstitution of Rab8a in aging DCs enhances antigen cross-presentation and facilitates their homing to secondary lymphoid organs (SLO)

As the cytokine production by the Rab8a reconstituted DCs was enhanced, we assessed whether such cells had improved antigen-presentation potential. *In-vitro* generated BMDCs from aged animals and those reconstituted of Rab8a along with the cells from the younger animals were FACS sorted (purity ~95%) (Figure 2.17.B). Equal number of cells from different groups were pulsed with ovalbumin for two hours and then co-cultured with CFSE labelled OT1 cells for 72 hours to measure the proliferating T cells. We observed a four-fold increase in the frequencies of

OT1 cells that divided at least once when co-cultured with the antigen-pulsed DCs from young (~65.0% ± 0.56) and the Rab8a-OE aged DCs (~60.37% ± 0.30) as compared to the control aged cells (~16.53% ± 0.15) (Figure 2.8.L and M). In separate experiments, we measured the ability of BMDCs from different groups to display antigenic peptide by pulsing them with varying concentration of SIINFEKL peptide or ovalbumin. We did observe significantly increased frequencies of proliferating $CD8^+$ T cells when DCs of aged mice were reconstituted with Rab8a as compared to the control cells but the effects were milder (Figure 2.11.B-C, 2.10.N-O, 2.12 A-D). Addionally *in vitro* generated NKD ($NK1.1^-/GR1^-$), MKD ($F4/80^-/GR1^-$) depleted cDC2s were also pulsed with ovalbumin and co-cultured with OT1 cells. After 72 hrs post co-culture OT1 cell proliferation was measured using flow cytometry and the proliferated CFSE diluting OT1 cells are plotted as individual peaks. CSFE diluting OT1 cells were comparable in different peaks of OT1 cells when cDC2s from young and Rab8a-OE were used as compared to aged cDC2s from both NKD and MKD condition. However the frequency of CFSE diluting cells from aged condition were maximum at peak 0, 1, and 2 indicated that these cells divided least in further divisions indicating the dysfunctionality of cDC2s of aged animals. Interestingly we observed a clear 6th peak in Rab8a-OE and young conditions in MKD (where NK cells were not depleted but monocytes, macrophages and granulocytes were depleted) suggested that expression of NK1.1 by cDC2s might be influencing the antigen presentation ability of cDC2s. (Figure 2.14.D-E and 2.14.F-G)). A similar trend in OT1 cells proliferation was also visualized as observed for non-depleted cells (Figure 2.15A-D). The above observation suggested that there might be influence of above molecules on the cDC2s because in case of MKD cDC2s differential $CD8^+$ T cells proliferation was observed in comparison to NKD and un-depleted cells from aged animals than young and Rab8a-OE.

Separately BMDCs generated from young, aged and Rab8a-OE conditions by using GMCSF+IL4 (GDCs) and Flt3l (FDCs) were also pulsed with OVA for 2hrs and 24hrs and followed these cells were co-cultured with CFSE labelled OT1 cells for 72 hrs and cell division was acquired using flow cytometer. CFSE proliferation from each condition was plotted as individual peak to determine the frequency of CFSE diluting cells at each division and a total of 6 division was found. However in both the case where cDC2s were generated either from GMCSF+IL4 or Flt3l and pulsed for 2hrs, maximum OT1 cells were present at peak 0 and 1 in a setup where aged cDC2s were co-cultured with OT1 cells than young and Rab8a-OE DCs condition whose proliferation were comparable at different division (Figure 2.15.A-D and 2.15.F-I). Additionally we observed a small restoration in *in vitro* antigen presentation from aged cDC2s when they were pulsed for 24hrs where OT1 cells divided from peak 0 to 2 but could not compensate in further cell divisions suggests dysfunctionality of cDC2s in aged animals are cell intrinsic (Figure 2.15.A-D and 2.15.F-I).

Rab8a reconstituted DCs of aged animals presented exogenous antigens more efficiently to activate antigen specific $CD8^+$ T cells *ex vivo*, we therefore evaluated their immune potentiation effects *in vivo*. Schematic of the experiments is shown in Figure 2.11.D. $CD45.1^+$ congenic animals that were previously injected with CFSE labelled OT1 cells ($1x10^6$) were transferred with Ova-pulsed control BMDCs or those reconstituted with Rab8a from aged mice. In a separate group, similarly prepared Ova-pulsed BMDCs from young animals were injected. All the recipients showed equal distribution of OT1 cells the following day of transfer (Figure 2.18.A). Three days later, frequencies of the divided donor OT1 cells were measured in the peripheral blood as well as different lymphoid organs. The percentage of divided OT1 cells in the peripheral blood and splenic tissues of recipients of aged DCs were 33.3% and 25.3%, respectively (Fig 2.11.E and F). We

observed upto a two-fold increase in their frequencies in Rab8a-OE DCs (48.2% and 54.4%) and young DCs (47.5% and 36.1%) in peripheral blood and splenic tissues (Figure 2.11.E and F). In other lymphoid organs, the recipients of aged DCs had the lowest frequencies of OT1 cells while those receiving Rab8a-OE DCs and young DCs had upto 10-fold increase in the proportion of such cells in different lymph nodes (Figure 2.11.G and 2.18C). The OT1 cells in different organs showed the highest proliferation rates in the recipients of Rab8a-OE DCs and young DCs and those transfused with BMDCs of aged animals showing the least division rates (Figure 2.11.G and 2.18.C). In the same experiment we also measured the frequency of transferred BMDCs ($CD45.2^{+}CD11C^{+}$ cells) from different groups to assess homing potential. The recipients of BMDCs from aged animals (0.59%) had two-fold higher frequencies of these cells in comparison to the recipients of young (0.29%) and Rab8a-OE (0.23%) animals (Figure 2.11.H and 2.18.D and E). The distribution of DCs could be dictated by their expressed chemokine receptors such as CCR7 (13). Lower frequencies of BMDCs expressing CCR7 from aged mice as compared to those of young and Rab8a-OE cells could explain their poor homing to SLO (Figure 2.11.I and 2.18.G). Similarly, the transferred DCs of young animals and those reconstituted with Rab8a populated spleen in comparable frequencies but were ~2-fold lower than those from aged animals (Figure 2.18.D and E). The expanded OT1 cells and the distribution of Ova-pulsed DCs showed a direct correlation (Figure 2.11.G, 2.18.D and E). To explain the differential distribution of BMDCs of aged, Rab8a-OE and young animals, we measured the expression of molecules such as CCR5 and CCR7. For measuring the expression of CCR7 on BMDCs, cells were first *ex-vivo* pulsed with IAV for 16 hours to simulate a situation encountered during infection of mice. $CD11b^{+}CD11c^{+}$ cells that expressed CCR7 were more abundant among Rab8a-OE (37.50 ± 0.36 %) and those from young animals (~41 ± 0.20 %) as compared to those of aged animals (26.5 ± 0.5 (Figure 2.11.I).

Similar trends were observed for the expression of CCR5, a chemokine receptor that facilitates the migration of DCs to inflamed tissues. Therefore, Rab8a reconstitution enhanced homing potential of DCs to both SLO and at the inflammatory tissues. Addionally similar experimental setup was used as where DCs from young, aged and Rab8a-OE conditions were generated using Flt3l and transferred into gender matched congenic mice which were already transferred with CFSE labelled OT1 cells and *in vivo* antigen presentation was measured and comparable CFSE dilution was measured in young and Rab8a-OE DCs recipients than aged DCs recipients (Figure 2.16A-C).

The data, therefore, showed that Rab8a over expression of DCs of an aging host not only promotes cross antigen-presentation but also enhances their migratory potential for efficient sensing of pathogens and priming of antigen specific $CD8^+$ T cells.

Figure 2.11

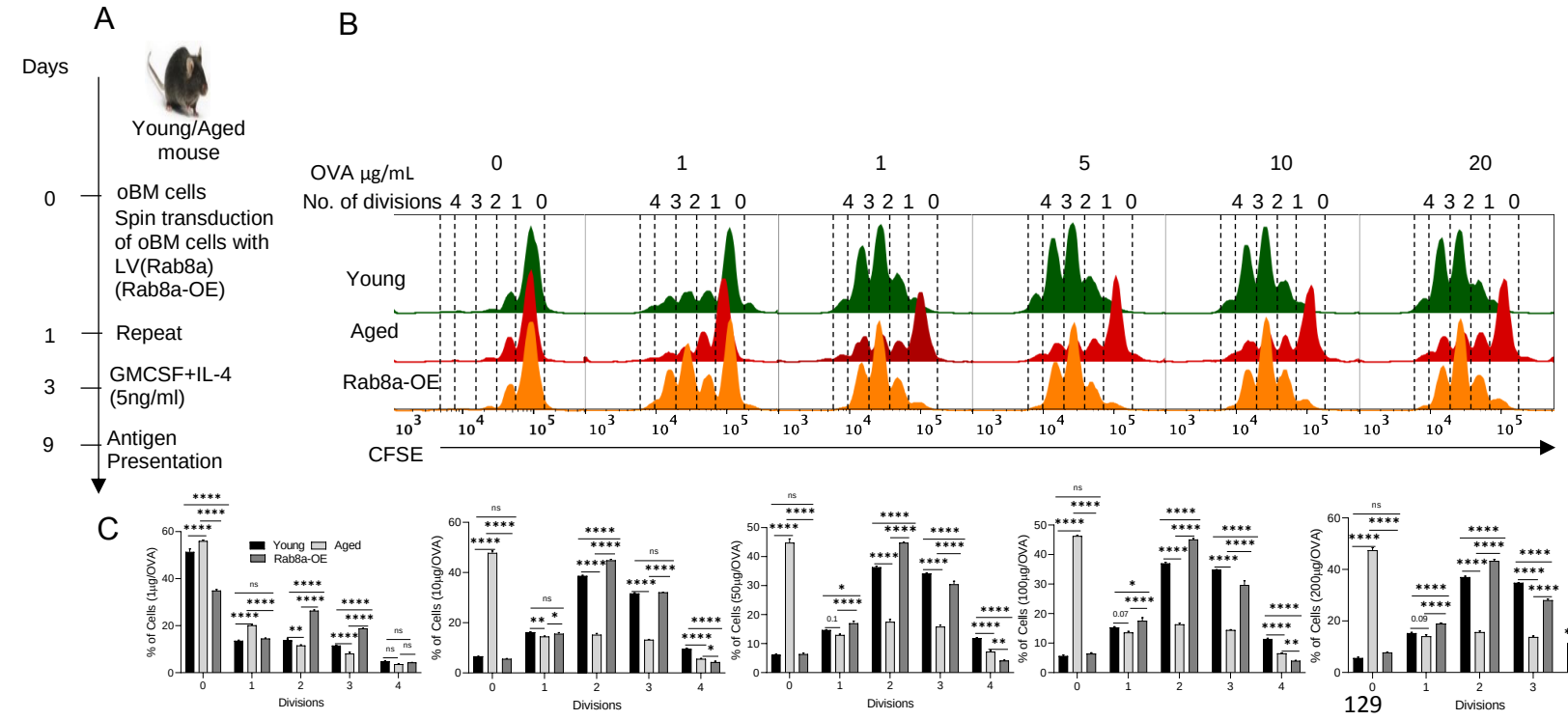

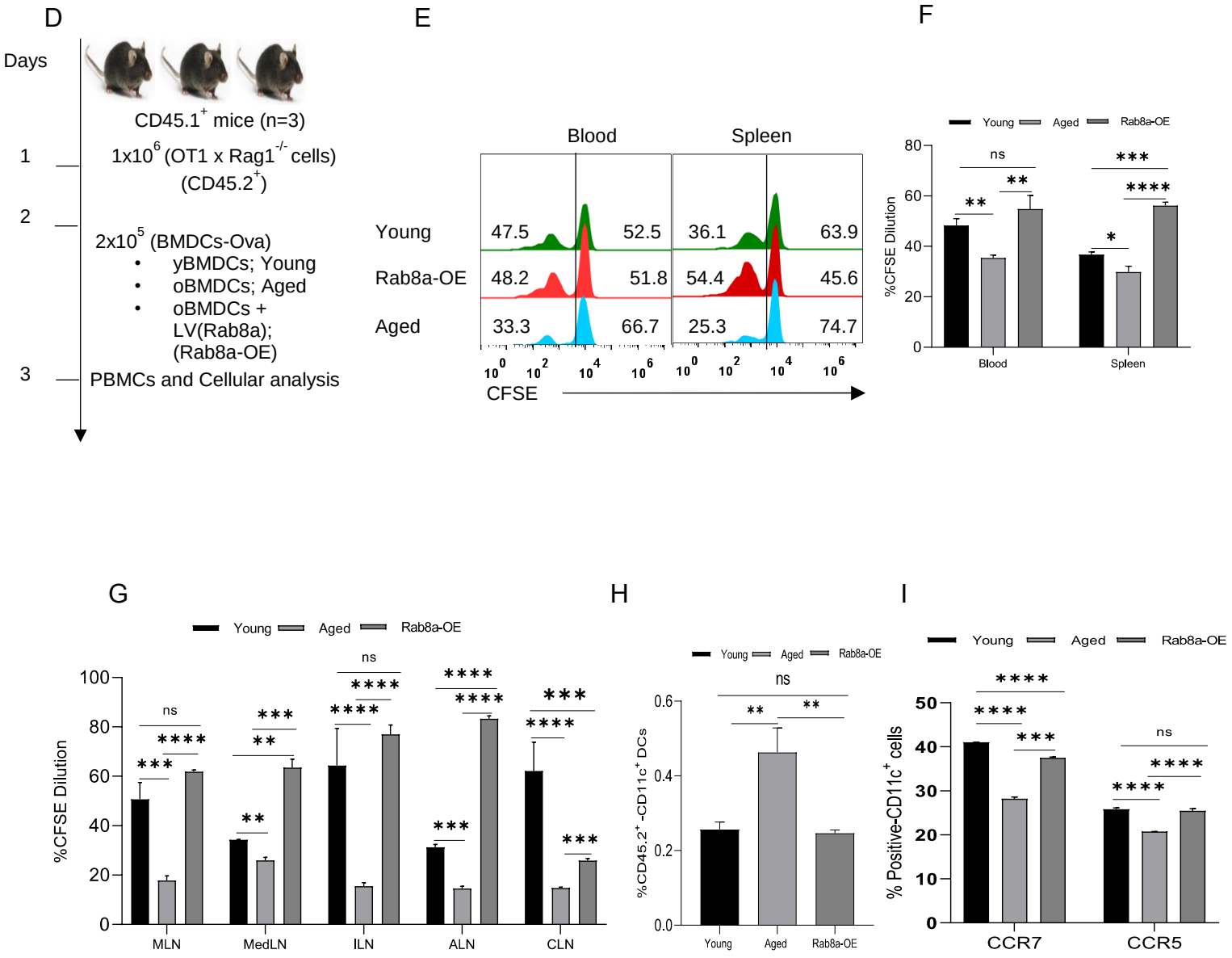

Figure 2.11: Restoration of Rab8a in bone marrow cells of aged mice enhances the antigen presentation ability of aged BMDCs.

A. Schematic representation of the experiment is shown. BMDCs were generated from young, aged and Rab8a-OE bone marrow cells. 6 days post onset of culture, the cells were harvested and the BMDCs were sorted based on CD11c staining. The sorted BMDCs were pulsed with varying concentrations of ovalbumin for 2hrs. The antigen stimulated BMDCs were then co-cultured with

CFSE labelled OTI cells in order to measure the antigen presentation ability as a function of OTI cell proliferation. B. Overlaid histograms show the CSFE dilution in each condition. C. Bar graph show the cumulative data for (B). D. A schematic of the experiment is shown. 2x105 ovalbumin pulsed BMDCs generated from young, aged and Rab8a-OE BM cells were transferred into CD45.1 animals which were already infused with CSFE labelled OT1 cells. 72hrs post BMDC transfer, the animals were then sacrificed and in-vivo CD8 T cells proliferation was measured. E. Overlaid histograms showing the frequency of CSFE diluting CD8 T cells in blood and spleen. F. Bar graph showing the cumulative data of (E) (n=3). Data represents Means ± SEM. ****p<0.0001; ***p<0.001;**p<0.01;*p<0.05, ns p>0.05. (One way ANOVA). G. Bar graph show the cumulative data of percent CFSE dilution in different lymph-nodes. H. Bar graph show the percent $CD45.2^{+}CD11c^{+}$ donor BMDCs in the peripheral blood of each group. Bar graph show the frequency of $CCR5^{+}CD11c^{+}$ and $CCR7^{+}CD11c^{+}$ BMDCs generated from different conditions is shown. The experiments were repeated at least twice and representative data from one of the experiment is shown.

Figure 2.12

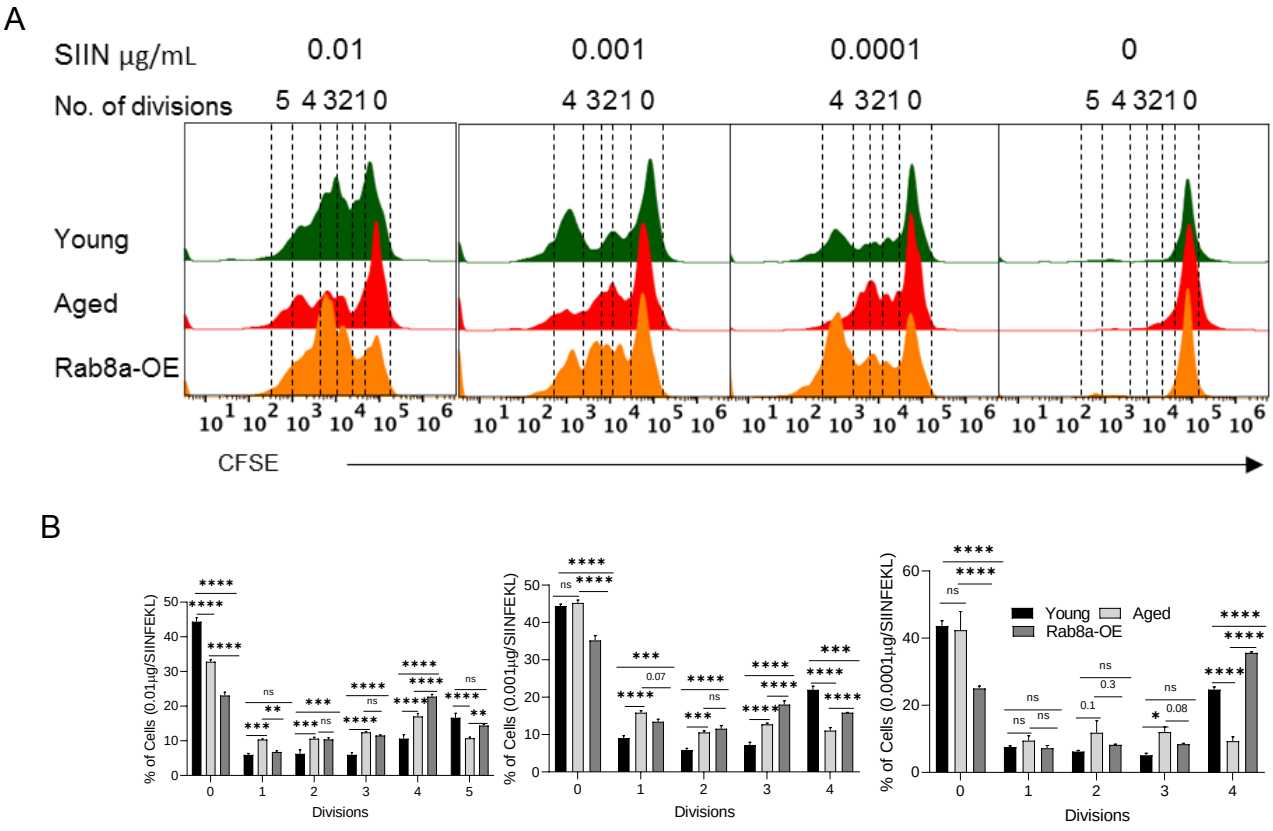

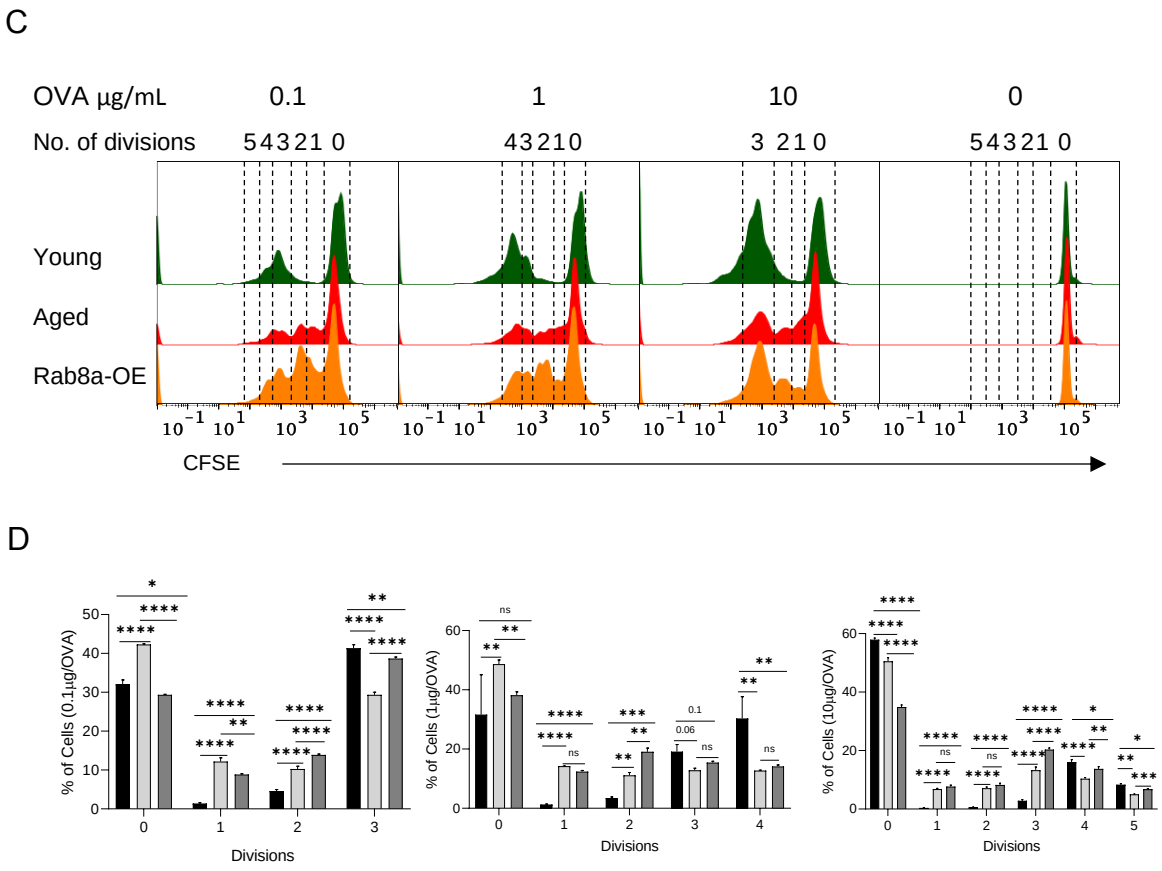

Figure 2.12 Reconstitution of Rab8a in aged BMDCs promotes antigen cross presentation.

A-B. Representative offset histograms show the proliferating OT1 cells in in-vitro culture when BMDCs were pulsed with varying concentrations of SIINFEKL peptide (A) or ovalbumin (B). C-D. Bar graphs show the cumulative data on frequencies of cells in each division. Mean ± SEM values are shown and one way ANOVA was used to assess statistical differences. ****p<0.0001; ***p<0.001;**p<0.01;*p<0.05, ns p>0.05.

Figure 2.13

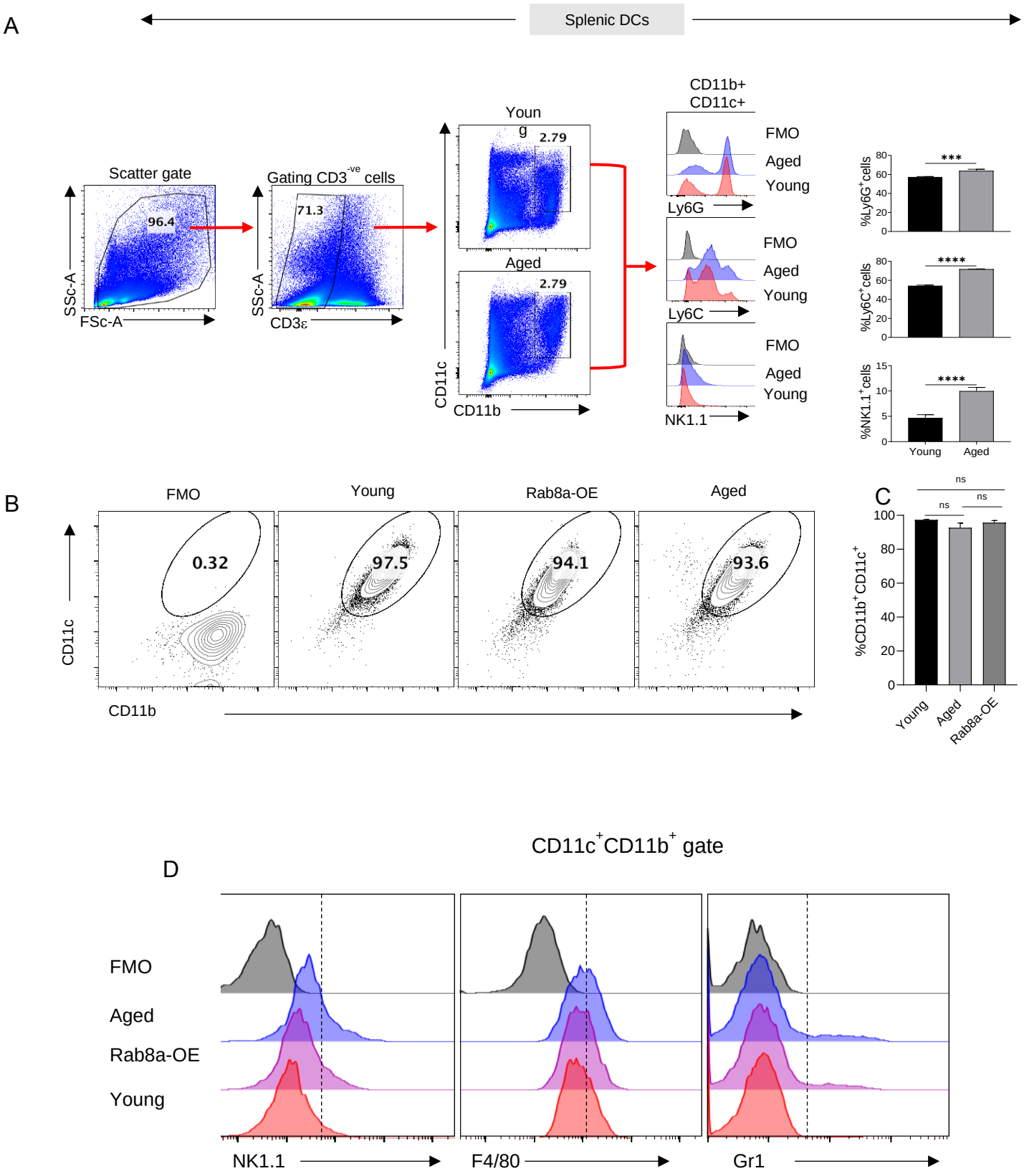
A
Splenic DCs
Scatter gate
96.4
SSc-A
FSc-A
Gating CD3-ve cells
71.3
SSc-A
CD3ε
Youn
g
2.79
Aged
2.79
CD11c
CD11b
CD11b+
CD11c+
FMO
Aged
Young
Ly6G
FMO
Aged
Young
Ly6C
FMO
Aged
Young
NK1.1
%Ly6G+cells
%Ly6C+cells
%NK1.1+cells
***
****
****
Young
Aged
B
FMO
Young
Rab8a-OE
Aged
0.32
97.5
94.1
93.6
CD11c
CD11b
C
ns
ns
ns
%CD11b+CD11c+
Young
Aged
Rab8a-OE
D
CD11c+CD11b+ gate
FMO
Aged
Rab8a-OE
Young
NK1.1
F4/80
Gr1

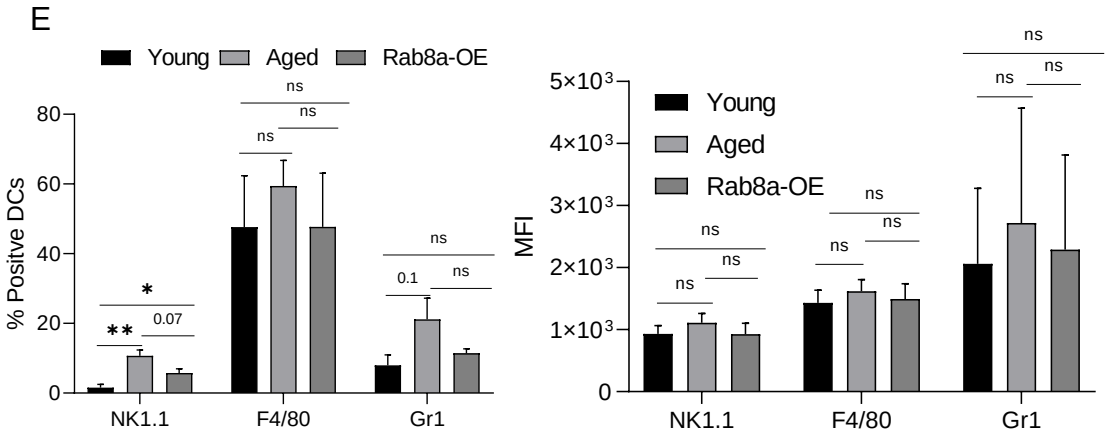

Figure 2.13: Phenotypic profiling of splenic DCs and BMDCs generated using GM-CSF/IL4.

A. Gating strategy to analyse the expression of Ly6C (monocytic marker), Ly6G (neutrophil marker) and NK1.1 (NK cell marker) cells by splenic $CD11c^{+}CD11b^{+}$ DCs. The analysis was used using four animals in each group. The experiments were repeated two times and data from one such experiment are shown by representative FACS plots. B. Representative FACS plots show the frequencies of $CD11c^{+}CD11b^{+}$ BMDCs generated from using GM-CSF/IL-4 cultures. C. Bar Graph shows the cumulative data of a representative experiment. D. Representative offset histograms show the expression of markers associated with NK cells (NK1.1), macrophages (F4/80) and granulocytes (GR1; Ly6C/Ly6G) on $CD11c^{+}CD11b^{+}$ cDC2s. E-F. Bar graphs show the cumulative data for frequency of such cells (E) and the MFI values (F) for the expression of each of the markers. Experiments were repeated three times data from one such experiment is shown as Mean ± SEM values. One way ANOVA was used to assess statistical differences. ****$p<0.0001$; ***$p<0.001$;**$p<0.01$;*$p<0.05$, ns $p>0.05$.

Figure 2.14

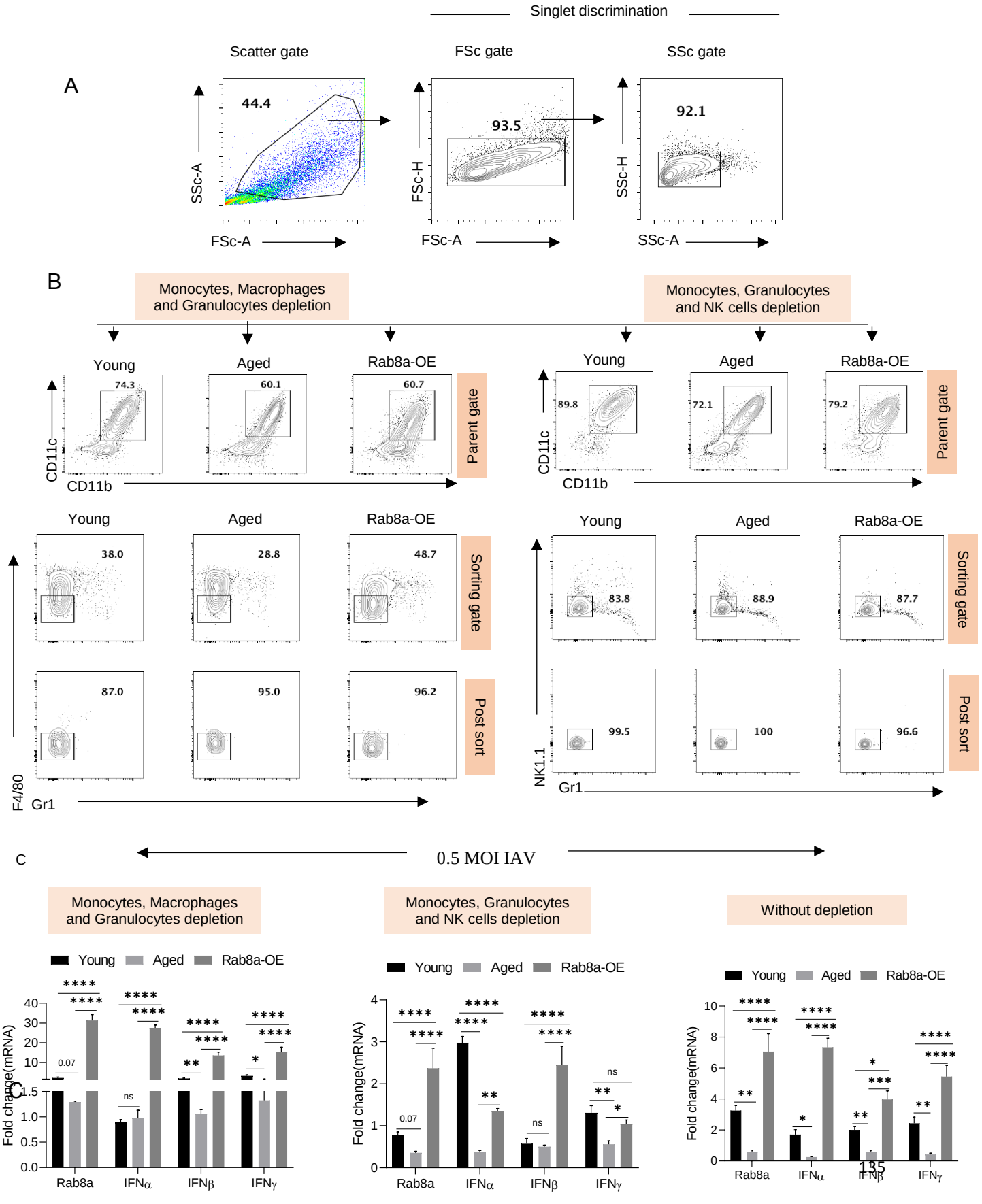
Singlet discrimination
A
Scatter gate
FSc gate
SSc gate
44.4
93.5
92.1
SSc-A
FSc-A
FSc-H
SSc-H
B
Monocytes, Macrophages and Granulocytes depletion
Monocytes, Granulocytes and NK cells depletion
Young
Aged
Rab8a-OE
74.3
60.1
60.7
89.8
72.1
79.2
CD11c
CD11b
Parent gate
38.0
28.8
48.7
83.8
88.9
87.7
Sorting gate
87.0
95.0
96.2
99.5
100
96.6
Post sort
F4/80
Gr1
NK1.1
C
0.5 MOI IAV
Without depletion
Young
Aged
Rab8a-OE
Fold change(mRNA)
Rab8a
IFNα
IFNβ
IFNγ

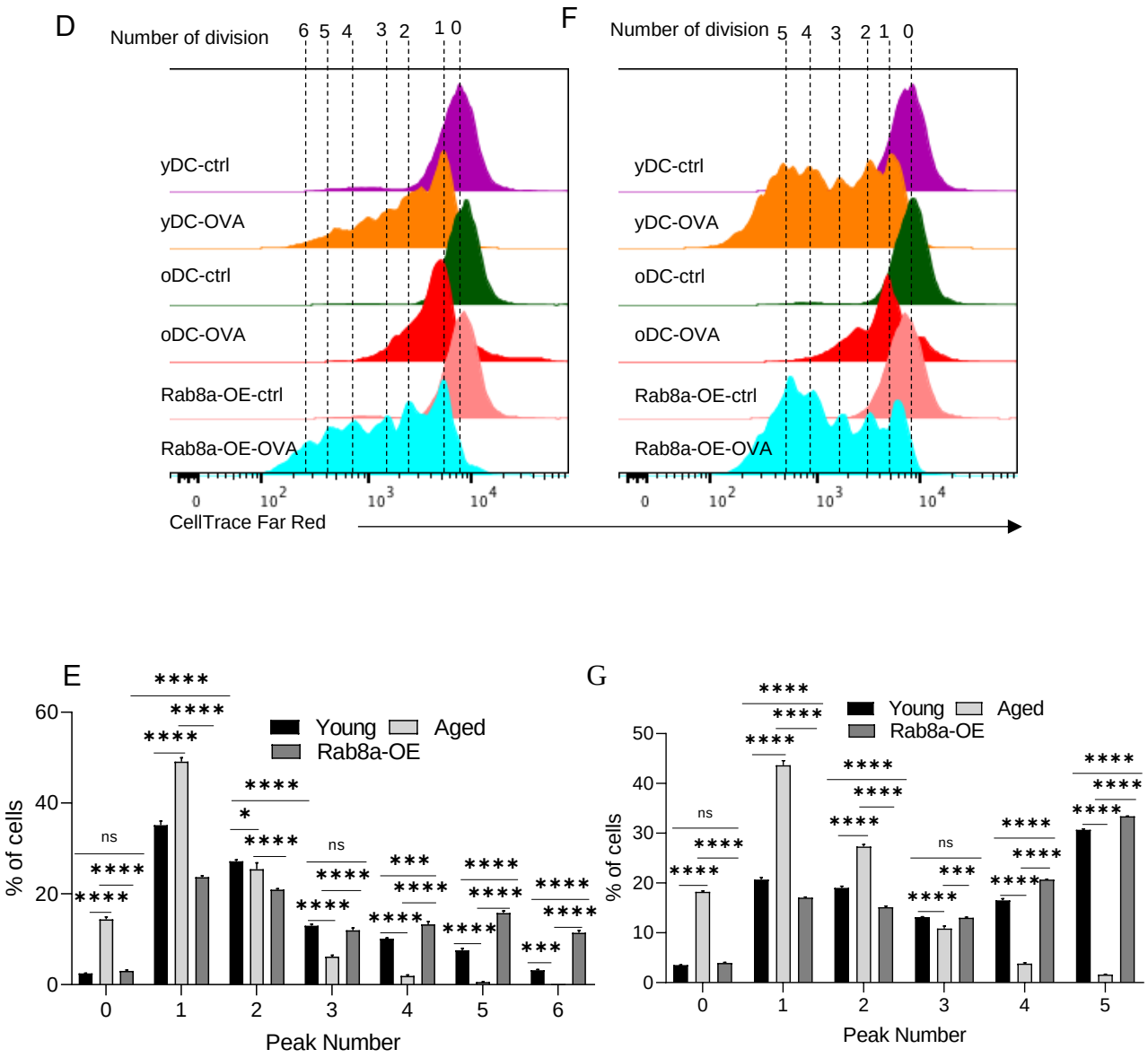

Figure 2.14: Gating strategy and depletion of key molecules (Ly6G/Ly6C/F4/80/NK1.1) expressing cDC2s in order to reveals its role in antigen presentation.

A. Gating strategy to discriminate the singlet population out of total live cells. B. Representative FACS plot show the frequency of $CD11b^{+}/CD11c^{+}$ DCs in indicated conditions out of which the double negative population in one case ($F4/80^{-}$/ $GR1^{-}$) and in other ($NK1.1^{-}/GR1^{-}$) were sorted out. Post sort is also shown for the respective samples. C. $CD11b^{+}/CD11c^{+}$ DCs depleted for indicated condition along with un-depleted GMCSF+IL4 derived DCs were pulsed with 0.5 MOI IAV for 3hrs and then the above cells were used for isolating RNA and qPCR was done to amplify the genes shown in the bar graphs. D. Representative overlaid histogram show the frequency of CFSE dilution of OT1 cells upon co-culture with $CD11b^{+}/CD11c^{+}$ but $F4/80^{-}$/ $GR1^{-}$ ovalbumin pulsed

cells which were depleted for the cells expressing molecules for monocytes, macrophages and granulocytes. E. Bar graph show the cumulative data of (D). F. Representative overlaid histogram show the frequency of CFSE diluting OT1 cells upon co-culture with $CD11b^{+}/CD11c^{+}$ but $NK1.1^{-}$ $/GR1^{-}$ ovalbumin pulsed cells which were depleted for the cells expressing molecules for monocytes, granulocytes and NK cells. G. Bar graph show the cumulative data of (G). Cumulative data is summarized by bar diagram (n=3). Mean ± SEM values are shown and one way ANOVA was used to assess statistical differences. ****p<0.0001; ***p<0.001;**p<0.01;*p<0.05, ns p>0.05.

Figure 2.15

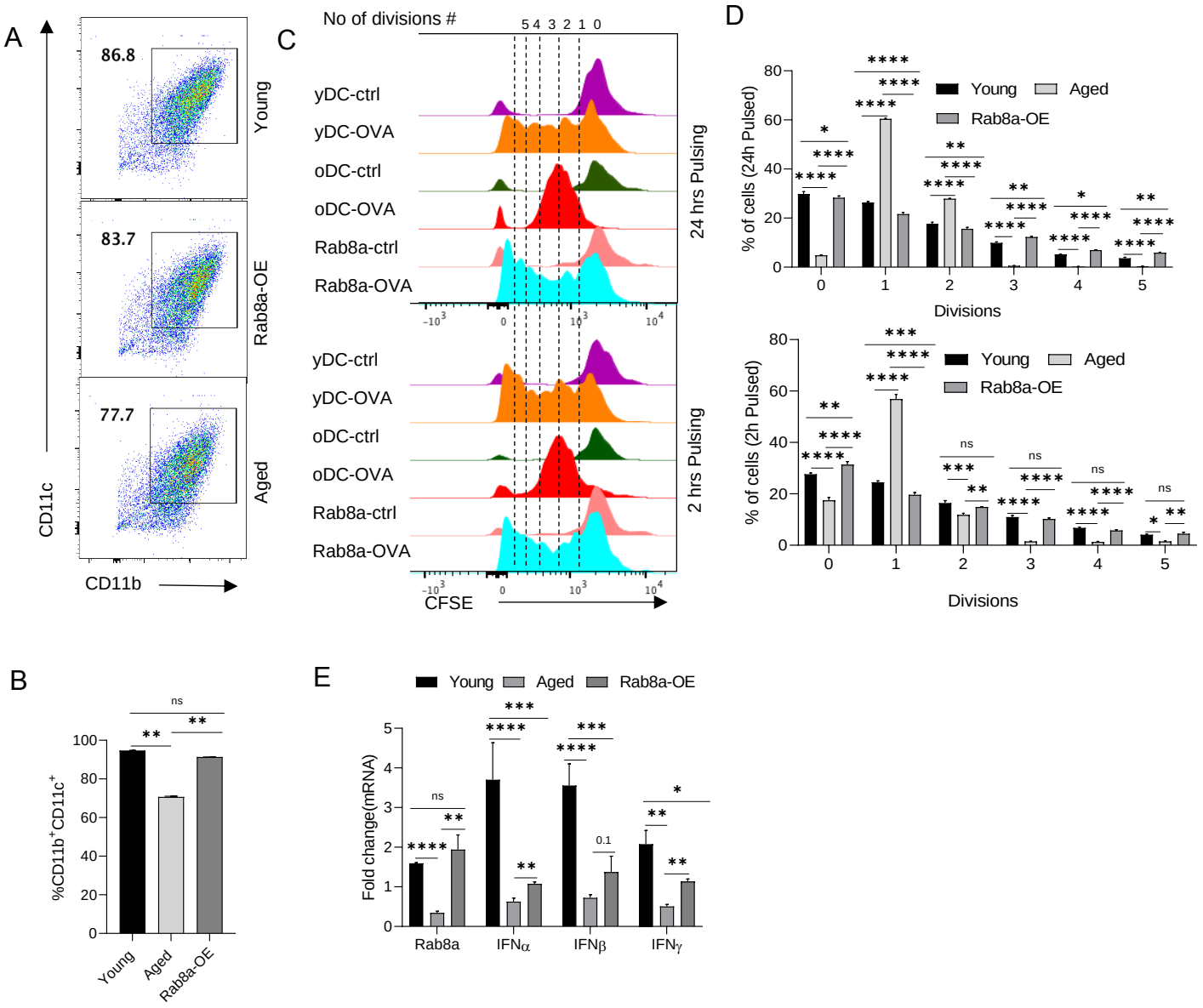

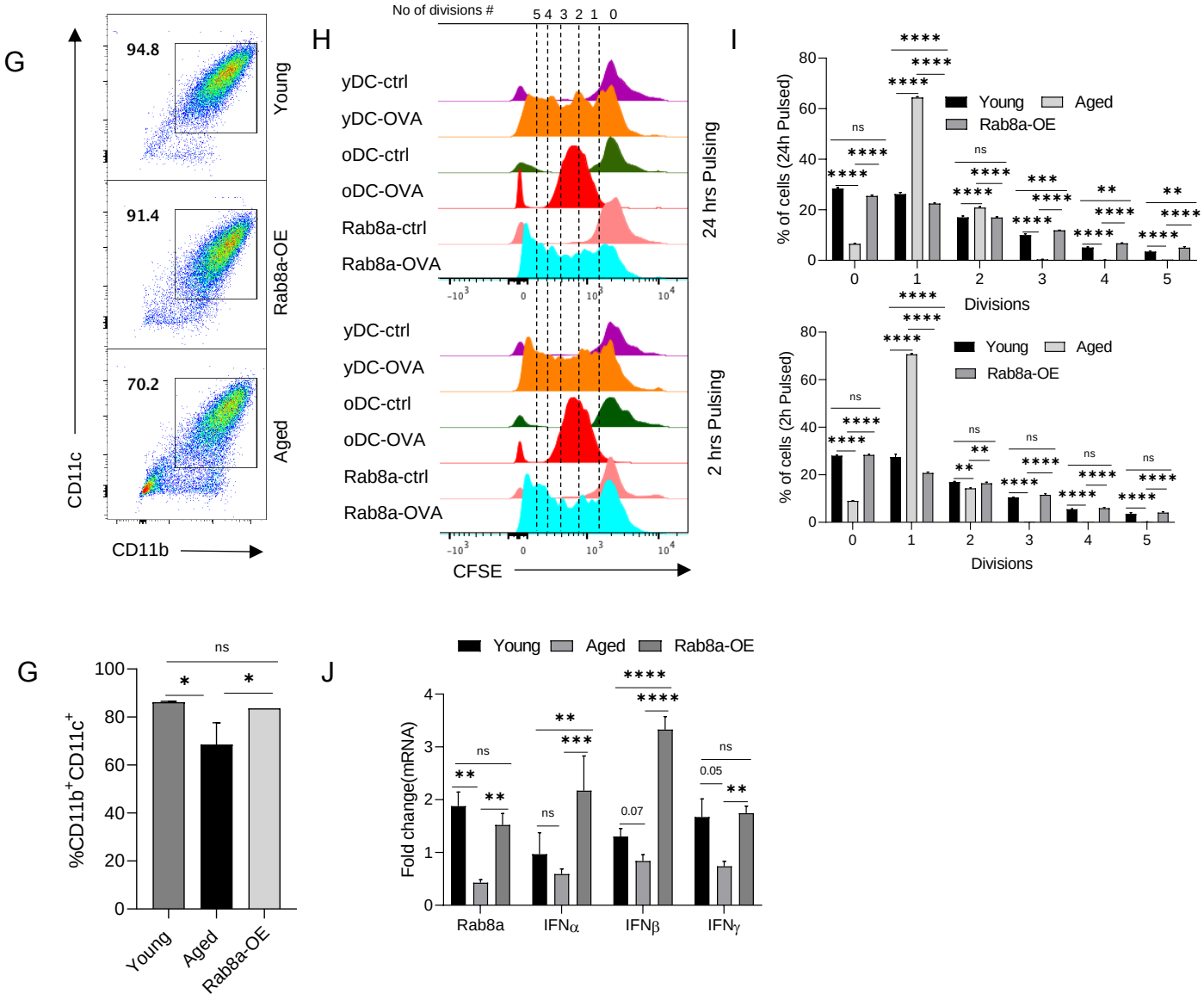

Figure 2.15: A comparative analysis of GM-CSF/IL-4 and Flt-3l induced BMDCs reconstituted of Rab8a in enhancing in-vitro antigen presentation.

Young, aged and Rab8a-OE bone marrow cells were cultured for 6 days with either GM-CSF/IL-4 or Flt3l to generate CD11c+CD11b+ cDC2s. The cells were then pulsed with OVA for 2hrs and 24hrs and co-cultured with CFSE labelled OT1 cells for 72 hrs to assay CFSE dilution by the proliferating OT1 cells. A and B. Representative FACS plots (A) and bar graphs (B) show the frequencies of cDC2s as indicated. C. Representative offset histograms show the frequencies of CFSE diluting OT1 cells co-cultured with GM-CSF/IL-4 induced ova pulsed BMDCs in indicated conditions. D. Bar graphs show the frequencies of CFSE diluted cells within each division of CFSE

diluted OT1 cells. E. cDC2s generated using GM-CSF/IL-4 were pulsed with 0.5MOI IAV for 3hrs and the transcript abundance of IFNα, IFNβ, and IFNγ along with Rab8a was measured and is shown by bar graphs. F and G. Representative FACS plots (F) and bar graphs (G) show the frequencies of cDC2s as indicated. H. Representative offset histograms show the frequencies of CFSE diluting OT1 cells co-cultured with Flt-3l induced ova pulsed BMDCs in indicated conditions. I. Bar graphs show the frequencies of CFSE diluted cells within each division of CFSE diluted OT1 cells. J. cDC2s generated using Flt-3l were pulsed with 0.5MOI IAV for 3hrs and the transcript abundance of IFNα, IFNβ, and IFNγ along with Rab8a was measured and is shown by bar graphs. The experiments were performed four times and data from one such representative experiment is shown. Mean ± SEM values are shown and one way ANOVA was used to assess statistical differences. ****$p<0.0001$; ***$p<0.001$;**$p<0.01$;*$p<0.05$, ns $p>0.05$.Rab8a reconstituted DCs generate effective antigen-specific memory $CD8^+$ T cell response

We evaluated how Rab8a reconstituted DCs generate memory response of $CD8^+$ T cells. We transferred $CD45.1^+$ congenic animals with CFSE labelled OT1 cells ($1x10^6$) and the recipients were analyzed for equal distribution of OT1 cells the next day (Figure 2.19.A-B). In the randomly distributed groups of OT1 recipients, $5x10^5$ of the sorted Ova-pulsed BMDC from aged animals, Rab8a-OE aged cells and young animals were infused and the expansion kinetics of OT1 cells was measured. Blood form the mice was collected at three and six days of BMDCs transfer, and expanded donor OT1 cells were analysed. As compared to the animals receiving DCs of aged animals, recipients of Rab8a-OE cells and DCs of young animals had >3-fold increase in the frequencies of donor OT1 cells in their peripheral blood at 3days post transfer (dpt). An increase was also evident at 6dpt (Figure 2.17.B-C, 2.19.D and E). The expanded cells were allowed to further differentiate into memory cells for a month and the persisting donor cells were then recalled by intranasal infection of animals with IAV (WSN-SIINFEKL) to assess their anti-viral properties. All the infected animals showed a transient reduction in body weight (Figure 2.19.F). Frequency

of $CD44^{hi}CD45.2^{+}$ $CD8^{+}$ T cells in the peripheral blood of animals receiving Rab8a-OE DC (10.6%) and the young DCs (11%) in comparison to the recipients of aged DCs (1.3%) were upto a 10-fold higher on 6 dpi (Figure 2.17.D). Sacrificed animals were then analysed for different lymphoid and non-lymphoid organs for enumerating the frequency of expanded donor cells. The recipients of BMDCs from aged, Rab8a-OE and young animals had 0.64%, 4.34%, and 7.87% of OT1 cells in medLN, 1.46%, 3.06% and 3.3% in spleens and 25.70%, 80% and 48.70% in lungs, respectively (Figure 2.17.E, 2.19.G). Thus, OT1 cells were upto ~10-fold higher in the draining LN and upto 4-fold higher in lung tissues of animals receiving aged DCs reconstituted of Rab8a or young animals as compared to those receiving such cells from of aged animals. The functionality of the expanded cells was monitored by stimulating such cells with cognate peptide and performing ICCS assays. $IFN\gamma^{+}CD8^{+}$ T cells in the recipients of BMDCs from aged, Rab8a-OE and young animals were 7.58%, 23.56% and 28.8% and in medLN, 29.43%, 51.9% and 45.42% in spleens and 5.66%, 41.81% and 67.7% in lungs, respectively (Figure 2.17.F, 2.19.H-J). Similar results were obtained for IFN-γ^{-}TNF-α^{+} and IFN-γ^{+}TNF-α^{+} donor cells with the more frequencies of cells recovered from the recipients of young and Rab8a-OE DC than those receiving such cells from the aged animals (Figure 2.19.H-J). The viral loads in the lung tissues were better controlled in the recipients of Rab8a-OE BMDCs and those of young animals as compared to those receiving the control cells from aged animals as determined by plaque assays and qRT-PCR (Figure 2.17.G and H). Recipients of BMDCs overexpressing Rab8a and as well as those of young animals in comparison to those receiving control cells from aged animals had viral titres reduced by >100-fold (Figure 2.17.H). Furthermore, lung tissues in the recipients of BMDCs from aged animals as compared to those receiving Rab8a-OE BMDCs as well as those from young animals displayed extensive haemorrhagic lesions, indicating a pronounced tissue damaging response due to less

efficient viral control (Figure 2.17.I). Addionally Flt3l based DCs generated from young, aged and Rab8a-OE conditions were ovalbumin pulsed and adoptively transferred into gender matched congenic mice which were already transferred with OT1 cells, followed by these animals were left for 1 month to generate persisting memory cells. Later on these persisting cells were recalled and expanded donor cells were measured in spleen and lungs. A significant increase in the frequency of expanded donor cells was measured in Rab8a-OE DCs recipients than aged DCs recipients. However a comparable frequency virus specific donor cells was present in young DCs recipients (Figure 2.16.E-G). ICCS assay also revealed a significant increase in the frequency of cytokine producing donor cells in lungs and spleen or Rab8a-OE DCs recipients than aged DCs recipients however a comparable frequency of expanded donor cells was observed in Rab8a-OE vs young DCs recipients (Figure 2.16.H-J).

Therefore, Rab8a reconstituted BMDCs from aged animals restored the age-related impairment in their antigen presentation potential to prime $CD8^+$ T cells to confer to the host a better protection against viral infection.

Figure 2.16

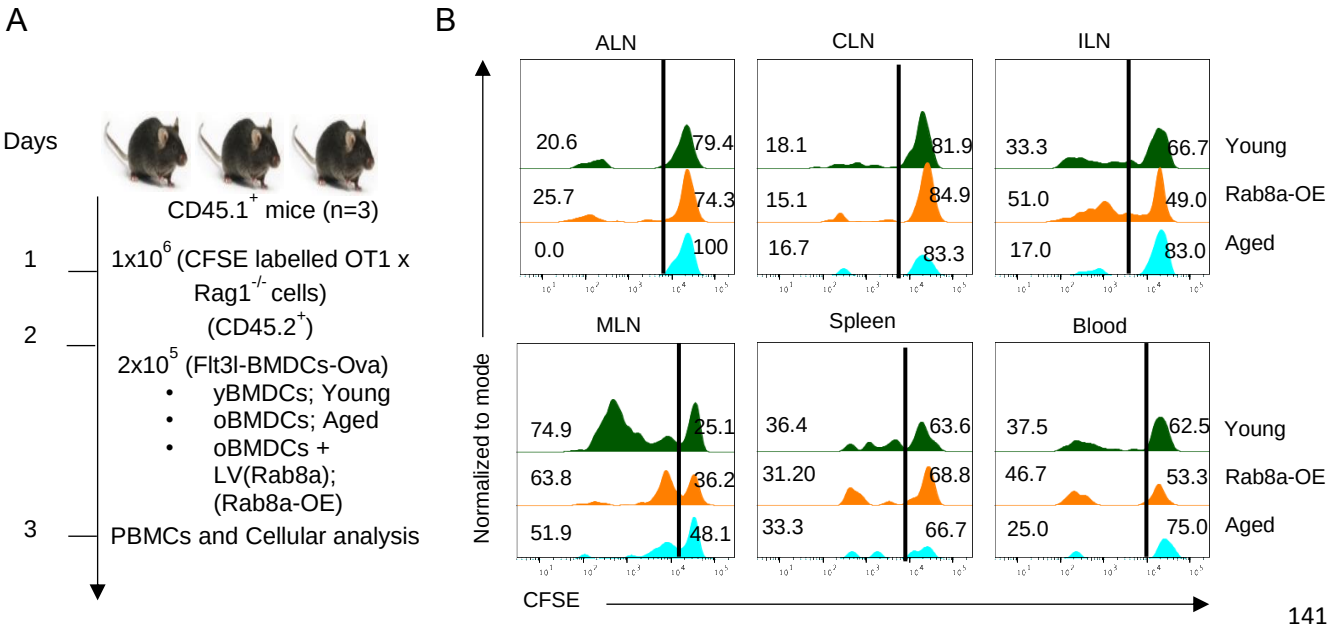

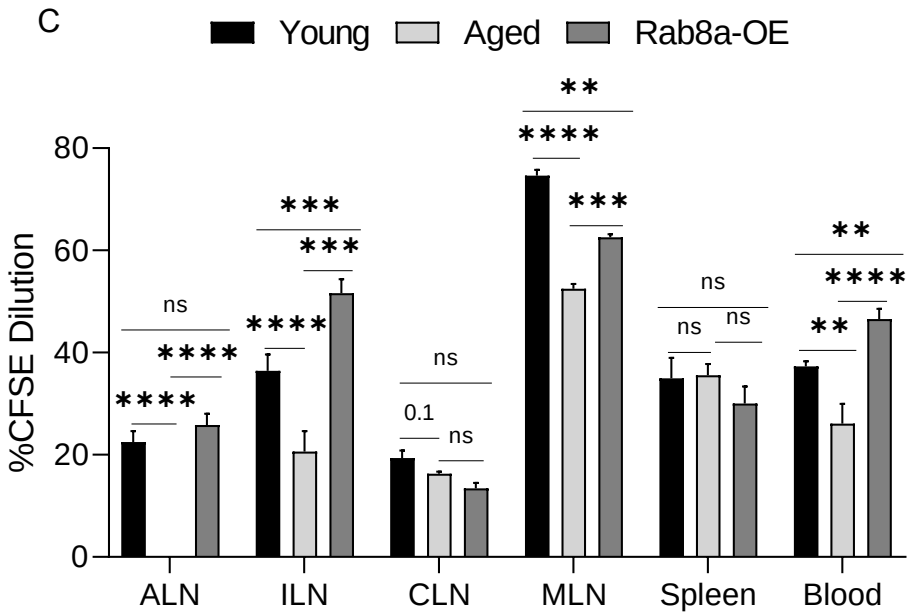
C
Young
Aged
Rab8a-OE
%CFSE Dilution
80
60
40
20
0
ALN
ILN
CLN
MLN
Spleen
Blood
ns
0.1
**
****
***

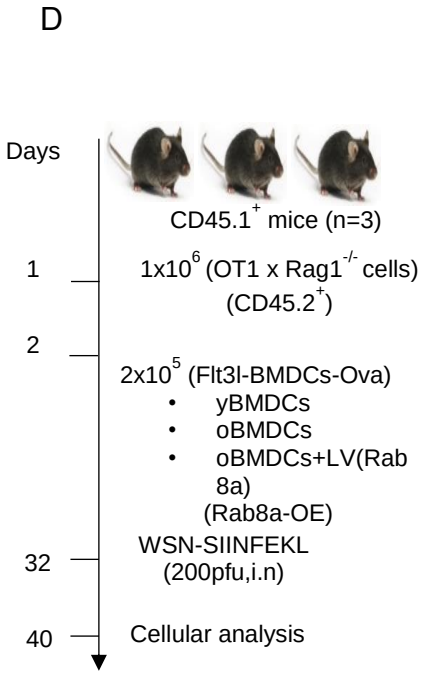
D
Days
CD45.1+ mice (n=3)
1
1x10^6 (OT1 x Rag1-/- cells)
(CD45.2+)
2
2x10^5 (Flt3l-BMDCs-Ova)
• yBMDCs
• oBMDCs
• oBMDCs+LV(Rab 8a)
(Rab8a-OE)
32
WSN-SIINFEKEL
(200pfu,i.n)
40
Cellular analysis

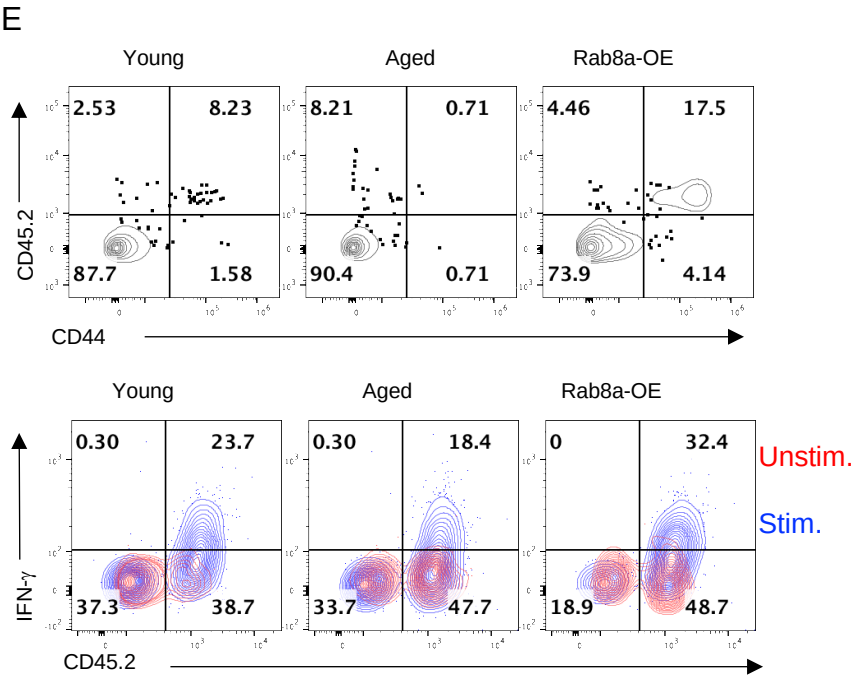
E
Young
Aged
Rab8a-OE
CD45.2
CD44
2.53
8.23
87.7
1.58
8.21
0.71
90.4
0.71
4.46
17.5
73.9
4.14
IFN-γ
CD45.2
0.30
23.7
37.3
38.7
0.30
18.4
33.7
47.7
0
32.4
18.9
48.7
Unstim.
Stim.

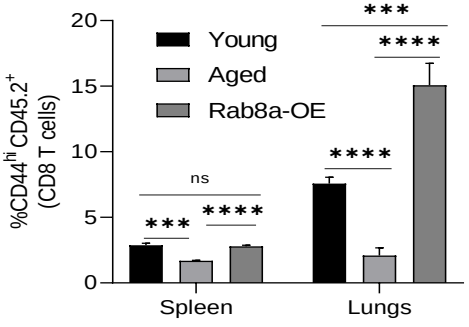
F
%CD44hiCD45.2+ (CD8 T cells)
Young
Aged
Rab8a-OE
20
15
10
5
0
Spleen
Lungs
ns
***
****

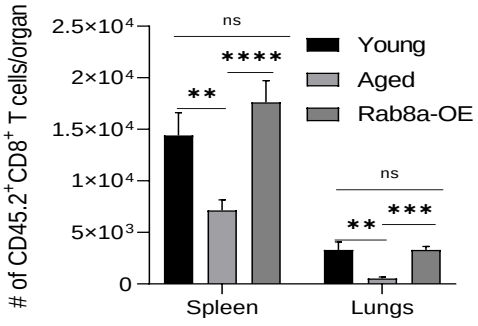
G
# of CD45.2+CD8+ T cells/organ
2.5×10⁴
2×10⁴
1.5×10⁴
1×10⁴
5×10³
0
Young
Aged
Rab8a-OE
Spleen
Lungs
ns
**
***
****

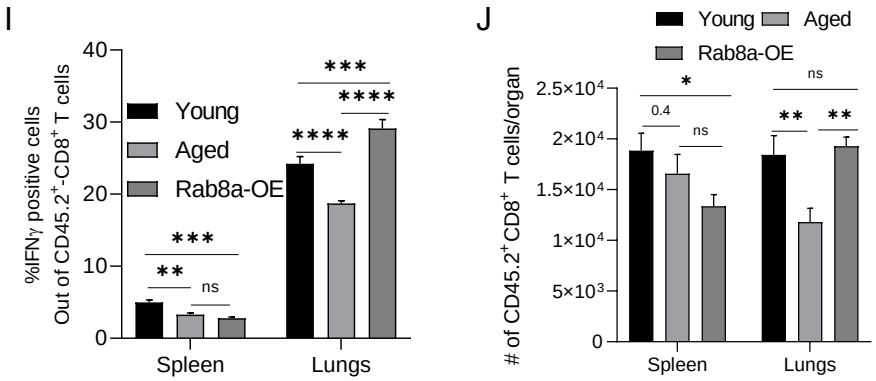

Figure 2.16: Reconstitution of Rab8a in bone marrow cells of aged animals restored the functionality of Flt3l derived cDC2s *in-vivo*.

A. Schematic of experiment showing the details of timeline used for measuring the *in vivo* antigen presentation ability of Flt3l derived cDC2s in CD45.1 congenic animals. B. Young, aged and Rab8a-OE bone marrow cells were added with Flt3l for 6 days in order to generate cDC2s ($CD11b^+/CD11c^+$) (n=3). Later on these cDC2s were pulsed with ovalbumin and adoptively transferred into gender matched CD45.1 animals (n=3) which were already transferred with CFSE labelled OT1 cells and then post 72hrs post DCs transfer these animals were sacrificed and different lymph-nodes (ALN, CLN, ILN and MLN), spleen and peripheral blood were collected and then the CFSE dilution was measured and shown in the form of representative overlaid histogram. C. Bar graphs showing the cumulative data of (B). D. Schematic of experiment used for measuring the generation and expansion of memory $CD8^+$ T cells at tissue site of infection (n=4) upon recall with IAV. E Representative FACS plot show the expanded virus specific donor cells in the lungs of different DCs recipients. F-G. Bar graphs show the frequency (F) and counts (G) of total expended donor cells in different organs of mice. H. Representative overlaid FACS plot shown to reveal the frequency of IFNγ positive donor OT1 cells in lungs of infected mice upon pulsing them with cognate peptide. I-J. Bar graphs show the frequency (I) and counts (J) of $IFN\gamma^+CD45.2^+$ $CD8^+$ T cells in spleen and lungs determined by ICCS. Mean ± SEM values are shown and one way ANOVA was used to assess statistical differences. ****$p<0.0001$; ***$p<0.001$;**$p<0.01$;*$p<0.05$, ns $p>0.05$.

Figure 2.17

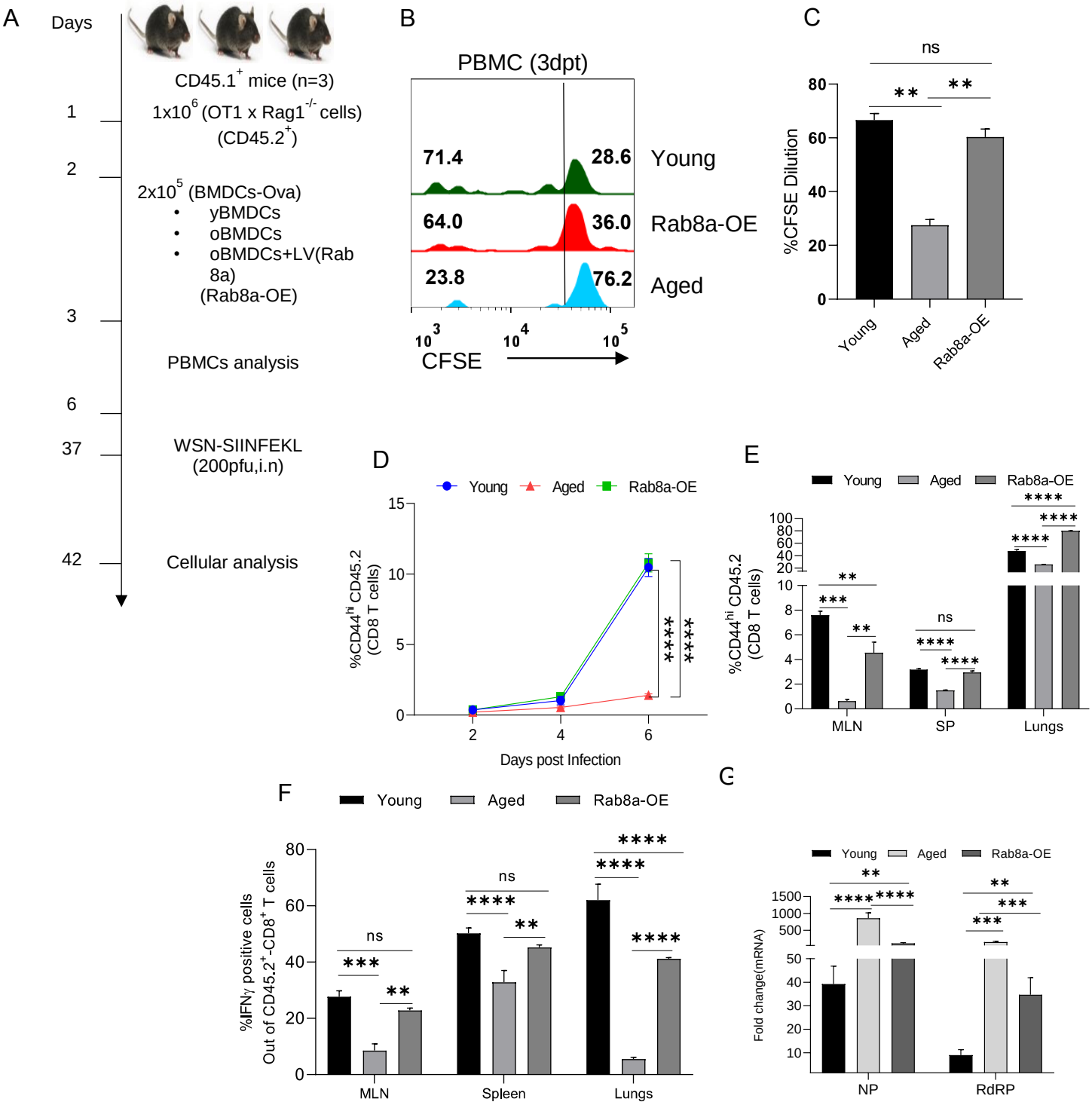
A
Days
CD45.1+ mice (n=3)
1
1x10^6 (OT1 x Rag1-/- cells) (CD45.2+)
2
2x10^5 (BMDCs-Ova)
• yBMDCs
• oBMDCs
• oBMDCs+LV(Rab 8a) (Rab8a-OE)
3
PBMCs analysis
6
37
WSN-SIINFEKL (200pfu,i.n)
42
Cellular analysis
B
PBMC (3dpt)
71.4
28.6
Young
64.0
36.0
Rab8a-OE
23.8
76.2
Aged
CFSE
C
%CFSE Dilution
ns
Young
Aged
Rab8a-OE
D
Young
Aged
Rab8a-OE
%CD44hi CD45.2 (CD8 T cells)
Days post Infection
E
%CD44hi CD45.2 (CD8 T cells)
MLN
SP
Lungs
F
%IFNγ positive cells Out of CD45.2+-CD8+ T cells
MLN
Spleen
Lungs
G
Fold change(mRNA)
NP
RdRP

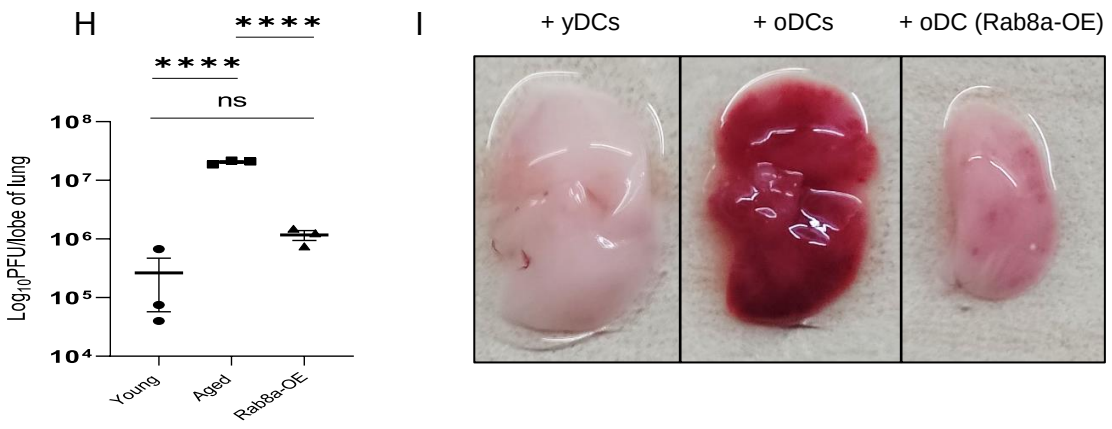

Figure 2.17: Reconstitution of Rab8a in the bone marrow of aged animals led to the restoration of the priming and presentation abilities to T cells in the BMDCs recipient animals

A. Schematic of the experiment is shown. *In-vitro* generated BMDCs from young, aged and Rab8a-OE BM cells were sorted, pulsed with ovalbumin for 2hrs, washed and adoptively transferred into sex matched congenic $CD45.1^+$ animals infused with CFSE OT1 cells for measuring the antigen presentation ability of different BMDCs in-vivo. B. Overlaid histogram show the expansion of the transferred CFSE labelled $CD8^+$ T cells post 3 days post BMDCs transfer. C. Bar-graph show the cumulative data of (B). D. Line graph show the kinetics of expanded virus specific donor $CD8^+$ T cells in the peripheral blood of BMDCs recipient animals post WSN-SIINFEKL infection (n=3). Data represents Means ± SEM. ****$p<0.0001$; ***$p<0.001$;**$p<0.01$;*$p<0.05$, ns $p>0.05$. (One way ANOVA). E. Bar graph showing the frequency of expanded virus specific donor CD8 T cells in indicated lymphoid and non-lymphoid organs post WSN-SIINFEKL infection. F. Bar graphs show the results of ICCS assays for functionality assessment are shown. G. Bar graph show the viral titer in the lungs of infected mice using influenza NP and RdRP specific primers. H. Summary plot showing the viral titre in infected lungs using plaque assay. I. Representative images of lungs of each group showing the relative haemorrhagic lesions in different BMDCs recipient animals is shown. The experiments were repeated at least two times and representative data from one of the experiment is shown (n=3). Data represents Means ± SEM. ****$p<0.0001$; ***$p<0.001$;**$p<0.01$;*$p<0.05$, ns $p>0.05$. (two way ANOVA).

Figure 2.18

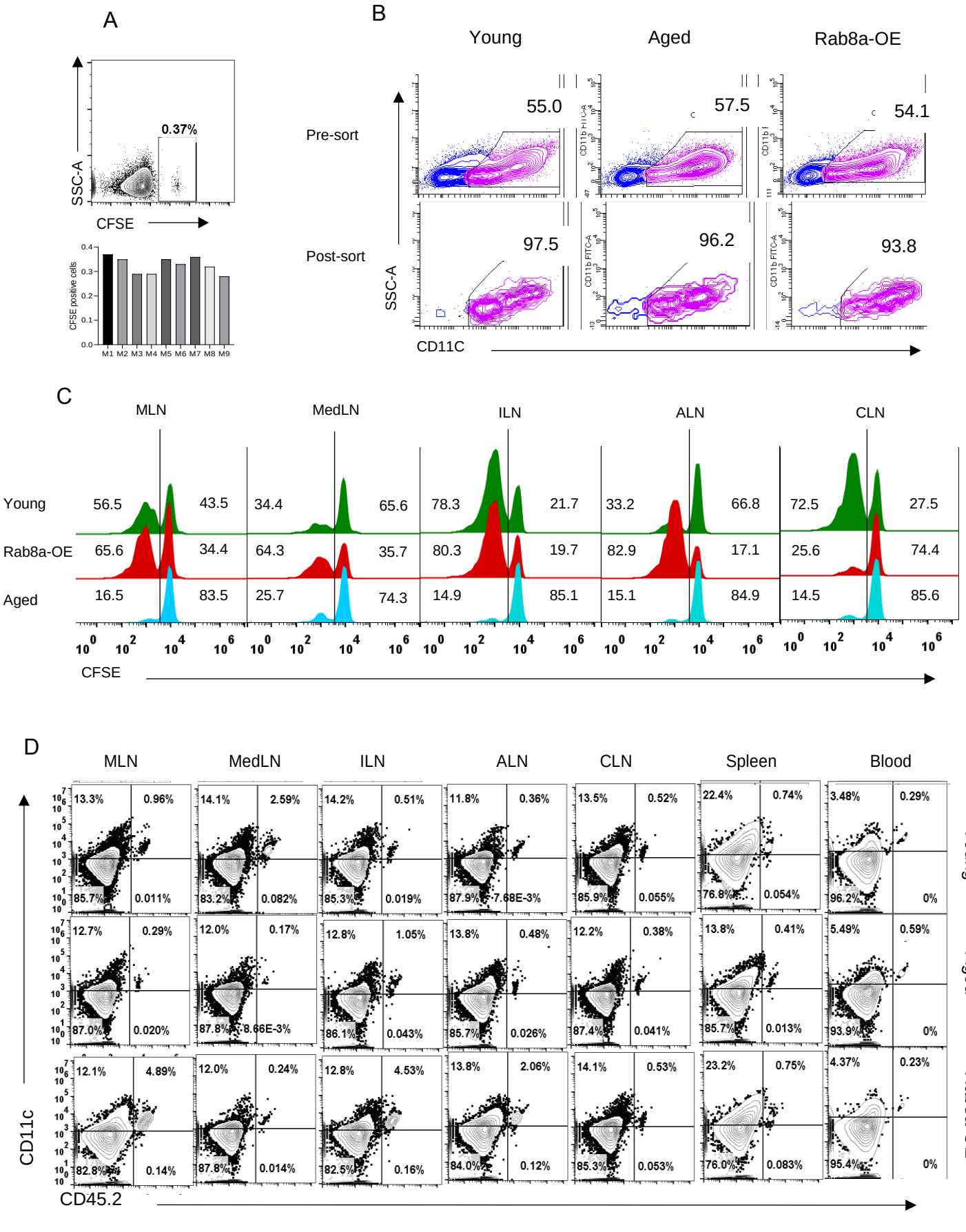
A
0.37%
SSC-A
CFSE
CFSE positive cells
M1 M2 M3 M4 M5 M6 M7 M8 M9
B
Young
Aged
Rab8a-OE
Pre-sort
Post-sort
55.0
57.5
54.1
97.5
96.2
93.8
SSC-A
CD11C
C
MLN
MedLN
ILN
ALN
CLN
Young
Rab8a-OE
Aged
56.5 43.5 34.4 65.6 78.3 21.7 33.2 66.8 72.5 27.5
65.6 34.4 64.3 35.7 80.3 19.7 82.9 17.1 25.6 74.4
16.5 83.5 25.7 74.3 14.9 85.1 15.1 84.9 14.5 85.6
CFSE
D
MLN
MedLN
ILN
ALN
CLN
Spleen
Blood
Young
Aged
Rab8a-OE
13.3% 0.96% 85.7% 0.011%
14.1% 2.59% 83.2% 0.082%
14.2% 0.51% 85.3% 0.019%
11.8% 0.36% 87.9% 7.68E-3%
13.5% 0.52% 85.9% 0.055%
22.4% 0.74% 76.8% 0.054%
3.48% 0.29% 96.2% 0%
12.7% 0.29% 87.0% 0.020%
12.0% 0.17% 87.8% 8.66E-3%
12.8% 1.05% 86.1% 0.043%
13.8% 0.48% 85.7% 0.026%
12.2% 0.38% 87.4% 0.041%
13.8% 0.41% 85.7% 0.013%
5.49% 0.59% 93.9% 0%
12.1% 4.89% 82.8% 0.14%
12.0% 0.24% 87.8% 0.014%
12.8% 4.53% 82.5% 0.16%
13.8% 2.06% 84.0% 0.12%
14.1% 0.53% 85.3% 0.053%
23.2% 0.75% 76.0% 0.083%
4.37% 0.23% 95.4% 0%
CD11c
CD45.2

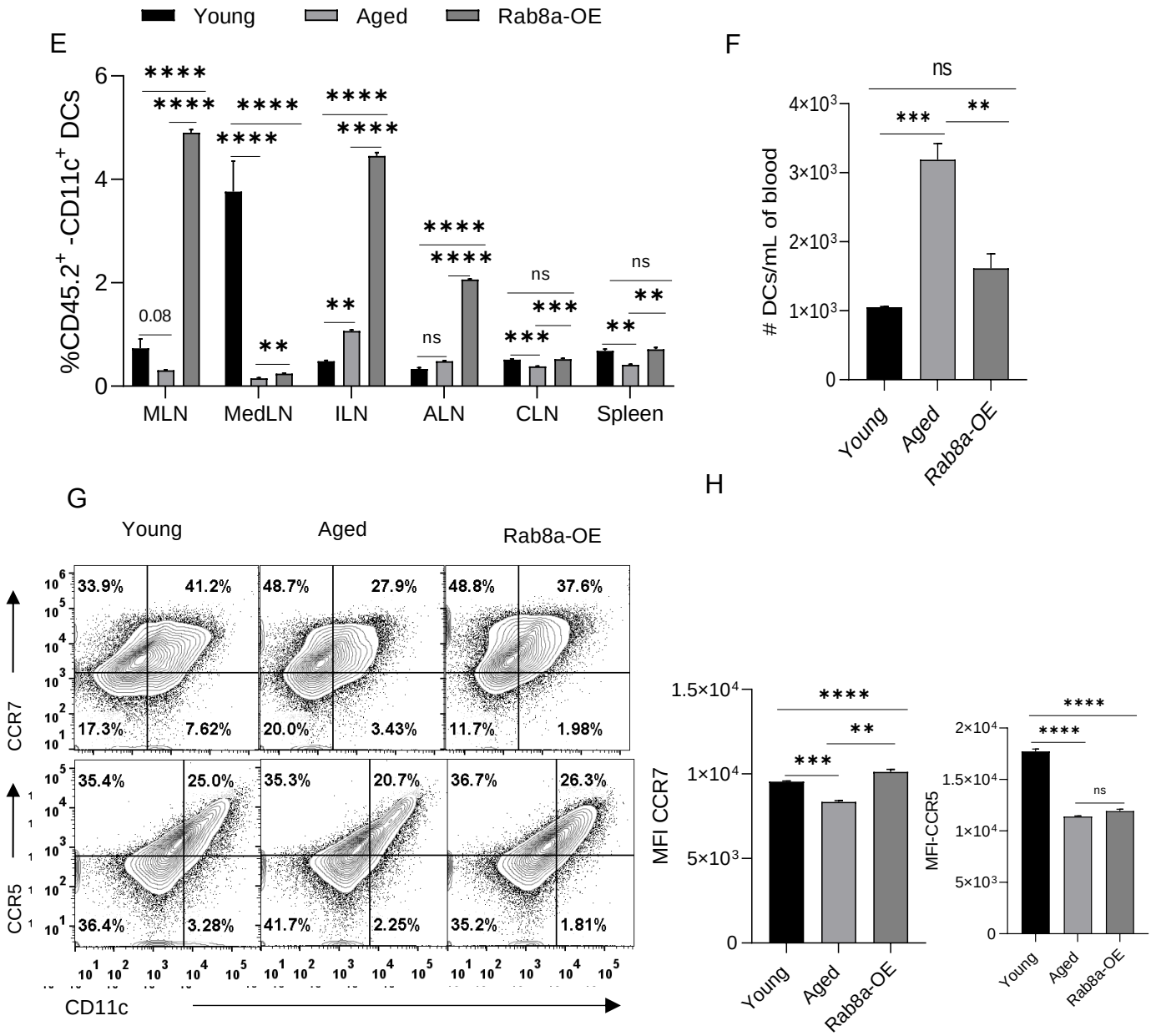

Figure 2.18: OT1 transfer status for in-vivo DCs immunization experiment and in-vitro antigen presentation ability of DCs generated from Rab8a overexpressing BM cells of aged mice.

A. Overlaid histogram showing the % GFP^+ BM cells in order to show the transduction efficiency of Rab8a-OE lentiviruses. B-C. FACS plot and bar graph showing the $CFSE^+$ cells and transfer status of $CFSE^+$ cells in CD45.1 mice before transferring the ovalbumin pulsed BMDCs.

D. Representative overlaid histogram show the proliferating OT-I cells in the peripheral circulation at 6 days post DC transfer. E. Bar graph show the cumulative data of (D). Data represents Means ± SEM. ****p<0.0001; ***p<0.001;**p<0.01;*p<0.05, ns p>0.05 (one way ANOVA). F. Line graph show the change in bodyweight of recipient animals after intranasal WSN-SIINFEKL infection in each group. G. Representative FACS plot show the frequency of expanded virus specific donor OT-I cells in different organs of BMDC recipients after WSN-SIINFEKL infection. H. Representative FACS plot show the frequency of cytokine (TNFα and IFNγ) producing donor cells in different organs of recipients. I-J. Bar graph show the frequency of TNFα-IFNγ double positive (I) and TNFα positive (J) cells in different organs of BMDC recipients. K-L. Representative overlaid histogram show the proliferating $CD8^{+}$T cells in *in-vitro* culture when BMDCs from different conditions were pulsed with varying concentration of SIINFEKL peptide (K) or ovalbumin (L). M-N. Bar graph show the cumulative data of K-L. Data represents Means ± SEM. ****p<0.0001; ***p<0.001;**p<0.01;*p<0.05, ns p>0.05 (two way ANOVA). The experiments were repeated at least three times and representative data from one of the experiment is shown.

Figure 2.19

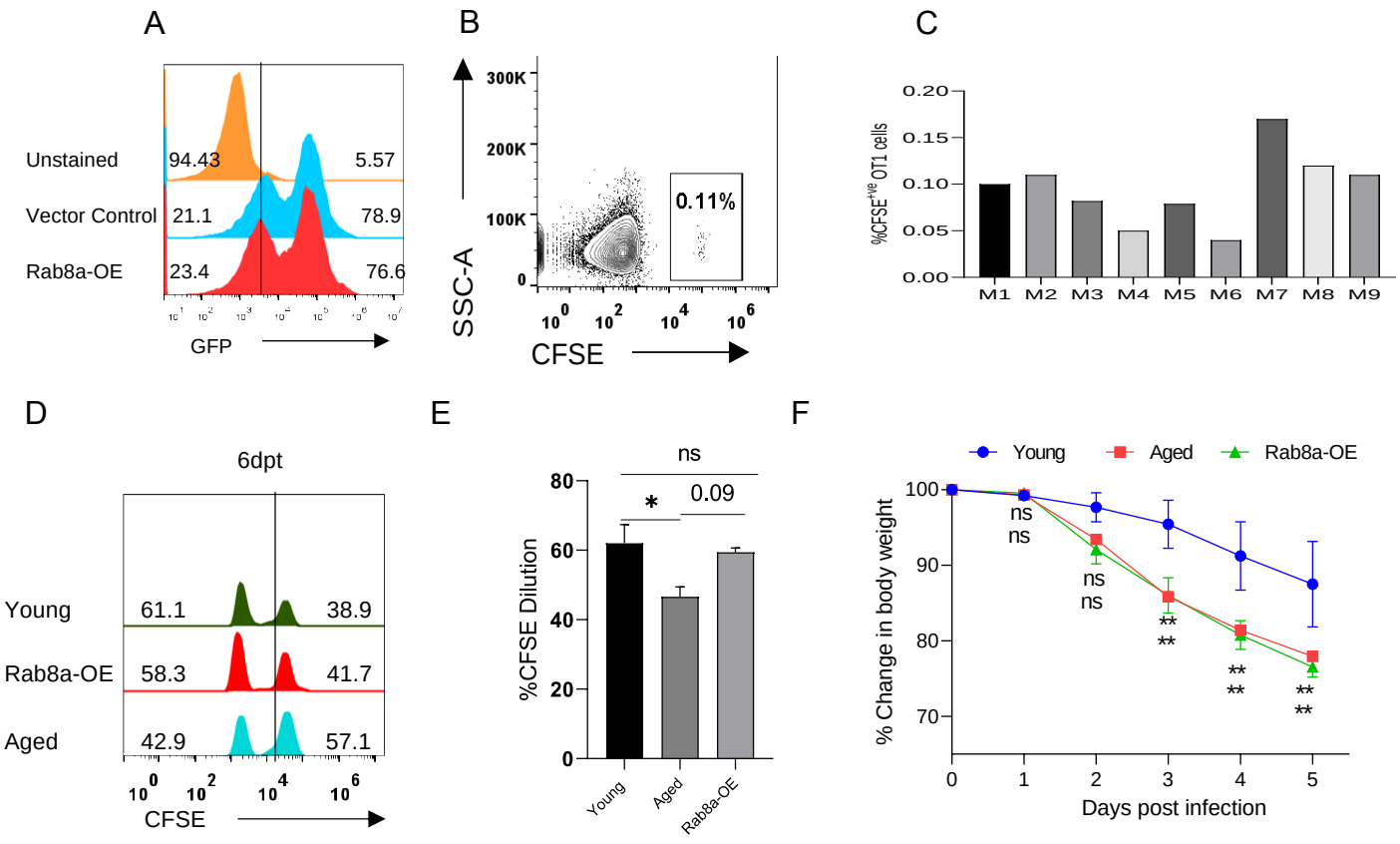

G

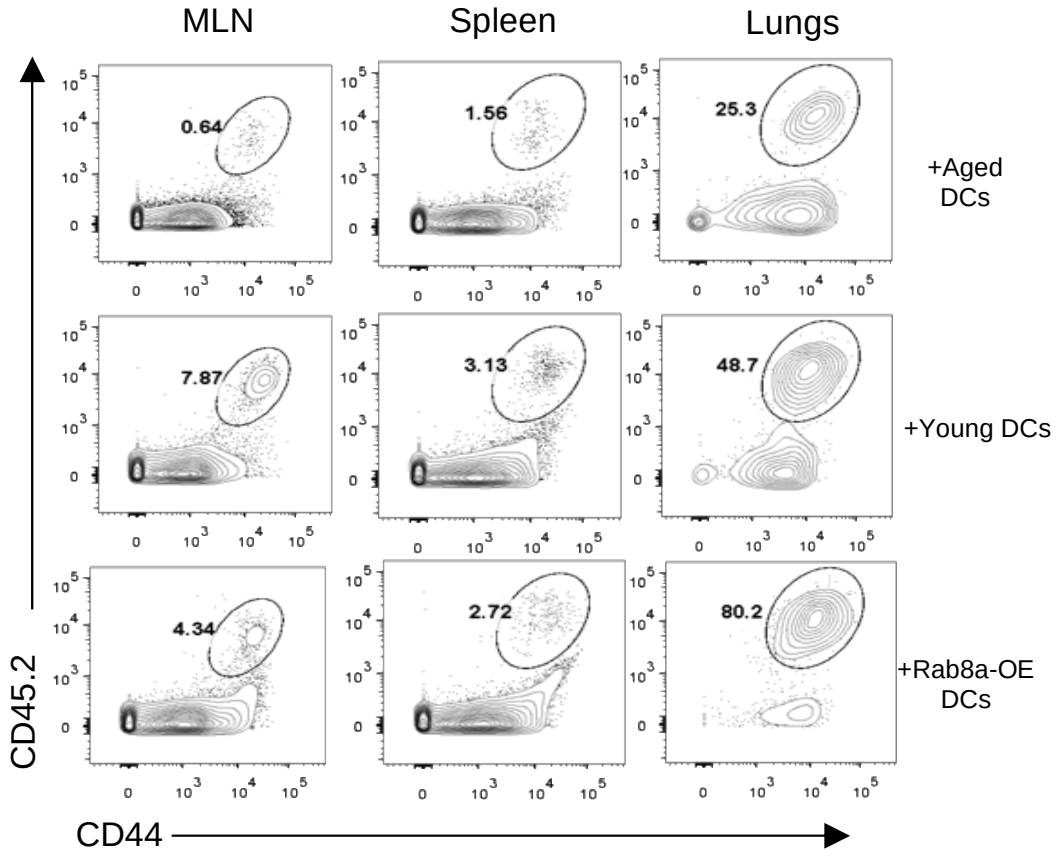
MLN
Spleen
Lungs
0.64
1.56
25.3
+Aged DCs
7.87
3.13
48.7
+Young DCs
4.34
2.72
80.2
+Rab8a-OE DCs
CD45.2
CD44

H

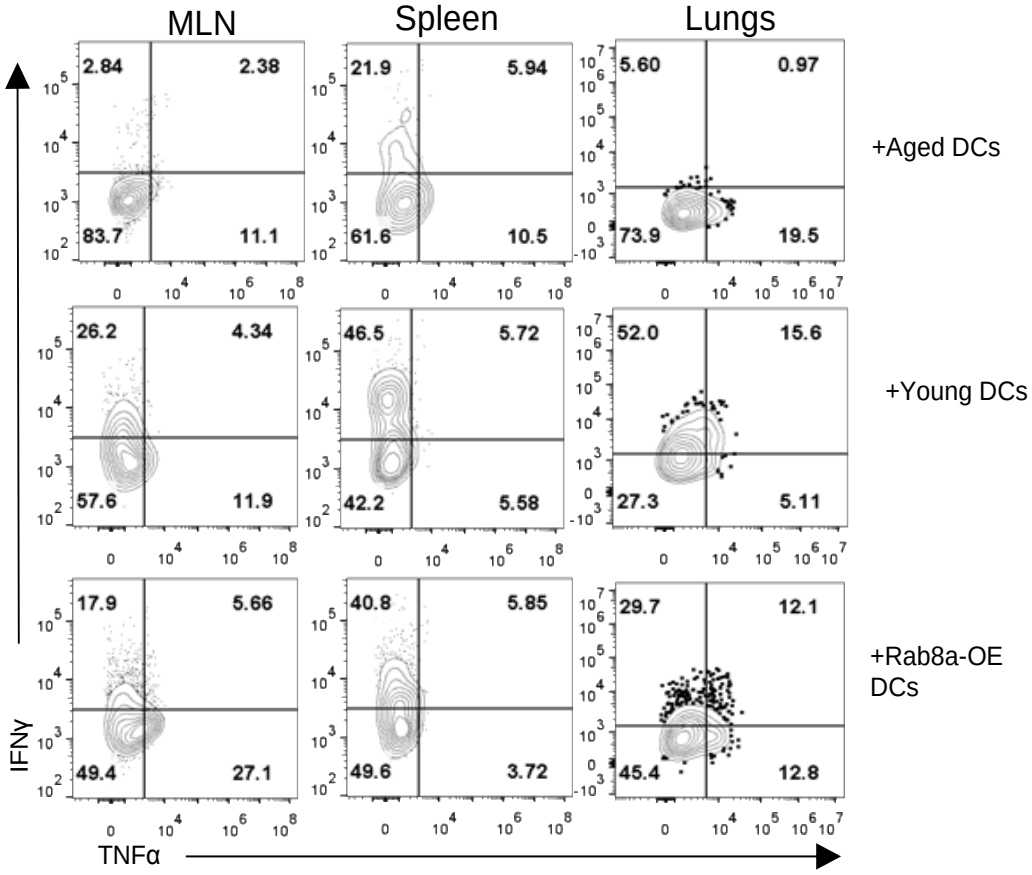
MLN
Spleen
Lungs
2.84
2.38
83.7
11.1
21.9
5.94
61.6
10.5
5.60
0.97
73.9
19.5
+Aged DCs
26.2
4.34
57.6
11.9
46.5
5.72
42.2
5.58
52.0
15.6
27.3
5.11
+Young DCs
17.9
5.66
49.4
27.1
40.8
5.85
49.6
3.72
29.7
12.1
45.4
12.8
+Rab8a-OE DCs
IFNγ
TNFα

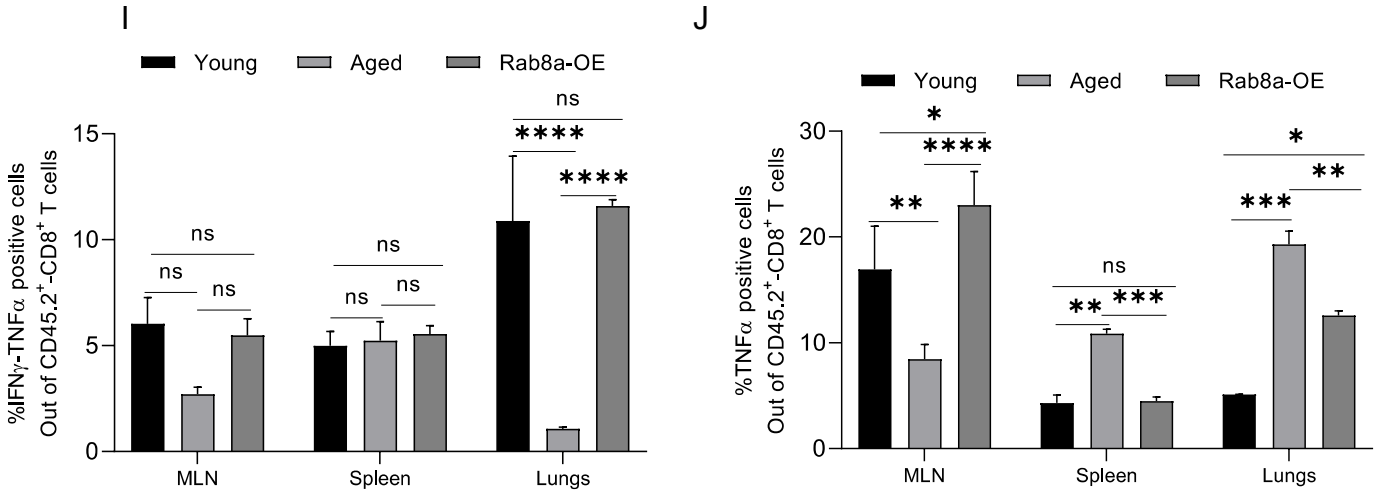

Figure 2.19: Rab8a overexpressing DCs of aged animals expand antigen-specific CD8$^+$ T cells *in vivo*.

A. Overlaid histogram showing the % GFP$^+$ BM cells in order to show the transduction efficiency of Rab8a-OE lentiviruses. B-C. FACS plot and bar graph showing the CFSE$^+$ cells and transfer status of CFSE$^+$ cells in CD45.1 mice before transferring the ovalbumin pulsed BMDCs. D. Representative overlaid histogram show the proliferating OT-I cells in the peripheral circulation at 6 days post DC transfer. E. Bar graph show the cumulative data of (D). Data represents Means ± SEM. ****p<0.0001; ***p<0.001;**p<0.01;*p<0.05, ns p>0.05 (one way ANOVA). F. Line graph showing the change in bodyweight of recipient animals after intranasal WSN-SIINFEKL infection in each group. G. Representative FACS plot show the frequency of expanded virus specific donor OT-I cells in different organs of BMDC recipients after WSN-SIINFEKL infection. H. Representative FACS plot show the frequency of cytokine (TNFα and IFNγ) producing donor cells in different organs of recipients. I-J. Bar graph show the frequency of TNFα-IFNγ double positive (I) and TNFα positive (J) cells in different organs of BMDC recipients. Data represents Means ± SEM. ****p<0.0001; ***p<0.001;**p<0.01;*p<0.05, ns p>0.05 (two way ANOVA). The experiments were repeated at least three times and representative data from one of the experiment is shown.

Rab8a reconstitution in bone marrow cells promoted signalling via mTOR pathway for enhancing survival

To gain insights into the molecular events following depletion or the overexpression of Rab8a in bone marrow cells differentiated into BMDCs, transcriptional changes and signalling events were analysed. Rab8a depleted bone marrow cells had significantly reduced expression of *IGF1R and PI3K,* both constituting the complex required for cellular growth and survival (Figure 2.20.B). A significant decrease in the expression of *Akt1, Akt2* and *Akt3* was also observed in the Rab8a depleted cells (Figure 2.20.C). However, the expression of *Tsc1* and *Tsc2* was significantly increased in the BMDCs knockdown of Rab8a (Figure 2.20.D). Other key genes involved in nutrient sensing such as mTOR, and the components of mTORC1 and mTOC2 such as *Rictor, Raptor* and *SIN1* along with S6K, a positive regulator of cellular growth and survival were also downregulated in Rab8a depleted cells (Figure 2.20.D-E). Following a reconstitution of Rab8a in bone marrow cells of aged animals, the expression of all the genes except for *Raptor* and *Rictor* was upregulated. *Raptor* and *Rictor* were further enhanced in expression following addition of GM-CSF and IL-4 in the differentiating cells (Figure 2.20.F-J).

To measure the expression of key molecules required for differentiation of bone marrow cells into BMDCs, cell lysate from different conditions were subjected to immunoblotting. Depletion of Rab8a was confirmed using anti-Rab8a antibody (Figure 2.20.J). While the baseline expression levels of Akt1 and its phosphorylated version (pAkt1) were high in bone marrow cells of young animals as compared to those from aged animals, both were further increased in differentiated BMDCs (Figure 2.20.J). Following Rab8a depletion, the expression levels of Akt1 as well as pAkt1 were reduced in bone marrow cells as well as BMDCs (Figure 2.20.K). A reconstitution of Rab8a led to the increased expression of both Akt1 and pAkt1 in steady state

conditions as well as after differentiation into BMDCs (Figure 2.20.J). GAPDH signal served as loading controls for different samples. To quantify the levels of Akt1 and pAkt1, flow cytometric analysis was also performed (Figure 2.20.K-P). Differentiated DCs of young animals expressed higher levels of Akt1, pAkt1 as well as Rab8a (Figure 2.20.K and N). An over expression of Rab8a in BMDCs of aged animals upregulated the expression of both Akt1 and pAkt1 and its genetic depletion reduced the expression (Figure 2.20.K and N). Rab8a induced modulation of expression were more evident for pAkt1 which could indicate their rapid response to enhance cytokine production, antigen-presentation as well as longevity (Figure 2.20.L-P). Taken together, the expression data showed that a reconstitution of Rab8a promoted cellular growth and survival due to signalling events involving mTOR pathway.

Figure 2.20

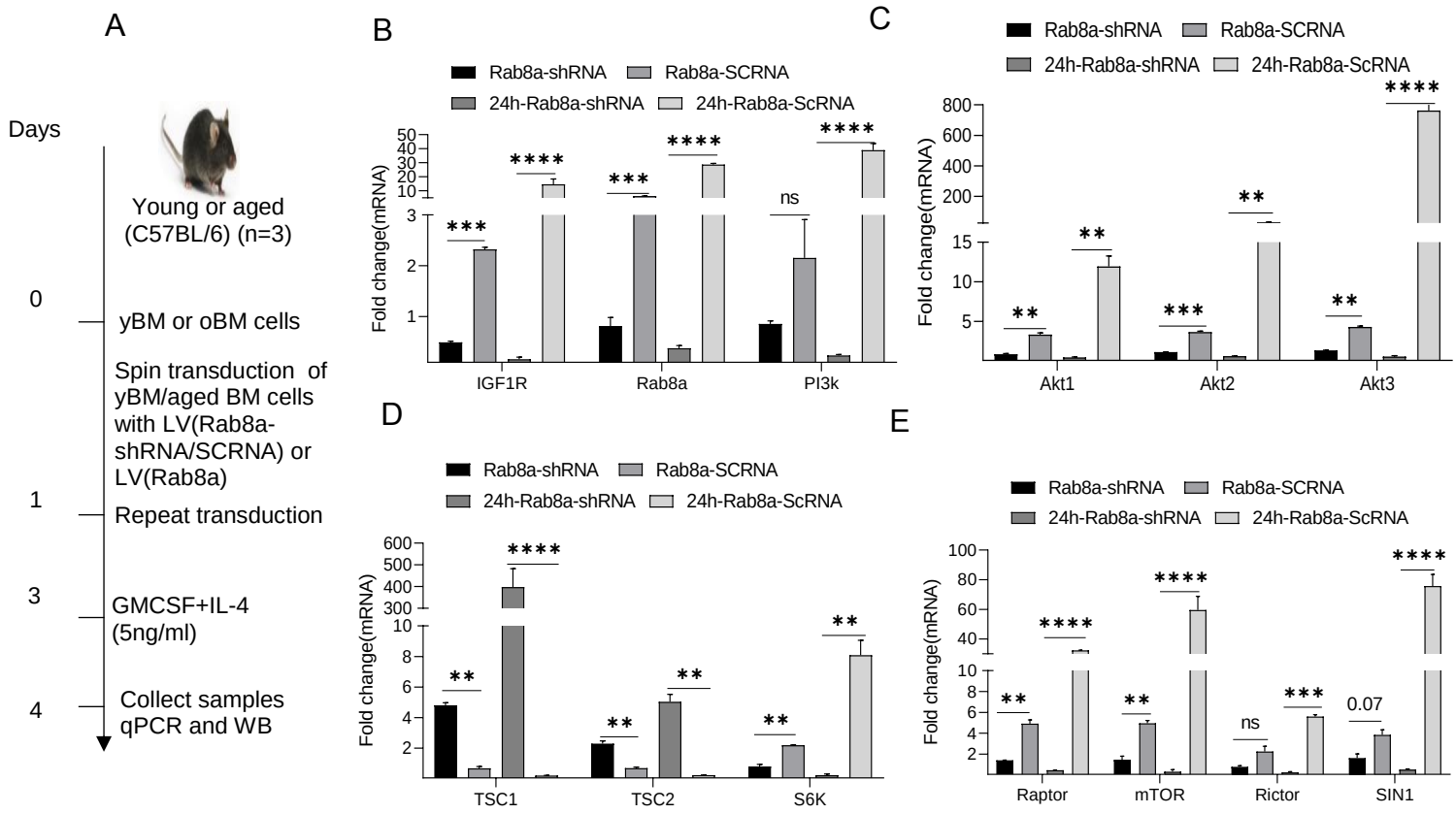

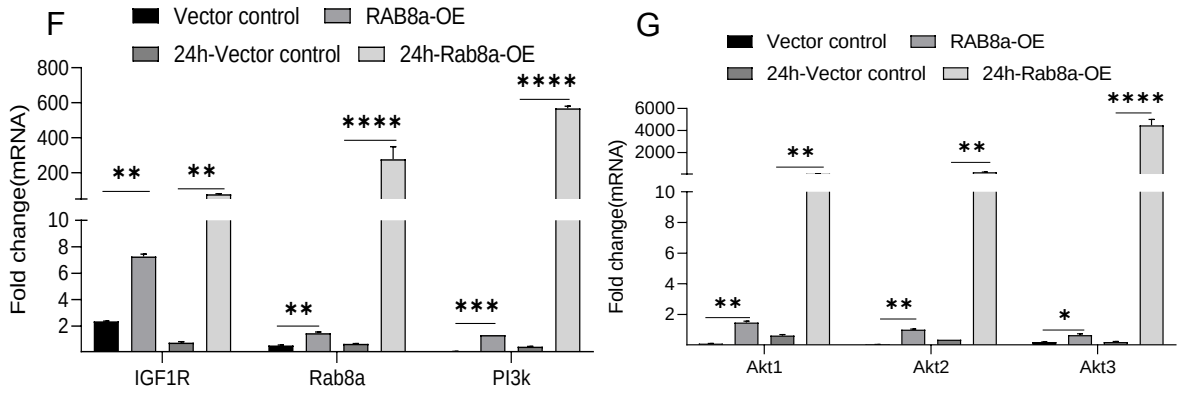
F
Vector control
RAB8a-OE
24h-Vector control
24h-Rab8a-OE
Fold change(mRNA)
IGF1R
Rab8a
PI3k
G
Akt1
Akt2
Akt3

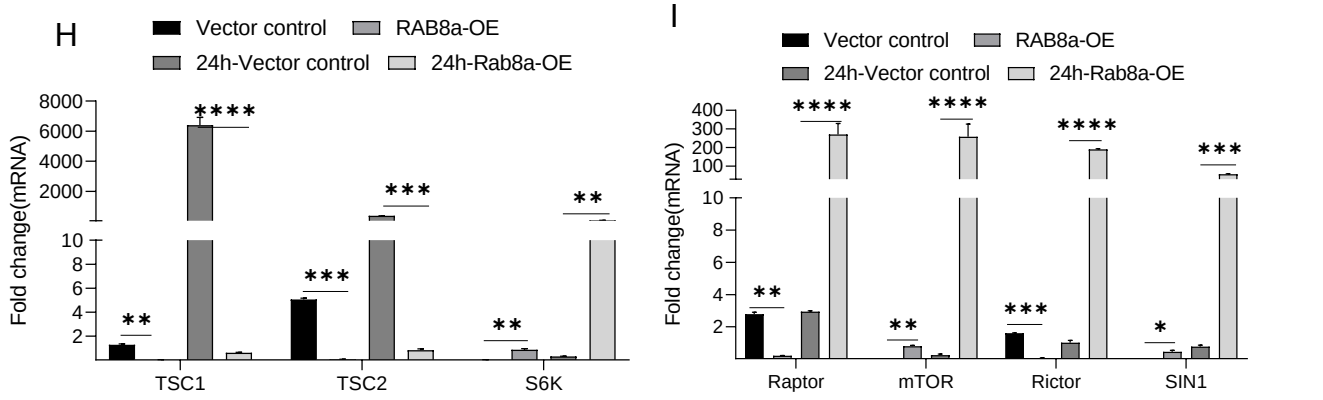
H
I
Vector control
RAB8a-OE
24h-Vector control
24h-Rab8a-OE
Fold change(mRNA)
TSC1
TSC2
S6K
Raptor
mTOR
Rictor
SIN1

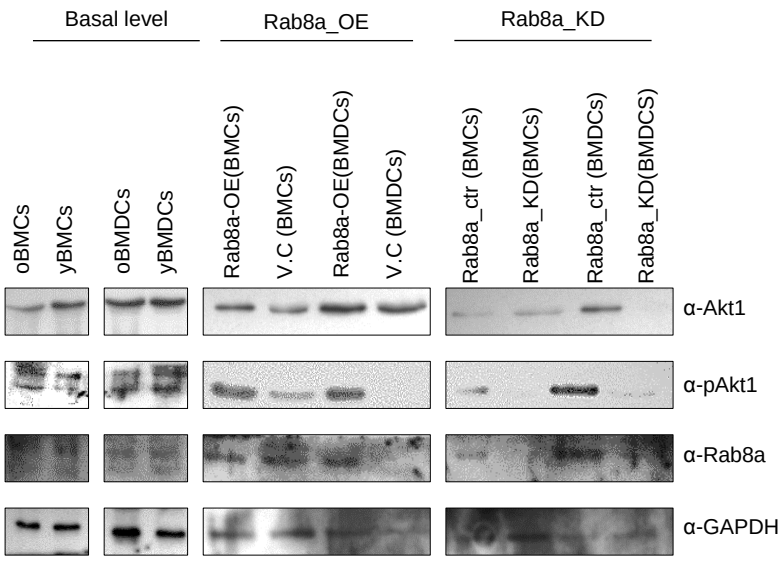
J
Basal level
Rab8a_OE
Rab8a_KD
oBMCs
yBMCs
oBMDCs
yBMDCs
Rab8a-OE(BMCs)
V.C (BMCs)
Rab8a-OE(BMDCs)
V.C (BMDCs)
Rab8a_ctr (BMCs)
Rab8a_KD(BMCs)
Rab8a_ctr (BMDCs)
Rab8a_KD(BMDCS)
α-Akt1
α-pAkt1
α-Rab8a
α-GAPDH

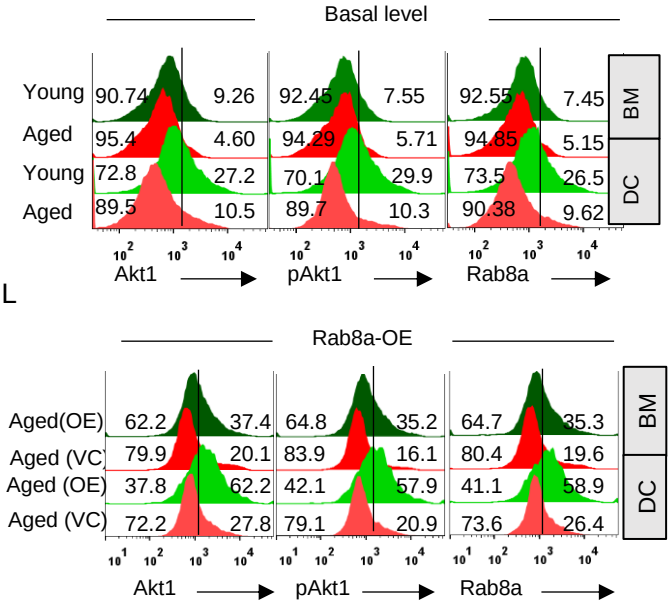
K
Basal level
Young
Aged
Young
Aged
90.74
9.26
92.45
7.55
92.55
7.45
95.4
4.60
94.29
5.71
94.85
5.15
72.8
27.2
70.1
29.9
73.5
26.5
89.5
10.5
89.7
10.3
90.38
9.62
BM
DC
Akt1
pAkt1
Rab8a

L
Rab8a-OE
Aged(OE)
Aged (VC)
Aged (OE)
Aged (VC)
62.2
37.4
64.8
35.2
64.7
35.3
79.9
20.1
83.9
16.1
80.4
19.6
37.8
62.2
42.1
57.9
41.1
58.9
72.2
27.8
79.1
20.9
73.6
26.4
BM
DC
Akt1
pAkt1
Rab8a

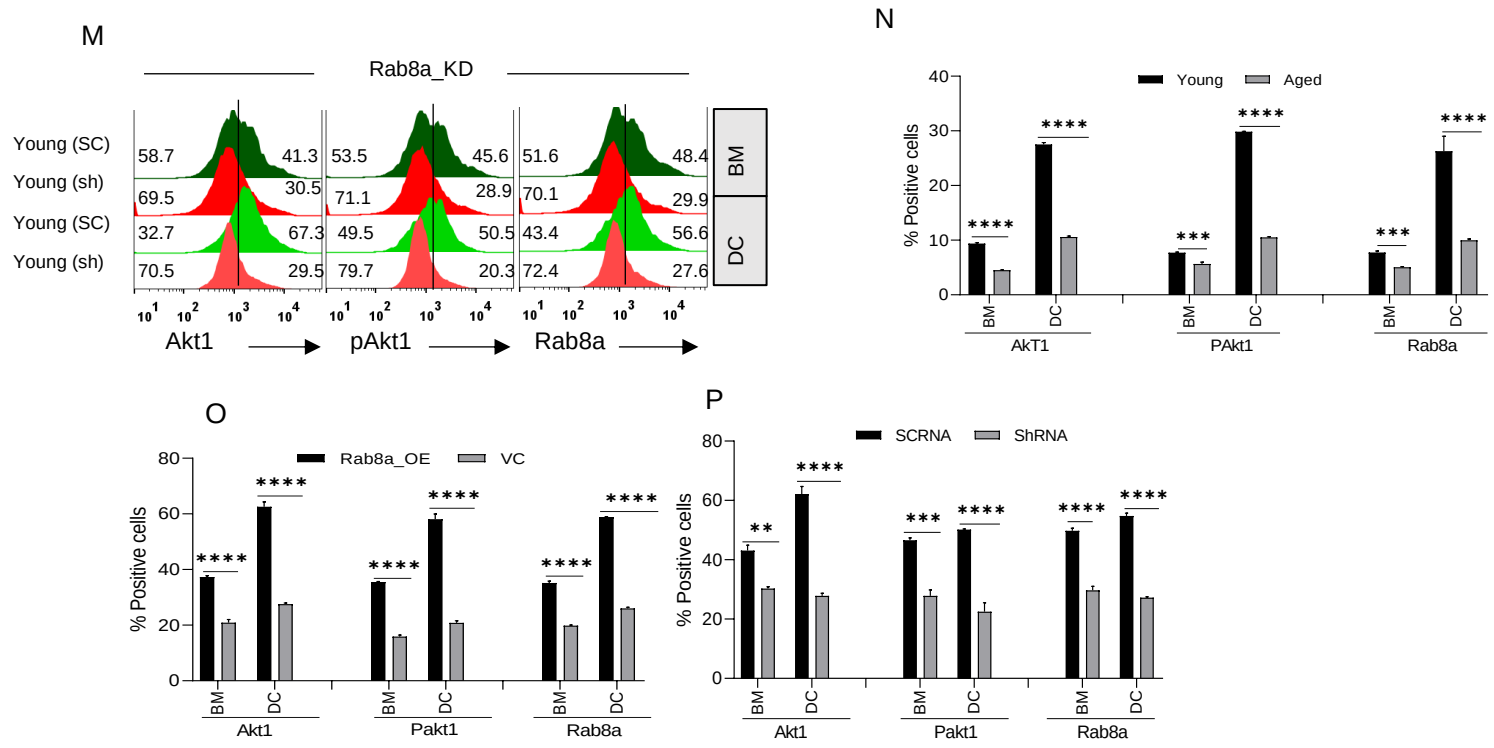

Figure 2.20: Rab8a is critically required for functional differentiation of BMDCs.

A. Schematic of experiment where WT young and aged animals were sacrificed and their bone marrow cells were spin transduced using Rab8a-shRNA or scrambled construct harbouring lentiviruses for knockdown of Rab8a. Additionally Rab8a was overexpressed in aged bone marrow using Rab8a overexpression construct harbouring lentiviruses. The Rab8a-knocked down and overexpressing bone marrow cells along with their controls were cultured in media supplemented with GMCSF and IL4 for 24hrs. This was followed by RNA isolation and cDNA preparation and the transcript abundance of different genes involved in the functional differentiation of BMDCs was measured by qRT-PCR. B-I. Bar graphs showing the expression data in terms of fold change for different genes in each group. Data represents Means ± SEM. ****p<0.0001; ***p<0.001;**p<0.01;*p<0.05, ns p>0.05 (two way ANOVA). J. Western blots show the protein levels of Akt1, pAkt1, Rab8a and GAPDH in the indicated groups are shown. K. Representative overlaid histogram show the expression of Akt1, Pakt1 and Rab8a at basal level in BM cells and

in BMDCs after addition of cytokines for 24hrs. L. Representative overlaid histogram show the expression of Akt, Pakt1 and Rab8a upon overexpression of Rab8a in aged BM cells and after addition of cytokines for 24hrs. M. Representative overlaid histogram revealing the expression of Akt, Pakt1 and Rab8a upon knockdown of Rab8a in young BM cells and after addition of cytokines for 24hrs. N-P. Bar graphs show the cumulative data of K-M. Data represents Means ± SEM. ****p<0.0001; ***p<0.001;**p<0.01;*p<0.05, ns p>0.05 (two way ANOVA). The experiments were repeated twice and representative data from one of the experiment is shown.

Rab8a controls the turnover of class I MHC molecules to enhance antigen presentation.

Rab8a reconstituted BMDCs preferentially expanded $CD8^+$ T cells. We reasoned that the effects could be due to differential turnover or the trafficking pattern of class I MHC molecule following Rab8a expression. BMDCs from young, aged and Rab8a-OE aged cells were generated and pulsed with graded concentrations of SIINFEKL peptide or the whole protein. $CD11c^+$ cells were analysed for display of peptide-MHC class I (H-$2K^b$-SIINFEKL) by flow cytometry. A significant increase in the H-$2K^b$-SIINFEKL displaying DCs was evident in BMDCs from young as well as Rab8a-OE cells in comparison to the those from aged animals (Figure 2.21A-B and 2.22.A-C). DCs displaying p-MHC class I engage with specific $CD8^+$ T cells for activating CTLs. We, therefore, captured initial events involving OT1 cells and cognate antigen-pulsed DCs generated from young, aged and Rab8a-OE cells. *In-vitro* generated BMDCs from different conditions were sorted and labelled with CellTrace™ Far Red dye. The labelled BMDCs were pulsed with either SIINFEKL peptide for 45 minutes or with OVA for 2hrs and then co-incubated with CFSE labelled OT1 cells for 6 or 12hrs and conjugates with double positivity were analysed. Rab8a-OE BMDCs as well as the cells from young animals formed such conjugates more frequently as compared to those from the aged mice following SIINFEKL-peptide and ovalbumin pulse (Figure 2.21.C, 2.22.D).

To understand the role of subcellular compartments in facilitating Rab8a-driven cross antigen presentation, we performed confocal analysis of DCs from young and aged animals as well as those overexpressing (Rab8a-OE aged) with and without antigen-pulsing. A significant increase in the expression of Rab8a was observed after pulsing BMDCs with ovalbumin (Figure 2.21.D, E and 2.23.A). BMDCs generated from the cells of both young and Rab8a-OE condition but not those from aged mice displayed elevated expression of Rab8a following an antigen-pulse (Figure 2.21.D, 2.21.F and 2.23.A). Rab11 is preferentially localized in recycling endosome, a compartment where class I MHC molecules are abundantly present [19]. Following an exogenous antigen pulse, the processed peptides displaying class I MHC molecule are exported to plasma membrane via phagosome for engaging specific TCRs of $CD8^+$ T cells. We, therefore, assessed the levels of Rab11 in BMDCs generated from young, Rab8a-OE aged cells and the control aged cells. A significant increase in the expression of Rab11 was observed following Rab8a overexpression in the aging BMDCs which further increased following ovalbumin pulse (Figure 2.21.D-F and 2.23.A). Both Rab8a and Rab11 showed a significantly higher co-localization in BMDCs generated from young and Rab8a-OE aged cells than the control aged BMDCs (Figure 2.21.D, H and 2.23.A). Therefore, Rab8a reconstituted DCs of aged animals were enriched with endosomal recycling compartment (ERC) that can then promote efficient trafficking of class I MHC molecules to plasma membrane. Whether or not the ERCs are enriched in peptide-MHC complexes following Rab8a reconstitution of aged BMDCs pulsed with Ova was also analysed. While the un-pulsed BMDCs showed no staining for H-$2K^b$-SIINFEKL, ovalbumin pulsed cells showed substantially increased levels (Figure 2.21.D, G and 2.23.A). Interestingly, a significant increase in the expression of H-$2K^b$-SIINFEKL was observed in BMDCs generated from young and Rab8a-OE aged cells than the control aged BMDCs (Figure 2.21.D, G and 2.23.A). We also

observed higher co-localization of H2-K^b-SIINFEKL with both Rab8a and Rab11 in OVA-pulsed BMDCs of young and Rab8a-OE BMDCs when compared with those from the BMDCs of aged mice (Figure 2.21.D, H and 2.23.A). We also observed an increase in the expression of both Rab8a and Rab11 in BMDCs of young and those of aged animals that overexpressed Rab8a (Rab8a-OE) following Ova pulse using western blotting and flow cytometry (Figure 2.21 I, J and 2.23.B). Taken together, we conclude that after internalization of Ova protein, Rab8a modulates the expression of Rab11 and promotes the transport of peptide-MHC class I to the ERCs which eventually display such complexes on the surface of DCs to enhance cross antigen-presentation. We observed an altered shape of BMDCs from aged mice upon pulsing with Ova while no such differences were evident in the cells from young and Rab8a-OE conditions (unpublished observation). Such alteration could be driven by differential actin polymerization, a highly energy dependent process (20). We performed intracellular staining with Alexa Fluor™ 488 Phalloidin (Thermo Fisher Scientific) to quantify the total actin content of cells and observed a significant increase in the frequency of phalloidin-Alexa Fluor 488 positive cells in BMDCs generated from Rab8a-OE (~60%) than aged (~27%) and young BM cells (~43.2%) (Figure 2.21.K-M). The above data were also supported by a significantly lower expression of phalloidin on per cell expression basis (Figure 2.21.M). Our results also correlated with earlier reports where formation of cell protrusion and dorsal ruffle upon overexpression of Rab8a was observed (21). Above results suggested that overexpressing Rab8a in aged BM cells also restored their shape and probably the migratory potential of differentiated BMDCs for efficient functionality and homing.

Figure 2.21

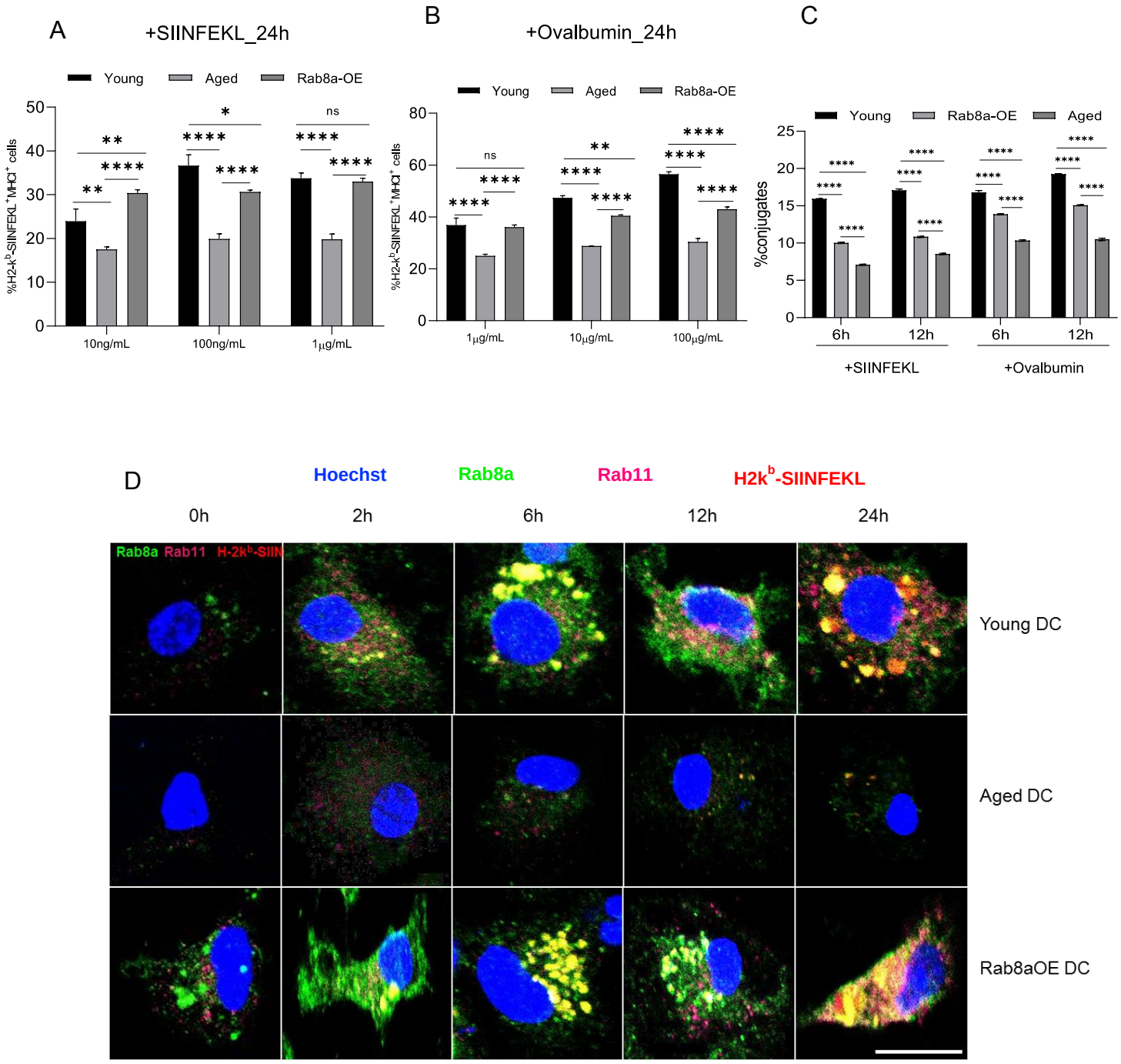
A
+SIINFEKL_24h
B
+Ovalbumin_24h
C
Young
Aged
Rab8a-OE
%H2-k^{b}-SIINFEKL^{+}MHCI^{+} cells
10ng/mL
100ng/mL
1μg/mL
10μg/mL
100μg/mL
%conjugates
6h
12h
+SIINFEKL
+Ovalbumin
D
Hoechst
Rab8a
Rab11
H2k^{b}-SIINFEKL
0h
2h
6h
12h
24h
Rab8a Rab11 H-2k^{b}-SIIN
Young DC
Aged DC
Rab8aOE DC

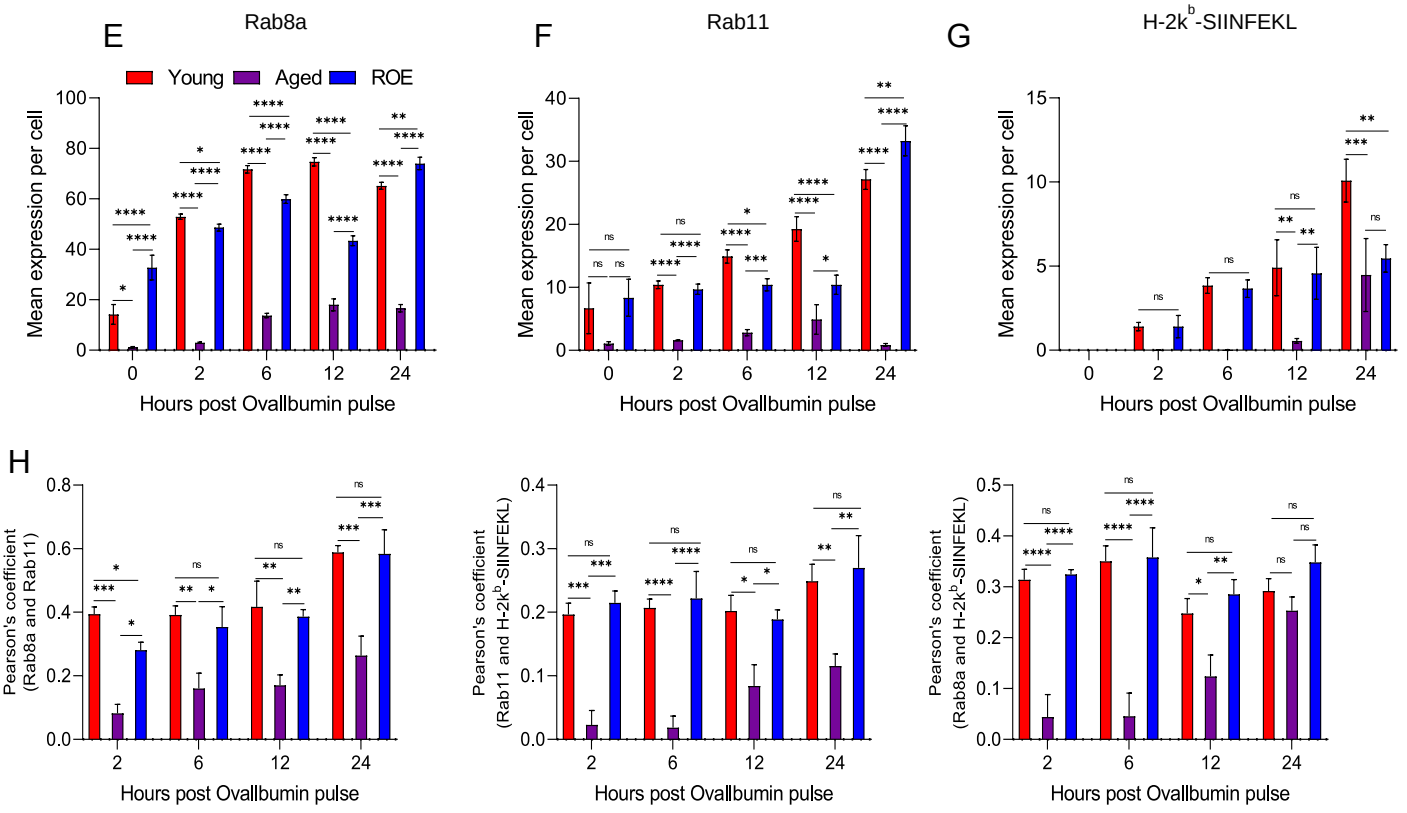
E
Rab8a
Young
Aged
ROE
Mean expression per cell
Hours post Ovallbumin pulse
F
Rab11
Mean expression per cell
Hours post Ovallbumin pulse
G
H-2k^b-SIINFEKL
Mean expression per cell
Hours post Ovallbumin pulse
H
Pearson's coefficient (Rab8a and Rab11)
Hours post Ovallbumin pulse
Pearson's coefficient (Rab11 and H-2k^b-SIINFEKL)
Hours post Ovallbumin pulse
Pearson's coefficient (Rab8a and H-2k^b-SIINFEKL)
Hours post Ovallbumin pulse

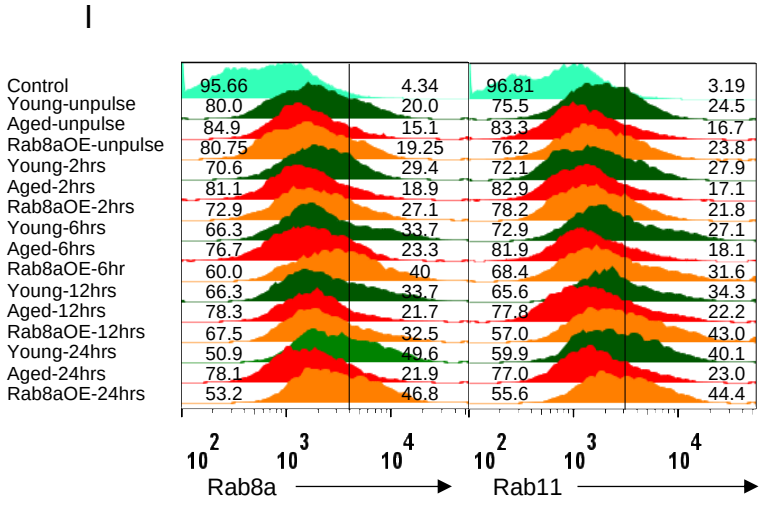
I
Control 95.66 4.34 96.81 3.19
Young-unpulse 80.0 20.0 75.5 24.5
Aged-unpulse 84.9 15.1 83.3 16.7
Rab8aOE-unpulse 80.75 19.25 76.2 23.8
Young-2hrs 70.6 29.4 72.1 27.9
Aged-2hrs 81.1 18.9 82.9 17.1
Rab8aOE-2hrs 72.9 27.1 78.2 21.8
Young-6hrs 66.3 33.7 72.9 27.1
Aged-6hrs 76.7 23.3 81.9 18.1
Rab8aOE-6hr 60.0 40 68.4 31.6
Young-12hrs 66.3 33.7 65.6 34.3
Aged-12hrs 78.3 21.7 77.8 22.2
Rab8aOE-12hrs 67.5 32.5 57.0 43.0
Young-24hrs 50.9 49.6 59.9 40.1
Aged-24hrs 78.1 21.9 77.0 23.0
Rab8aOE-24hrs 53.2 46.8 55.6 44.4
Rab8a
Rab11

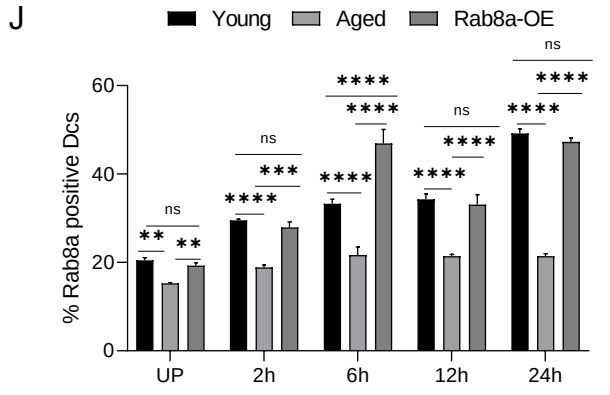
J
Young
Aged
Rab8a-OE
% Rab8a positive Dcs
UP
2h
6h
12h
24h

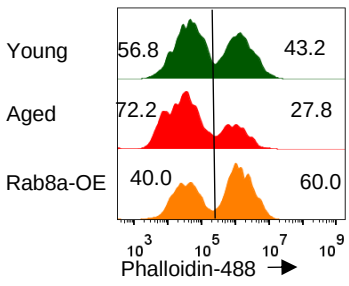
K
Young
Aged
Rab8a-OE
56.8
43.2
72.2
27.8
40.0
60.0
Phalloidin-488

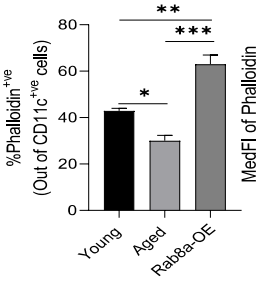
L
%Phalloidin+ve (Out of CD11c+ve cells)
Young
Aged
Rab8a-OE

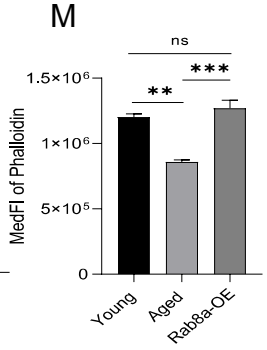
M
MedFI of Phalloidin
Young
Aged
Rab8a-OE

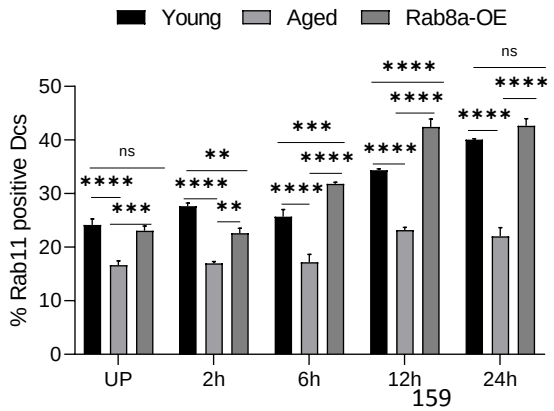
Young
Aged
Rab8a-OE
% Rab11 positive Dcs
UP
2h
6h
12h
24h

Figure 2.21: Rab8a is critical for the formation of immunological synapse using DCs and CD8 T cells.

A-B. Bar graphs summarizing the frequency of BMDCs of each group expressing SIINFEKL bound MHC-I complexes upon antigen pulse are shown. C. Bar graph summarizing the analysis for in vitro immune synapse formation assay are shown (n=3). Data represents Means ± SEM. ****p<0.0001; ***p<0.001;**p<0.01;*p<0.05, ns p>0.05 (two way ANOVA). D. Confocal microscopy images show the mean expression of Rab8a, Rab11 and H-2Kb-SIINFEKL upon pulsing with ovalbumin for different time points in indicated conditions. Scale bar = 10μm. E-H. Bar graphs shows the cumulative data of mean expression (E) of Rab8a (E), Rab11 (F) and H-2Kb-SIINFEKL (G) and their co-localization (H) in terms of Pearson's coefficient in BMDCs of each group upon pulsing with ovalbumin for different time points (n=3). Data represents Means ± SEM. ****p<0.0001; ***p<0.001;**p<0.01;*p<0.05, ns p>0.05. (two way ANOVA). I. Representative overlaid histogram show the relative abundance of Rab8a and Rab11 upon pulsing with ovalbumin in different indicated conditions. J. Bar graph show the cumulative data of I. K. Overlaid histogram showing the frequency of Phalloidin-AF488 positive dendritic cells from each group. L-M. Bar graph show the cumulative data of frequency (L) and MFI (M) of data presented in K (n=3). Data represents Mean ± SEM. ****p<0.0001; ***p<0.001;**p<0.01;*p<0.05, ns p>0.05. (one way ANOVA). The experiments were repeated twice and representative data from one of the experiment is shown.

Figure 2.22

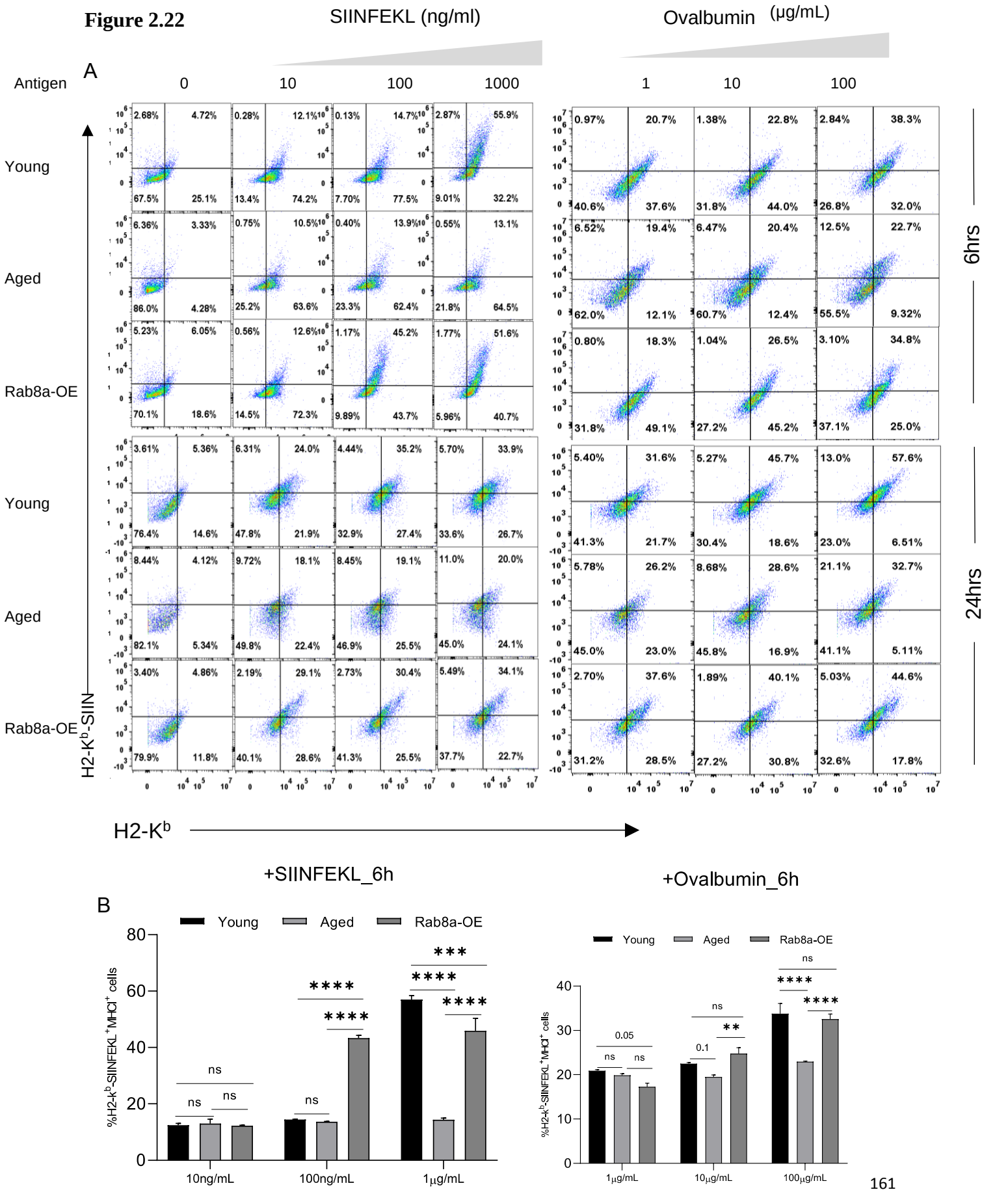
SIINFEKL (ng/ml)
Ovalbumin (µg/mL)
A
Antigen
0
10
100
1000
1
10
100
Young
Aged
Rab8a-OE
Young
Aged
Rab8a-OE
6hrs
24hrs
H2-K^b-SIIN
H2-K^b
+SIINFEKL_6h
+Ovalbumin_6h
B
Young
Aged
Rab8a-OE
%H2-K^b-SIINFEKL$^+$MHCI$^+$ cells
10ng/mL
100ng/mL
1µg/mL
1µg/mL
10µg/mL
100µg/mL
ns
****
***
**
0.05
0.1

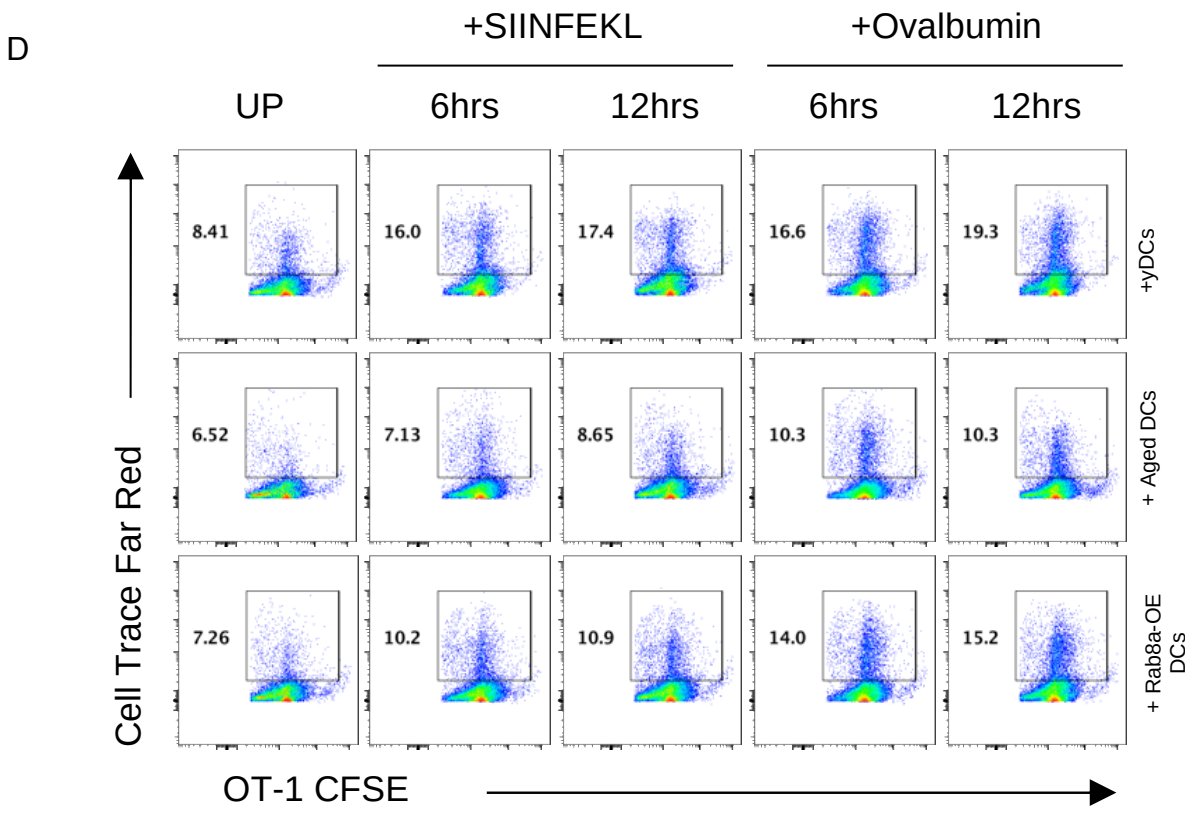

Figure 2.22: Reconstitution of Rab8a in BM cells of aged mice restore the antigen display on BMDCs. A. Representative FACS plot show the frequency of H-2Kb-SIINFEKL positive BMDCs out of total MHCI positive cells upon pulsing with varying concentration SIINFEKL peptide or ovalbumin for different time intervals. B-C. Bar graph show the cumulative data of SIINFEKL (B) or ovalbumin (C) pulsed BMDCs in each group. Data represents Means ± SEM. ****p<0.0001; ***p<0.001;**p<0.01;*p<0.05, ns p>0.05 (two way ANOVA). D. Representative FACS plot showing the *in-vitro* immune synapse formation which was measured by co-culturing the Cell trace far Red labelled pulsed BMDCs with CFSE labelled OT-I cells for indicated time points. The experiments were repeated at least three times and representative data from one of the experiment is shown.

Figure 2.23

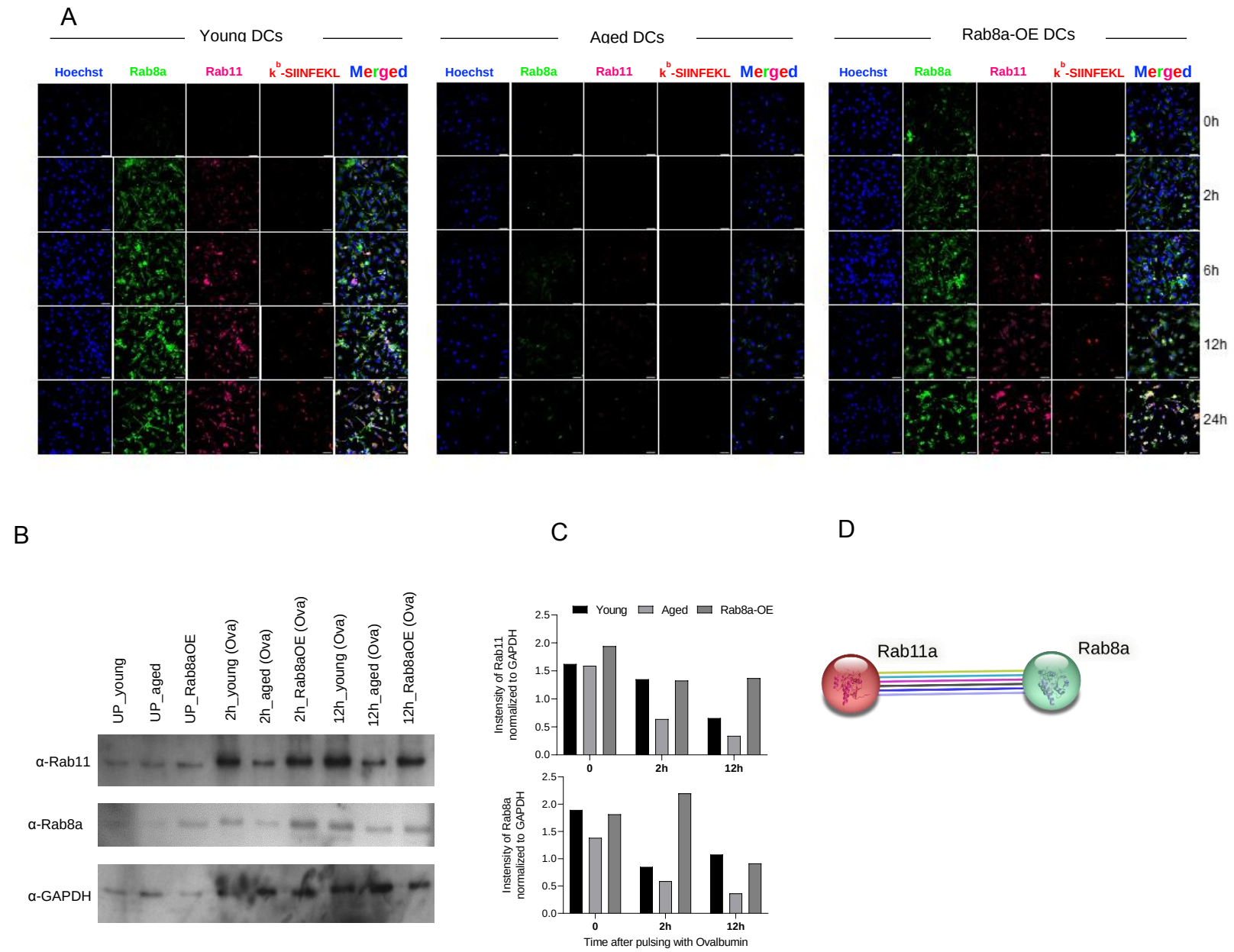
A
Young DCs
Aged DCs
Rab8a-OE DCs
Hoechst
Rab8a
Rab11
k^b-SIINFEKL
Merged
0h
2h
6h
12h
24h
B
UP_young
UP_aged
UP_Rab8aOE
2h_young (Ova)
2h_aged (Ova)
2h_Rab8aOE (Ova)
12h_young (Ova)
12h_aged (Ova)
12h_Rab8aOE (Ova)
α-Rab11
α-Rab8a
α-GAPDH
C
Young
Aged
Rab8a-OE
Instensity of Rab11 normalized to GAPDH
Instensity of Rab8a normalized to GAPDH
0
2h
12h
Time after pulsing with Ovalbumin
D
Rab11a
Rab8a

Figure 2.23: Overexpression of Rab8a in BM cells of aged mice modulates the expression of Rab11 and H-2Kb-SIINFEKL upon pulsing with ovalbumin.

A. Confocal microscopic images show the expression of Rab8a, Rab11 and H-2kb-SIINFEKL upon pulsing with ovalbumin. *In-vitro* generated BMDCs from young, aged and Rab8a-OE conditions were pulsed with ovalbumin for 0hrs, 2hrs, 6hrs, 12hrs and 24hrs and then were stained for the aforementioned markers and the images were acquired using Nikon A1 confocal microscope at 60x magnification. Scale bar=10μm. B. Western blot show the relative abundance of Rab8a and Rab11 upon pulsing with ovalbumin at different time intervals in indicated conditions. C. Bar graphs show the relative intensity of Rab11 and Rab8a normalized to control in indicated conditions. E. STRING network showing the co-expression of Rab8a with Rab11. The experiments were repeated at least three times and representative data from one of the experiment is shown.

Discussion

WHO estimates that by 2030, one out of six people will be above 60 years (https://www.who.int/news-room/fact-sheets/detail/ageing-and-health). This poses a great challenge to health care system since aged population exhibit higher susceptibility to infection and respond poorly to vaccination (22). Therefore, it becomes imperative to devise immune potentiating strategies in the aging population. We attempted to elucidate the molecular intricacies associated with loss of DCs' function in the aging host since these cells are involved in the initiation of an antigen specific T cell response and thus link innate and adaptive systems (23). Conventional dendritic cells are divided into two subset viz CDC1s and CDC2s. Out of them CDC1s are widely widely known for its role in cross presenting antigenic epitope to $CD8^+$ T cells in clearing the viral infection and supress the growth of tumor (24). Age associated impaired function of CDC1s are observed which involved dimished Type I IFN production along with compromised cross antigen presentation (25). Transcriptomic analysis of $CD11b^+/CD11c^+$ cDC2s from aged and young mice showed an attrition of the type I IFN pathway. Accordingly, BMDCs as well as splenic DCs from mice lacking type I IFN response because of IFN receptor knockout exhibited impaired differentiation and functionality as was also observed in DCs of aged humans. Additionally, molecules downstream to growth factor receptors that influence differentiation of DCs were also reduced in the expression in DCs of both aged and IFNRKO mice. One such molecule Rab8a, a small GTPase was shown to be critically involved in the differentiation and functionality of DCs. Rab8a depleted bone marrow precursors of young animals failed to efficiently differentiate into DCs while its reconstitution in those of aged mice reversed the phenotype. Furthermore, Rab8a reconstituted BMDCs displayed better functionality that involved

survival, cytokine production, homing and efficiency in engaging with T cells. Therefore, reconstitution of Rab8a can induce immune potentiation in aged individuals.

Type I IFNs (IFNα/β) are a major class of antivirals that act by inducing IFN stimulated genes (ISGs) that makes the susceptible cells refractory to viral propagation. Other functions of Type I IFNs are promoting upregulation of MHC and costimulatory molecules (CD80 and CD86) both required for efficiently priming T cells (26, 27). IFNs response in DCs enhances cross-presentation of antigens during viral infection in addition to promoting cellular migration (28). Respiratory viral pathogens such as SARS-CoV2 and IAV cause severe lesions in aged individuals29, 30). COVID-19 caused a more severe disease in individuals above the age of 80 years as compared to those below 50 years (31, 32). A comparative analysis of SARS-CoV infected young and aged macaques showed an enhanced immune-mediated pulmonary pathologies and elevated levels of IL-8 but significantly reduced levels of IFNβ in the infected lung tissues of the latter group (31). Furthermore, an exogenously administered IFNβ ameliorated pulmonary lesions in the infected animals (34). Diminished type I IFN response was also evident in patients with severe COVID-19 (35). A compromised type I IFN response initially after infection could fail to control the viral load and paved the way for a protracted pathology and poor prognosis of viral infection. We observed an attenuation of type I IFN signalling in DCs of aged mice and humans which could in part help explain the vulnerability of aging population to develop severe disease following viral infection.

Cytokine (GM-CSF and IL-4) induced differentiation of DCs recruits molecules such as Rab8a and triggers Akt activation by PI3K (36, 37). Akt inhibits the expression of Tsc1 and 2 which regulate signalling via mTORC1. With the negative regulation removed, mTORC1 promotes proliferation, survival and differentiation of DCs (37, 38). Our RNA seq data showed a

downregulation of genes involved in mTOR signalling within the aged bone marrow cells. Additionally, the growth factor receptors, CSFRA, IGF1R, and their downstream adaptor, Rab8a, were reduced in expression in the bone marrow of aged as well as IFNRKO mice (37). To directly test the role of signalling via growth receptors, we modulated the levels of Rab8a and assessed responsiveness of DCs. While an shRNA mediated knockdown of Rab8a in young bone marrow cells resulted in impaired differentiation, a reconstitution of bone marrow cells of aged mice with Rab8a generated functionally competent DCs by potentially involving PI3K-AKT-mTORC1 axis. The investigated functional properties that were regained by the Rab8a reconstituted DCs of aging host included efficient expression of type I IFNs and ISGs, MHC and costimulatory molecules and antigen uptake, processing and presentation and leading to an efficient viral control. Therefore, reconstitution of Rab8a largely restored function of incapacitated DCs of an aging host. However, we did not establish a direct role of Rab8 mediated events and a compromised IFN response leading to reduced functions of DCs of aging host but at subcellular level such events might be connected given its role in facilitating cellular secretions.

Rab8a localize in different cellular compartments such as plasma membrane (39), macropinosomes (40), recycling endosomes (41) microtubules and pseudopodia as well as the exocytic vesicles. It is also essential for the fusion of exocytic vesicles to the plasma membrane (42). Overexpression of Rab8a is known to promote the formation of cell protrusion and dorsal ruffles (43) and enhances membrane trafficking (40). A colocalization of Rab8a with Rab11 as well as Rab22a was evident (41, 40). Since Rab11 and Rab22a have been implicated in antigen cross-presentation, our observation that Rab8a overexpressing aged DCs exhibit not only an enhanced expression of Rab11 but also their efficient colocalization with the peptide-MHC complexes following an antigen pulse (19, 4). This could help explain the underlying subcellular

trafficking events of immune potentiation achieved by Rab8a overexpressing DCs. An increase in the MFI of Rab8a around the cell periphery upon antigen stimulation further suggested its role in transport and fusion of peptide-MHCI complex containing vesicles to the plasma membrane, thus mediating antigen presentation. Consequently, such DCs better engaged with the cognate TCR expressing $CD8^+$ T cells. With the expansion of antigen specific $CD8^+$ T cells, the virus infection could be better resolved generating a pool of persisting memory. We indeed observed enhanced early immunological memory in the recipients of Rab8a overexpressing DCs as compared to those receiving DCs of aged animals. These observations therefore could have implications not only in managing viral infections but also enhancing vaccine efficacy along with anti-tumour response in the aging population. That the modified DCs induced immune potentiation by expansion of effector $CD8^+$ T cells and the generation of memory pool obviate the need to have persisting DCs in the host. DCs being short lived population are unlikely to pose long-term toxicity because of genetic modification. Our observation that Rab8a critically controls the functionality and differentiation of DCs and reconstitution of the same in DCs from aged individuals could, therefore, represent a viable option to reconstitute immune function and improve the existing strategies to provide aged individuals with long-term protection against viral infections.

References

1. Pennock, N.D., White, J.T., Cross, E.W., Cheney, E.E., Tamburini, B.A. and Kedl, R.M., 2013. T cell responses: naive to memory and everything in between. Advances in physiology education, 37(4), pp.273-283.
2. Weyand, C.M. and Goronzy, J.J., 2016. Aging of the immune system. Mechanisms and therapeutic targets. Annals of the American Thoracic Society, 13(Supplement 5), pp.S422-S428.
3. Nikolich-Žugich, J., 2018. The twilight of immunity: emerging concepts in aging of the immune system. Nature immunology, 19(1), pp.10-19.
4. Ponnappan, S. and Ponnappan, U., 2011. Aging and immune function: molecular mechanisms to interventions.
5. Crooke, S.N., Ovsyannikova, I.G., Poland, G.A. and Kennedy, R.B., 2019. Immunosenescence and human vaccine immune responses. Immunity & ageing, 16, pp.1-16.
6. Pinti, M., Appay, V., Campisi, J., Frasca, D., Fülöp, T., Sauce, D., Larbi, A., Weinberger, B. and Cossarizza, A., 2016. Aging of the immune system: focus on inflammation and vaccination. European journal of immunology, 46(10), pp.2286-2301.
7. Long, E.O., Burshtyn, D.N., Clark, W.P., Peruzzi, M., Rajagopalan, S., Rojo, S., Wagtmann, N. and Winter, C.C., 1997. Killer cell inhibitory receptors: diversity, specificity, and function. Immunological reviews, 155(1), pp.135-144.

8. Rodriguez-Barbosa, J.I., Schneider, P., Weigert, A., Lee, K.M., Kim, T.J., Perez-Simon, J.A. and Del Rio, M.L., 2019. HVEM, a cosignaling molecular switch, and its interactions with BTLA, CD160 and LIGHT. Cellular & molecular immunology, 16(7), pp.679-682.
9. Filén, S. and Lahesmaa, R., 2010. GIMAP proteins in T-lymphocytes. Journal of signal transduction, 2010.
10. Tolksdorf, F., Mikulec, J., Geers, B., Endig, J., Sprezyna, P., Heukamp, L.C., Knolle, P.A., Kolanus, W. and Diehl, L., 2018. The PDL1-inducible GTPase Arl4d controls T effector function by limiting IL-2 production. Scientific reports, 8(1), p.16123.
11. Fang, M., Li, P., Wu, X. and Xu, Y., 2015. Class II transactivator (CIITA) mediates transcriptional repression of pdk4 gene by interacting with hypermethylated in cancer 1 (HIC1). Journal of Biomedical Research, 29(4), p.308.
12. McLellan, A.D., Kapp, M., Eggert, A., Linden, C., Bommhardt, U., Bröcker, E.B., Kämmerer, U. and Kämpgen, E., 2002. Anatomic location and T-cell stimulatory functions of mouse dendritic cell subsets defined by CD4 and CD8 expression. Blood, The Journal of the American Society of Hematology, 99(6), pp.2084-2093.
13. Hong, W., Yang, B., He, Q., Wang, J. and Weng, Q., 2022. New insights of CCR7 signaling in dendritic cell migration and inflammatory diseases. Frontiers in pharmacology, 13, p.841687.
14. Nan, Y., Wu, C. and Zhang, Y.J., 2017. Interplay between Janus kinase/signal transducer and activator of transcription signaling activated by type I interferons and viral antagonism. Frontiers in immunology, 8, p.1758.
15. Joffre, O.P., Segura, E., Savina, A. and Amigorena, S., 2012. Cross-presentation by dendritic cells. Nature Reviews Immunology, 12(8), pp.557-569.

16. Sehrawat, S., Koenig, P.A., Kirak, O., Schlieker, C., Fankhauser, M. and Ploegh, H.L., 2013. A catalytically inactive mutant of the deubiquitylase YOD-1 enhances antigen cross-presentation. Blood, The Journal of the American Society of Hematology, 121(7), pp.1145-1156.
17. Hickman, H.D., Reynoso, G.V., Ngudiankama, B.F., Cush, S.S., Gibbs, J., Bennink, J.R. and Yewdell, J.W., 2015. CXCR3 chemokine receptor enables local CD8+ T cell migration for the destruction of virus-infected cells. Immunity, 42(3), pp.524-537.
18. Luo, L., Wall, A.A., Yeo, J.C., Condon, N.D., Norwood, S.J., Schoenwaelder, S., Chen, K.W., Jackson, S., Jenkins, B.J., Hartland, E.L. and Schroder, K., 2014. Rab8a interacts directly with PI3Kγ to modulate TLR4-driven PI3K and mTOR signalling. *Nature communications*, *5*(1), p.4407.
19. Nair-Gupta, P., Baccarini, A., Tung, N., Seyffer, F., Florey, O., Huang, Y., Banerjee, M., Overholtzer, M., Roche, P.A., Tampé, R. and Brown, B.D., 2014. TLR signals induce phagosomal MHC-I delivery from the endosomal recycling compartment to allow cross-presentation. Cell, 158(3), pp.506-521.
20. Pollard, T.D. and Cooper, J.A., 2009. Actin, a central player in cell shape and movement. Science, 326(5957), pp.1208-1212.
21. Peränen, J., Auvinen, P., Virta, H., Wepf, R. and Simons, K., 1996. Rab8 promotes polarized membrane transport through reorganization of actin and microtubules in fibroblasts. The Journal of cell biology, 135(1), pp.153-167.
22. Gardner, I.D., 1980. The effect of aging on susceptibility to infection. Reviews of infectious diseases, 2(5), pp.801-810.

23. Palucka, K. and Banchereau, J., 1999. Dendritic cells: a link between innate and adaptive immunity. Journal of clinical immunology, 19, pp.12-25.
24. Hildner, K., Edelson, B.T., Purtha, W.E., Diamond, M., Matsushita, H., Kohyama, M., Calderon, B., Schraml, B.U., Unanue, E.R., Diamond, M.S. and Schreiber, R.D., 2008. Batf3 deficiency reveals a critical role for CD8α+ dendritic cells in cytotoxic T cell immunity. Science, 322(5904), pp.1097-1100.
25. Connors, J., Taramangalam, B., Cusimano, G., Bell, M.R., Matt, S.M., Runner, K., Gaskill, P.J., DeFilippis, V., Nikolich-Žugich, J., Kutzler, M.A. and Haddad, E.K., 2022. Aging alters antiviral signaling pathways resulting in functional impairment in innate immunity in response to pattern recognition receptor agonists. GeroScience, 44(5), pp.2555-2572.
26. Katze, M.G., He, Y. and Gale Jr, M., 2002. Viruses and interferon: a fight for supremacy. Nature Reviews Immunology, 2(9), pp.675-687.
27. Marckmann, S., Wiesemann, E., Hilse, R., Trebst, C., Stangel, M. and Windhagen, A., 2004. Interferon-β up-regulates the expression of co-stimulatory molecules CD80, CD86 and CD40 on monocytes: significance for treatment of multiple sclerosis. Clinical & Experimental Immunology, 138(3), pp.499-506.
28. Parlato, S., Santini, S.M., Lapenta, C., Di Pucchio, T., Logozzi, M., Spada, M., Giammarioli, A.M., Malorni, W., Fais, S. and Belardelli, F., 2001. Expression of CCR-7, MIP-3β, and Th-1 chemokines in type I IFN-induced monocyte-derived dendritic cells: importance for the rapid acquisition of potent migratory and functional activities. Blood, The Journal of the American Society of Hematology, 98(10), pp.3022-3029.

29. Channappanavar, R. and Perlman, S., 2020. Age-related susceptibility to coronavirus infections: role of impaired and dysregulated host immunity. The Journal of clinical investigation, 130(12), pp.6204-6213.
30. Mueller, A.L., McNamara, M.S. and Sinclair, D.A., 2020. Why does COVID-19 disproportionately affect older people?. Aging (albany NY), 12(10), p.9959.
31. Verity, R., Okell, L.C., Dorigatti, I., Winskill, P., Whittaker, C., Imai, N., Cuomo-Dannenburg, G., Thompson, H., Walker, P.G., Fu, H. and Dighe, A., 2020. Estimates of the severity of coronavirus disease 2019: a model-based analysis. The Lancet infectious diseases, 20(6), pp.669-677.
32. Yanez, N.D., Weiss, N.S., Romand, J.A. and Treggiari, M.M., 2020. COVID-19 mortality risk for older men and women. BMC public health, 20(1), pp.1-7.
33. Singh, D.K., Singh, B., Ganatra, S.R., Gazi, M., Cole, J., Thippeshappa, R., Alfson, K.J., Clemmons, E., Gonzalez, O., Escobedo, R. and Lee, T.H., 2021. Responses to acute infection with SARS-CoV-2 in the lungs of rhesus macaques, baboons and marmosets. Nature microbiology, 6(1), pp.73-86.
34. Channappanavar, R., Fehr, A.R., Zheng, J., Wohlford-Lenane, C., Abrahante, J.E., Mack, M., Sompallae, R., McCray, P.B., Meyerholz, D.K. and Perlman, S., 2019. IFN-I response timing relative to virus replication determines MERS coronavirus infection outcomes. The Journal of clinical investigation, 129(9), pp.3625-3639.
35. Hadjadj, J., Yatim, N., Barnabei, L., Corneau, A., Boussier, J., Smith, N., Péré, H., Charbit, B., Bondet, V., Chenevier-Gobeaux, C. and Breillat, P., 2020. Impaired type I interferon activity and inflammatory responses in severe COVID-19 patients. Science, 369(6504), pp.718-724.

36. Van de Laar, L., Coffer, P.J. and Woltman, A.M., 2012. Regulation of dendritic cell development by GM-CSF: molecular control and implications for immune homeostasis and therapy. Blood, The Journal of the American Society of Hematology, 119(15), pp.3383-3393.
37. Sukhbaatar, N., Hengstschläger, M. and Weichhart, T., 2016. mTOR-mediated regulation of dendritic cell differentiation and function. Trends in immunology, 37(11), pp.778-789.
38. Linke, M., Fritsch, S.D., Sukhbaatar, N., Hengstschläger, M. and Weichhart, T., 2017. mTORC 1 and mTORC 2 as regulators of cell metabolism in immunity. FEBS letters, 591(19), pp.3089-3103.
39. Armstrong, J., Thompson, N., Squire, J.H., Smith, J., Hayes, B. and Solari, R., 1996. Identification of a novel member of the Rab8 family from the rat basophilic leukaemia cell line, RBL. 2H3. Journal of cell science, 109(6), pp.1265-1274.
40. Hattula, K., Furuhjelm, J., Tikkanen, J., Tanhuanpää, K., Laakkonen, P. and Peränen, J., 2006. Characterization of the Rab8-specific membrane traffic route linked to protrusion formation. Journal of cell science, 119(23), pp.4866-4877.
41. Rowe, R.K., Suszko, J.W. and Pekosz, A., 2008. Roles for the recycling endosome, Rab8, and Rab11 in hantavirus release from epithelial cells. Virology, 382(2), pp.239-249.
42. Grigoriev, I., Yu, K.L., Martinez-Sanchez, E., Serra-Marques, A., Smal, I., Meijering, E., Demmers, J., Peränen, J., Pasterkamp, R.J., van der Sluijs, P. and Hoogenraad, C.C., 2011. Rab6, Rab8, and MICAL3 cooperate in controlling docking and fusion of exocytotic carriers. Current Biology, 21(11), pp.967-974.
43. Peränen, J., 2011. Rab8 GTPase as a regulator of cell shape. Cytoskeleton, 68(10), pp.527-539.

44. Cebrian, I., Croce, C., Guerrero, N.A., Blanchard, N. and Mayorga, L.S., 2016. Rab22a controls MHC-I intracellular trafficking and antigen cross-presentation by dendritic cells. EMBO reports, 17(12), pp.1753-1765.
45. Kaur, M., Kumar, D., Butty, V., Singh, S., Esteban, A., Fink, G.R., Ploegh, H.L. and Sehrawat, S., 2018. Galectin-3 regulates γ-herpesvirus specific CD8 T cell immunity. IScience, 9, pp.101-119.
46. Sehrawat, S., Kirak, O., Koenig, P.A., Isaacson, M.K., Marques, S., Bozkurt, G., Simas, J.P., Jaenisch, R. and Ploegh, H.L., 2012. CD8+ T cells from mice transnuclear for a TCR that recognizes a single H-2Kb-restricted MHV68 epitope derived from gB-ORF8 help control infection. Cell Reports, 1(5), pp.461-471.
47. Singh, S., Dahiya, S., Singh, Y.J., Beeton, K., Jain, A., Sarkar, R., Dubey, A., Tehseen, A. and Sehrawat, S., 2022. Robust anti-SARS-CoV2 single domain antibodies cross neutralize multiple viruses. IScience, 25(7).
48. Sharma, Y., Sarkar, R., Jain, A., Singh, S., Shekhar, C., Shanmugam, C., Dhanavelu, M., Tembhurne, P., Kaul, R. and Sehrawat, S., 2021. A mouse model of PPRV infection for elucidating protective and pathological roles of immune cells. Frontiers in Immunology, 12, p.630307.
49. Schmittgen, T.D. and Livak, K.J., 2008. Analyzing real-time PCR data by the comparative CT method. Nature protocols, 3(6), pp.1101-1108.
50. Tehseen, A., Kumar, D., Sarkar, R., Singh, S., Dubey, A. and Sehrawat, S., 2022. Glucocorticoid signaling mediates CD8+ T cell memory differentiation. bioRxiv, pp.2022-07.

Appendix

Table1. List of qPCR primers (5'-3') used for measuring the expression of respective genes in mouse cDNA

Gene name	Forward Primer	Reverse Primer	Product Size
IFNα	GGACTTTGGATTCCCGCAGGA	GTGGAGGTCATTGCAGAATGAG	169
IFNβ	CCAGCTCCAAGAAAGGACGA	CGCCCTGTAGGTGAGGTTGAT	85
IFNγ	TTCTTCAGCAACAGCAAGGC	TCAGCAGCGACTCCTTTTCC	165
IFITM1	CGACAGCCACCACAATCAAC	CCCACCATCTTCCTGTCCCT	148
IFIT1	AGCACACATTGAAGAAGCCCT	GTAGCCAGAGGAAGGTGATGC	148
ISG15	ACGATTTCCTGGTGTCCGTG	AGGGTAAGACCGTCCTGGAG	136
OAS1A	TGCCCTATCTGACACATTAGC	TTTCATCATATCTATGGTCCCCCAG	130
OAS1g	GCCCTTGAGTGGCTACAACA	TGTGATAAAGCTGATCGTTGCT	127
OAS2	AGTGACATGGTGGGAGTGTT	TCCAGAGCTGAATGGACTCCTA	157
OAS3	TGACCCGACAGGCAACCT	TCACACAGCGGCCTTTACC	139
STAT1	CGTGCAGTGAGTGAGTGAGAG	GAGTTGGGCAAGCGATCCG	151
STAT2	TCCGCTGTTCGCTATCTTGG	TGCGCCATTTGGACTCTTCT	138
IRF9	GCAAAGAGGGGTATGGTAAGGA	TCGGAAGTCTTGCTTGCCTG	180
HPRT	CTGGAGCAAGTCTTACAGTCC	GCGTCGTGATTAGCCATGATG	135

Table2. List of qPCR primers (5'-3') used for assessing the expression of respective genes in human PBMCs

Primer name	Forward Primer	Reverse Primer	Product size
IFITM1	CCGTGAAGTCTAGGGACAGG	TGTCACAGAGCCGAATACCA	152
ISG15	GTGGACAAATGCGACGAACC	TCGAAGGTCAGCCAGAACAG	158
OAS2	GAGAAAAGCCAAAGAAGCGGG	ATCAGGGTATGGGGGAGAAGT	176
STAT1	TGTGAAGTTGAGAGATGTGAATGAG	TCGTTCTGGTGCCAGCATTT	173
STAT2	GCTGCACTTGGGAGTGATGA	TCCTGAATGTCCCGGCAGAA	149
OAS3	AGAAGCCCAGGCCTATCATC	GGATGCCATTCCGTCCCAT	135
IFIT1	CTCTGCCTATCGCCTGGATG	AGCTTCAGGGCAAGGAGAAC	132
IRF9	CCTCCAGCCAAGACAATGGAA	CCAGCAAGTATCGGGCAAAG	180
IFNα	TCGTATGCCAGCTCACCTTTT	CAGCATGGTCCTCTGTAAGGG	158
IFNβ	ACGCCGCATTGACCATCTAT	AGCCAGGAGGTTCTCAACAAT	107
IFNγ	TGAATGTCCAACGCAAAGCA	CTGGGATGCTCTTCGACCTC	122
18s rRNA	GGCCCTGTAATTGGAATGAGTC	CCAAGATCCAACTACGAGCTT	150

Table3. List of qPCR primers (5'-3') used for measuring the expression of genes of mTOR pathway

Primer Name	Forward Primer	Reverse Primer	Product Size
RAB8A	CCATGGGTATCATGCTGGTCT	AGTCGAGTGCCAGCTTTTCTC	186
IGF1R	AATCCTCCAACTCTGCCCAA	TTCTGATGGGTATTTTGTCTTTGGA	121
Pi3k	TGGGACCACTTGGTAGAAGAAC	GGGGCAGTGTTTGCAGG	115
Akt1	CCGCCTGATCAAGTTCTCCT	TGCCCACAGTAGAAACATCCT	200
Akt2	TCCACAAACGTGAATGCCAG	AGGCAGCGTATGACAAAGGT	173
Akt3	ACACCACCTGAAAAGTATGACGA	GGAACTTATTCCCGTCCGCT	107
TSc1	CTGAGCCGCTGCAAGCTA	TGCAGTGGTACCAAAGGCTTTAC	128
TSc2	ATGAGAGACCCAAAAGCAGAA	GGAGAACACATATCGGGCCA	151
S6k	AGGGGGCTATGGAAAGGTTTT	ATGTTCCGCTCTGCTTTCGT	141
mTOR	TTGGCATAACAGATCCTGACCCTG	GGTCATTCAGAGCCACAAACAG	100
Rictor	CGCTCGTGGGCAGGTATTAT	AGCAGACCTCGCCTTATTTCC	109
Raptor	CAGAAGTGCGTGAGTCTGGT	AAAGAATGGGCTGTGCCTGA	141
SIN1	GGGACTTCCGGGCTTCA	GAGCTTGCCCAGGATGTATGT	142

Table4. List of PCR primers (5'-3') used for the cloning of Rab8a shRNA into pLKO.1-GFP and cDNA sequences into pLenti-GFP vector.

Primer	Sequences
RAB8a_FP	CGACTCTAGAATGGCGAAGACCTACGATTAC
RAB8a_RP	GGTGGATCCTGCAGATCCTCTTCAGAGATGAGTTTCTGCTCCAGGAGACTGCACCGGAAG
RAB8a_TS1	CCGGACCGGTCCGGACTCGATTGAGAAATTCAAGAGATTTCTCAATCGAGTCCGGGAATTCC
RAB8a_BS1	GGAATTCCCGGACTCGATTGAGAAATCTCTTGAATTTCTCAATCGAGTCCGGACCGGTCCGG
RAB8a_TS2	CCGGACCGGTGCCTTCAACTCCACATTCATCAAGAGTGAATGTGGAGTTGAAGGCGAATTCC
RAB8a_BS2	GGAATTCGCCTTCAACTCCACATTCACTCTTGATGAATGTGGAGTTGAAGGCACCGGTCCGG
RAB8a_SC.TS1	CCGGACCGGTGAGCGATTGGACATACATCTCAAGAGGATGTATGTCCAATCGCTCGAATTCC
RAB8a_SC.BS1	GGAATTCGAGCGATTGGACATACATCCTCTTGAGATGTATGTCCAATCGCTCACCGGTCCGG
RAB8a_SC.TS2	CCGGACCGGTACTTTTGCACACCACTACCTCAAGAGGGTAGTGGTGTGCAAAAGTGAATTCC
RAB8a_SC.BS2	GGAATTCACTTTTGCACACCACTACCCTCTTGAGGTAGTGGTGTGCAAAAGTACCGGTCCGG